

**AGE-INDUCED DESYNCHRONIZATION BETWEEN CLOCK
AND IMMUNE GENES EXPRESSION IN MICROGLIA AND
OTHER PERIPHERAL CLOCKS IN MALE WISTAR RATS:
CHRONOBIOTIC ROLE OF CURCUMIN**

*A thesis submitted to University of Hyderabad for the award of
the degree
Doctor of Philosophy
In
Animal Sciences*



Supervisor:
Prof. Anita Jagota

By:
Neelesh Babu Thummadi

**Department of Animal Biology
School of Life Sciences
University of Hyderabad
P.O. Central University
Hyderabad 500 046, Telangana, India**

July, 2019

Reg. No.: 12LAPH08

University of Hyderabad

(A Central University by an Act of Parliament)

Department of Animal Biology

School of Life Sciences

P.O. Central University, Gachibowli, Hyderabad-500046



CERTIFICATE

This is to certify that the thesis entitled “*Age-induced desynchronization between clock and immune genes expression in microglia and other peripheral clocks in male Wistar rats: chronobiotic role of curcumin*” submitted by Mr. **Neelesh Babu Thummadi** bearing registration number **12LAPH08** in partial fulfillment of the requirements for award of **Doctor of Philosophy** in the School of Life Sciences is a bona fide work carried out by him under my supervision and guidance.

This thesis is free from plagiarism and has not been submitted previously in part or in full to this or any other University or Institution for award of any degree or diploma.

Further, the student has the following publications before submission of the thesis for adjudication and has produced the evidence for the same in the form of acceptance letter or the reprint in the relevant area of his research.

A. Publications:

1. Neelesh Babu Thummadi, Anita Jagota (2019) Aging renders desynchronization between clock and immune genes in male Wistar rat kidney: chronobiotic role of curcumin. **Biogerontology** 20(4):515–532 (ISSN: 1389-5729, Springer Nature); **(Part of thesis: Objective II)**
2. Anita Jagota, Neelesh Babu Thummadi (2017) Hormones in Clock regulation During Ageing. In: Rattan SIS, Sharma R (eds) Hormones and Ageing and Longevity. Healthy Ageing and Longevity, vol 6. Springer, Cham, pp 243–265 (ISBN: 978-3-319-63000-7, Springer)
3. Anita Jagota, Neelesh Babu Thummadi*, Kowshik Kukkemane* (2019) Circadian regulation in Hormesis: Health and Longevity (eds Rattan S and Marios Kariasis) in “The Science of Hormesis in Health and Longevity.” Chapter 22 pp 223-233. Academic press (* equal contribution) (ISBN: 978-0-12-814253-0, Elsevier)
4. Anita Jagota, Kowshik Kukkemane*, Neelesh Babu Thummadi* Biological Rhythms and Aging. In “Models, Molecules and Mechanisms in Biogerontology.” Springer Nature (in Press) (* equal contribution)

and

has made presentations in the following conferences:

B. Presentations in Conferences:

1. International conference on 'Recent trends in Neurological and Psychiatric *Research*' (SNCI – 2016) "Daily chronomics of clock genes expression and specific inflammatory markers in peripheral clock – Liver: Middle age perturbations" **Poster Presentation**, December 2016, CSIR-CCMB, Hyderabad, Telangana, India, as part of 30th Annual meeting of Society for Neurochemistry India (SNCI). **(International)**
2. Academia Sinica-UOH (Indo-Taiwan) joint workshop on **Frontiers in Life Sciences** "Age induced alterations in clock genes and inflammatory parameters in peripheral clock – Liver" **Poster Presentation**, September 2016, School of Life Sciences, University of Hyderabad, Hyderabad, India. **(International)**

Further, the student has passed the following courses towards the fulfillment of course work required for the award of Ph.D.

Course Code	Name	Credits	Pass/Fail
AS 801	Seminar 1	1	Pass
AS 802	Research Ethics & Management	2	Pass
AS 803	Biostatistics	2	Pass
AS 804	Analytical Techniques	3	Pass
AS 805	Lab Work	4	Pass

Supervisor

Head of the Department

Dean of the School

University of Hyderabad
(A Central University by an Act of Parliament)
Department of Animal Biology
School of Life Sciences
P.O. Central University, Gachibowli, Hyderabad-500046



DECLARATION

I, **Neelesh Babu Thummadi**, hereby declare that this thesis entitled "*Age-induced desynchronization between clock and immune genes expression in microglia and other peripheral clocks in male Wistar rats: chronobiotic role of curcumin*" submitted by me under the guidance and supervision of **Prof. Anita Jagota** is an original and independent research work. I also declare that it has not been submitted previously in part or in full to this university or any other University or Institute for the award of any degree or diploma.

Date:

Name: Neelesh Babu Thummadi

Signature of the Student

Reg. No.: 12LAPH08

ACKNOWLEDGEMENTS

*I express my deepest gratitude to my supervisor **Prof. Anita Jagota** for allowing me to work under her guidance in the wonderful field of chronobiology and immunology. Words fall short to describe the kindness and the encouragement she showed since the day I began my journey in Ph.D. I am extremely delighted to work under **Prof. Anita Jagota** whom I cherish as a true mentor. I will forever remember her support and enthusiasm in science which helped me in learning and shaping myself as a better student.*

*I am extremely thankful to my doctoral committee members **Prof. B. Senthilkumaran** and **Prof. Naresh Babu Sepuri** for their encouragement and suggestions throughout my Ph.D.*

*I am grateful to Head, Department of Animal Biology **Prof. Anita Jagota** and the former Heads **Prof. Jagan Pongubala** and **Prof. Senthilkumaran** for allowing me to use the department facilities.*

*I am thankful to Dean, School of Life Sciences, **Prof. S. Dayananda** and former Deans **Prof. K.V.A. Ramaiyya**, **Prof. P. Reddanna** and **Prof. RP. Sharma** for allowing me to use school facilities.*

*I extend my thanks all the **faculty members** of Dept. of Animal Biology and School of Life Sciences for their timely suggestions.*

*I take this opportunity to thank the family members of **Prof. Anita Jagota**, **Shri Laxminarayana Jannu**, **Navya** and **Nishant** for always being cordial.*

*I thank all the **Office staff** from Animal Biology department, School of life sciences, Animal house and administrative wing for their timely help.*

*I thank my former lab mates **Dr. Ushodaya M**, **Dr. Dileep Kumar Reddy**, **Dr. Lakshmi B**, and **Dr. Vinod Ch.** for creating conducive environment in the lab.*

*I especially thank my labmates **Dr. Varsha S Prasad**, **Kowshik K**, and **Minurani Dalai** for being there with me. I thank the other labmates **Sushree Abhidathri Sharma**,*

Zeeshan Akhtar Khan, Sultan Khan, Santosh K Das, K Vidila Jing for their help and support.

*I thank **Mr. Balakrishna** for his assistance in the lab.*

*I thank **Kavya** and **Mr. Senthil** for being very good friends with me.*

*I thank my friends from the University of Hyderabad, **Sirish, Lokiya, Swaroop, and Siva** for making my stay more pleasant.*

*I thank all the Professors from my Integrated M.Sc. who helped me a lot. I especially thank **Dr. C Madhav Reddy** and **Dr. T Chandrashekar** for their kindness and support.*

*I thank my friends from my Integrated M.Sc. **Naveen, Bushan, Varaprasad, Khaja, Siva, Ganesh, Suresh, Balaji, Sivarjuna, Pramod, Nagarjuna, and Mallikarjun***

*I thank all my school **Teachers** who invigorated the passion for science in me.*

*I thank all my school **friends**.*

*I thank my **Parents, sister, brothers, cousins** and all the **near and dear** who has unfathomable love and care towards me.*

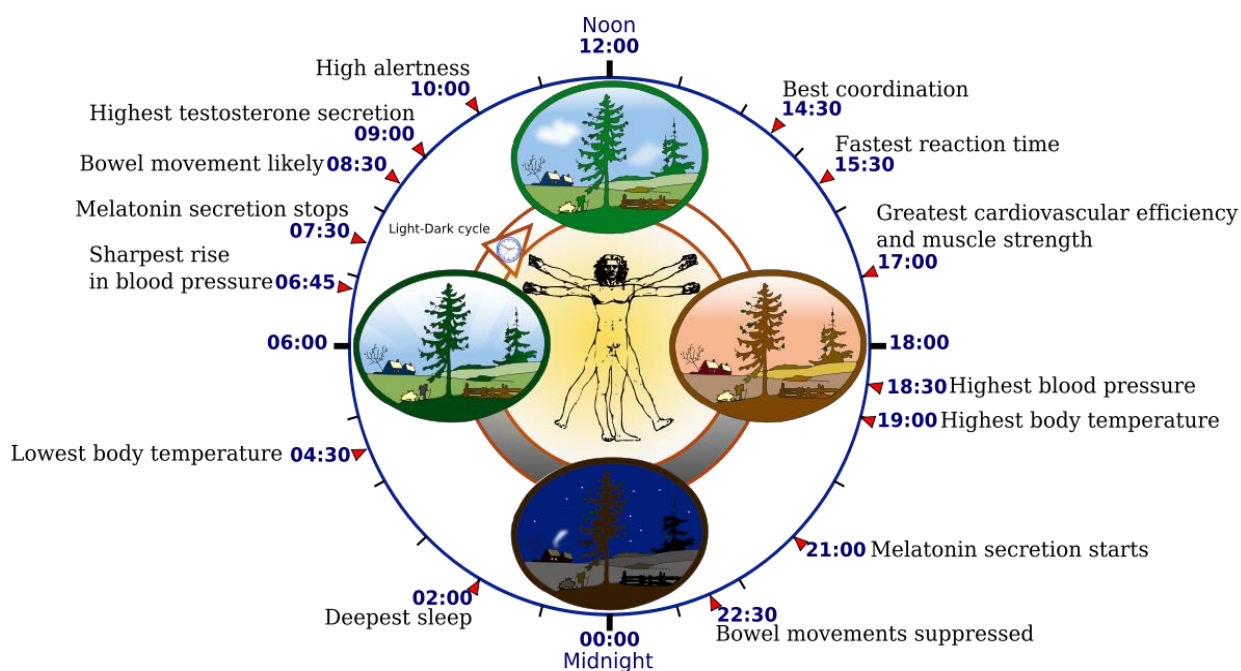
Contents

<i>Chapter I Introduction and Review of Literature</i>	1
Circadian rhythms	2
Circadian clock	4
Suprachiasmatic nucleus (SCN)	4
Molecular mechanism of circadian clock	9
Peripheral clocks	12
Aging	17
Aging and clock dysfunction	17
Aging and peripheral clocks dysfunction	19
I. Aging, Microglia and clock dysfunction	19
II. Aging, Liver and clock dysfunction	26
III. Aging, Kidney and clock dysfunction	30
IV. Aging, Spleen and clock dysfunction	32
Inflammaging and NF-κB pathway in clock dysfunction	33
Aging and Serotonin mediated inflammation in clock dysfunction	34
Curcumin as a therapeutic drug	36
Hypothesis	38
<i>Objectives</i>	39
<i>Chapter II Materials and Methods</i>	41
<i>Chapter III Results</i>	50
<i>Chapter IV Discussion</i>	152
<i>Summary and Conclusions</i>	168
<i>References</i>	172
<i>Appendices</i>	187
List of Figures	188
List of Tables	192
Abbreviations	193
<i>Publications</i>	198

Chapter I Introduction and Review of Literature

Circadian rhythms

During the evolution, it is the adaptation of the organisms that resulted in the synchrony of their physiological, behavioural and metabolic functions to the daily light dark cycles. This adaptation had lead the organisms to execute most of their biological activities in a rhythmic pattern with the near 24 hour periodicity which are called as circadian rhythms (Jagota 2012). The term circadian rhythm was coined from the Latin *circa* – around; *diem* – a day. The circadian rhythms exist in various organisms ranging from single cell organisms like cyanobacteria to highly evolved mammals (Edgar et al. 2012). With circadian rhythms, organisms are able to anticipate the environmental changes and make use of the resources like light and food in better way (Sharma 2003). In mammals, circadian rhythms are observed in several physiological functions like sleep-wake cycles, body temperature, blood pressure, melatonin secretion etc. (Fig. 1). Synchrony between the physiologies is essential for the metabolic homeostasis (Li and Lin 2016).



https://en.wikipedia.org/wiki/Circadian_rhythm#/media/File:Biological_clock_human.svg

Fig. 1: This diagram depicts the circadian patterns typical of someone who rises early in morning, eats lunch around noon, and sleeps at night (10 p.m.). Although circadian rhythms tend to be synchronized with cycles of light and dark, other factors - such as ambient temperature, meal times, stress and exercise can influence the timing as well.

Parameters of circadian rhythms

Endogenous: Circadian rhythms exist even in the constant conditions i.e. in the absence of any external cue such as light. In constant darkness, mammals exhibit free-running period which is denoted by Greek letter ' τ '.

Entrainable: In spite of being endogenous, circadian rhythms will be reset in the presence of a given external cue and the process of resetting is termed as 'entrainment'. Any stimuli that can cue an entrainment is termed as zeitgeber (time giver). In the process of resetting, a zeitgeber can induce phase alteration of a circadian rhythm. Depending on the time and type of zeitgeber, phase advance or phase delay can be observed in the circadian rhythms (Fig. 2).

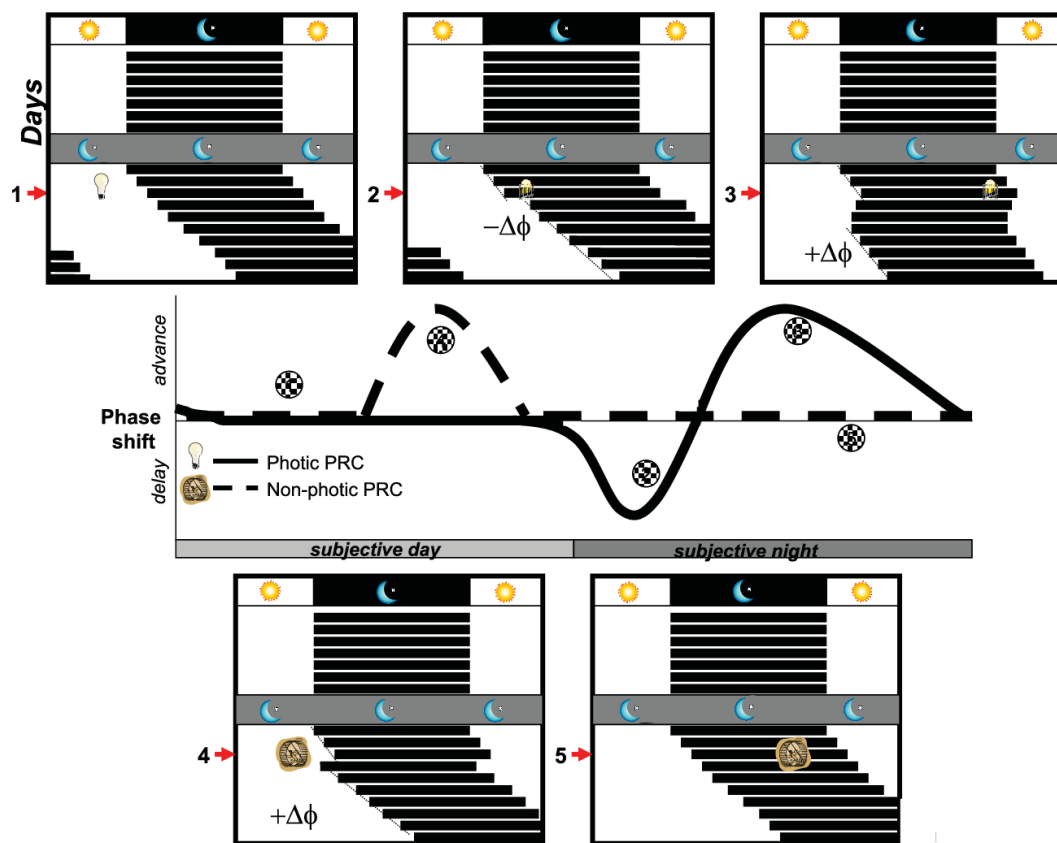


Fig. 2: Phase response curves of circadian rhythms. In the top panel, actograms represent the response of locomotor activity rhythms to a light pulse during 1) the subjective day, 2) the early subjective night (inducing a phase delay of the rhythm), and 3) the late subjective night (inducing a phase advance). The bottom panel represents a nonphotic stimulus (such as a novel running wheel) presented 4) in the middle of the subjective day (inducing a phase advance of the rhythm) or 5) during the subjective night (no response). The central graph is a representation of both phase response curves, a PRC to light (solid line), and a PRC to a nonphotic stimulus (dashed line), indicating the numbers of the manipulations shown in the corresponding actograms (Golombek and Rosenstein 2010).

Temperature compensated: Variations in physiological temperatures influence the kinetics of biomolecules but it cannot alter the periodicity of the circadian rhythms in mammals. This property is referred as temperature compensation.

Circadian clock

In the living organisms, there exists a circadian timing system that maintains the circadian rhythms with near 24 h periodicity of several physiologies and behaviour and keeps in synchrony with the light dark cycles (Jagota 2012). Circadian clock maintains the circadian rhythms not only in response to the external cues but also to the endogenous signals within the biological system (Ueda et al. 2005). A well synchronized circadian clock is highly essential for the proper maintenance of homeostasis of an organism (Kim et al. 2019). The architecture and the mechanism of the circadian clock varies from insects to mammals with increase in complexity and functions. In the light of the importance of circadian clock, Nobel Prize in physiology and medicine in 2017 was awarded jointly to Jeffrey C. Hall, Michael Rosbash and Michael W. Young for their discovery of molecular mechanism involved in circadian rhythms in *Drosophila* (Callaway and Ledford 2017). In mammals, the central circadian clock is located in Suprachiasmatic nucleus (SCN) (Takahashi 2017).

Suprachiasmatic nucleus (SCN)

Suprachiasmatic nucleus is group of neurons that is present below the hypothalamus, above the optic chiasm, and on either side of the 3rd ventricle (Fig. 3a, 3b) with 10,000 in number on each side (Hastings et al. 2018). It serves as the principal pacemaker or master clock that regulates the overt circadian rhythms. SCN is functionally distinct into two compartments i.e. core and shell which are diverse in their neuronal distribution, neuropeptide secretions, gene expression pattern etc. (Evans et al. 2015). Shell is characterized by the presence of arginine vasopressin (AVP) neurons, whereas, the core is densely populated with vasoactive intestinal peptides (VIP) neurons (Morin 2007) (Fig. 3c, 3d, 3e). Individual neurons in SCN has the capacity to sustain the circadian rhythms of neuronal firing, gene expression and calcium concentration ($[Ca^{2+}]_i$) (Noguchi et al. 2017). Interestingly, SCN exhibits higher electric activity during the circadian day in both diurnal and nocturnal animals (Hastings et al. 2018). In the process of entrainment of circadian rhythms, SCN involves three major steps (i) perceiving of the external stimuli such as light, (ii) processing and intra communication of the received information (iii) transmission of the processed signals to other tissues and synchronise them to the given stimuli.

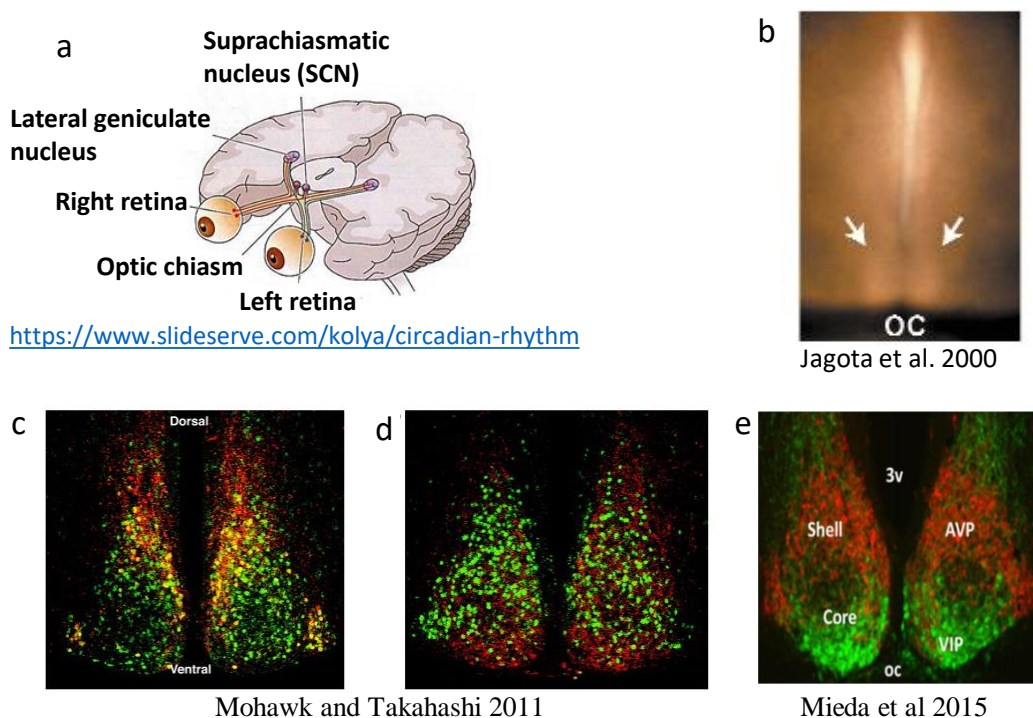


Fig. 3: (a) Suprachiasmatic nucleus located at either side of optic chiasm. (b) Coronal slices of hamster SCN. Arrows show SCN; OC, optic chiasm (Jagota et al. 2000). Expression of neuropeptides in the mammalian suprachiasmatic nucleus (SCN) demonstrated by photomicrographs of mouse SCN slices. The bilateral nuclei are located directly above the optic chiasm and positioned on either side of the third ventricle. Slices were obtained from transgenic mice expressing the CLOCKD19 mutant protein tagged with hemagglutinin (HA) in secretogranin positive cells (expression of the HA-tagged transgene protein product is shown in green). Sections were immunostained to detect expression of the neuropeptides (c) arginine vasopressin (AVP, red) and (d) vasoactive intestinal polypeptide (VIP, red). AVP expression is observed most prominently in the dorsal SCN, whereas VIP expression is strongest in the ventral SCN. Cells expressing both CLOCKD19-HA (expressed throughout the nucleus) and the peptide of interest appear yellow (Mohawk and Takahashi 2011). (e) Different compartments of SCN (Mieda et al. 2015).

Afferent pathways

There are three afferent pathways to receive the information from external zeitgeber and transmit to SCN (Fig. 4). In mammals, retinohypothalamic tract (RHT), geniculohypothalamic tract (GHT), and raphe nuclei are identified as primary afferent pathways (Reghunandanan and Reghunandanan 2006). Light is the major zeitgeber which transmits through the monosynaptic retinohypothalamic tract (Jagota 2012). Glutamate and pituitary adenylate cyclase-activating polypeptide (PACAP) serve as the major neurotransmitters from RHT. RHT neurons excited with light stimulation release glutamate into the core of SCN which is rich in VIP neurons (Webb et al. 2013). PACAP from retinal ganglionic cells may help in potentiating the action mechanism

of glutamate on the core of SCN (Webb et al. 2013). GHT arising from the intergeniculate leaflet (IGL) projects into the SCN region where RHT inputs into the SCN (Hanna et al. 2017). IGL receives the photic information from a branch of RHT. Thus GHT helps as a secondary or indirect photic messenger and also it serves to transmit non-photic signals like motor activity (Saderi et al. 2013). Neuropeptide Y (NPY), GABA and enkephalin (ENK) are identified as potential neurotransmitters involved in GHT pathway to SCN in various species (Albers et al. 2017). The third input pathway raphe mainly projects the serotonergic neurons to the central pacemaker with serotonin as major neurotransmitter. In addition, SCN responds to the raphe nuclei through dorsomedial hypothalamus nucleus to alter the serotonin levels. In response to this raphe nuclei signals to SCN about the activity status (Deurveilher and Semba 2008). This provides a significant and sustainable circadian rhythms.

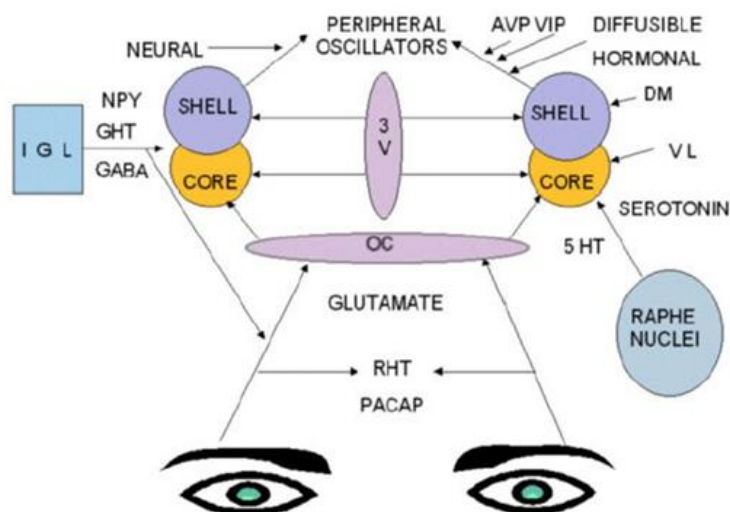


Fig. 4: Afferent inputs of the SCN. RHT: Retinohypothalamic tract, GHT: Genuculohypothalamic tract, OC: Optic chiasm, 3V: Third ventricle, IGL: Intergeniculate leaflet, DM: Dorsomedial SCN, VL: Ventrolateral SCN, NPY: Neuropeptide Y, GABA: Gamma amino butyric acid, PACAP: Pituitary adenylate cyclase-activating polypeptide (Reghunandan and Reghunandan 2006).

Intra-SCN communications

To have the robust and sustained circadian rhythms a strong and integrated intra-SCN communication is highly needed (Reghunandan and Reghunandan 2006). GABA, VIP and AVP are most essential neurotransmitters as potential SCN synchronizers. GABA is expressed by most of the SCN neurons and are GABAergic (Albers et al. 2017). It was shown that GABA can exhibit dual effects where it can be excitatory during the day and at night it can be inhibitory (Wagner et al. 2001). In SCN, nearly 9 – 24% of neurons express VIP which acts through VPAC₂ receptor that is expressed in nearly 60% of neurons in SCN, and results in change in

neuronal firing rate (Reghunandan and Reghunandan 2006). Through VPAC₂, VIP can reset the rhythms in the presence of light and also can help in sustaining the existing rhythm (Jones et al. 2018). In SCN, AVP is produced by one third of the neurons where its synthesis and secretion is in circadian manner (Mieda et al. 2015). AVP acts through V1a receptors and plays an excitatory role which leads to increased amplitude of neuronal firing rates in the subjective day (Li et al. 2008).

Efferent pathways

To synchronize the circadian rhythms to the external stimuli SCN has to signal the other peripheral tissues and organs, this is carried out by the efferent pathways (Fig. 5). SCN relays its signals to the nearest regions like hypothalamus, thalamic nuclei, paraventricular nucleus, dorsomedial nucleus, subparaventricular zone. SCN innervations not only ends in hypothalamus but extend to several other regions like salivary glands, liver etc. (Hastings et al. 2018).

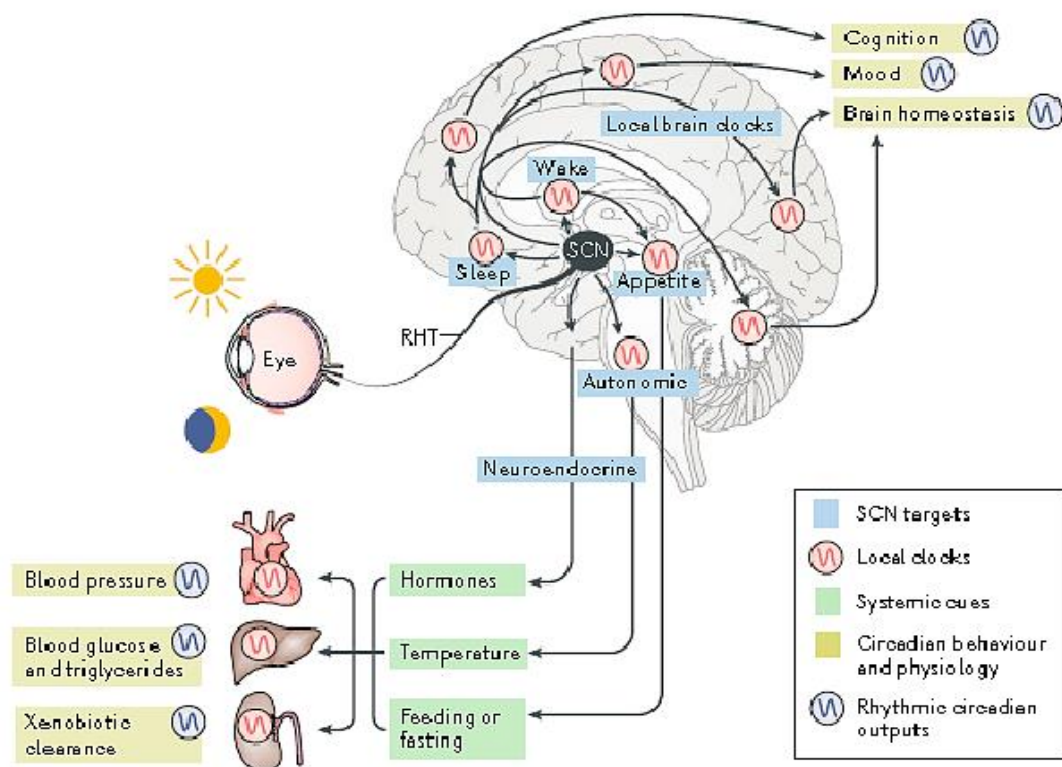


Fig. 5: The SCN receives direct retinal innervation via the retinohypothalamic tract (RHT) to ensure its synchronization to day–night cycles. The SCN clock projects to various brain centres, many of which contain local circadian clocks that direct behavioural (for example, feeding–fasting and sleep–wakefulness), autonomic and neuroendocrine circadian rhythms. These systemic cues synchronize the local molecular clocks of peripheral tissues, and these local clocks in turn direct local programs of circadian gene expression that regulate physiological rhythms critical to health (for example, rhythms relating to mental alertness, blood pressure, triglyceride metabolism and renal function (Hastings et al. 2018).

VIP and AVP are the essential neurotransmitters that are involved in the efferent pathway signaling. In addition to these neurotransmitters several other neurochemicals like somatostatin (SS), calbindin (CalB), calretinin (CALR), Galanin (Gal), Angiotensin II (ANG II), Prokineticin 2 (PK2) etc. are identified as potential signaling molecules. Apart from the neurotransmitters, several other humoral molecules like TGF α are identified as important signaling molecules (Kramer et al. 2001). Of all the signaling mechanisms, one pathway plays an essential role in regulating the circadian rhythms i.e. the melatonin secretion from the pineal gland. Melatonin synthesis and secretion is explained in Fig.6.

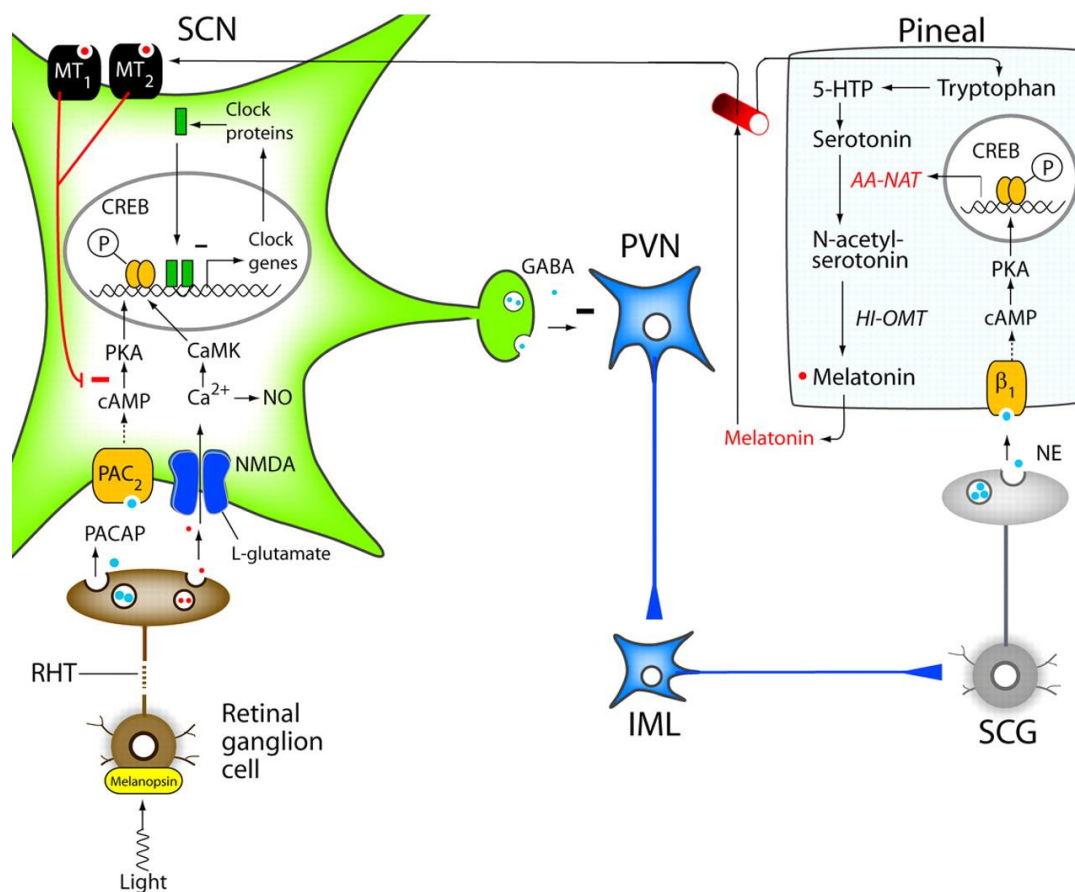


Fig. 6: The most prominent projection of the SCN is to the subparaventricular zone, located ventral to the paraventricular nucleus (PVN), and to the dorsomedial nucleus of the hypothalamus. The subparaventricular zone projects to the medial preoptic region and is involved in control circadian rhythms of body temperature. The dorsomedial nucleus, which receives SCN both directly and via the subparaventricular zone, controls a wide range of circadian responses, including the sleep–wake cycle, corticosteroid secretion, and feeding, via projections to other hypothalamic targets, including the ventrolateral preoptic area, the PVN, and the hypocretin/orexin neurons of the posterior lateral hypothalamus. The SCN also sends a direct inhibitory projection to PVN neurons controlling sympathetic output to the pineal gland (Benarroch 2008).

Melatonin is considered as the messenger of the darkness as it signals the animals about the absence of light and its upsurge is observed at dark periods in both diurnal and nocturnal animals (Jagota and Thummadi 2018). Melatonin is a potent circadian synchronizer in several tissues and acts through melatonin receptors like MT1, MT2 and MT3 in various tissues. SCN is one among those tissues which receives the signals from melatonin. This pathway provides a feedback mechanism for the SCN. Melatonin suppress the neuronal activity levels of SCN in the night time and can reduce the VP levels in SCN as an immediate effect. Melatonin can also exert long term effect like phase shifting and amplifying the circadian rhythms in SCN (Reghunandan and Reghunandan 2006). Owing to its circadian synchronizing property, melatonin has been well studied for its chronobiotic properties (Mattam and Jagota 2014).

Molecular mechanism of circadian clock

In between receiving the stimuli and relaying it to the other organs, SCN employs a highly conserved molecular mechanism that plays a non-replaceable role in generating and sustaining the circadian rhythms (Jagota 2012). Molecular mechanism is comprised of dedicated set of core clock genes like *Clock*, *Bmal1*, *Per1*, *Per2*, *Cry1* and *Cry2* etc. and their products. They form tightly regulated transcriptional and translational feedback loop (TTFLs) mechanisms that result in the near 24 h rhythms in their expression that exerts overt rhythms in several physiologies (Fig. 7). CLOCK and BMAL1 acts as limbs of positive feedback loop, while PER and CRY shares the negative limb of the feedback loop (Takahashi 2017). CLOCK and BMAL1 heterodimerize to form the basic helix-loop-helix-PAS (PER-ARNT-SIM) transcription factor (Huang et al. 2012). They bind with histone acetyltransferase (HAT) p300 and CREB binding protein which now can bind to the chromatin (Lee et al. 2010). E-box elements are the binding sites of the CLOCK:BMAL1 heterodimer (Kwon et al. 2006). Several clock controlled genes (CCGs) including *Periods* and *Cryptochromes* have E-box elements at their promoter site. Once CLOCK:BMAL1 heterodimer binds to the E-box elements it initiates the transcription of the CCGs including periods and cryptochromes. But the stability of the PERIODS and CRYPTOCHROMES decide the length of the period of circadian rhythms. PER undergoes subsequent degradation by β -TrCP ubiquitination when PER gets phosphorylated at regulatory sites (Buhr and Takahashi 2013). On the other hand CRY also undergoes degradation by SCF (Skp1/Cullin/F-box protein) E3 ligase complex (SCF^{Fbx13}).

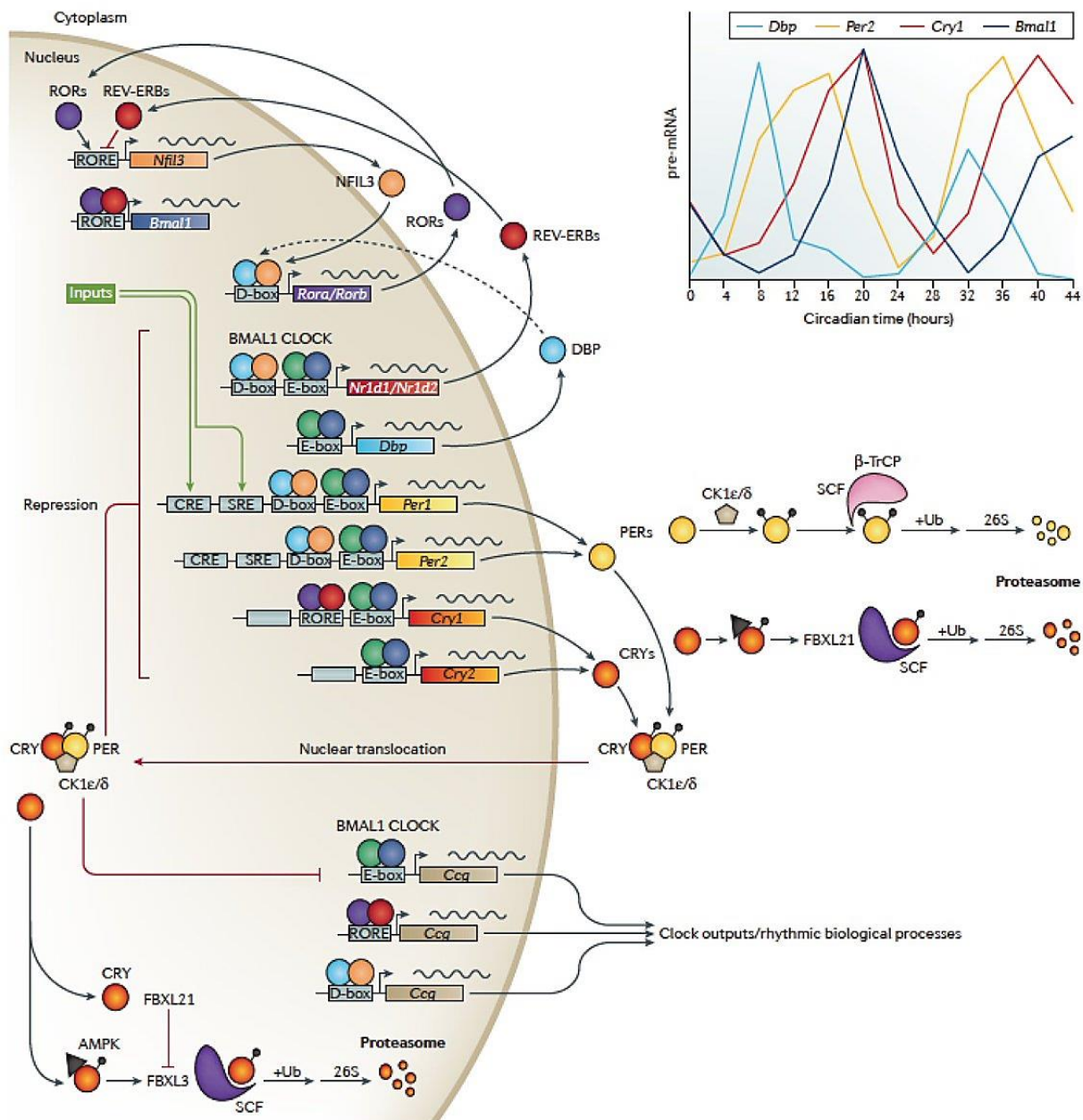


Fig. 7: The circadian gene network in mammals. At the core, CLOCK and BMAL1 activate the *Per1*, *Per2*, *Cry1* and *Cry2* genes, whose protein products interact and repress their own transcription. The stability of the PER and CRY proteins are regulated by parallel E3 ubiquitin ligase pathways. CLOCK and BMAL1 also regulate the nuclear receptors, Rev-erb α/β , which rhythmically repress the transcription of *Bmal1* and *Nfil3* that is driven by the activators, ROR α/β . NFIL3 in turn represses the PAR-bZip factor, DBP, to regulate a rhythm in the ROR nuclear receptors. These three interlocked transcriptional feedback loops represent the three major transcriptional regulators of the majority of cycling genes. Different combinations of these factors generate different phases of transcriptional rhythms as exemplified by the RNA profiles of *Dbp*, *Per2*, *Cry1* and *Bmal1* in the mouse liver (Takahashi 2017).

However, SCF^{Fbx21} rescues CRY from degradation by SCF^{Fbx13} as it has least ubiquitination activity than SCF^{Fbx13} (Yoo et al. 2013). Towards the evening when PER and CRY protein levels

reach a critical level they bind with each other and also binds with Casein kinase 1 δ (CK1 δ) and also with CK1 ϵ (Gallego and Virshup 2007). This PER complex relocates to the nucleus and binds to the CLOCK:BMAL1 complex to repress its activity.

During the process of repression PER complex consists at least 25 proteins which also includes SIN3-HDAC and Hp1 γ -Suv39h histone methyltransferase, where they initiate the deacetylation of histones and repress the CLOCK:BMAL1 transcription activity (Takahashi 2017). This repression on CLOCK:BMAL1 complex would repress the transcription of periods and cryptochromes and other CCGs, thus PER and CRY fulfills the negative feedback loop. Towards the late night, transcription of *Periods* and *Cryptochromes* decline and also as the half-life of PER and CRY is very low they undergo subsequent degradation by ubiquitination by selective E3 ligases. This would make PER complex to relieve the repression on the CLOCK:BMAL1 complex. Therefore, towards the beginning of the day, CLOCK:BMAL1 complex can initiate the cycle of transcription anew. Apart from this transcriptional activation and repression, the circadian rhythms are sustained by the help of an auxiliary feedback mechanism. Rev-erba/ β and Rora/ β are also among the CCGs that are transcriptionally activated by CLOCK:BMAL1 complex. Rev-erba/ β can bind to the ROR response elements (RRE) in the promoter of *Bmal1* and inhibit its transcription, whereas Rora/ β can competitively bind to the RRE in promoter region to induce the transcription of *Bmal1* (Partch et al. 2014).

Synchronization of the molecular clock

As an endogenous property, the time period to complete one cycle of transcriptional activation and repression almost takes 24 hours which can be seen as free running period. *Period* gene plays a significant role in determining the period length of an organism. Studies have shown that a familial mutation for period gene can determine the length of the period in humans. Familial advanced sleep phase disorder (FASPD) is one of the disorders associated with the mutations in PER2 and CSNK1D, where the individuals show phase advance in their sleep-wake cycles by several hours in comparison to normal individuals (Toh et al. 2001; Jones et al. 2013). PER proteins not only decide the endogenous period length they also respond to the external cues like photic signal and helps in sustaining the synchrony. For instance, PER1 and PER2 can be induced even in CLOCK:BMAL1 independent manner in the presence of light (Fig. 8). CREB responsive elements are present in the promoter region of *Period* genes, in the presence of the light CREB gets activated and initiate the transcription of *Period* genes (Jagannath et al. 2013).

However, this photic induced transcription of *Period* genes appears to be restricted to the light hitting the retina in night time alone or during the constant darkness condition. This phenomenon corresponds to the time period where animals show response in behavior with phase advance or phase delay of the period. This adaptation is considered as the resetting.

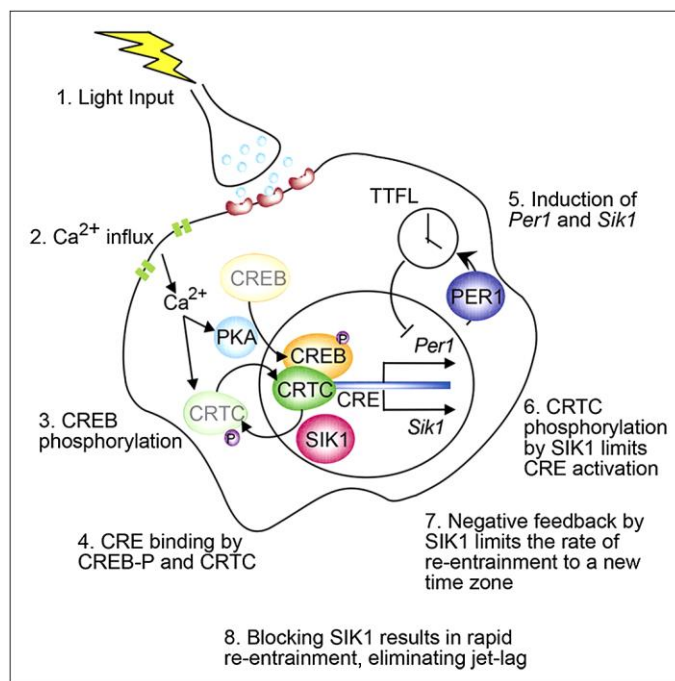


Fig. 8: An entrainment stimulus causes CRTC1 to coactivate CREB, inducing the expression of *Per1* and *Sik1*. SIK1 then inhibits further shifts of the clock by phosphorylation and deactivation of CRTC1. Knockdown of *Sik1* within the SCN results in increased behavioral phase shifts and rapid re-entrainment following experimental jet lag. Thus SIK1 provides negative feedback, acting to suppress the effects of light on the clock. This pathway provides a potential target for the regulation of circadian rhythms (Jagannath et al. 2013).

Peripheral clocks

SCN synchronizes the rhythms of several physiologies in almost all the other organs to the given environmental cue. In order to achieve the synchrony, almost all the cells in other organs possess a similar circadian molecular machinery as seen in SCN (Fig. 9). With the help of neurotransmitters and humoral signals SCN communicates with the peripheral clocks and brings synchrony with environmental cues. Peripheral clocks have the ability to self-sustain the circadian rhythms. It was first shown in the fibroblast cells that even after several propagations they still possess an active circadian rhythms (Balsalobre et al. 1998). It was shown that cultures of lung and liver could generate 20 or more cycles of *Per2* expression (Yoo et al. 2004).

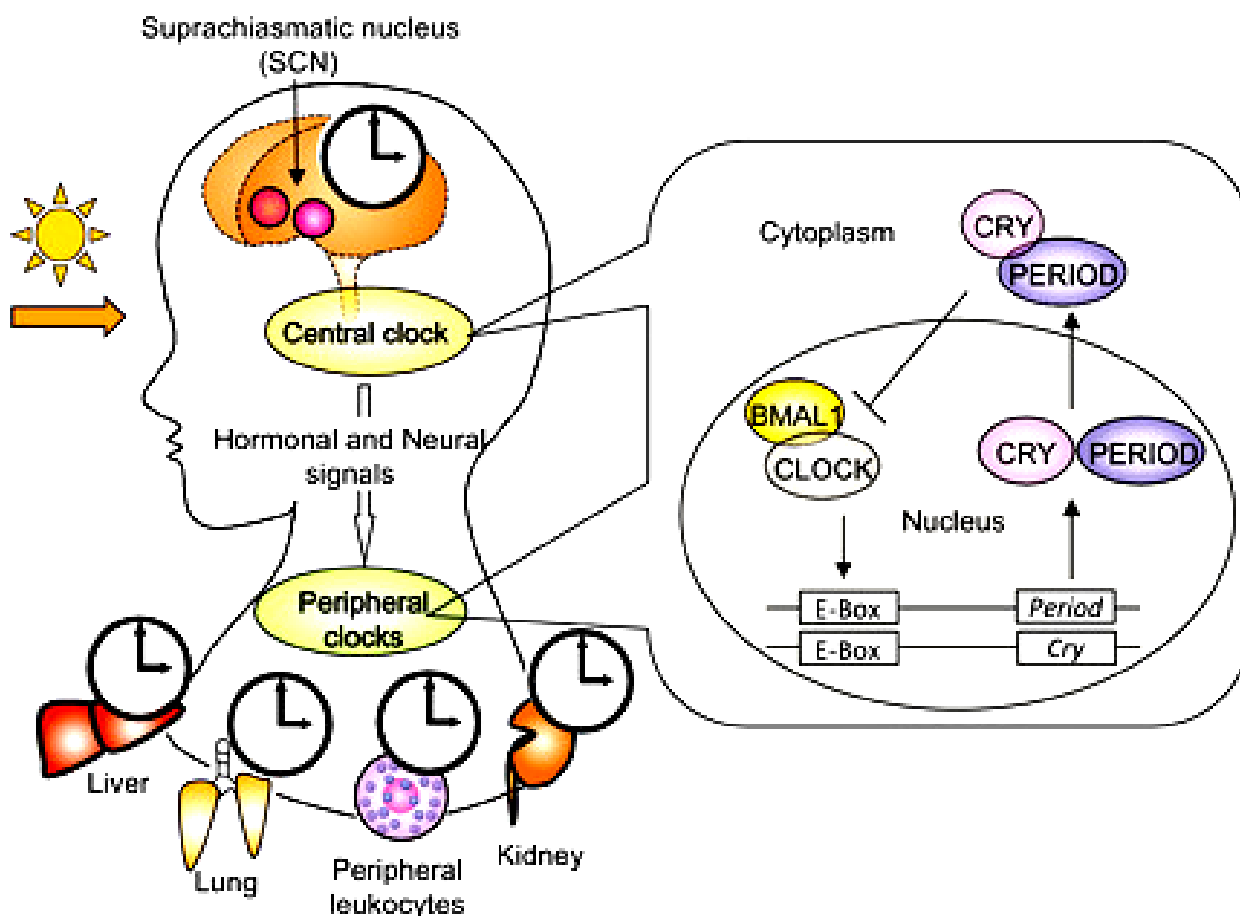


Fig 9: The mammalian circadian clock consists of the central oscillator, located in the suprachiasmatic nucleus (SCN) of the hypothalamus, and peripheral oscillators present in virtually all cell types. Light activates a specific group of photoreceptors in the retina that are connected to the central SCN clock, which synchronizes and entrains peripheral circadian clock via neural and endocrine pathways. The molecular mechanisms of rhythm generation are cell autonomous and highly conserved in the SCN (the central clock) and peripheral cells (the peripheral clocks) (Nakao et al. 2015).

However, to maintain the synchrony between the peripheral clocks *in vivo* the role of SCN is unreplacable. In the SCN lesioned animals, the phases of the rhythmic cycles between the peripheral clocks were completely different from each other (Guo et al. 2006). This explains the reason why SCN is considered as master clock and other peripheral clocks as slave clocks. Though there exists the clock machinery in peripheral tissues they show a 4h delay in the expression of clock genes compared to master clock SCN. This delay is probably because of the rapid input of electric signals perceived from photic signals to the SCN neurons but the delayed input to peripheral clocks through humoral signals (Balsalobre 2002). Peripheral clocks regulate several physiological functions in rhythmic pattern. For instance: the detoxification process shown by kidney, liver and intestines (Gachon et al. 2006). Energy metabolism, carbohydrate and

lipid metabolism, renal plasma flow, blood pressure, heart beat rate, immunity etc. are few among the daily oscillations that are regulated by peripheral clocks (Fig. 10). In spite of their self-ability to generate rhythms all these peripheral clocks are synchronized by the SCN timing cues (Dibner et al. 2010).

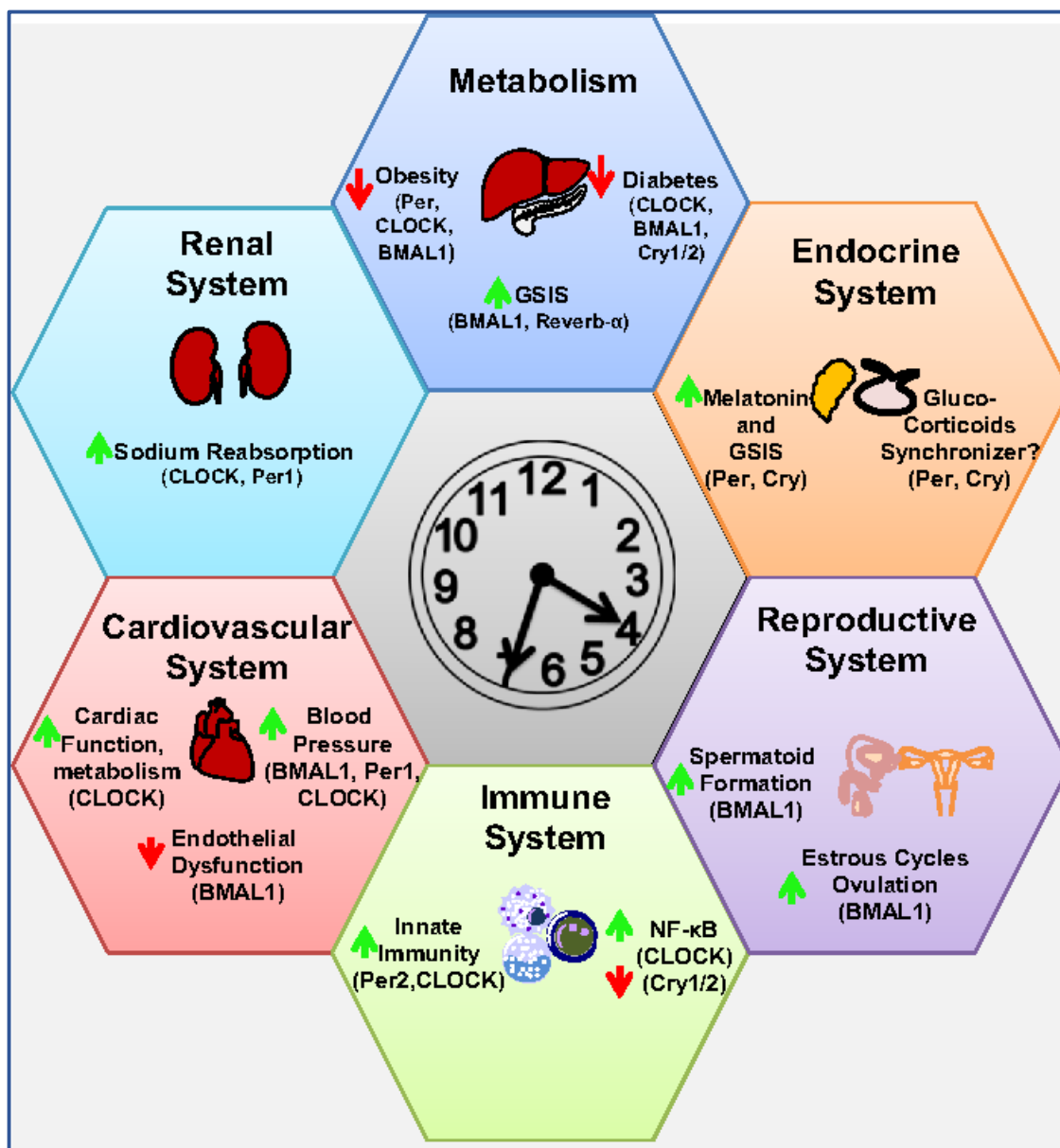


Fig. 10: Integrative role for the circadian clock in the regulation of physiological function. Circadian proteins listed in parentheses dictate which proteins have been implicated in regulating the process in question. If a protein is not listed, it does not imply that it is not involved, but that it has not yet been tested. Green arrows represent induction by the circadian protein; red arrows represent repression (Richards and Gumz 2013).

Clock and immunity

With the pioneering work in 1960s and 1970s, it was observed that mice responds to numerous pathogens and associated byproducts like endotoxins, exotoxins, and also pro-inflammatory cytokines, in a diurnal manner. It was reported that hematopoietic cells migration to the tissues occurs preferentially in the active phase of animal (Scheiermann et al. 2013). In correspondence to that, it was reported that in bone marrow homing of hematopoietic stem cells (HSCs) and neutrophils; monocyte recruitment to muscle cells occurs at the night time in mice (Scheiermann et al. 2012). All these studies led to a reasoning how circadian rhythms are interlinked with immunity. The studies on the macrophages and lymphocytes in recent years helped us to understand the clock mechanism in relation to immunity. The presence of circadian clock was first reported in spleen, lymph nodes, and macrophages in mice (Keller et al. 2009). It was shown that the clocks in these cells can sustain autonomously in ex vivo. It was also observed that these cells express the inflammatory genes like tumor necrosis factor α (TNF α) and interleukin 6 (IL-6) in a circadian manner in the presence of lipopolysaccharide (LPS) (Keller et al. 2009). Later, Bollinger et al. 2011 has shown the robust clock genes expressions in CD4⁺ T and reported that the temporal programming of interleukin 2 (IL-2), interleukin 4 (IL-4), interferon γ (IFN- γ) and CD40L expression in CD4⁺ T cells are under the control of the clock genes. A direct link between clock genes and immune response was first reported in Gibbs et al. 2012. They have shown that REV-ERB α is a key molecule to link circadian clock and immunity in mice (Fig. 11). Lam et al. 2013 has shown that REV-ERB α can reduce the expression of matrix metalloproteinase 9 (*Mmp9*) and *Cx3cr1* in macrophages. REV-ERB α also regulates the important inflammatory roles in macrophages such as migration, adhesion, and integrin activation through the chemokine ligand 2 (*Ccl2*) (Sato et al. 2014). Further, Narasimamurthy et al. 2012 has proven that Cry in macrophages regulate the expression of TNF α and IL-6 protein secretions. In Cry1^{-/-} Cry2^{-/-} mice, cAMP levels increase which activates protein kinase A (PKA) that in turn induces the phosphorylation of p65 leading to the activation of nuclear factor kappa-light-chain-enhancer of activated B cells (NF- κ B). Eventually, there will be increased expression of IL-6, TNF α and chemokine ligand 1 (CXCL1) (Narasimamurthy et al. 2012). In splenic natural killer (NK) cells, PER1 was shown to play a significant role in regulating their immunological functions where there was altered expression of IFN γ , perforin and granzyme B in *Per1*^{-/-} mice (Logan et al. 2013). Earlier it was shown that the rhythmicity of these factors will be suppressed by inducing the chronic jet lag (Logan et al. 2012). Leukocyte trafficking shows

circadian variation and was shown to be under the regulation of BMAL1 and also similar results were reported with chronic SCN arrhythmia (Scheiermann et al. 2012; Prendergast et al. 2013).

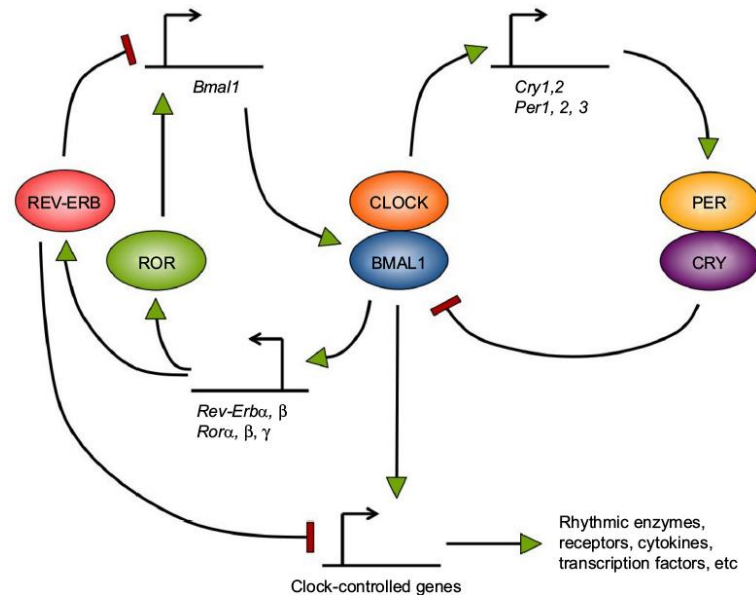


Fig. 11: Most cells in the organism have a circadian clock, whose mechanism relies on a set of clock genes. The CLOCK/BMAL1 transcription factor complex positively regulates *Per* and *Cry* genes. PER and CRY proteins accumulate and then form complexes, enter the nucleus, and inhibit their own expression by repressing CLOCK/BMAL1 activity. In parallel, CLOCK/BMAL1 activates the *Rev-Erb* and *Ror* genes. ROR factors positively regulate *Bmal1* gene expression, whereas REV-ERB factors repress it. Clock transcription factors, such as CLOCK/BMAL1 and REV-ERB α , also regulate rhythmically the transcription of many other genes termed clock-controlled genes, which encode various types of proteins and constitute the output of the circadian clock (Nobis et al. 2016).

Circadian clock machinery is observed not just in innate immune cells but also in adaptive immune cells like T and B cells (Scheiermann et al. 2018). Circadian clock is essential for the development of immune cells, where BMAL1 was shown to be important for the development of B cells (Sun et al. 2006). Number of T and B cells are present more in number in blood during the night in humans and at day in mice that correspond to the activity of the organism (Scheiermann et al. 2018). Also in the lymph nodes the number of lymphocytes are present more in number in the early active phase of organism (Druzd et al. 2017). BMAL1 plays a significant role in the trafficking of the T cells (Druzd et al. 2017). In T cells, lack of CLOCK protein shows blunted rhythms of T cells responses after stimulating T cell receptor (TCR) (Fortier et al. 2011). In macrophages, dendritic cells and B cells toll like receptor 9 (TLR9) shows the rhythmic expression which is in turn under the regulation of *Per2* (Silver et al. 2012). All this increasing evidences suggest that clock and immunity are tightly interlinked. However, with the aging the circadian clock and immunity shows disruption.

Aging

Aging is a unidirectional and irreversible process that is characterized by the progressive deterioration of physiological homeostasis which leads to impaired physiological functions (López-Otín et al. 2013). Aging has been attributed with nine hall-marks such as telomere attrition, genomic instability, epigenetic alterations, deregulated nutrient sensing, loss of proteostasis, stem cell exhaustion, cellular senescence, mitochondrial dysfunction, and altered intercellular communication (Fig. 12). Aging invariably affects all the tissues and the circadian rhythms of several physiological processes like sleep-wake cycles, behavior, metabolism, immunity etc.

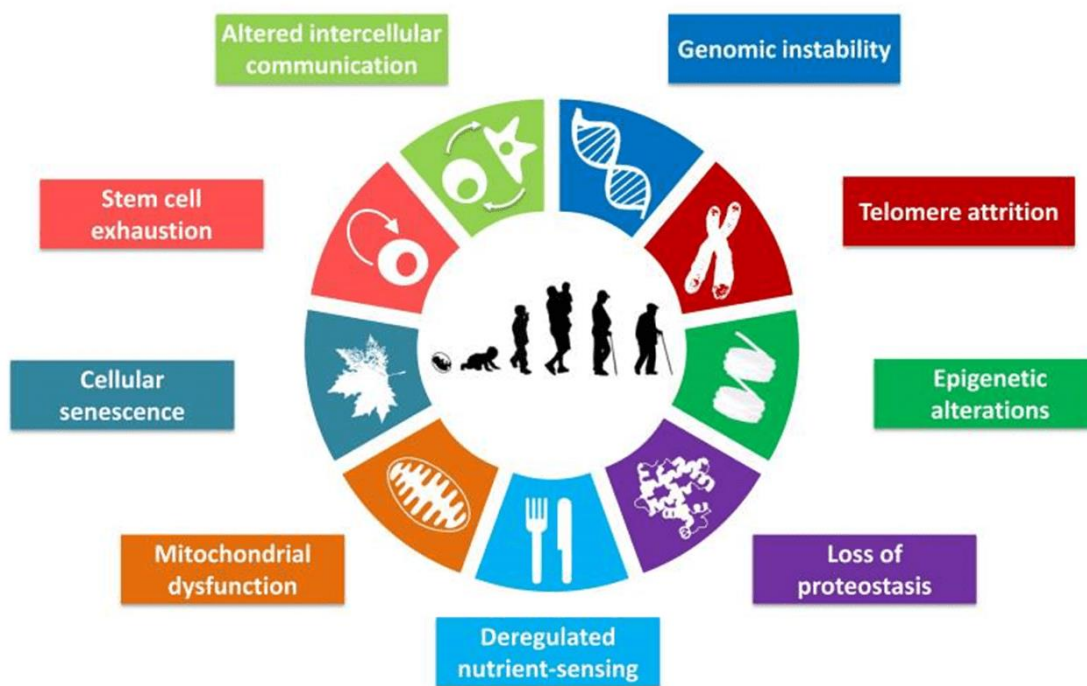


Fig. 12: Hallmarks of aging: The scheme enumerates the nine hallmarks described in this Review: genomic instability, telomere attrition, epigenetic alterations, loss of proteostasis, deregulated nutrient sensing, mitochondrial dysfunction, cellular senescence, stem cell exhaustion, and altered intercellular communication (López-Otín et al. 2013).

Aging and clock dysfunction

Sleep-wake cycle is the foremost overt circadian rhythm that gets affected with the aging. Elderly subjects may suffer from advanced sleep phase syndrome (ASPS) with irregular sleep-wake patterns (Jagota 2005) (Fig. 13) Aging severely dampens the circadian rhythms of locomotor activities, temperature etc. however, transplantation of fetal SCN into the older animals rescued

the circadian rhythms (Li and Satinoff 1998) suggesting the importance of functional central clock in maintenance of homeostasis. Controversial results are shown on the size of the SCN, where in few reports the volume and number of cells in SCN were shown to be reduced (Tsukahara et al. 2005).

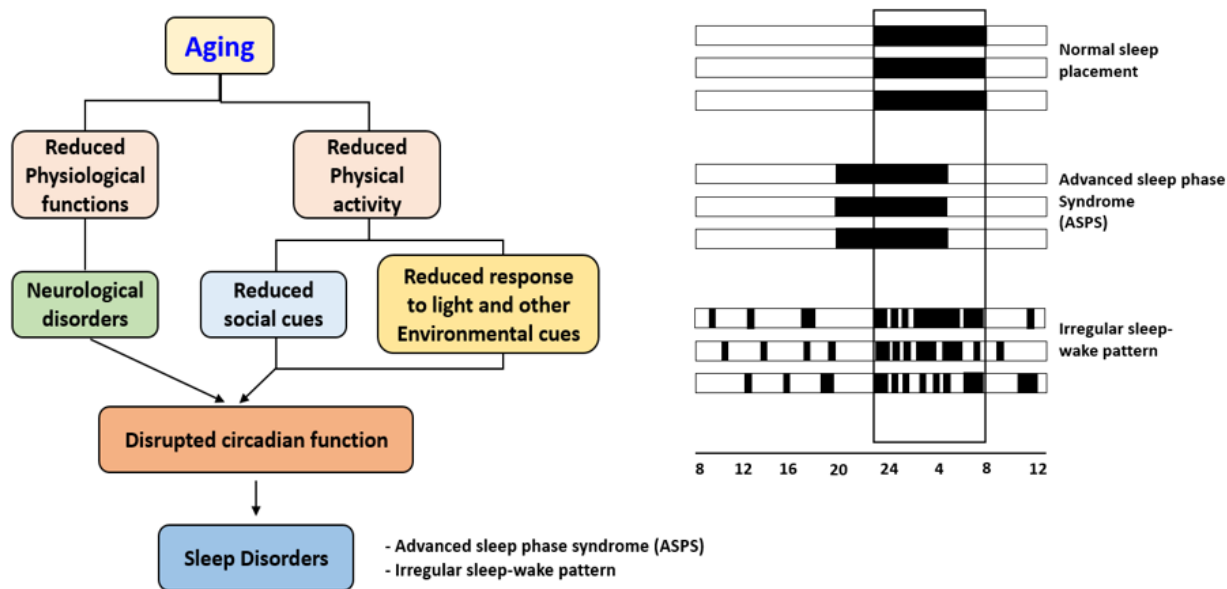


Fig. 13: Schematic diagram showing various sleep disorders associated with disturbances of the circadian system. The open bars represent intervals during which wakefulness typically occurs, black bars correspond to usual sleep times in normal and pathological conditions and vertical rectangle represents desired sleep time. Individuals with advanced sleep phase syndrome (ASPS), sleep earlier than desired time, whereas individuals with irregular sleep-wake pattern such as sleep disorder breathing (SDB); periodic leg movement in sleep (PLMS), and rapid eye movement (REM); behavioral disorder (RBD) etc. may have disturbed sleep at other than desired times also (Jagota 2005).

The expression of AVP and VIP also reduces in older subjects over 80 years in SCN (Wu et al. 2007). Aging dampens the SCN activity, where there is alteration in synchrony in firing patterns of SCN neurons (Nakamura et al. 2011). In older animals, most of the SCN neurons fire out of phase when compared to young animals (Farajnia et al. 2012). Sensitivity toward the zeitgebers also decreases with aging, decreasing the functional output of SCN (Hood and Amir 2017).

Molecular clock also gets affected with aging. From our laboratory, we have reported the altered clock genes *rBmal1*, *rPer1*, *rPer2*, *rCry1* and *rCry2* expression and phase of rhythm in aged (24 month) SCN (Mattam and Jagota 2014). We have also reported the altered serotonin

metabolism (Reddy and Jagota 2015), expressed protein profiles (Jagota and Mattam 2017) in aged SCN. Further, we have reported the altered rhythms of NO (Vinod and Jagota 2016), *Socs1* (Vinod and Jagota 2017), and anti-oxidant enzymes activity (Manikonda and Jagota 2012) in the peripheral clocks. In correspondence to aging and altered circadian clock, several reports suggest that disturbance in circadian clock can accelerate the aging phenotype. *Bmal1* knockdown in mice has shown accelerated aging phenotype and reduced the lifespan (Yang et al. 2016). However, *Per1,2^{-/-}* mice did not show variations in the young age in comparison to wild type, but at 12-14 months they exhibited premature aging with loss of fertility and soft tissue, and kyphosis (Lee 2005). This further strengthens the relation between aging and circadian dysfunction. Aging is also characterized by increased inflammatory status in several cell types and tissues, this phenomenon is called as ‘inflammaging’. The altered inflammatory status in the elderly may play substantial role in developing disease and progression (Park et al. 2014). However, most of the studies in peripheral clocks were confined to the macrophages, but there are no significant studies in microglia, the immune cells in central nervous system and other peripheral clock like liver, kidney and spleen.

Aging and peripheral clocks dysfunction

I. Aging, Microglia and clock dysfunction

Microglia

Microglia are the resident macrophages of the central nervous system (CNS) and they are the persistent immune cells which are highly susceptible to the changes in the microenvironment of the brain (Davalos et al. 2005). They comprise nearly 12% of the total glial population in the brain (Gomez-Nicola and Perry 2015). Microglia were first characterized by Pio del Rio-Hortega and he termed the name ‘microglia’ (Kettenmann et al. 2011). They are derived from haematopoietic lineage during embryo development and migrate into the CNS as monocytic cells, where they get colonized (Eglitis and Mezey 1997; Priller et al. 2001). In mouse, macrophages enter brain parenchyma around E9 and microglia also undergo different phases of differentiation based on the signals from the developing nervous system. Proteins like colony stimulating factor 1 (CSF1), transforming growth factor- β (TGF- β), IL-34 are known to signal the development of microglial cells. Though microglia and macrophages are similar in many characteristic features there are several variations in their core gene expression profiles. The total number of microglia remains almost same throughout the lifespan (Kettenmann et al. 2011).

Depending on the physiological status of an organism, microglia transforms into various forms in CNS. Once the microglia reach the brain parenchyma they transform into ramified form and remain to stay in that form until there is physiological disturbance.

Resting microglia

In the young age, microglia possess a steady state which is a resting phenotype that is morphologically characterized by ramified processes. The steady state microglia performs the continuous surveillance of the surroundings in the brain (Nimmerjahn et al. 2005). The interactions between the neurons and microglia suppress the activation of microglia and helps to maintain the steady state (Fig. 14). Neurons secrete CX3C-chemokine ligand 1 (CX3CL1) which binds to the CX3C-chemokine receptor 1 (CX3CR1), a cell membrane receptor of microglia, and restrains the microglia activity (Saijo and Glass 2011). In addition, cell to cell interactions between neurons and microglia also restricts the activation of microglia. For instance: the neuronal cell surface proteins like CD200, CD47 and CD22 binds to the microglial cell surface proteins CD200R, CD172 and CD45 respectively and maintains the steady state (Ransohoff and Cardona 2010). Steady state microglia helps in normal brain development with their synaptic pruning activity (Paolicelli et al. 2011) (Fig. 15).

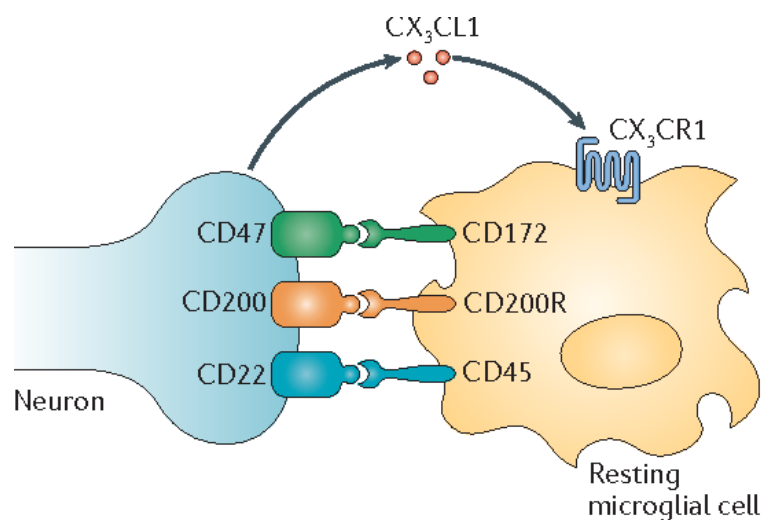


Fig. 14: (a) Under steady-state conditions, microglia exhibit an extensively ramified morphology and a resting phenotype. This phenotype is maintained in part through neuron-derived signals, including CX3C-chemokine ligand 1 (CX3CL1), CD47, CD200 and CD22, which act through corresponding receptors expressed by microglia (Saijo and Glass 2011).

Microglia with its immune related proteins involves in the improvement of synapse formation in the developing brain (Hong et al. 2016). Microglia makes a contact with the synapses and engulfs the synapses that are not showing more neuronal activity in other words the experience

(Tremblay et al. 2010; Schafer et al. 2012). Immune proteins like complement proteins and fractalkine receptors plays a substantial role in the synaptic pruning, where their ablations caused the abnormalities in the synapse formation in pre-natal and postnatal neuronal development (Paolicelli et al. 2011; Squarzoni et al. 2014). Microglia continues to perform synapse pruning even in the adult brain, where the abnormalities in the synapse pruning in the adult brain causes the impairment in the learning and motor functions (Parkhurst et al. 2013).

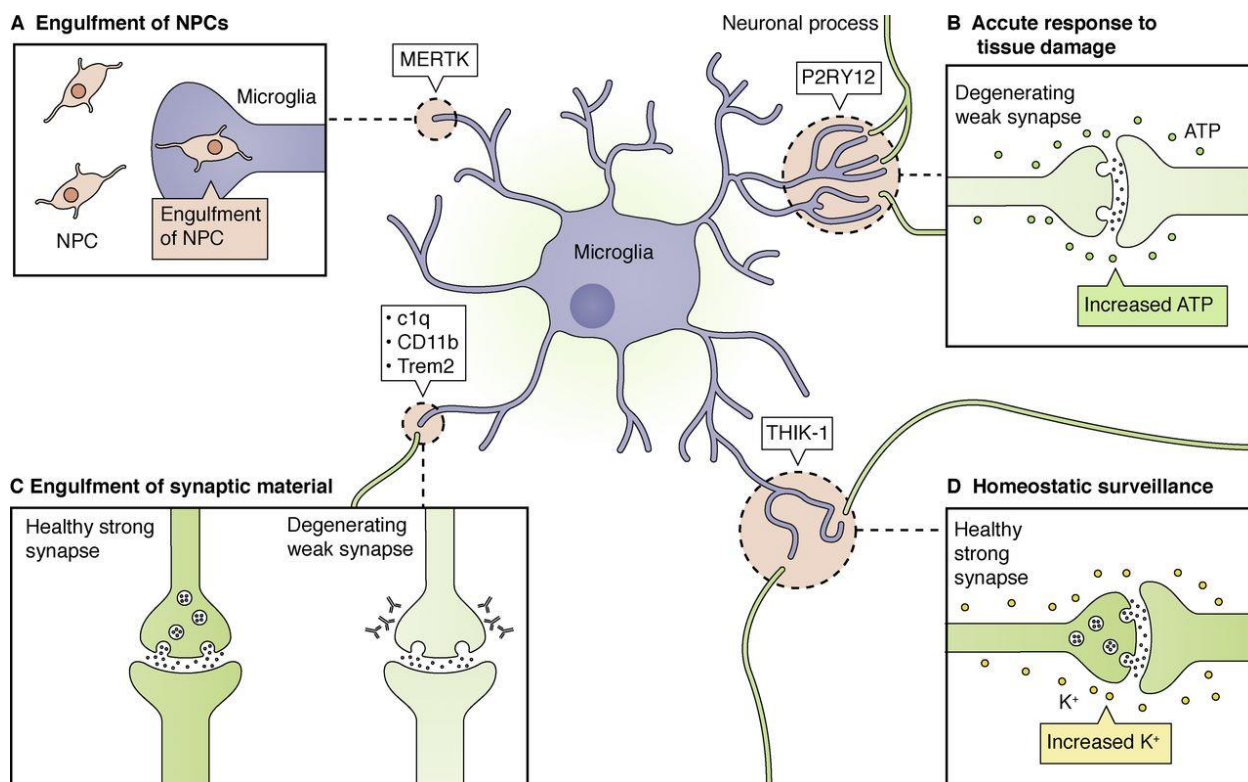


Fig. 15: Homeostatic functions of microglia. (A) At various time points of neurogenesis, microglia display a critical role in regulating the number of neural progenitors through phagocytosis (B) Microglia respond acutely to CNS damage by sensing ATP through P2RY12 signaling (C) Engulfment of synaptic material in development and disease is regulated by complement-mediated recognition (D) Homeostatic surveillance by microglial processes is regulated by the potassium channel THIK-1 (Norris and Kipnis 2018).

Microglia activation

Microglia shows two kinds of activation such as classical activation (M1) and alternate activation (M2) (Fig. 16). Microglia readily gets classically activated (M1) in the presence of immunogen such as lipopolysaccharide (LPS) and also pro-inflammatory molecules in the CNS. M1 microglia secretes pro-inflammatory molecules like tumour necrosis factor- α (TNF- α), interleukin-1 β (IL-1 β), IL-12, nitric oxide (NO), prostaglandins (PGs), reactive oxygen species

(ROS), chemokines, etc. Microglia also recruits the other immune cells like macrophages to the inflammatory site to further augment the immune responses (Carniglia et al. 2017).

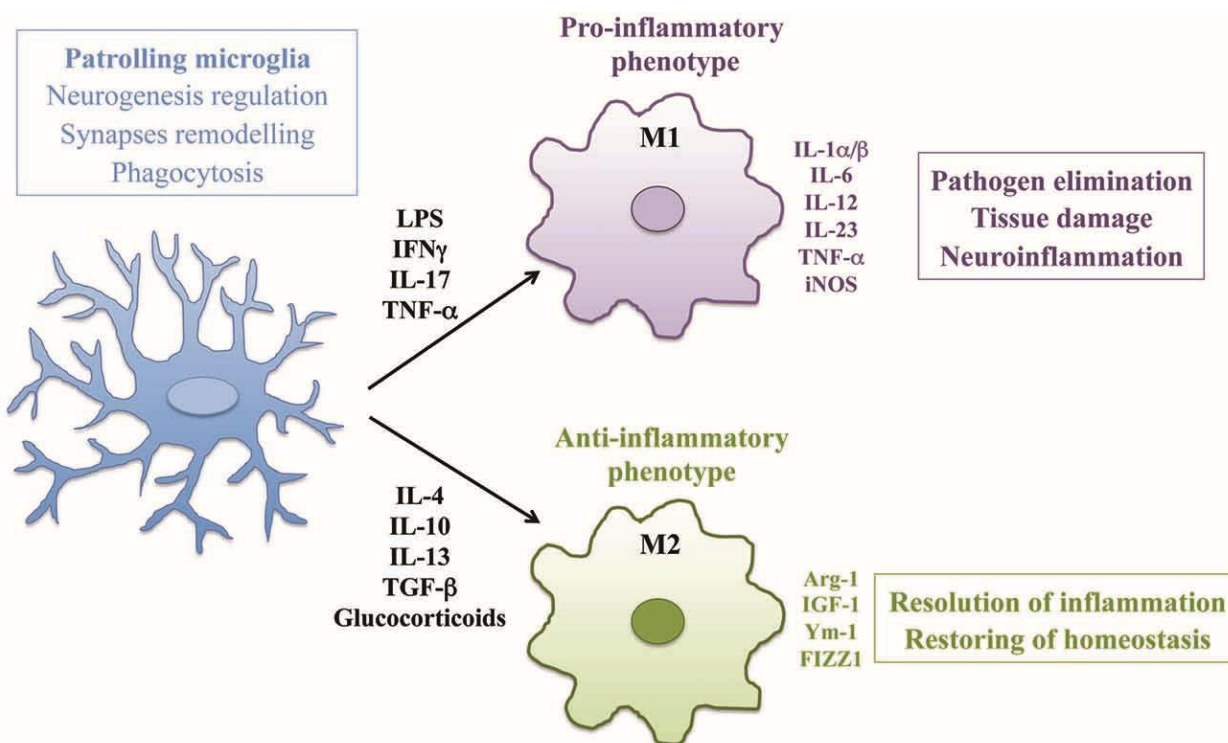


Fig. 16: Activation and polarization of microglia in resting conditions and during neuroinflammation. The morphology and the phenotype associated with different functional states of microglia are represented. In physiological conditions patrolling microglia regulate central nervous system (CNS) homeostasis. In neuroinflammation microglia assume ameboid morphology and acquire classical M1 or alternative M2 phenotype according to the nature of local milieu (Salvi et al. 2017).

It is further essential that increased inflammatory status of microglia should be dampened once the inflammatory stimuli is resolved. In the presence of the anti-inflammatory molecules microglia will acquire the alternate activation (M2). During this state, microglia release the anti-inflammatory molecules like transforming growth factor- β (TGF- β), IL-10, etc. These molecules signal the other inflammatory and non-inflammatory cells to block the release of pro-inflammatory molecules and to induce tissue repairing. If the activation of microglia is not resolved it may cause a severe damage to the healthy cells in the vicinity and may lead to the neurodegeneration as seen in several neuropathologies like PD and AD (Fig. 17).

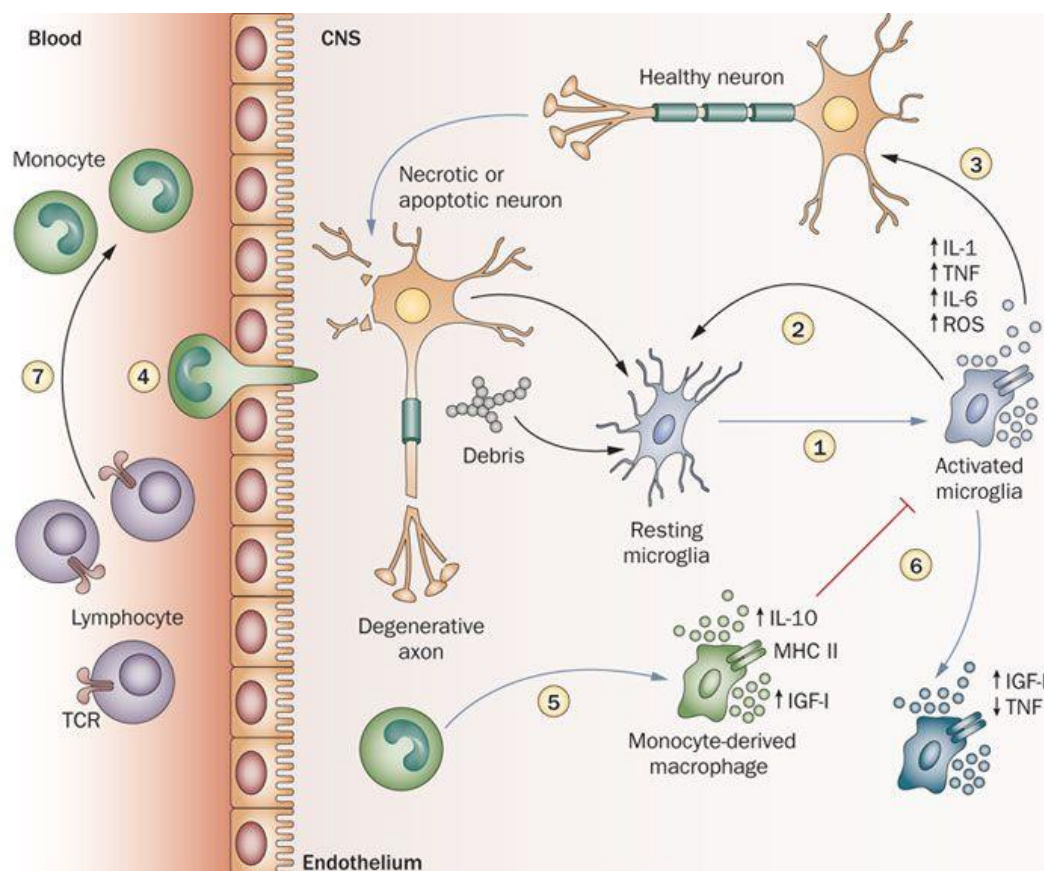


Fig. 17: Dying cells and/or the accumulation of debris or aggregated proteins activate resting microglia in the CNS (1). Activated microglia phagocytose debris and aggregated proteins while concurrently secreting toxic compounds, including pro-inflammatory cytokines (such as IL-1, TNF and IL-6) and ROS. If the microglial response is uncontrolled or prolonged, these toxic agents contribute to the development of a self-sustaining neurotoxic cycle that involves further activation of naive microglia (2) and loss of surrounding neurons (3). At this stage (equilibrium stage), assistance from the systemic immune system becomes essential to control local inflammation. Blood-derived monocytes infiltrate the damaged parenchyma (4) and differentiate locally into macrophages (5). These cells efficiently engulf debris, secrete growth factors and anti-inflammatory cytokines, and suppress microglial activation (6). Under neurodegenerative conditions, resident microglia are unable to provide these essential functions. T-helper lymphocytes (mainly CD4⁺ T cells) augment the recruitment of blood monocytes to the CNS (7) and, hence, indirectly regulate the phenotype of microglia (6) (Schwartz and Shechter 2010).

Clock in microglia

Like all the other immune cells microglia also possess the circadian clock that shows robust oscillations in the expression of clock genes (Fonken et al. 2015). It is the molecular clock within the microglia that regulates the sleep-wake cycle dependent oscillations of synaptic strength of neurons (Hayashi et al. 2013). Circadian clock regulates the rhythmic expression of lysosomal cysteine protease Cathepsin S (CatS), which in turn modify the perineuronal environment and

regulates the diurnal oscillations of the synaptic strength. Aberrations in the CatS was shown to increase the locomotor functions and failed to decrease the synaptic strength in the sleep phase (Hayashi et al. 2013). It is essential to reduce the synaptic strength during the sleep as to acquire and consolidate new information with wakening. The loss of circadian regulation of CatS may lead to the neuropsychiatric disorders like depression and impairment in cognition (Chi-Castañeda and Ortega 2018). Clock also regulates the circadian expression of ATP receptors of P2Y subtype (P2YR, a G protein-coupled receptor), P2Y₁₂R (Hayashi et al. 2013) in microglia. ATP from the glial cells plays significant role in synaptic transmission throughout the neuronal activity. Extension of microglial processes are regulated by P2Y₁₂R, which in turn depends on the ATP. Disruption in P2Y₁₂R resulted in aberrant synaptic strength, whereas with the upregulation of P2Y₁₂R, the microglial processes extended in the dark phase which are retracted partially in the light phase that lead to decreased synaptic strength (Hayashi et al. 2013b). It was shown that ATP can induce the expression of core clock gene *Per1* via P2X7R in microglia (Nakazato et al. 2011). Overexpression of *Per1* enhanced the memory formation (Sakai et al. 2004), suggesting that *Per1* has role in synaptic plasticity. ATP also enhances the expression of signaling molecules like TNF- α , plasminogen, IL-1 β (Chi-Castañeda and Ortega 2018) that are important in the synaptic plasticity (Ikegaya et al. 2003; Becker et al. 2013; Liu et al. 2014). Some of these immune molecules were shown to express rhythmically in microglial cells (Fonken et al. 2015).

Effect of aging on microglia

The number of Iba1⁺ microglia in the aged rat hippocampus doesn't vary in comparison to young brain (VanGuilder et al. 2011), however, microglia number was significantly decreased in aged nigrostriatal system and cortex (Sharaf et al. 2013). Cultured microglial cells from aged mice expressed elevated basal levels of pro-inflammatory molecules like TNF α , IL6 and IL1 β (Sierra et al. 2007). Similar results were observed previously from the whole brain extract (Godbout et al. 2005) and in microglia from old brains (Ye et al. 1999). With LPS administration, microglia showed increased expression of pro-inflammatory molecules (Sierra et al. 2007). It was a general observation that microglia upon aging shows increased activation, and with the inflammatory stimuli, microglia shows enhanced response in aged animals (Lee et al. 2013). This phenomenon is considered as priming of microglia (Fig. 18). In the older subjects microglia possess de-ramified morphology which is very similar to the activated microglia. The de-ramified microglia shows increased expression of MHC-II than the normal microglia (Norden and Godbout 2013).

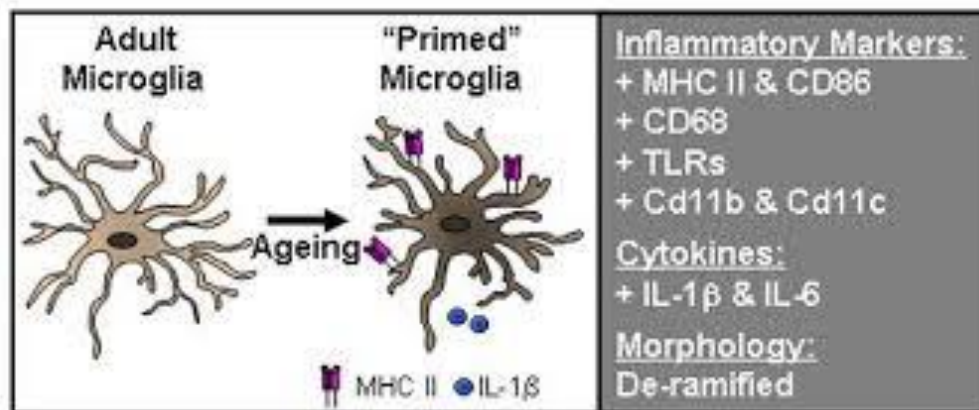


Fig. 18: Evidence of microglial priming in the aged brain: In normal aging there is increased mRNA and protein expression of several inflammatory markers on microglia. In older rodents and non-human primates these include proteins associated with antigen presentation, (MHC II and CD86), scavenger receptors (CD68), pattern associated recognition receptors (Toll-like receptors), and integrins (CD11b and CD11c). There are also detectable increases in inflammatory cytokines and decreases in anti-inflammatory cytokines in the aged brain. In several aging models the morphology of the microglia is more de-ramified. Collectively these findings are interpreted to indicate that microglia of the aged brain maintain a primed or activated immune profile (Norden and Godbout 2013).

Microglia has been reported to involve in age associated pathologies like PD and AD. In young brain microglia has several beneficial roles, however, with aging the primed microglia are hypothesized to be detrimental in their functions (Fig. 19). In PD patients, increased inflammation is observed with microglia activation and increased expression of pro-inflammatory molecules (Hirsch and Hunot 2009). Reactive molecules from the dying neurons activate the microglia through pattern recognition receptors (PRRs) and purinergic receptors that may progress PD (Saijo and Glass 2011). In correspondence to this, administering LPS into substantia nigra can induce damage to the dopaminergic neurons, also media conditioned with TLR4-activated microglia can induce damage to the dopaminergic neurons (Dutta et al. 2008). Microglia are seen surrounding senile plaques in AD brains (Dickson et al. 1992). Lack of amyloid clearing function of microglia was also reported in AD (Flanary 2005). Altered functional status of microglia was shown to be cytotoxic in AD (Sawada et al. 2007). It was proposed that it is the dysfunctional microglia but not the activated microglia that leads to the pathologies in AD (Bernhardi 2007).

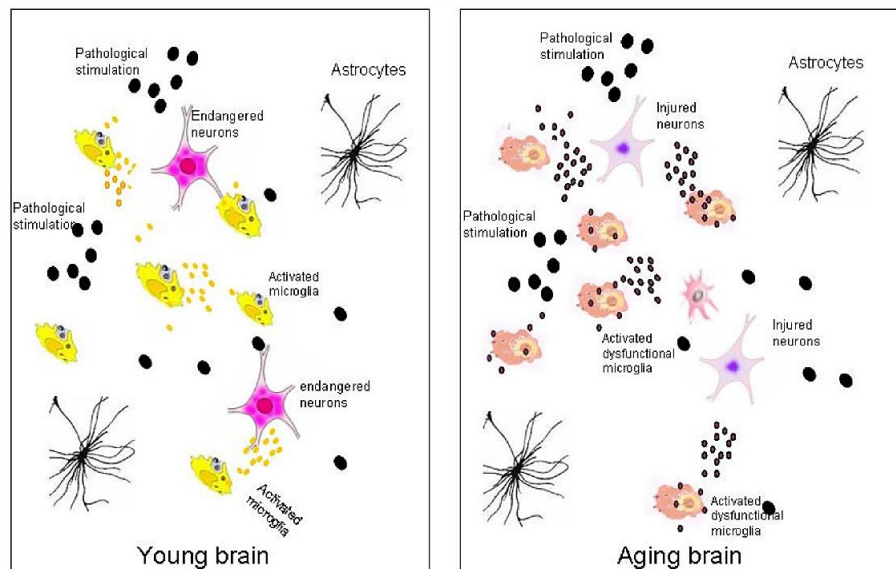


Fig. 19: Age-primed microglia hypothesis of Parkinson's disease. Microglia functions differentially in the substantia nigra of the young (left) and aged (right) brain. Left: When facing pathogenic stimuli (large black dots), the healthy microglia in the young brain respond by releasing neurotrophic factors (small yellow dots) to support the endangered dopaminergic neurons and limit neuronal damages. Right: In the aged brain the microglia are primed with aging and function abnormally. When exposed to pathogenic stimuli, they are overactivated and release excessive oxidative stress and inflammatory factors (small black dots), which damage the vulnerable dopaminergic neurons and eventually lead to neurodegeneration (Luo et al. 2010).

II. Aging, Liver and clock dysfunction

Clock in liver

Liver is the prime site of metabolism for carbohydrates, lipids, amino acids, bile acid, and also it helps in detoxification process. Liver has an active circadian clock machinery and it has the maximum number of genes exhibiting the circadian rhythms in their expression (Zhang et al. 2014). Transcriptome analysis of liver has revealed two peaks of gene transcripts that were rhythmically expressed at the beginning of light and dark phases. They perhaps represent different physiological activities like detoxification activity and energy demand during the rest and activity phase. Interestingly, proteins of several of these genes showed similar pattern of expression (Reinke and Asher 2016). Most of the crucial physiologies in liver are regulated by circadian clock (Fig. 20). From our laboratory we have shown that nitric oxide (NO) exhibit daily oscillations in liver (Vinod and Jagota 2016). Lipid peroxidation shows daily rhythms with maximum at beginning of night phase where the activity of anti-oxidant enzymes was observed to be minimum (Manikonda and Jagota 2012).

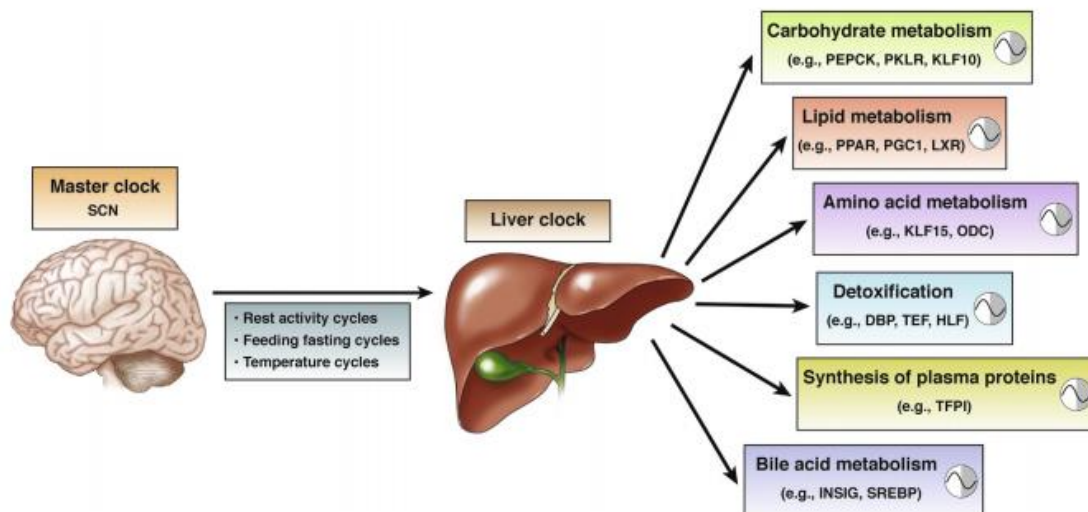


Fig. 20: Circadian regulation of liver physiology. The hypothalamic master clock synchronizes peripheral oscillators, such as the liver clock, via rhythmic activity, feeding, and temperature cues. The liver clock drives the cyclic expression of master regulators and rate-limiting enzymes of key hepatic metabolic outputs (Reinke and Asher 2016).

The vital enzymes involved in the hexose sugar metabolism like glucose transporters, glucagon receptor peaks at the early evening (Reinke and Asher 2016). Enzymes involved in lipid metabolism like glycerol-3-phosphate acyltransferase [GPAT], 1-acyl-glycerol-3-phosphate acyltransferase [AGPAT], etc. exhibit circadian oscillations (Adamovich et al 2014). Similarly, proteins involved in the cholesterol metabolism like 3-hydroxy-3-methylglutaryl-coenzyme A (HMG-CoA) reductase express maximum at the day time. The rhythmic expression of active T3 from inactive T4 depends on the rhythmic expression of deiodinase 1 in liver. The thyroid hormone receptor also express rhythmically that matches with the oscillating levels of T3 and T4 in serum. Circadian clock also regulates the rhythmic expression of immune genes in liver (Panda et al 2002; Storch et al 2002; Akhtar et al 2002; Zhang et al 2014).

Clock aberrant mice are hyperphagic, hyperglycemic and obese (Turek et al. 2005). Insulin was reported to regulate the expression of *Clock* gene through forkhead box O3 (FOXO3) in liver (Chaves et al. 2014). N6-methyladenosine (m⁶A) mRNA methylation is essential for the lipid metabolism. However, BMAL1 regulates the methylation of m⁶A RNA in liver (Zhong et al. 2018). *Per2* shows oscillations as internal time keeping mechanism of liver and also responds to the external cues as interlink for synchrony (Reddy and Maywood 2007). Rev-erba provides a link between the clock and metabolism. Heme which is cofactor was known to be the ligand of REV-ERBa (Raghuram et al. 2007). Heme binds to REV-ERBa and negatively regulates the

expression of gluconeogenic gene (Yin et al. 2007). Absence of REV-ERB α increased the levels of glucose and triglycerides (Cho et al. 2012). However, administration of REV-ERB α ligands showed weight loss, decreased lipogenic expression and enhanced the glucose and lipid metabolism in obese animals (Solt et al. 2012). The accumulating data suggest that circadian clock and the metabolism are tightly interlinked where circadian disruption that can be seen in shift workers can result in metabolic syndromes (Ferrell and Chiang 2015) (Fig. 21).

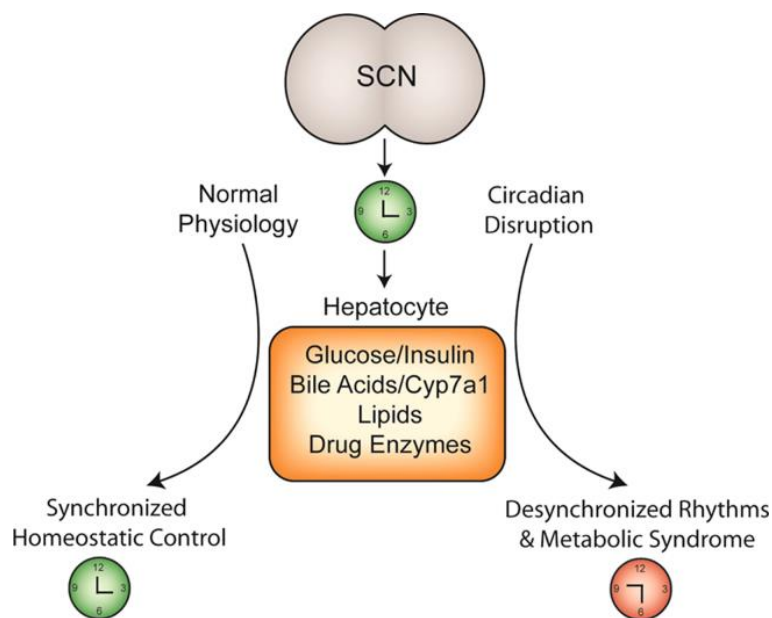


Fig. 21: The suprachiasmatic nucleus (SCN) generates endogenous biological rhythms, ensuring that internal physiology is synchronized with the external environment. Under normal conditions, rhythms in glucose and insulin, bile acids, lipids and drug enzymes contribute to homeostatic control of liver physiology. Under conditions of circadian disruption, including shift work, perturbations in these physiological rhythms result in desynchronized timing between SCN and the periphery and are associated with diabetes, obesity, and other symptoms of metabolic syndrome (Ferrell and Chiang 2015).

With aging, the amount of the blood in liver decreases by 20-40% (Zeeh and Platt 2002). There is reduction in the liver cell mass (Wakabayashi et al. 2002). The fenestrations of sinusoidal endothelial cells become thickened, reducing the molecular exchange from and to the liver (McLean et al. 2003). There is decrease in the levels of bilirubin and albumin, while there is an increase in alkaline phosphatase. Also, the activities like cholesterol metabolism reduces with aging resulting in increase in blood cholesterol and fat (Tietz et al. 1992). Mitochondrial functions decline in liver with aging which may be a reason for the delayed liver regeneration (Poulose and Raju 2014). There is decline in the oxidative capacity in liver (Campanelli 2012). At molecular level, there is accumulation of multiprotein C/EBP α -Brm-HDAC1 complex which blocks the promoter sites for elongation factor 2 (E2F), which could be the reason for

decreased regenerative capacity of liver cells (Wang et al. 2008). There is accumulation of senescent hepatocytes, immune cells etc. in aged liver (Aravinthan and Alexander 2016) (Fig. 22). Also there is increased recruitment of inflammatory cells in the liver with aging (Maeso-Díaz et al. 2018). With aging the circadian rhythms in liver are known to dampen (Hood and Amir 2017). NO rhythms were altered with progression in age (Vinod and Jagota 2016). Circadian rhythms of circulating lipid components were dampened and showed phase alterations in the elderly subjects (Singh et al. 2016). Lipid peroxidation rhythm was reported to alter with aging (Manikonda and Jagota 2012). 24-h glucose rhythms showed significant variations with the aging (Wijsman et al. 2013). Plasma cortisol showed variations in phase and amplitude in the old age (Cauter et al. 1996). These variations could be the result of altered or dampened circadian expression of clock genes in the peripheral clocks (Yamazaki et al. 2002). These altered rhythms could be causative for metabolic disorders like diabetes, hypertension, and dyslipidemia etc. (Hood and Amir 2017).

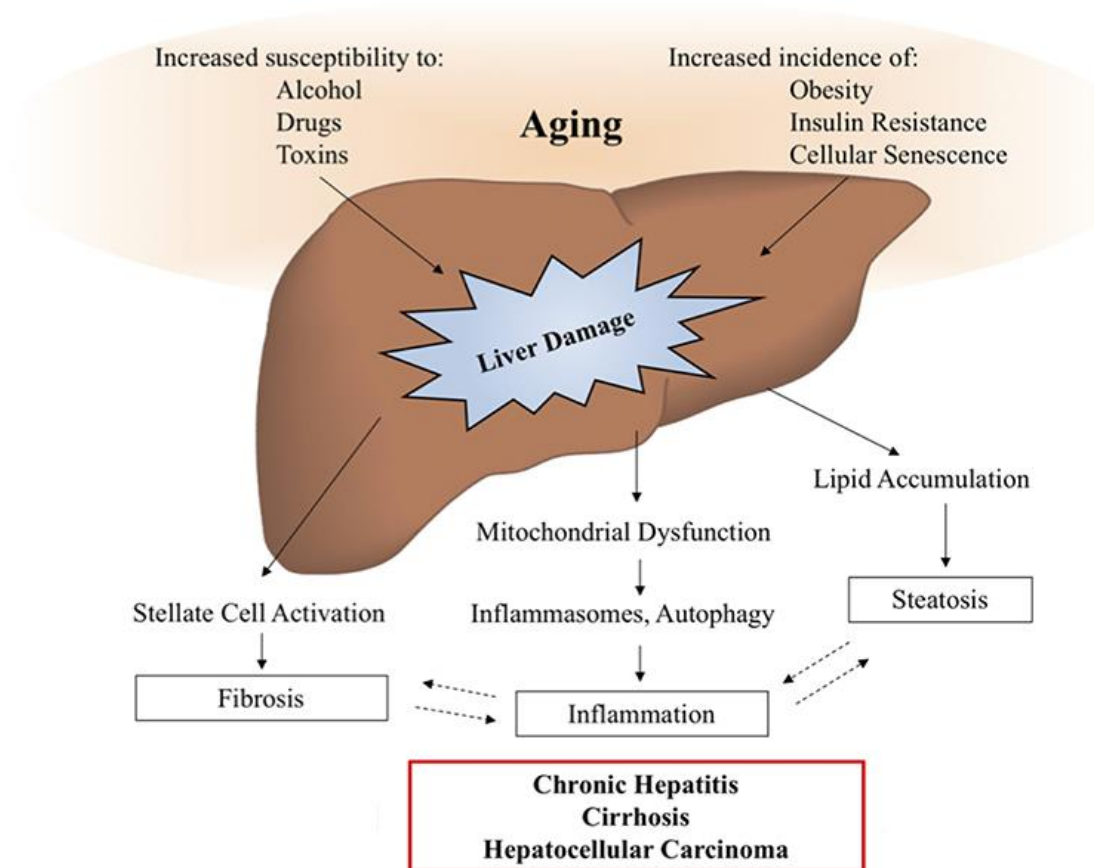


Fig. 22: Aging and liver disease. With increasing age, the liver becomes more susceptible to damage, while the prevalence of metabolic disease, obesity, and cellular senescence are known to increase. These insults lead to the activation of signaling pathways driving liver pathology, such as inflammation, steatosis, and fibrosis, which are often involved in positive feedback loops, further exacerbating the symptoms of liver disease. (modified from Stahl et al. 2018).

III. Aging, Kidney and clock dysfunction

Clock in kidney

Kidney plays vital role in maintaining blood pressure by perpetually filtering blood, removing waste materials, maintaining electrolytes and fluid homeostasis in circadian manner (Hara et al. 2017) (Fig. 23). Circadian oscillations in kidney can be seen in Glomerular Filtration Rate (GFR), electrolyte excretion, urine production, and renal blood flow (Stow and Gumz 2011). Recent investigations clearly suggest that BMAL1 plays critical role in circadian regulation of blood pressure in mice (Douma et al. 2018). Cry1/Cry2 double knockout mice also exhibit loss of circadian rhythms in blood pressure (Doi et al. 2010). NHE3 (sodium hydrogen antiporter 3), an important protein involved in maintenance of sodium balance and blood pH, is known to be a CCG with E-box elements in its promoter (Saifur et al. 2005). Likewise, PER1 regulates expression of α ENaC (alpha subunit of epithelial Na⁺ channel), an essential protein for regulation of salt and water reabsorption (Gumz et al. 2009).

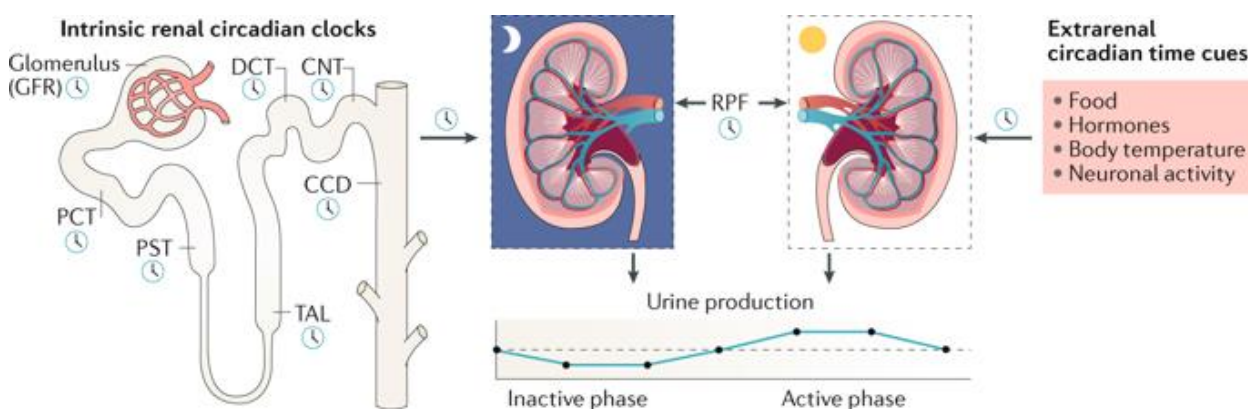


Fig. 23: Intrinsic circadian clocks in the kidneys. Renal plasma flow (RPF), glomerular filtration rate (GFR), podocytes and tubular cells are regulated by renal intrinsic clocks, resulting in a circadian rhythm in urine output. Extrarenal circadian time cues (including those provided by nutrients, hormones, body temperature and the activity of the nervous system) synchronize the rhythms of the intrinsic renal clocks. CCD, cortical collecting duct; CNT, connecting tubule; DCT, distal convoluted tubule; PCT, proximal convoluted tubule; PST, proximal straight tubule; TAL, thick ascending limb (Firsov and Bonny 2018).

Similarly, various sodium transporters, water channels, vasopressin receptors that are critical for kidney physiology are under the circadian regulation (Stow and Gumz 2011). Zuber et al. 2009, profiled the circadian expression of genes in different regions of kidney using microarray analysis. Ribosome profiling has revealed that at least 41% of transcripts which are expressed circadian manner and 55% of translated proteins show circadian variations (Castelo-Szekely et al. 2017). These genes involve in maintaining the homeostasis of kidney (Firsov and Bonny

2018). Disruption in the circadian clock genes alters the physiology of the kidney that can be reflected in the circadian rhythms of cardiac output, and BP (Duguay and Cermakian 2009). The altered circadian rhythms of renal physiologies are known to cause chronic kidney disease, kidney stones, and renal fibrosis, hypertension (Firsov and Bonny 2018).

Aging as a global process, invariably affects physiology of kidney, leading to several comorbidities (Braun et al. 2016) (Fig. 24). With aging non-sclerosed glomeruli decrease in number, there is loss of tubules, increase in tubular diverticuli frequency, vascular changes (Denic et al. 2016). Anatomical changes include nephrosclerosis, nephron hypertrophy, and the functional nephrons decrease in number. Circadian pattern of blood pressure was also known to alter with age that may lead to adverse conditions (Hart and Charkoudian et al. 2014).

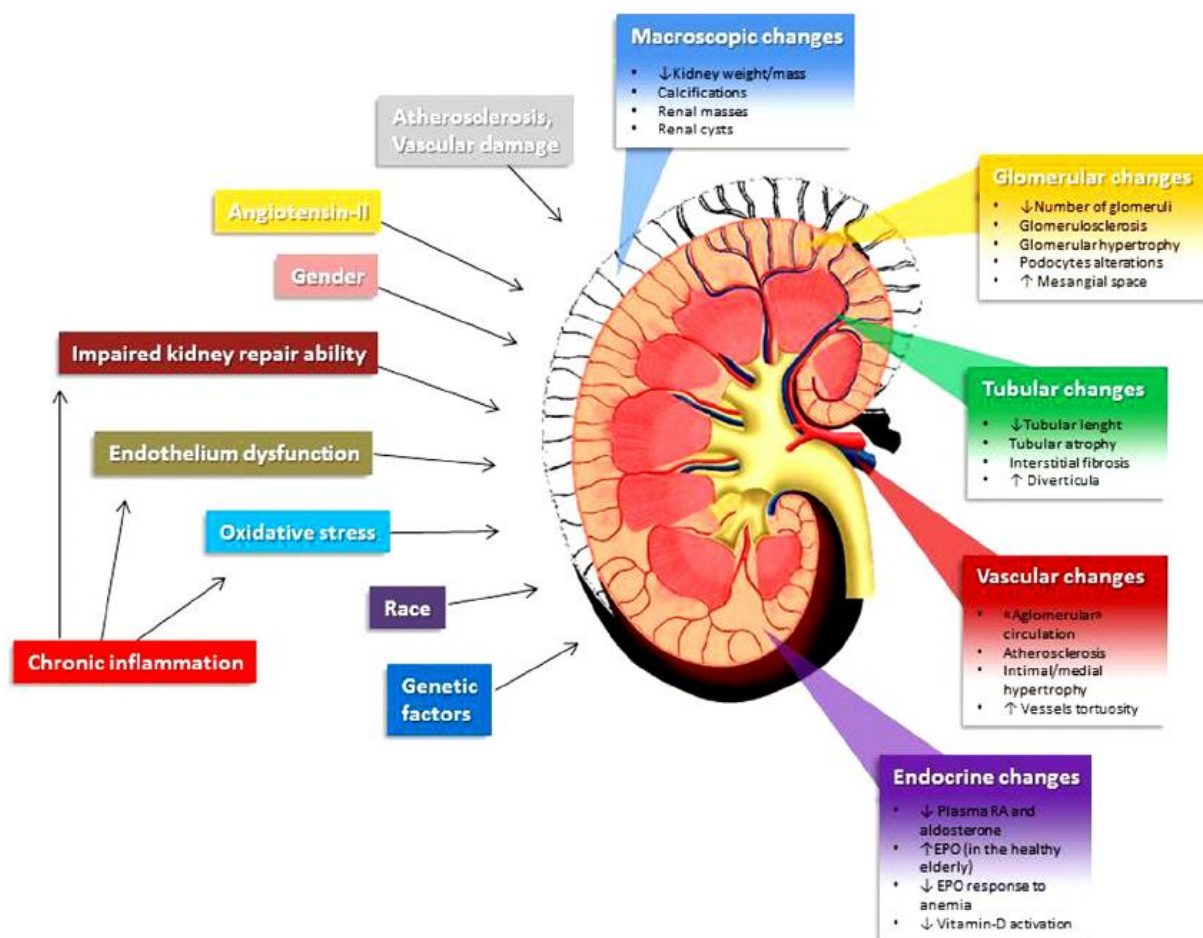


Fig. 24: Macroscopic and microscopic changes in the aging kidney and risk factors (Bologna et al. 2014).

In addition, aging was associated with chronic inflammation, where increased lymphocytes, macrophages and inflammatory proteins like IL1, IL2, TNF α are observed in kidney (Bologna

et al. 2014; Xi et al. 2014). Increased inflammatory proteins cause cellular senescence. These cells further release higher amounts of inflammatory proteins resulting in fibrosis and parenchymal involution (Bolognani et al. 2014). Age associated increased activity of NF- κ B had been attributed to chronic kidney diseases (CKD) (Chen et al. 2016).

IV. Aging, Spleen and clock dysfunction

Clock in spleen

Spleen primarily acts as blood filter and also plays important role as a part of immune system. It is secondary lymphoid organ which initiates the immune responses against bloodborne antigens (Cesta 2006). Spleen can be differentiated into two compartments i.e. white pulp and red pulp. Red pulp is the site for the removal of old erythrocytes, platelets and apoptotic cells (Mebius and Kraal 2005). White pulp is the site for resident macrophages, B cells and dendritic cells (Mebius and Kraal 2005). Red and white pulp are demarcated by marginal zone composed of fibroblastic reticular cells (Martin and Kearney 2002). Spleen is the site for mononuclear phagocyte system, it provides the repository for the monocytes and they will be transferred to the site of injury in various tissues (Swirski et al. 2009).

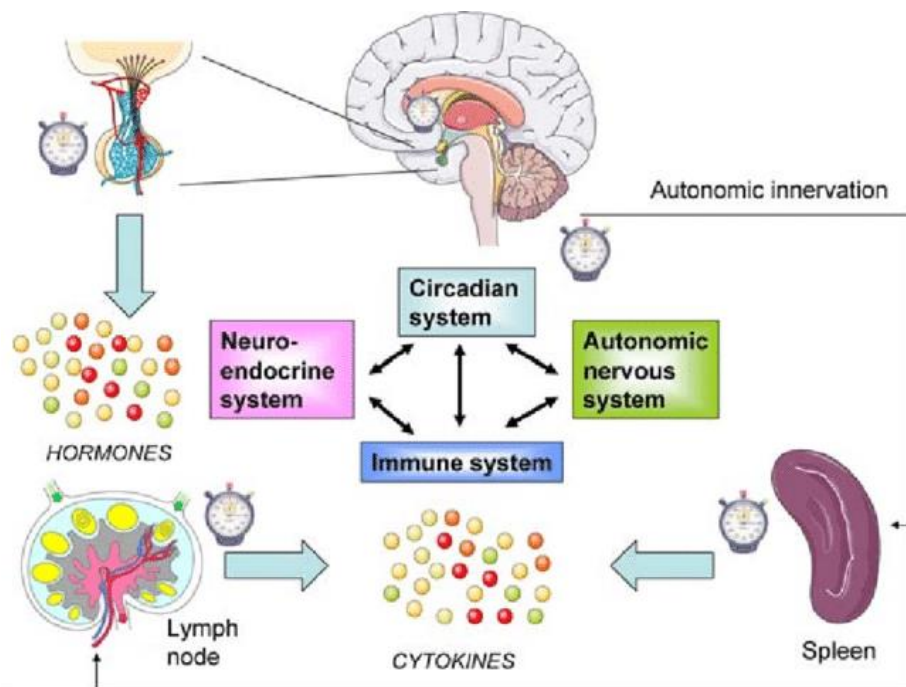


Fig. 25: Temporal interactions among the neuroendocrine system, the autonomic nervous system and the immune system as adaptive mechanisms to the environmental changes (Esquifino et al. 2007).

Spleen shows circadian expression of inflammatory molecules which can be regulated by the central clock SCN (Fig. 25). Spleen exhibits 24 hour rhythms in immune response (Esquifino et al. 1992). Natural killer cells isolated from the spleen showed robust circadian TTFLs (Arjona and Sarkar 2005). Also inflammatory molecules IFN- γ , TNF- α showed rhythmic expression. Similarly, macrophages isolated from spleen exhibit circadian expression core clock genes and several inflammatory genes (Keller et al. 2009; Silver et al. 2012).

With aging, marginal zone that surrounds the B cell follicle in white pulp of spleen shows altered distribution of macrophages and they don't form the boundary along marginal zone (Aw et al. 2016; Turner and Mabbott 2017a). The functionality of the macrophages of marginal zone also severely compromised to acquire dextran particles (Birjandi et al. 2011). Further, the localization and the movement of B cells between B cell follicle and marginal zone is also reduced in spleen (Turner and Mabbott 2017a). This impairment may not be the result of functional variation in B cells but loss of function of splenic stromal cells (Turner and Mabbott 2017b). Also, T and B cell compartmentalisation is compromised with reduced boundaries (Aw et al. 2016). In humans, spleen showed increased atrophy with the aging (Turner and Mabbott 2017b). Immunologically, aged spleen showed increased expression of IL-6 than the young age spleen in mice (Park et al. 2014). Further, the production of IL-6 in the presence of LPS was observed to be higher in aged spleen (Park et al. 2014). There are no evidences as to what happens to the circadian clock in the aged spleen.

Inflammaging and NF- κ B pathway in clock dysfunction

NF- κ B (nuclear factor kappa-light-chain-enhancer of activated B cells), a protein complex with its transcription factor activity regulates the expression of several cytokines and helps in cell survival (Fig. 26). It is essentially involved in immune responses in several immune and non-immune cells. NF- κ B also plays substantial role in synapse formation and memory consolidation (Kaltschmidt and Kaltschmidt 2016). NF- κ B belongs to class of "rapid-acting" transcription factors, where they are present in an inactive form and becomes activated in the presence of stimuli. Factors like LPS, reactive oxygen species (ROS), TNF- α , interleukins etc. can activate NF- κ B through receptors such as toll like receptor 4 (TLR4), TNFR etc. Further, it was well established that NF- κ B mediated transcription of cytokines like TNF- α , IL-6, IL- β are involved in the chronic inflammation and inflammaging (Watroba and Szukiewicz 2016).

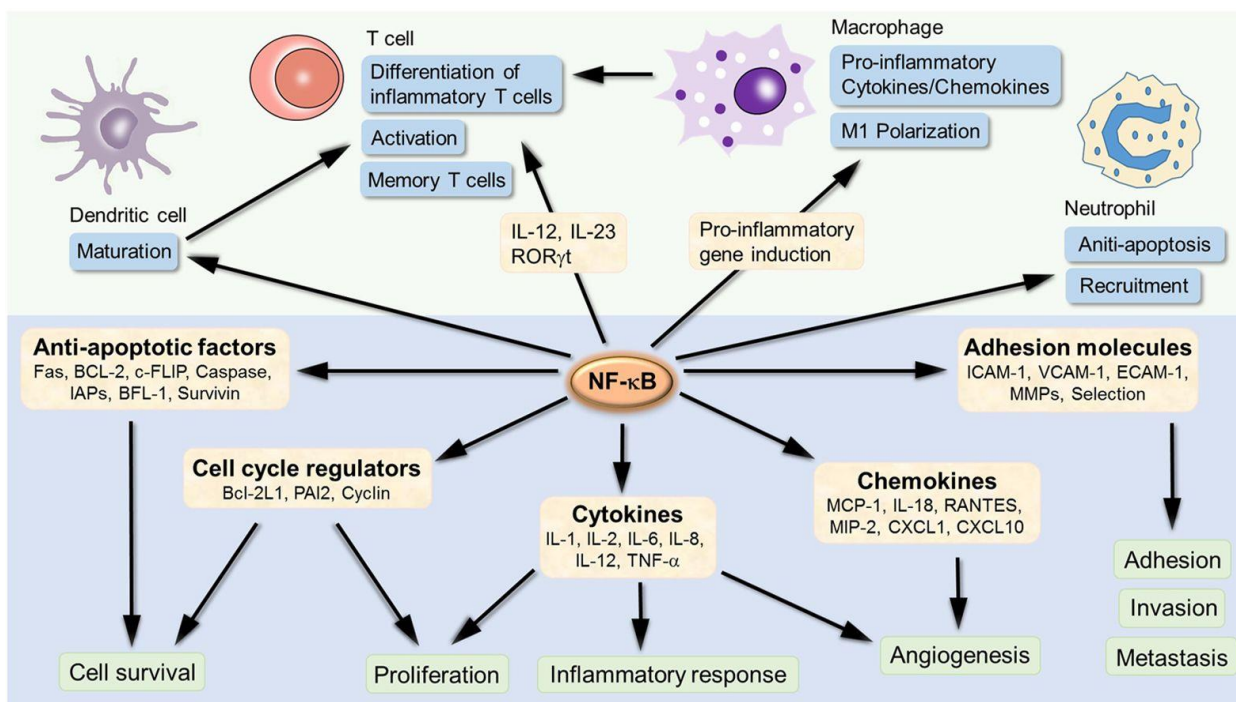


Fig. 26: NF- κ B target genes involved in inflammation development and progression. NF- κ B is an inducible transcription factor. After its activation, it can activate transcription of various genes and thereby regulate inflammation. NF- κ B target inflammation not only directly by increasing the production of inflammatory cytokines, chemokines and adhesion molecules, but also regulating the cell proliferation, apoptosis, morphogenesis and differentiation (Liu et al. 2017).

With aging, soluble tumor necrosis factor receptors (STNF-RI and STNF-RII), TNF α , IL-6, high-sensitive C reactive protein (hsCRP), and IL-18 were significantly increased in humans (Morrisette-Thomas et al 2014). Cytokines like IL-6 play significant role in aging and considered as marker for inflammaging (Franceschi et al 2017). A mutation in IL6 was known to cause longevity in human (Bonafè et al 2001).

Aging and Serotonin mediated inflammation in clock dysfunction

As it was mentioned earlier, serotonin (5-hydroxytryptamine (5-HT)) plays an important role as neurotransmitter in regulating circadian rhythms like sleep-wake cycles, mood, appetite etc. Apart from this, serotonin in peripheral organs have immune-modulatory functions (Fig. 27). Immune cells have serotonin receptors of various classes (5-HT₁, 5-HT₂, 5-HT₃, 5-HT₄, and 5-HT₇), serotonin transporter (SERT), and enzymes required for serotonin synthesis and degradation (Herr et al. 2017). Through these receptors serotonin modulates the immune responses. Serotonin was shown to modulate the secretion of several cytokines such as TNF- α ,

IL-1 β , IL-8/CXCL8, IL-6, and IL-12p40 (Durk et al. 2005). It was shown that serotonin is needed at lower concentration for the basal expression of IL-6 and TNF- α (Kubera et al. 2005). Serotonin also helps in recruiting neutrophil cells and phagocytosis of bacteria. It also induce the T cell stimulation, and superoxide release (Herr et al. 2017). With aging, we have previously reported that serotonin levels decrease and phase of the rhythm alters in SCN (Jagota and Kalyani 2010). We have also reported the altered serotonin metabolism in aged rat SCN (Reddy and Jagota 2015). Interestingly, in rotenone induced Parkinson's disease (RIPD) rat model, serotonin metabolism altered and the serotonin levels were significantly decreased (Mattam and Jagota 2015). Serotonin also decreases in the platelets with aging (Taborskaya et al. 2016). Altered serotonin metabolism is a risk factor for several age-associated disorders like diabetes, cardiovascular diseases, Alzheimer's disease (AD), Parkinson's disease (PD) etc. (Rehman and Masson 2001; Mattson et al. 2004; Benninghoff et al. 2012). Inflammation can modulate the serotonin metabolism (Capuron et al. 2003), therefore, increased inflammatory status or inflammaging may contribute to the altered serotonin metabolism and vice versa.

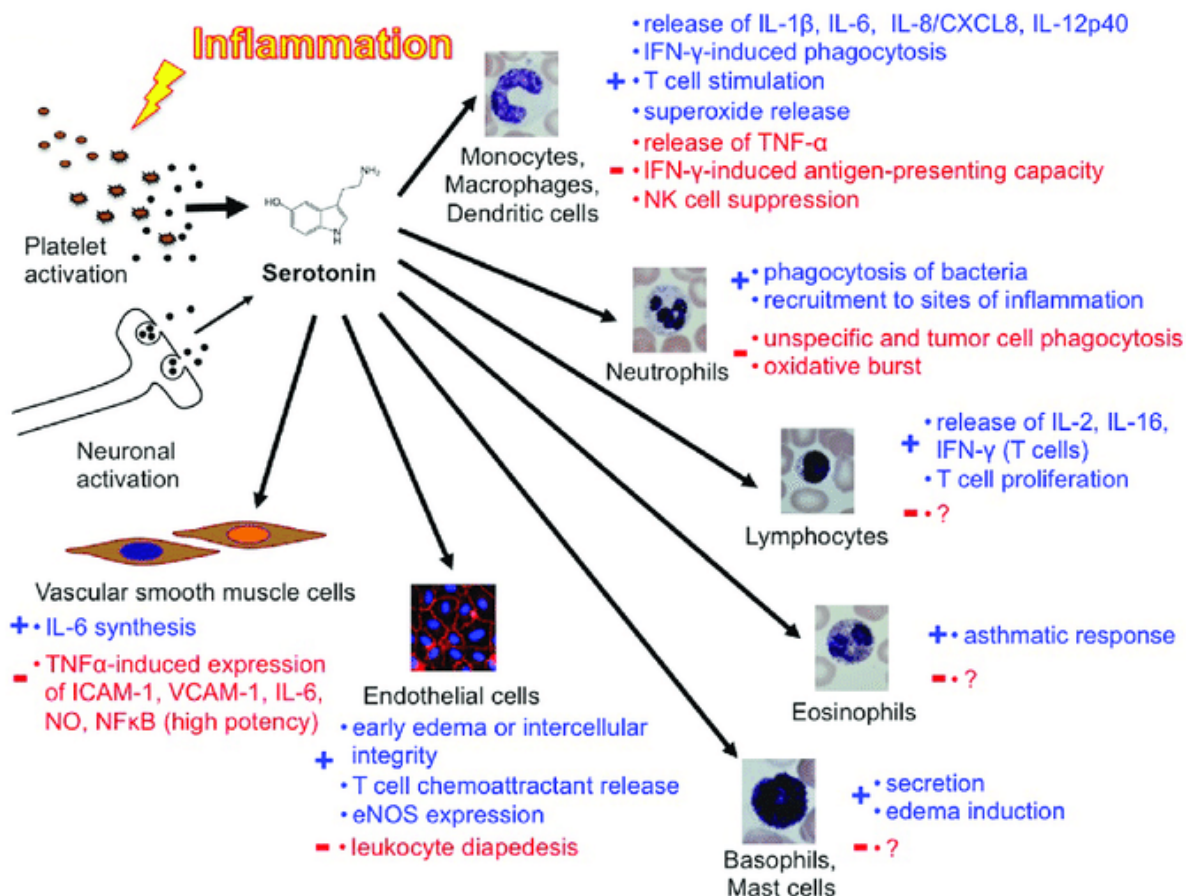


Fig. 27: Overview of the complexity of the function of platelets and serotonin in inflammation and immunity (Herr et al. 2017).

Curcumin as a therapeutic drug

Curcumin is hydrophobic polyphenol extracted from rhizome of *Curcuma longa* commonly called as turmeric (Anand et al. 2007) (Fig. 28). In India, it has been used as food preservative and herbal medicine for centuries. Curcumin is a pleiotropic molecule which has various properties such as anti-oxidant, anti-inflammatory, anti-carcinogenic, anti-microbial, anti-aging etc. (Fig. 29) (Hewlings and Kalman 2017).

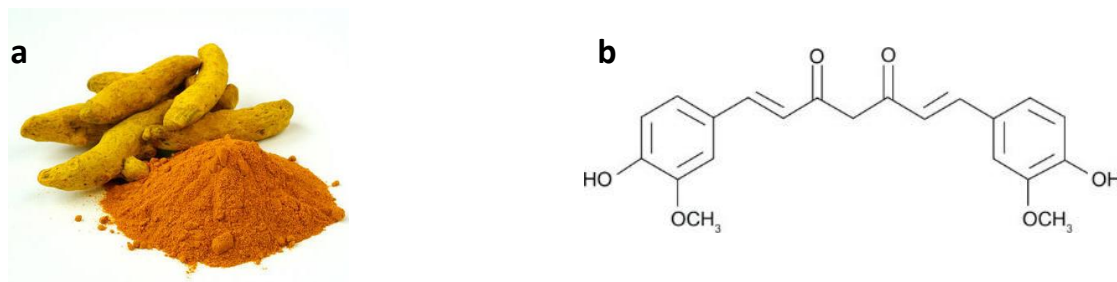


Fig. 28: (a). Curcumin; (b). Chemical structure of curcumin - bis- α,β -unsaturated β -diketone, [(*E, E*)-1,7-bis (4-hydroxy-3-methoxyphenyl)-1,6-heptadiene-3,5 dione] (Xu et al. 2018).

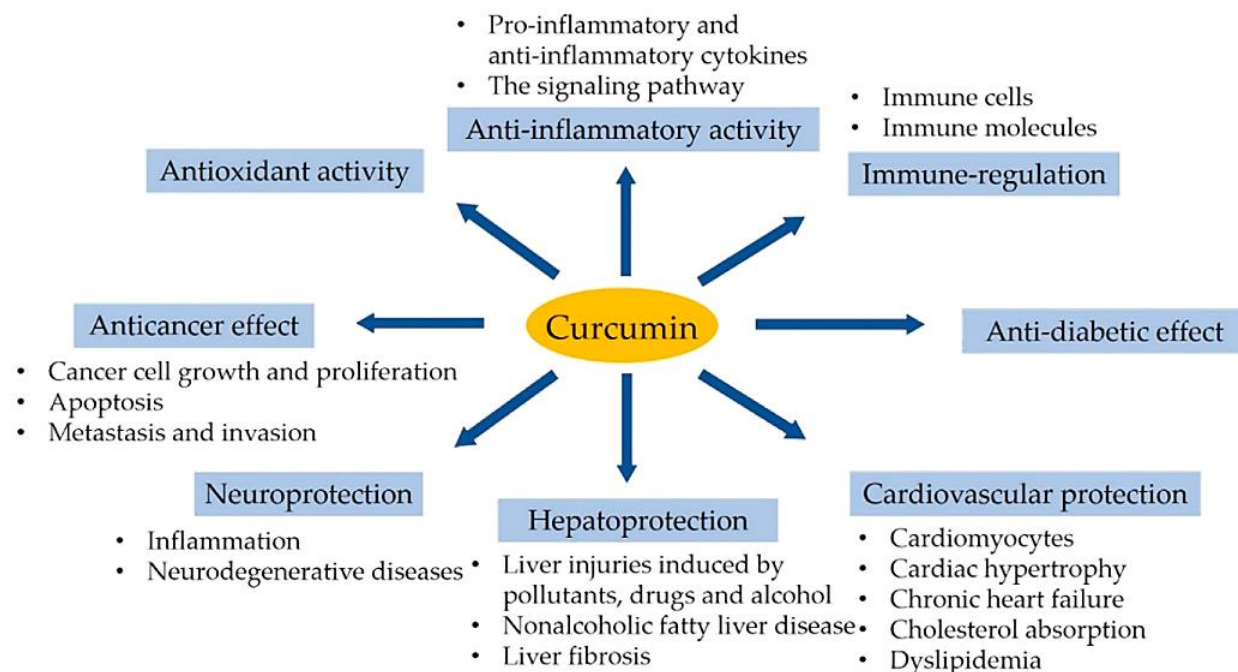


Fig. 29: A summary of the bioactivity and health benefits of curcumin, including antioxidant, anti-inflammatory, immune-regulatory, anticancer, neuroprotective, hepatoprotective, cardiovascular protective, and anti-diabetic effects (Xu et al. 2018).

Curcumin exerts its beneficial properties by interacting with several molecular targets such as transcription factors, growth factors and associated receptors, kinases, adhesion molecules, inflammatory molecules, enzymes, apoptotic proteins, etc. (Zhou et al. 2011). Curcumin was shown to reduce NF- κ B and TNF- α mediated inflammatory diseases such as rheumatoid arthritis, multiple sclerosis, Crohn's disease, psoriasis, PD, AD (Zhou et al. 2011; Panahi et al 2016). Further, curcumin also inhibits the production of interleukins like IL-6, IL-1 β by blocking NF- κ B and MAPK pathways (Cho et al. 2007). Curcuminoids have shown to increase the activity of superoxide dismutase (SOD), catalase, and also enhanced the levels of lipid peroxidase and glutathione peroxidase (Sahebkar et al. 2015). Curcumin also improved several metabolic syndromes like obesity, hyperglycemia, hypertension, etc. (Hewlings and Kalman 2017). From our laboratory, we have shown that curcumin has chronobiotic role. With the aging, the clock genes showed altered expression pattern in SCN (Mattam and Jagota 2014), upon curcumin administration, the clock genes were differentially restored in aged rat SCN (Kukkemane and Jagota 2019). We have also reported the restoratory property of curcumin on 5-HT and 5-HIAA levels in ethanol induced SCN and pineal (Jagota and Reddy 2007).

Hypothesis

With this literature background we understood that aging results in alteration in the circadian clock machinery in central clock which may lead to several pathologies. However the effect of aging on the circadian machinery in peripheral clocks like microglia, liver, kidney and spleen are not well elucidated. Aging is linked with inflammation in various tissues and cell types which leads to the progression of pathologies like PD, AD, hepatic cancer, chronic kidney diseases, splenomegaly etc. The reasons behind the ‘inflammaging’ is still unclear. Since circadian clock regulates the immune responses, studying the daily variations of clock and immune genes would help us addressing the cause for inflammaging. Therefore, to understand the chrono-immune attritions with aging, we are interested to study the role of aging on the daily rhythms of clock genes (*rBmal1*, *rPer1*, *rPer2*, *rCry1*, *rCry2*, *rRev-erba*, and *rRora*) and immune genes (*rNf-κb1*, *rTnfa*, *rIl6*, *rTlr4*, and *rTlr9*), as well as neurotransmitter serotonin (5-HT) in peripheral clocks. Further, we were interested to evaluate the chronobiotic role of curcumin on these genes with aging. Finally, to understand the interlink between circadian clock and immune responses we have administered lipopolysaccharide (LPS), an endotoxin present on the outer membrane of gram negative bacteria that elicits inflammatory responses. Further, to understand the role of NF-κB on the LPS induced changes in clock and immune genes expression in microglia, liver, kidney and spleen, we have administered Pyrrolidine dithiocarbamate (PDTC) which is an active NF-κB inhibitor.

Objectives

Objective I: The chronomics of various gene expression in microglial cells

- A. To study age induced alterations of
- Clock genes – *rBmal1*, *rPer1*, *rPer2*, *rCry1*, *rCry2*, *rRev-erba*, *rRora*
 - Inflammatory genes - *rNf- κ b1*, *rTnfa*, *rIl6*, *rTlr4*, *rTlr9*
 - Microglia resting genes - *rCx3cr1*, *rCd172*, *rCd45*
- B. To study the effect of curcumin administration on the age induced alterations of clock, inflammatory and microglia resting genes expression

Objective II: The chronomics of various gene expression and 5-HT in liver, kidney and spleen

- A. To study age induced alterations of clock, inflammatory genes expression and 5-HT
- B. To study the effect of curcumin administration on the age induced alterations of clock, inflammatory genes expression and 5-HT

Objective III: Effect of NF- κ B inhibitor on Lipopolysaccharide (LPS) induced alterations of clock genes expression in microglia, liver, kidney and spleen

- A. To study the effect of LPS on the clock and immune genes expression
- B. To evaluate the role of rNF- κ B in LPS induced alterations of clock and immune genes expression

Chapter II Materials and Methods

Animals: All the studies were conducted on male Wistar rats. The rats were maintained individually in standard polypropylene cages with temperature maintained at 23 ± 1 °C, with relative humidity 55 ± 6 %; under light-dark cycle (LD) 12:12 [lights were on at 06:00 AM (Zeitgeber time (ZT)-0) and lights were off at 6:00 PM (ZT-12)] for 2 weeks prior to experiments. Food and water was provided *ad libitum*. Cages were changed at random intervals. Dim red light was used for handling the animals in the dark (Mattam and Jagota 2014).

For aging studies: Animals were divided into three age groups: Group A – 3 months (m), Group B – 12 m and Group C – 24 m. Each group (n=48) was sub divided into three groups (I) Control (C) (II) Vehicle treatment (VT) and (III) Curcumin treatment (CT) with n=16 in each sub group.

Control: Group A (I), B (I) and C (I) animals (n=48) did not receive any treatment.

Vehicle treatment: Group A (II), B (II) and C (II) animals (n=48) were administered with 0.5 % carboxy methyl cellulose (CMC) orally at ZT-11 for 15 days.

Curcumin treatment: 100 mg/ml w/v of curcumin (Sigma) was suspended in 0.5 % carboxy methyl cellulose (CMC). Required amount of curcumin was mixed freshly with CMC and stirred for at least 30 minutes. For 15 days, Group A (III), B (III) and C (III) animals (n=48) were administered with curcumin (300 mg/kg body weight) orally at ZT-11, since it showed differential restoratory properties in rat central clock SCN (Kukkemane and Jagota 2019).

For LPS studies: 3 m male Wistar rats were used for this study. Animals were divided into two groups: Group D – Vehicle-treated group, Group E – lipopolysaccharide (LPS) treated group. Group F – Pyrrolidine dithiocarbamate (PDTC) treated group, Group G – LPS+PDTC treated group.

Vehicle treatment: Group D animals (n=16) were administered with 50 μ L saline intraperitoneally at ZT-12.

LPS treatment: LPS, an immunogen present on the gram negative bacteria was used to elicit inflammatory response (Okada et al. 2008) and to understand clock and immune interactions in various peripheral clocks. LPS was dissolved in physiological saline and administered to group E animals with a single dose of 1 mg/kg body weight intraperitoneally at ZT-12 (n=16) (Curtis et al. 2014).

Pyrrolidine dithiocarbamate (PDTC) administration: PDTC is a potent inhibitor of NF- κ B (Yang et al. 2017) and was used to analyze the role of NF- κ B in clock and immune interactions.

PDTC was dissolved in physiological saline and administered with a single dose of 100 mg/kg body weight intraperitoneally at ZT-11 to group F animals (n=16) (Sato et al. 1999).

LPS and PDTC treatment: Group G animals were treated with PDTC at ZT-11 and with LPS at ZT-12 (n=16).

Tissue collection for aging studies: Animals of group A (I, II, III), B (I, II, III) and C (I, II, III) were sacrificed at various time points ZT-0, 6, 12 and 18 (n = 4 at each time point; n=16 for four time points in each sub group) on 16th day.

Tissue collection for LPS studies: Animals of group D, E, F and G were sacrificed at various time points ZT-6, 12, 18 and 0/24 beginning from ZT-6 (n = 4) i.e. 12 h after respective treatments.

Tissue preparation: From the animals of all groups, liver, kidneys, and spleen were removed carefully at each time point, and snap frozen in liquid N₂. Tissues were stored at -80° C until further use. Microglia isolation was performed immediately.

Microglia isolation: Rats were anesthetized with diethyl ether and perfused through the left ventricle of heart with 1x PBS. Brains were removed carefully and cleared from the meninges. Each brain was split into two halves and each half was homogenized separately in 5 mL of 1x PBS with tissue dissociating enzyme papain (40 units/mL) (Sigma Aldrich) in it. Homogenates were incubated at 37°C for 20 minutes (min). Homogenates were filtered through cell strainer (corning) of 70µ pore size to obtain single cell suspension. Cell suspensions were centrifuged at 500 x g for 10 min at 18°C. Cell pellets were resuspended in 1x PBS without papain in it. Cell suspensions were centrifuged at 500 x g for 10 min at 18°C. Cell pellet from each half of the brain was collected into 15 mL centrifuge tube and mixed with 4 mL of 37% percoll, it was underlaid by 4 mL of 70% percoll and overlaid by 4 mL of 30% percoll, and on top of it 2 mL of 1x HBSS (Invitrogen) was carefully overlaid. The tube was centrifuged (Kubota) at 200 x g for 40 min at 18°C with least acceleration and deceleration. After the centrifugation, the debris was carefully removed from the top layer. Microglial cells would appear as a ring at the interphase of 70% and 37% percoll. We collected 2-3 mL of interphase mostly from the 37% segment. The collected interphase was diluted thrice with 1x HBSS and mixed thoroughly. The homogenate was centrifuged at 500 x g for 10 min at 18°C. The cell pellets were collected into 1.5 mL eppendorf tubes and washed twice with 500 µL of 1x HBSS and centrifuged at 500 x g for 5 min at 4°C. Cell pellets from the two halves of the same brain were mixed and continued for either flow cytometry or RNA isolation (Cardona et al. 2006).

Percoll gradients: Percoll (GE) is a low viscous density gradient medium for separation of cells and other subcellular components. To make a gradient with percoll, we mixed 9 parts of pure percoll with 1 part of 10x HBSS which now can be considered as 100% percoll. To make 70% percoll we mixed 7 parts of 100% percoll and 3 parts of 1x HBSS. To make 37% percoll, we mixed 3.7 parts of 100% percoll with 6.3 parts of 1x HBSS. To make 30% percoll, we mixed 3 parts of 100% percoll with 7 parts of 1x HBSS. Percoll gradients were prepared freshly just before the experiment.

Flow cytometry: To validate and enumerate the microglia in the isolated population of cells we have performed flow cytometric analysis. The isolated cells from each brain were counted under microscope using neubauer chamber. The cells were divided into various parts each with 10,000 cells in 100 μ L FACS buffer. Each part was incubated either with fluorescein isothiocyanate (FITC) conjugated CD45 antibody or phycoerythrin (PE) conjugated CD11b antibody. One part was incubated with both CD45 and CD11b antibodies. Cells were incubated with antibodies for 30 min in dark. Then cells were centrifuged and resuspended in 100 μ L FACS buffer. The cells were analyzed with Flow cytometry (Cardona et al. 2006).

RNA isolation from microglia: microglia isolated from single brain were homogenized in 1 mL of RNA Iso plus (Takara) and incubated at room temperature for 5 min. 200 μ L of chloroform was mixed with the homogenate and incubated for 5 min at room temperature. Then, centrifugation was done at 12,000 x g for 15 min at 4°C. The aqueous layer was isolated and mixed with equal volume of isopropanol and incubated for 10 min at room temperature. Then centrifuged at 12,000 x g for 15 min at 4°C. Supernatant was discarded and 75% ethanol was added to the pellet and centrifuged at 10,000 x g for 10 min at 4°C. Ethanol was discarded and pellet was air dried and resuspended in 20 μ L of diethyl pyrocarbonate (DEPC) treated water. RNA was quantified using nano drop (Thermo scientific) (Mattam and Jagota 2014).

RNA isolation from liver, kidney and spleen: Tissues from each time point were grinded in liquid nitrogen separately. 50 mg (dry weight) of tissue was taken for RNA isolation. 1 mL of RNA Iso plus (Takara) was used for homogenizing the tissue and followed the similar steps as mentioned above for RNA isolation. RNA pellet was dissolved in 50 μ L of DEPC treated water. RNA was quantified using nano drop (Thermo scientific) (Mattam and Jagota 2014).

cDNA synthesis: cDNA synthesis was performed using Bioline cDNA synthesis kit. 20 μ L reaction was performed using Thermo scientific PCR machine.

Table 1: Components used for the cDNA synthesis.

S. No.	Components	Volume (μL)
1	5x buffer	4
2	Reverse transcriptase enzyme	1
3	RNA	1 (μg)
4	Nuclease free water	required amount
	Total	20 μL

Table 2: Reaction set up for cDNA synthesis

S. No.	Temperature ($^{\circ}\text{C}$)	Time (min.)	cycles
1	25	10	1
2	42	15	1
3	48	15	1
4	85	5	1
5	4	∞	1

Quantitative Real time PCR (qRT-PCR): cDNA synthesized was diluted 1:10 times with nuclease free water. Sybr green (Invitrogen) detection method was used for the quantification of the mRNA expression in the samples. 10 μL reaction was used for the PCR reaction.

Table 3: components for qRT-PCR

S. No.	Components	Volume (μL)
1	SYBR Green	5
2	Forward primer	0.5
3	Reverse primer	0.5
4	cDNA	4
	Total	10 μL

Table 4: Reaction set up for qRT-PCR

Steps	Temperature ($^{\circ}\text{C}$)	Time	cycles
1	95	10 min	1
2	95	15 seconds (sec)	40
	60	60 sec	
3	Melt curve	-	1

Primers:

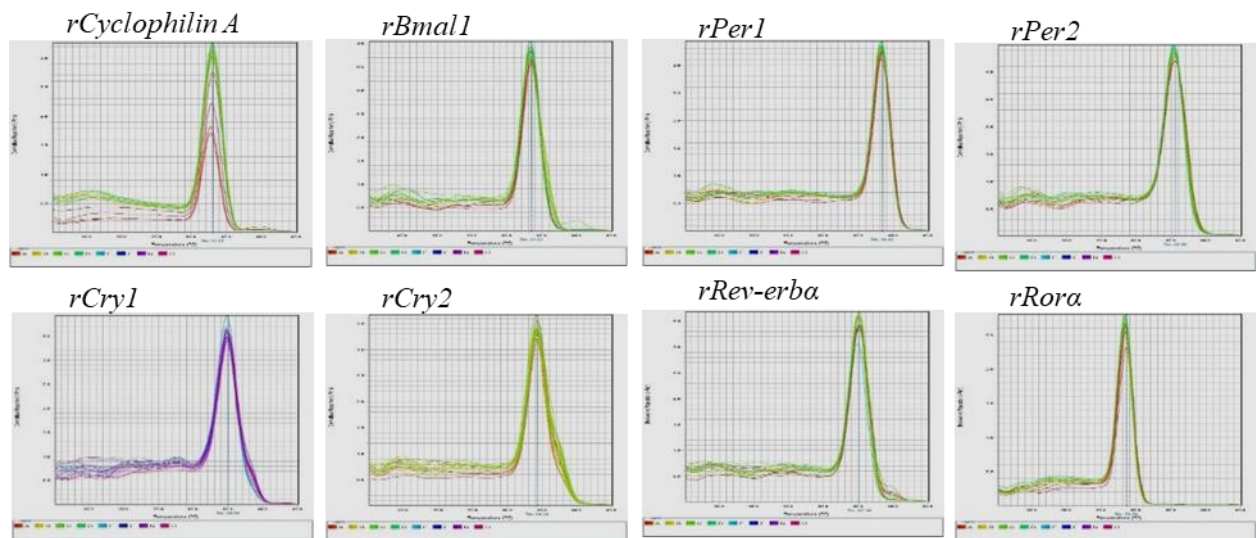
We have designed the primers for the clock genes (*rBmal1*, *rPer1*, *rPer2*, *rCry1*, *rCry2*, *rRev-erba*, *rRora*), immune genes (*rNf- κ b1*, *rTnfa*, *rIl6*, *rTlr4*, *rTlr9*), microglia resting genes (*rCx3cr1*, *rCd172*, *rCd45*) using IDT primer quest tool (Kukkemane and Jagota 2019).

Table 5: Primers list

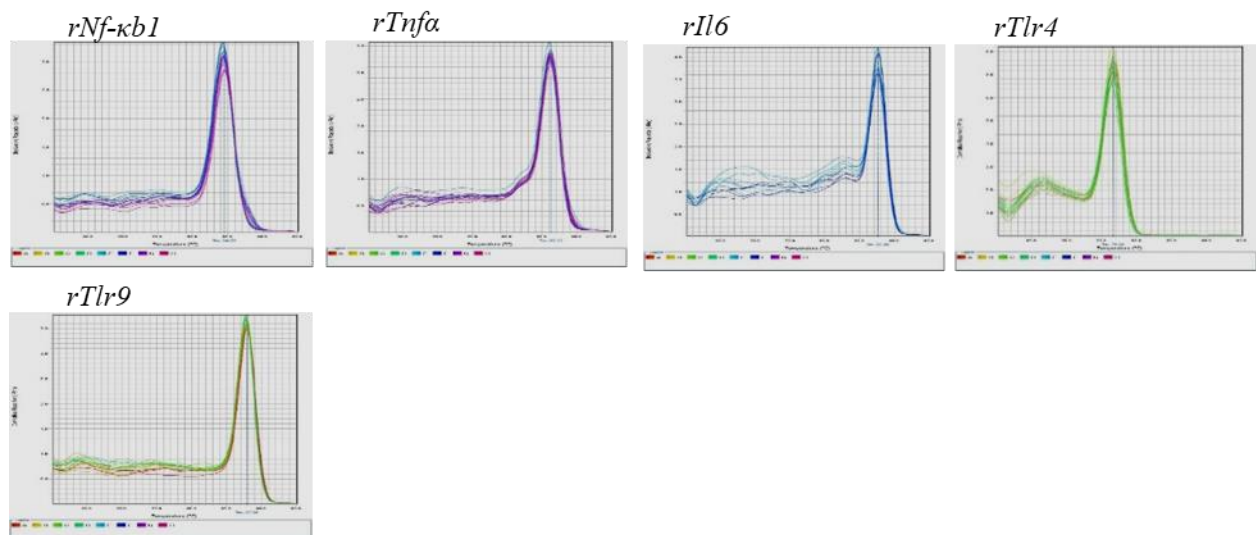
Gene	Forward Primer (5' – 3')	Reverse Primer (5' – 3')
Reference gene		
<i>rCyclophilin A</i>	CGCGTCTGCTTCGAGCTGTTT	GTCACCACCCTGGCACATGAAT
Clock genes		
<i>rBmal1</i>	GGCTTCTTTGGTACCAACATG	AATCCATCTGCTGCCCTGAGAAT
<i>rPer1</i>	GGCCAAGAAAGATACGTCGTCAG	ACACCACGCTCTCTGCCTTATTG
<i>rPer2</i>	AGCCACAGCCTGAACTAGAGACA	TCCTTGGTGAGGCCTAGCTTCT
<i>rCry1</i>	GGCGGAAACTGCTCTCAAGGA	CCAACACTCTGTGCGTCCTCTT
<i>rCry2</i>	CCATCGTCAACCACGCAGAGA	GGGACAGATGCCAACAGACAGAG
<i>rRev-erba</i>	GGTGACCTGCTCAATGCCATGTT	CGAGCGGTCTGCAGAGACAAGTA
<i>rRora</i>	TAGGATGTGCCGTGCCTTT	CAGGAGCGATCTGCTGACAT
Immune genes		
<i>rNf-κb1</i>	TACGATGGGACGACACCTCTACAC	GGTCTGCTCCTGCTGCTTTGA
<i>rTnfa</i>	GTCGTAGCAAACCACCAAGC	CCTTGAAGAGAACCTGGGAGTAG
<i>rIl6</i>	TCTCCGCAAGTAAGTGAAGGC	GCGTGGAGGAAAGGGAAAGA
<i>rTlr4</i>	GGCCTCCCTGGTGTGGATTT	TGGCTACCACAAGCACACTGAC
<i>rTlr9</i>	CTGGGACGTCTGGTACTGTTTC	CCGCACTCGAAGCTCGTTAT
Microglia resting genes		
<i>rCx3cr1</i>	GCTTCGTCCTGCCCTTGCTTAT	GCCTAATGGCTCTGGCCTTCTTC
<i>rCd172</i>	TGCTGGCACCTACTACTGTGTGA	CGGTGAAGAAGGTTTGCGGAGT
<i>rCd45</i>	CAAGTGGAGGCCAGTACAT	CACTGGGTGGATCTCTCTTCTTC

Dissociation curves for all the genes studied showed a single peak (Fig. 30) representing specific amplified target gene. Threshold cycle (Ct) values were obtained from the exponential phase of amplification plots. The relative quantitative expression of clock genes were obtained by normalizing each target gene expression with Cyclophilin A (Δ Ct = target gene Ct – Cyclophilin A Ct) in each sample and used $2^{-\Delta$ Ct method for analysis (Mattam and Jagota 2014).

Internal control gene and Clock genes:



Inflammatory genes:



Microglia resting genes:

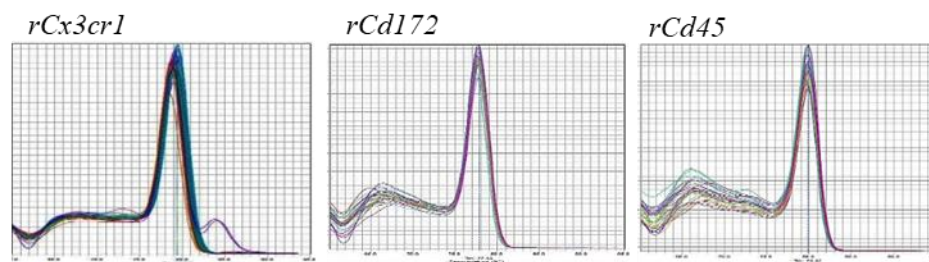


Fig. 30: Dissociation curves for clock, immune and microglia resting genes showing single peak

Serotonin estimation using Reverse phase High pressure liquid chromatography

Reverse phase HPLC (RP-HPLC) electro-chemical detection method was used to estimate the levels of serotonin (5-HT) at different time points such as ZT-0, 6, 12, and 18 in different age groups and curcumin treated groups in liver, kidney and spleen. Data acquisition and processing was done by using Empower 2 software (Waters). 10 mg tissue was homogenized in 100 μ L of 0.1 N perchloric acid containing 1mM of sodium bisulfate. Homogenate was sonicated for 5 seconds with 45% amplitude. Then, homogenate was centrifuged at 12,800 x g for 10 min at 4°C. Supernatant was collected and filtered through 0.22 μ m syringe filter. To estimate 5-HT, 50 μ L of the filtered homogenate was injected along with eluent A [10 % methanol; 0.1M citric acid; 0.1M sodium acetate, 50 mg/L EDTA (pH 4.1)] (Reddy and Jagota 2015).

Estimation: The amount of compound present in the sample was estimated by comparing the peak area measured in the sample to the standard peak area generated by analyzing the known amounts of standard compound (Fig. 31).

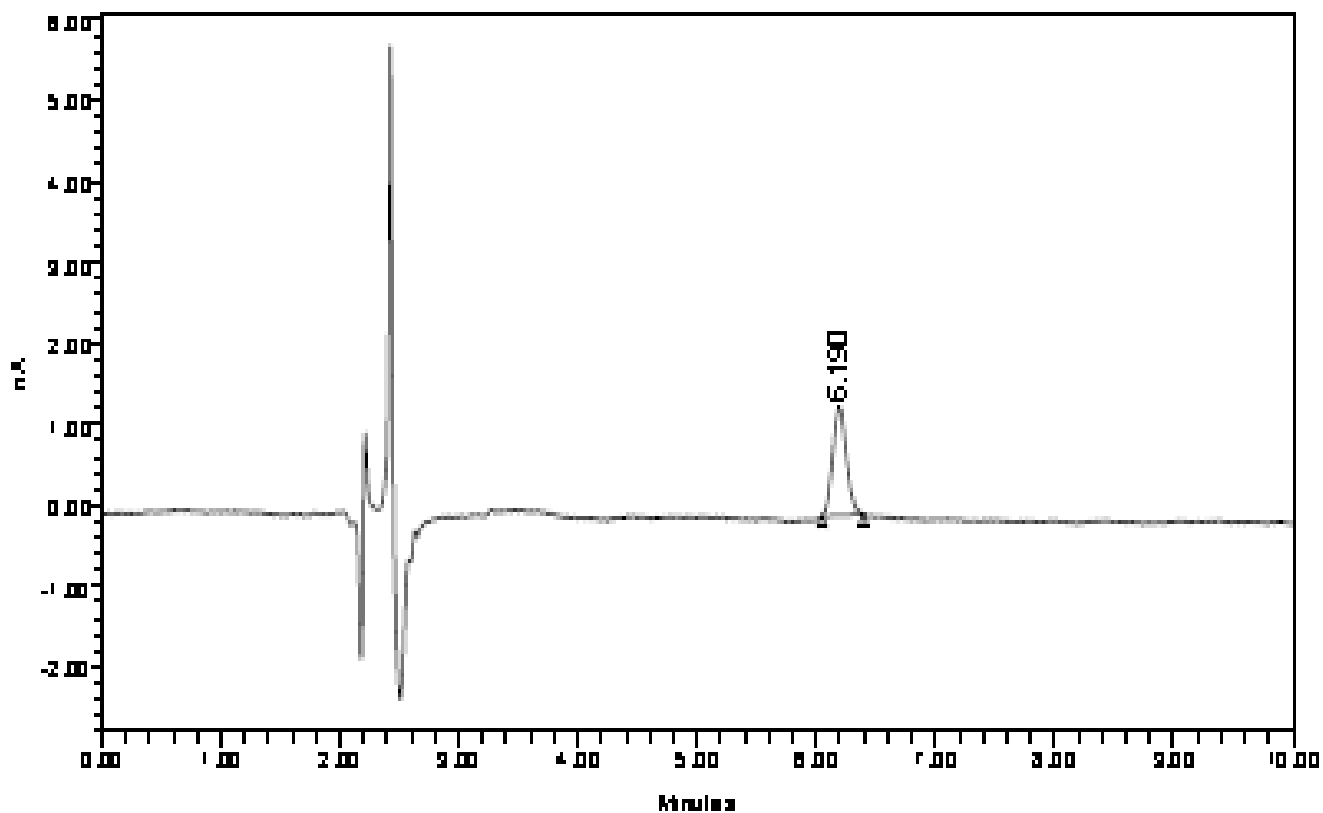


Fig. 31: Chromatogram showing the retention time for 5-HT.

Data analysis

Statistical analysis: Graph Pad Prism software was used for all the data analysis. Multiple comparisons among the four time points within the each age group were analyzed using one way ANOVA and followed by Post hoc Tukey's test. Student's t test was performed to compare mean 24 hour (h) levels between control and treatment groups. Daily pulse i.e. the ratio of maximum expression to minimum expression of a gene within each group was compared between control and treated groups using student's t test (Kukkemane and Jagota 2019). To understand how aging and treatment affected the expression pattern of genes we used circadian parameter 'phase shift' i.e. shift of maximum expression of gene expression to either earlier time point (phase advance) or later time point (phase delay).

Pearson correlation analysis: Using R-program (Kukkemane and Jagota 2019) Pearson correlation analysis was done. Pair wise correlations were analyzed in light (ZT-0, 6, 12) and dark (ZT-12, 18, 24/0) phase separately among *rBmal1*, *rPer1*, *rPer2*, *rCry1*, *rCry2*, *rRev-erba*, *rRora*, *rNf- κ b1*, *rTnfa*, *rIl6*, *rTlr4* and *rTlr9* genes in 3, 12 and 24 m vehicle-treated (VT) and curcumin treated (CT) liver, kidney and spleen samples. Similarly pairwise correlation was done within and among the clock genes, immune genes and microglia resting genes in 3, 12 and 24 m vehicle-treated (VT) and curcumin treated (CT) microglia (Kukkemane and Jagota 2019).

Gene to gene network analysis: We used weighted correlation network analysis (WGCNA) data mining package in R program to understand the gene to gene network alterations with the aging and curcumin treatment. Further, 'Cytoscape' software was used to develop the network images.

Chapter III Results

Flowcytometric analysis of microglia

The isolated cell pellet from density gradient centrifugation was analyzed for identification and quantification of microglial cells. In the brain, microglia and infiltrated macrophages are the only CD45 positive cells, but the expression of CD45 is higher in macrophages than in microglial cells. However, both the cell types have CD11b expression on their cell membrane but the other glial cells and neuronal cells lack its expression. Based on this differential expression of microglia and macrophage-specific protein expression, we have identified and enumerated the microglial cells in isolated cell pellet. We used PE-conjugated CD11b and FITC-conjugated CD45 antibodies to enumerate the microglial cells. We observed that nearly 80% of cells are microglial cells with less expression of CD45 than macrophages (Fig. 32).

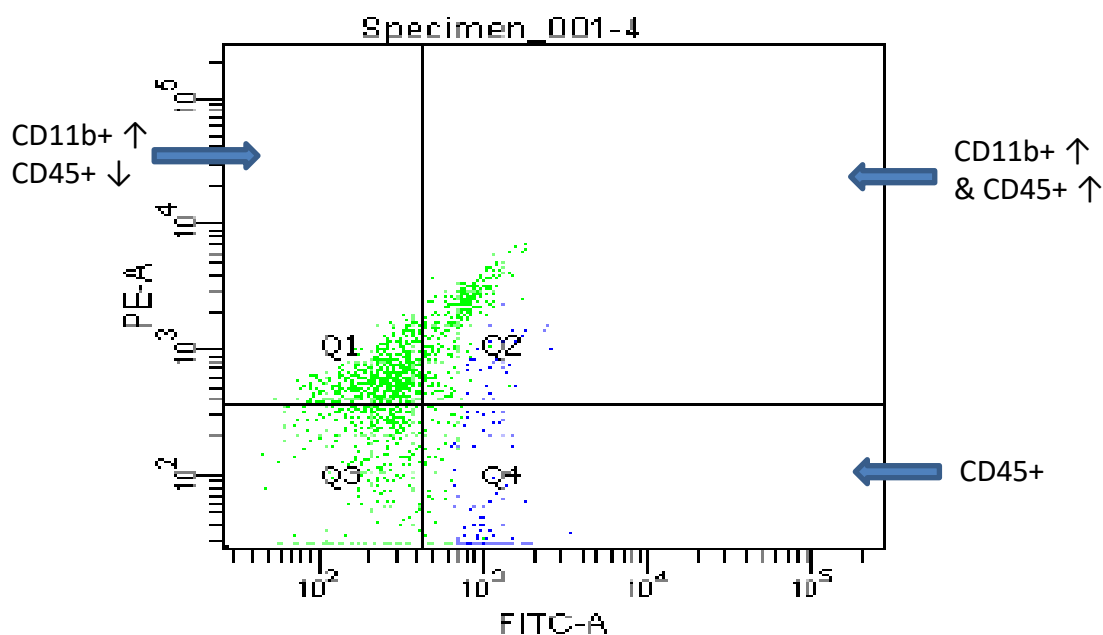


Fig. 32: Quadrant showing the microglia population. Q1 - cells with higher expression of CD11b and lesser expression of CD45. Q2 - cells with higher expression of CD11b and CD45. Q3 - cells with lesser expression of CD11b and CD45. Q4 - cells with higher expression of CD45 and lesser expression of CD11b. We consider the microglia positive cell population to be in Q1 since it has higher expression of CD11b and lesser expression of CD45. Nearly 80% of the total population belong to Q1. Therefore, nearly 80% of the population isolated from a single brain are microglial cells. (x-axis indicates the intensity of FITC fluorescence; y-axis indicates the intensity of PE fluorescence).

I. A. Age-induced alterations on mRNA expression of various clock, immune and microglia resting genes

Effect of aging on the daily rhythms of clock genes

We have studied the clock genes expression in C and VT group animals and we did not observe any change in both the groups. Core clock gene, *rBmal1* showed maximum expression at ZT-0 and minimum at ZT-6 in 3 m animals. In 12 and 24 m animals, the expression did not change in comparison to 3 m but the minimum expression was observed at ZT-12 and ZT-18 respectively. *rPer1* showed maximum expression at ZT-6 in 3, 12 and 24 m animals, but the minimum expression at ZT-0, ZT-12, and ZT-18 respectively. *rPer2* showed maximum expression was at ZT-12 in 3 m but in 12 and 24 m animals, 6 h phase advance was observed with maximum expression at ZT-0. *rCry1*, *rCry2*, and *rRora* showed maximum expression at ZT-0 in all age groups, but the minimum expression was observed at ZT-12 in 3 and 12 m; and at ZT-18 in 24 m animals. *rRev-erba* showed maximum expression at ZT-6 in all age groups, but the minimum expression was at ZT-18 in 3 and 24 m; at ZT-12 in 12 m animals (Fig. 33) (Table 6).

Effect of aging on the daily rhythms of immune genes

rNf- κ b1 showed maximum expression at ZT-6 and minimum expression at ZT-12 in 3 m animals. In 12 and 24 m animals, 6 h phase advance was observed with maximum expression at ZT-0. *rTnfa* and *rTlr4* showed maximum expression at ZT-6 and minimum expression at ZT-0 in 3 m, in 12 and 24 m animals 6 h phase advance was observed with maximum expression at ZT-0. *rTlr9* also showed maximum expression at ZT-6 and minimum expression at ZT-0 in 3 m animals, in 12 m animals maximum expression time point remained unchanged but in 24 m 6 h phase advance was observed. *rIl6* did not show rhythmic expression in 3 m animals, but in 12 and 24 m, rhythmic expression was observed with maximum expression at ZT-0 (Fig. 34).

Effect of aging on daily rhythms of microglia resting genes

rCx3cr1 showed maximum expression at ZT-6 in all age groups but the minimum expression was observed at ZT-0 in 3 m animals, at ZT-12 in 12 and 24 m animals. *rCd45* showed maximum expression at ZT-6 in all age groups but the minimum expression was observed at ZT-18 in 3 and 12 m, at ZT-12 in 24 m animals. *rCd172* showed maximum expression at ZT-6 and minimum expression at ZT-12 in 3 m, but in 12 and 24 m animals 6 h phase advance was observed with maximum expression at ZT-0 (Fig. 35) (Table 7).

Effect of aging on mean 24 h levels and daily pulse of clock genes

rBmall, *rCry1*, *rRev-erba*, and *rRora* did not show significant variation in mean 24 h levels in all age groups. *rPer1*, *rPer2*, and *rCry2* showed increased levels in 24 m in comparison to 3 m animals (Fig. 36). *rBmall*, *rPer1*, *rCry2*, and *rRev-erba* showed increased daily pulse in 12 m in comparison to 3 m animals. *rPer2*, *rCry1*, and *rRora* showed no significant variation in daily pulse with aging (Fig. 37) (Table 6).

Effect of aging on mean 24 h levels and daily pulse of immune genes

rTlr9 showed significantly increased expression in 12 m in comparison to 3 m animals. All the other immune genes did not vary with the aging (Fig. 36). *rNf- κ b1*, *rIl6* showed increased daily pulse in 12 m in comparison to 3 m animals. *rTnfa* showed increased daily pulse whereas, *rTlr9* showed decreased daily pulse in 12 and 24 m in comparison to 3 m animals. *rTlr4* did not vary in daily pulse with aging (Fig. 37) (Table 7).

Effect of aging on the mean 24 h levels and daily pulse of microglia resting genes

rCx3cr1 showed increased expression in 12 and 24 m in comparison to 3 m animals. *rCd45* showed increased expression in 12 m animals in comparison to 3 m animals. *rCd172* did not vary in expression levels with aging (Fig. 36). *rCx3cr1* showed decreased daily pulse in 24 m, *rCd172* showed increased daily pulse in 12 m in comparison to 3 m animals. *rCd45* did not alter in daily pulse with aging (Fig. 37) (Table 7).

Effect of aging on correlations among clock genes

In 3 m LP, *rBmall* and *rPer1*; *rPer1* and *rCry1*; *rPer2* and *rCry2*; *rPer2* and *rRev-erba*; *rPer2* and *rRora* showed negative correlation. *rBmall* and *rCry1*; *rBmall* and *rCry2*; *rBmall* and *rRora*; *rPer1* and *rRev-erba*; *rCry1* and *rCry2*; *rCry1* and *rRora*; *rCry2* and *rRora* showed positive correlation. In 3 m DP, *rPer1* and *rPer2* showed a negative correlation with all the other clock genes. Whereas, *rBmall*, *rCry1*, *rCry2*, *rRev-erba*, and *rRora* showed a positive correlation with each other. In 12 m LP and DP, all the clock genes showed a positive correlation with each other. In 24 m LP, *rPer2* and *rRev-erba*; *rCry1* and *rRev-erba* showed negative correlation. *rBmall* and *rRev-erba*; *rPer1* and *rCry1*; *rCry2* and *rRev-erba* did not show correlation. All the other genes showed a positive correlation with each other and with *rPer2*, *rCry1*, and *rRev-erba*. In 24 m DP, all the clock genes showed a positive correlation with each other (Fig. 38).

Effect of aging on correlations among immune genes

In 3 m LP, all the immune genes except *rIl6* showed a positive correlation with each other. *rIl6* showed a negative correlation with all the other immune genes. In 3 m DP, *rNf- κ b1* and *rTlr9*; *rTnfa* and *rTlr4*; *rTnfa* and *rTlr9*; *rTlr4* and *rTlr9* showed positive correlation. *rIl6* showed a negative correlation with other immune genes except *rNf- κ b1*. In 12 m LP and DP, all the immune genes showed a positive correlation with each other. Similarly, in 24 m LP and DP, all the immune genes showed a positive correlation (Fig. 38).

Effect of aging on correlations among microglia resting genes

In 3 m LP, *rCx3cr1*, *rCd172* and *rCd45* showed positive correlation with each other. In 3 m DP, they showed a negative correlation with each other. In 12 m LP, these genes showed a positive correlation with each other. In 12 m DP, *rCx3cr1* and *Cd45* showed a significant positive correlation. In 24 m LP, *rCx3cr1* and *Cd45* showed a significant positive correlation. In 24 m DP, *rCx3cr1* and *Cd172* showed a significant positive correlation (Fig. 38).

Effect of aging on correlations among clock, immune and microglia resting genes

In 3 m LP, *rBmall* and *rCry1* showed negative correlation with *rNf- κ b1*, *rTnfa*, *rTlr4* and *rTlr9*. *rPer1* and *rRev-erba* showed positive correlation with *rNf- κ b1*, *rTnfa*, *rTlr4* and *rTlr9*. *rIl6* showed a positive correlation with *rBmall*, *rCry1*, and *rCry2*, but showed a negative correlation with *rPer1*. *rCx3cr1*, *rCd172* and *rCd45* showed negative correlation with *rBmall*, *rPer2* and *rCry1*, but showed positive correlation with *rPer1* and *rRev-erba*. In 3 m DP, *rBmall*, *rCry1*, *rCry2*, *rRev-erba* and *rRora* showed negative correlation with *rTnfa*, *rTlr4* and *rTlr9*, but showed positive correlation with *rIl6*. *rBmall* and *rNf- κ b1*; *rCry1* and *rNf- κ b1* showed negative correlation. *rPer1* and *rTnfa*; *rPer1* and *rTlr4* showed a positive correlation. *rPer2* showed a positive correlation with *rNf- κ b1*, *rTlr4*, and *rTlr9*, but showed a negative correlation with *rIl6*. *rCx3cr1* showed negative correlation with *rBmall*, *rCry1*, *rCry2*, *rRev-erba* and *rRora*, but showed positive correlation with *rPer1* and *rPer2*. *rCd45* showed a negative correlation with *rPer1* and positive correlation with *rRev-erba*. In 12 m LP and DP, clock genes showed a significant and insignificant positive correlation with immune and microglia resting genes. Similarly, in 24 m LP and DP, all clock genes except *rRev-erba* showed a positive correlation with immune genes. *rPer1* and *rRev-erba* showed a significant positive correlation with *rCx3cr1*. *rBmall*, *rPer2*, *rCry1* and *rCry2* showed significant positive correlation with *rCd172*. In 24 m

DP, clock genes showed a significant and insignificant positive correlation with immune and microglia resting genes except *rCd45* (Fig. 38).

WGCNA analysis among clock, immune and microglia resting genes with aging

In 3 m, *rPer1* and *rRev-erba* showed strong interactions with immune and microglia resting genes. In 12 m, interactions among clock, immune and microglia resting genes increased. In 24 m, clock and immune genes showed strong interactions, whereas, *rCd172* showed interaction with clock and immune genes but other microglia resting genes lost interactions with clock genes (Fig. 39).

I. B. Chronobiotic role of curcumin on the age-induced alterations of clock, immune and microglia resting genes mRNA expression

Effect of curcumin on clock genes daily rhythms

Curcumin administration resulted in 6 h phase advance of *rBmal1* with maximum expression at ZT-18 in 3 m animals. However, in 12 and 24 m CT animals, the maximum expression did not vary in comparison to age-matched VT group. *rPer1* showed 6 h phase delay in 3 m CT and showed 12 h phase delay in 12 and 24 m CT animals in comparison to age-matched VT groups. *rPer2* showed 6 h phase delay in 3 m CT, 12 h phase delay in 12 m CT, 6 h phase advance in 24 m CT animals. *rCry1* showed 6 h phase advance in all age groups with curcumin treatment in comparison to VT animals. *rCry2* showed 12 h phase delay in 3 and 12 m CT animals, 6 h phase advance in 24 m CT animals. *rRev-erba* showed 12 h phase delay in 3 m CT, 6 h phase advance in 24 m CT, but the phase was not altered in 12 m CT in comparison to VT groups. *rRora* showed 6 h phase advance in 3, 24 m CT, 12 h phase delay in 12 m animals in comparison to age-matched vehicle groups (Fig. 33) (Table 6).

Effect of curcumin on daily rhythms of immune genes

Curcumin administration resulted in 12 h phase delay of *rNf- κ b1* in 3 m animals but did not alter in 24 m animals in comparison to age-matched VT animals. Interestingly, curcumin restored the phase of *rNf- κ b1* in 12 m in comparison to 3 m VT animals. *rTnfa* showed 12 h phase delay in 3 and 24 m CT animals in comparison to age-matched VT animals. Interestingly, curcumin restored *rTnfa* phase in 12 m in comparison to 3 m VT animals. *rIl6* showed rhythmicity in 3 m animals with maximum expression at ZT-0. In 12 m animals, curcumin abolished the rhythmicity which is similar to 3 m VT animals. In 24 m animals, curcumin showed 12 h phase delay in

comparison to age-matched VT animals. *rTlr4* showed 12 h phase delay in 3 m CT, 6 h phase advance in 24 m CT, but did not alter in 12 m CT animals in comparison to age-matched VT animals. *rTlr9* showed 12 h phase delay in 3 and 24 m CT, 6 h phase advance in 12 m CT in comparison to age-matched VT animals (Fig. 34) (Table 7).

Effect of curcumin on daily rhythms of microglia resting genes

Curcumin treatment resulted in 12 h phase delay of *rCx3cr1* and *rCd45* in 3 and 24 m animals, 6 h phase advance in 12 m animals. *rCd172* showed 12 h phase delay in 3 m CT and did not vary in 24 m CT in comparison to age-matched VT animals. Interestingly, curcumin restored the phase of *rCd172* in 12 m animals in comparison to 3 m VT animals (Fig. 35) (Table 7).

Effect of curcumin on mean 24 h levels and daily pulse of clock genes

With curcumin administration, *rBmal1* showed significantly increased expression in 3 and 24 m CT but did not vary in 12 m CT in comparison to age-matched VT animals. *rPer1* showed no alteration in 3 m CT, but significantly decreased in 12 and 24 m CT animals. *rPer2* showed significantly increased expression, but *rCry1*, *rCry2*, and *rRev-erba* showed decreased expression in all age groups in comparison to age-matched VT animals. *rRora* showed decreased expression in 3 and 24 m CT but did not alter in 12 m CT animals in comparison to VT groups (Fig. 36). Daily pulse of *rBmal1* showed the restoration in 12 m animals in comparison to 3 m VT animals but did not alter in 3 and 24 m with curcumin administration in comparison to age-matched VT animals. *rPer1* showed increased daily pulse in 3 and 24 m CT, but in 12 m, curcumin restored daily pulse in comparison to 3 m VT animals. *rPer2* and *rCry1* did not show alterations in daily pulse in all age groups with curcumin administration in comparison to age-matched VT animals. Daily pulse of *rCry2* showed no variation in 3 m CT, decreased in 12 m CT, increased in 24 m CT in comparison to age-matched VT animals. Daily pulse of *rRev-erba* did not alter in 3 and 24 m CT in comparison to age-matched VT animals, but curcumin restored daily pulse of *rRev-erba* in 12 m animals. Daily pulse of *rRora* showed no variation in 3 and 12 m CT but significantly increased in 24 m CT animals in comparison to VT animals (Fig. 37) (Table 6).

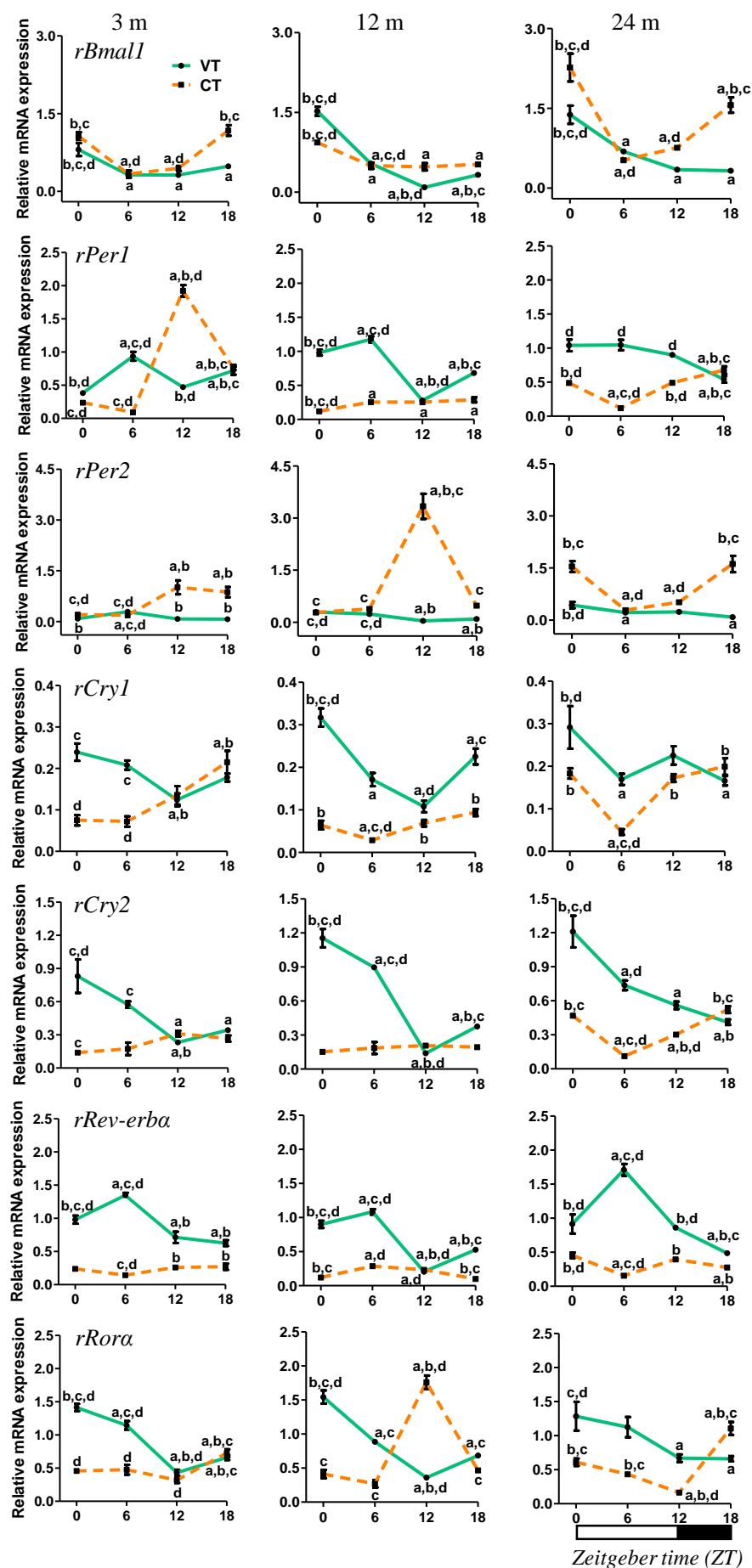


Fig. 33: Effect of curcumin administration on daily rhythms of various clock genes mRNA expression in 3, 12 and 24 months (m) old rat microglia. Each value is mean ± SEM (n = 4), $p \leq 0.05$ and expressed as relative mRNA expression. $p_a \leq 0.05$; $p_b \leq 0.05$, $p_c \leq 0.05$ and $p_d \leq 0.05$ (where ‘a’, ‘b’, ‘c’ and ‘d’ refers to comparison with ZT-0, ZT-6, ZT-12, and ZT-18 respectively within the group).

Effect of curcumin on mean 24 h levels and daily pulse of immune genes

Curcumin administration significantly decreased the expression of *rNf- κ b1* in 12 and 24 m animals in comparison to age-matched VT animals. Curcumin significantly reduced the levels of *rTnfa*, *rIl6* and *rTlr4* in all age groups in comparison to age-matched VT animals. Interestingly, in 12 m curcumin showed restoration of *rTlr9* levels in comparison to 3 m VT animals (Fig. 36).

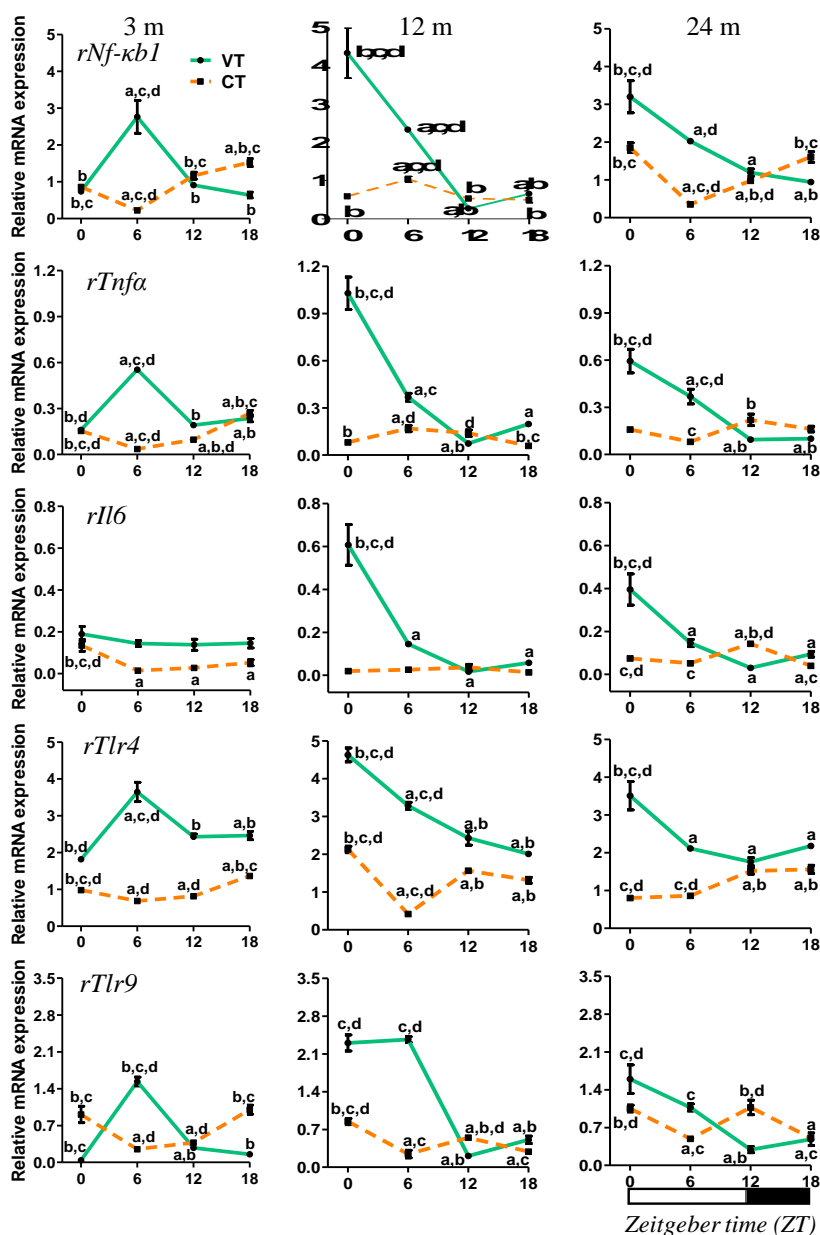


Fig. 34: Effect of curcumin administration on daily rhythms of various immune genes mRNA expression in 3, 12 and 24 months (m) old rat microglia. Each value is mean \pm SEM ($n = 4$), $p \leq 0.05$ and expressed as relative mRNA expression. $p_a \leq 0.05$; $p_b \leq 0.05$, $p_c \leq 0.05$ and $p_d \leq 0.05$ (where 'a', 'b', 'c' and 'd' refers to comparison with ZT-0, ZT-6, ZT-12, and ZT-18 respectively within the group).

Daily pulse of *rNf- κ b1* did not alter in 3 and 24 m CT in comparison to age-matched VT animals. Curcumin restored the daily pulse of in 12 m animals. Curcumin increased the daily pulse of *rTnfa* in 3 m animals but restored in 12 and 24 m animals in comparison to 3 m VT animals. Curcumin restored the daily pulse of *rIl6* in 12 m animals. Daily pulse of *rTlr4* did not alter in 3 and 24 m CT animals but increased in 12 m CT in comparison to age-matched VT animals. Curcumin reduced the daily pulse of *rTlr9* in all age groups in comparison to age-matched VT animals (Fig. 37) (Table 7).

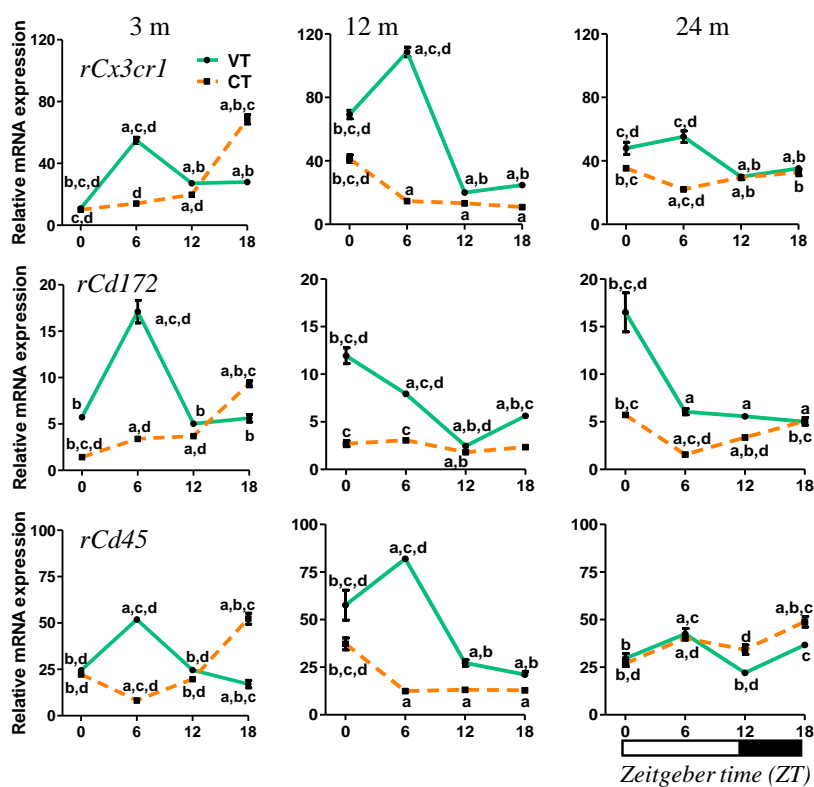


Fig. 35: Effect of curcumin administration on daily rhythms of microglia resting genes mRNA expression in 3, 12 and 24 months (m) old rat microglia. Each value is mean \pm SEM ($n = 4$), $p \leq 0.05$ and expressed as relative mRNA expression. $p_a \leq 0.05$; $p_b \leq 0.05$, $p_c \leq 0.05$ and $p_d \leq 0.05$ (where ‘a’, ‘b’, ‘c’ and ‘d’ refers to comparison with ZT-0, ZT-6, ZT-12, and ZT-18 respectively within the group).

Effect of curcumin on mean 24 h levels and daily pulse of microglia resting genes

Curcumin administration did not alter the levels of *rCx3cr1* in 3 m animals, but significantly reduced the levels and restored in 12 and 24 m in comparison to 3 m VT animals. *rCd172* showed reduced levels in all age groups with curcumin administration. *rCd45* showed decreased levels in 12 m CT but did not alter in 3 and 24 m CT animals in comparison to age-matched VT

animals (Fig. 36). Daily pulse of *rCx3cr1* was increased in 3 m CT but decreased in 12 and 24 m CT in comparison to age-matched VT animals. Curcumin resulted in an increased daily pulse of *rCd172* and *rCd45* in 3 m, decreased in 12 m, but did not alter in 24 m animals (Fig. 37).

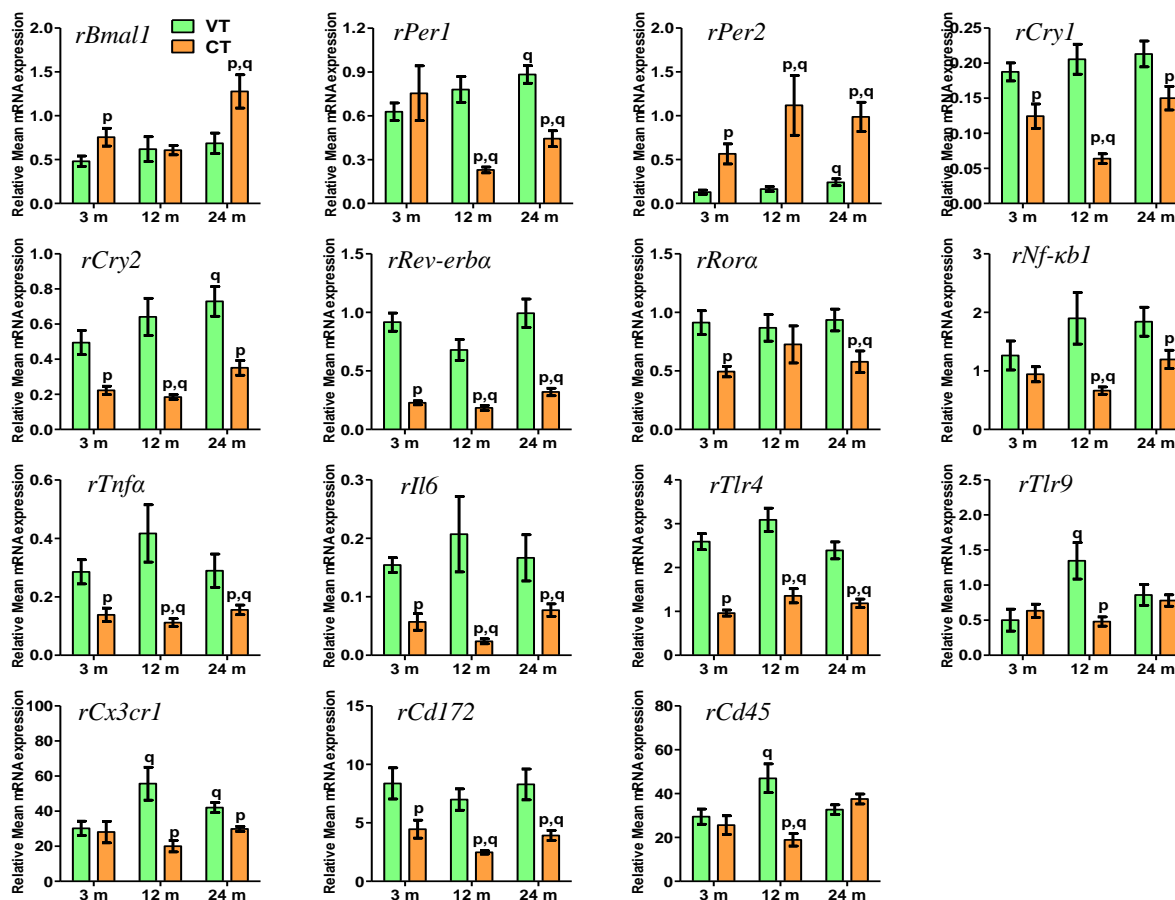


Fig. 36: Effect of curcumin administration on mean 24 hour (h) levels of clock, immune and microglia resting genes expression in 3, 12 and 24 months (m) old rat microglia. Each value is mean \pm SEM ($n = 4$), $p \leq 0.05$ and expressed as mean relative gene expression. $p_p \leq 0.05$ (where 'p' refers to comparison with the age-matched vehicle-treated group). $p_q \leq 0.05$ (where 'q' refers to comparison with 3 m vehicle-treated group).

Effect of curcumin on correlations among clock genes

In 3 m LP of CT animals, *rPer1*, *rPer2*, *rCry1*, and *rCry2* showed a positive correlation with each other but showed a negative correlation with *rBmall*. *rRora* showed negative correlation with *rPer1*, *rPer2*, *rCry1*, *rCry2* and *rRev-erba*, but showed positive correlation with *rBmall*. In 3 m DP of CT animals, *rPer1*, *rPer2*, *rCry1*, *rCry2* and *rRev-erba* showed positive correlation with each other. *rBmall* and *rPer1*; *rBmall* and *rPer2*; *rBmall* and *rCry2*; *rPer1* and *rRora* showed negative correlation. In 12 m LP of CT animals, curcumin showed restoration of

negative correlation between *rBmall* and *rPer1*; *rBmall* and *rPer2*; *rPer1* and *rCry1*; *rCry1* and *rRev-erba* in comparison to 3 m LP of VT group. In 12 m DP of CT animals, curcumin restored the negative correlation between *rBmall* and *rPer1*; *rBmall* and *rPer2*; *rPer2* and *rCry1* in comparison to 3 m DP of VT group. In 24 m LP of CT animals, curcumin restored the positive correlation between *rCry2* and *rRev-erba* in comparison to 3 m LP of VT group. In 24 m DP of CT animals, curcumin restored the negative correlation between *rPer1* and *rRev-erba*; *rPer2* and *rRev-erba* (Fig. 38).

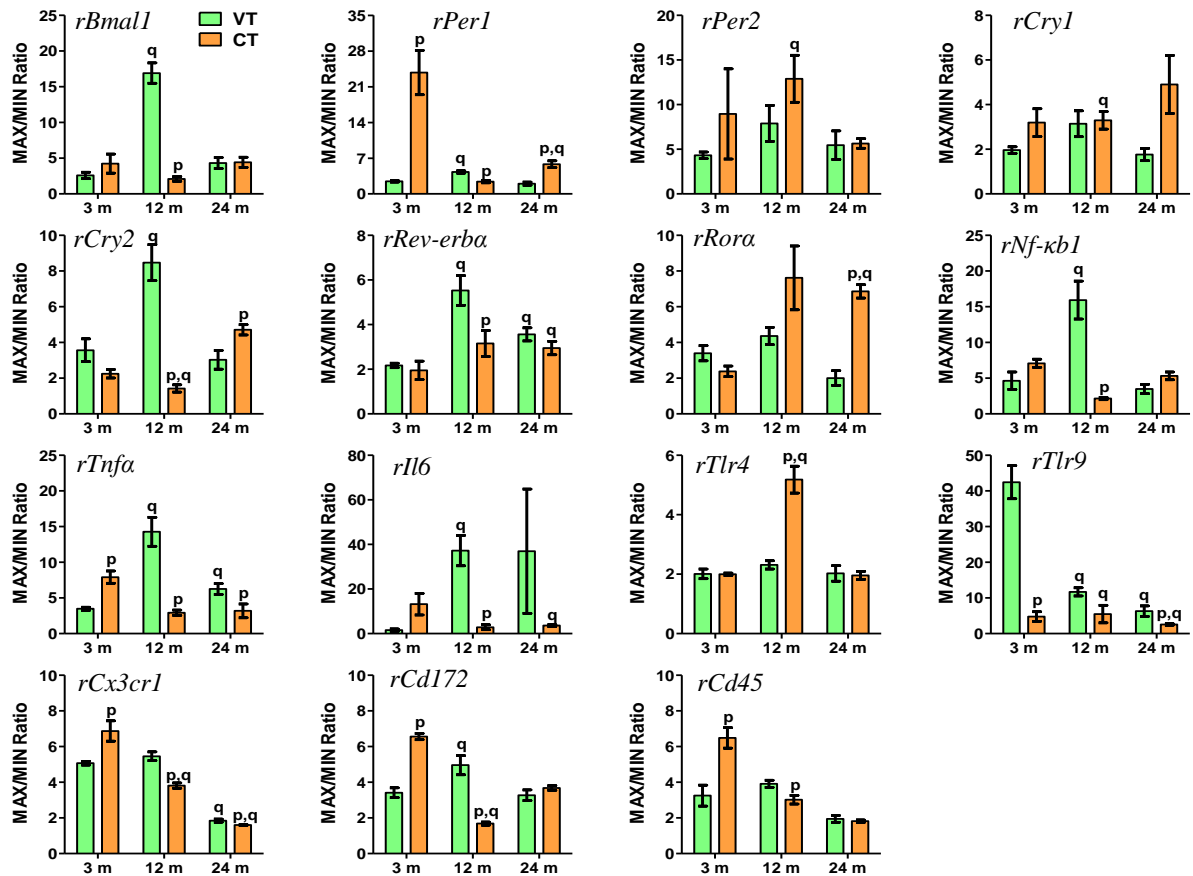


Fig. 37: Effect of curcumin administration on daily pulse of clock, immune and microglia resting genes expression in 3, 12 and 24 months (m) old rat microglia. Each value is mean \pm SEM ($n = 4$), $p \leq 0.05$ and expressed as mean relative gene expression. $p_p \leq 0.05$ (where ‘p’ refers to comparison with the age-matched vehicle-treated group). $p_q \leq 0.05$ (where ‘q’ refers to comparison with 3 m vehicle-treated group).

Effect of curcumin on correlations among immune genes

In 3 m LP of CT animals, *rNf-kb1* showed an insignificant positive correlation with other immune genes. Whereas the other immune genes showed a significant positive correlation with each other. In 3 m DP of CT animals, *rNf-kb1* showed a negative correlation with *rIl6*. *rTnfa* and *rTlr4*; *rTnfa* and *rTlr9*; *rIl6* and *rTlr9*; *rTlr4* and *rTlr9* showed negative correlation. In 12 m LP

of CT animals, curcumin showed partial restoration of negative correlation between *rNf- κ b1* and *rIl6*; *rIl6* and *rTlr4*. Curcumin restored the negative correlation between *rIl6* and *rTlr9*. In 24 m DP of CT animals, curcumin resulted in a positive correlation between *rNf- κ b1* and *rTlr4*; *rNf- κ b1* and *rTlr9*; *rTnfa* and *rIl6*; *rTlr4* and *rTlr9*. In 24 m LP of CT animals, curcumin showed a positive correlation between *rNf- κ b1* and *rTlr9*; *rTnfa* and *rIl6*; *rTnfa* and *rTlr4*, *rTnfa* and *rTlr9*; *rIl6* and *rTlr4*; *rIl6* and *rTlr9*. In 24 m DP of CT animals, curcumin showed restoration of negative correlation between *rNf- κ b1* and *rTnfa*; *rNf- κ b1* and *rIl6* (Fig. 38)

Effect of curcumin on the correlations among microglia resting genes

In 3 m LP of CT animals, curcumin showed a positive correlation between *rCx3cr1* and *rCd172* but showed a negative correlation between *rCd172* and *rCd45*. In 3 m DP of CT animals, curcumin altered the negative correlation among these genes into positive correlation. In 12 m LP of CT animals, curcumin showed a positive correlation between *rCx3cr1* and *rCd45*. In 12 m DP of CT animals, curcumin showed alteration of negative correlation among these genes into positive correlation. In 24 m LP of CT animals, curcumin showed positive correlation between *rCx3cr1* and *rCd172*, but negative correlation between *rCx3cr1* and *rCd45*; *rCd172* and *rCd45*. In 24 m DP of CT animals, curcumin showed a positive correlation between *rCx3cr1* and *rCd172* but showed partial restoration of negative correlation between *rCx3cr1* and *rCd45* (Fig. 38)

Effect of curcumin on the correlations among clock, immune and microglia resting genes

In 3 m LP of CT animals, *rPer1*, *rPer2*, *rCry1* and *rCry2* showed positive correlation with *rNf- κ b1* but showed negative correlation with *rIl6* and *rTlr9*. *rBmal1* showed positive correlation with *rTnfa*, *rIl6*, *rTlr4* and *rTlr9*. *rRev-erba* showed positive correlation with *rNf- κ b1*, *rTnfa* and *rTlr4*. *rRora* showed negative correlation with *rNf- κ b1*. In 3 m DP of CT animals, *rBmal1* and *rRora* showed positive correlation with *rTnfa*, *rTlr4* and *rTlr9*. *rPer2*, *rCry1*, *rCry2* and *rRev-erba* showed positive correlation with *rNf- κ b1*. *rPer1* showed negative correlation with *rTnfa*, *rIl6*, *rTlr4* and *rTlr9*. *rPer2*, *rCry1*, *rCry2* and *rRev-erba* showed positive correlation with *rIl6*. *rPer2* and *rCry2* showed negative correlation with *rTlr9*. In 12 m LP of CT animals, curcumin restored the negative correlation between *rBmal1* and *rNf- κ b1*; *rBmal1* and *rTnfa*; *rPer2* and *rNf- κ b1*; *rCry1* and *rNf- κ b1*; *rCry1* and *rTnfa*; *rCry2* and *rTlr4*. In 12 m DP of CT animals, curcumin restored the negative correlation between *rBmal1* and *rTnfa*; *rPer1* and *rNf- κ b1*; *rCry1* and *rNf- κ b1*; *rCry1* and *rTlr4*; *rCry1* and *rTlr9*; *rCry2* and *rNf- κ b1*; *rCry2* and *rTlr4*; *rCry2* and *rTlr9* (Fig. 38).

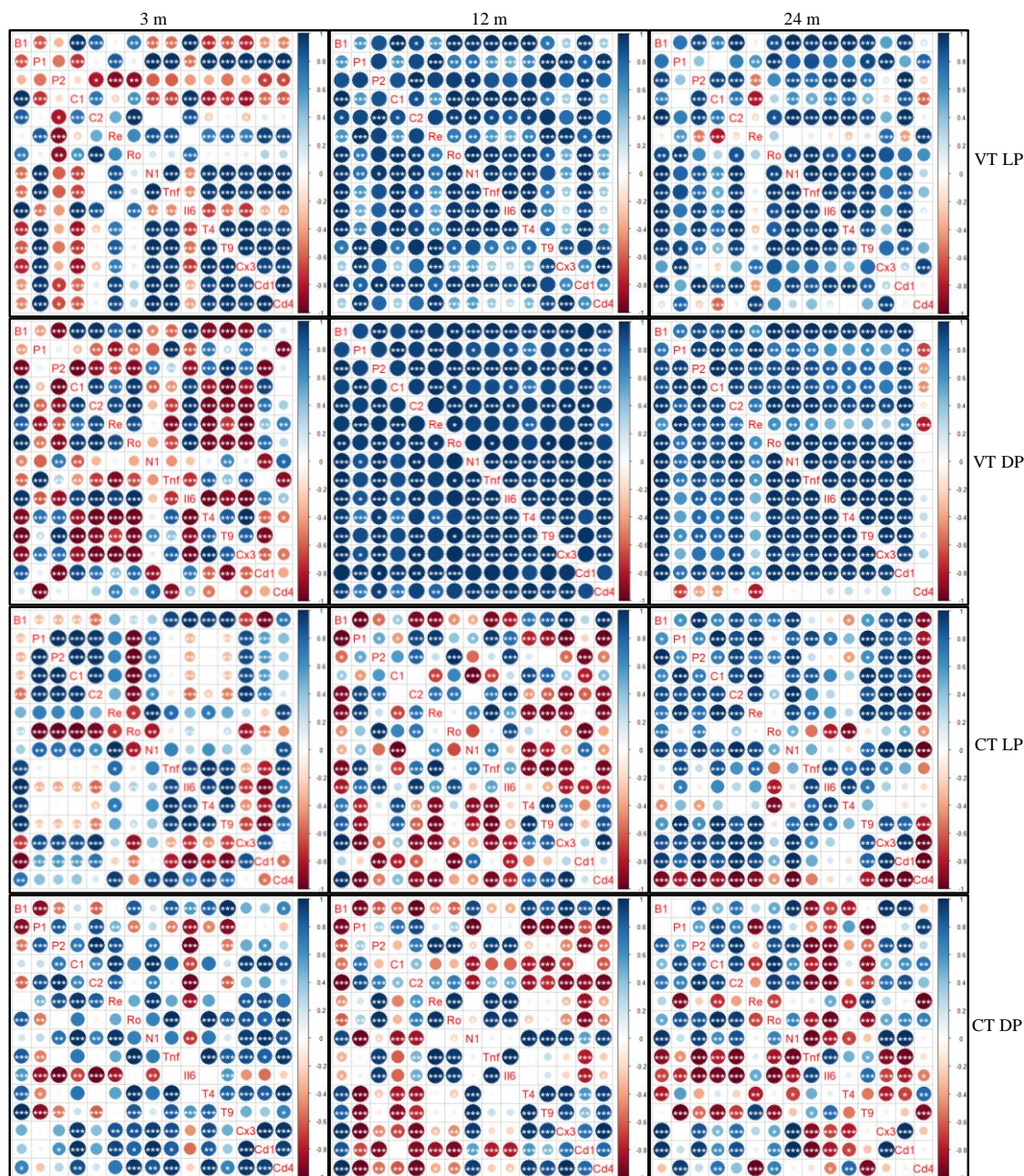


Fig. 38: Effect of curcumin administration on Pair wise correlations among clock, immune and microglia resting genes in light (ZT-0, 6, 12) and dark (ZT-12, 18, 24/0) phase of 3, 12 and 24 months (m) old rat microglia. (LP - light phase; DP - dark phase; VT - vehicle-treated; CT - curcumin treated). Intensity of color and size of circle represents correlation coefficient values between the genes. Where, positive correlations are indicated by shades of blue, negative correlations by shades of red, and white indicates no correlation. ‘*’, ‘**’, ‘***’ indicates statistically significant correlations ($p \leq 0.05$), ($p \leq 0.01$), ($p \leq 0.001$) respectively. (B1- *rBmall*; P1 - *rPer1*; P2 - *rPer2*; C1 - *rCry1*; C2 - *rCry2*; Re - *rRev-erba*; Ro - *rRora*; N1 - *rNfkb1*; Tnf - *rTnfa*; Il6 - *rIl6*; T4 - *rTlr4*; T9 - *rTlr9*; Cx3 - *rCx3cr1*; Cd1 - *rCd172*; Cd4 - *rCd45*).

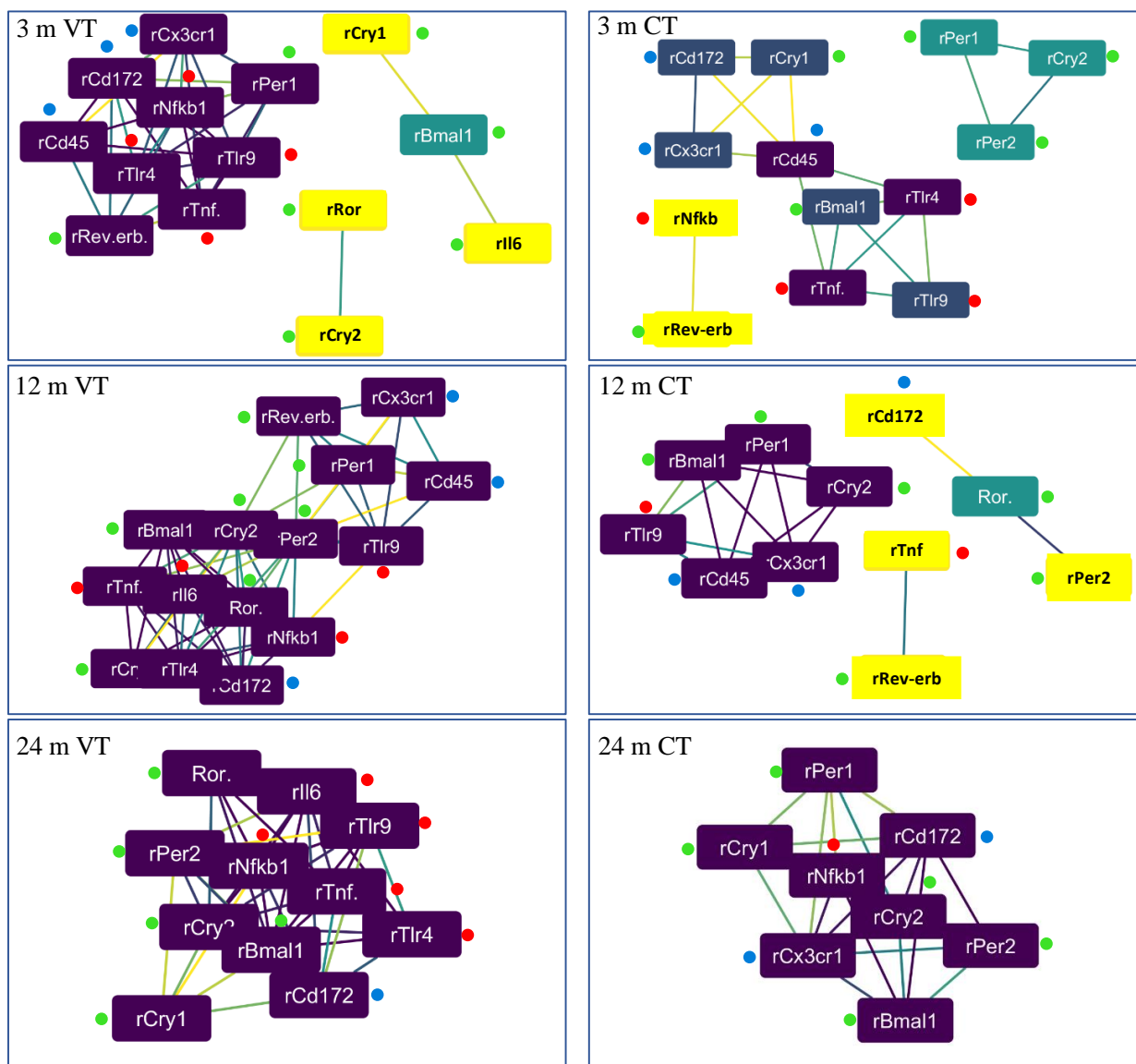


Fig. 39: WGCNA analysis between clock, immune and microglia gene clusters: Effect of aging on gene to gene network in 3, 12 and 24 m old rat microglia (left panel) and effect of curcumin administration (right panel). Color of the node indicates no. of interactions (highest—purple; intermediate—cyan and least—yellow). Color of an edge indicates the strength of interaction (strongest—purple; cyan—intermediate and weakest—yellow). Green, red and blue dots indicate clock, immune and microglia resting genes respectively.

Table 6: Effect of curcumin on age-induced alterations of clock genes expression

<i>Gene</i>		ZT-0	ZT-6	ZT-12	ZT-18	Mean 24 h levels	Max/min ratio
<i>rBmal1</i>	3 m VT	0.81 ± 0.12	0.32 ± 0.02	0.32 ± 0.01	0.48 ± 0.03	0.48 ± 0.06	2.59 ± 0.45
	3 m CT	1.07 ± 0.07	0.33 ± 0.07	0.44 ± 0.05	1.18 ± 0.1	0.76 ± 0.1 x	4.24 ± 1.33
	12 m VT	1.52 ± 0.08	0.54 ± 0.01	0.09 ± 0.01	0.33 ± 0.03	0.62 ± 0.14	16.91 ± 1.43 y
	12 m CT	0.93 ± 0.04	0.5 ± 0.06	0.48 ± 0.07	0.52 ± 0.01	0.61 ± 0.05	2.1 ± 0.34 x
	24 m VT	1.38 ± 0.17	0.69 ± 0.02	0.35 ± 0.03	0.33 ± 0.02	0.69 ± 0.12	4.32 ± 0.76
	24 m CT	2.27 ± 0.26	0.53 ± 0.03	0.76 ± 0.03	1.56 ± 0.14	1.28 ± 0.19 x,y	4.43 ± 0.7
<i>rPer1</i>	3 m VT	0.38 ± 0.03	0.94 ± 0.07	0.47 ± 0.02	0.72 ± 0.06	0.63 ± 0.06	2.46 ± 0.15
	3 m CT	0.24 ± 0.01	0.09 ± 0.02	1.92 ± 0.09	0.77 ± 0.04	0.75 ± 0.19	23.79 ± 4.35 x
	12 m VT	0.98 ± 0.04	1.18 ± 0.04	0.28 ± 0.03	0.68 ± 0.02	0.78 ± 0.09	4.29 ± 0.24 y
	12 m CT	0.12 ± 0.01	0.26 ± 0.03	0.25 ± 0.01	0.29 ± 0.04	0.23 ± 0.02 x,y	2.41 ± 0.23 x
	24 m VT	1.04 ± 0.09	1.05 ± 0.08	0.9 ± 0.03	0.54 ± 0.05	0.88 ± 0.06 y	2 ± 0.3
	24 m CT	0.49 ± 0.03	0.12 ± 0	0.49 ± 0.03	0.68 ± 0.06	0.44 ± 0.05 x,y	5.82 ± 0.68 x,y
<i>rPer2</i>	3 m VT	0.08 ± 0	0.29 ± 0.01	0.07 ± 0.01	0.07 ± 0.01	0.13 ± 0.02	4.33 ± 0.37
	3 m CT	0.2 ± 0.05	0.18 ± 0.04	1.01 ± 0.21	0.87 ± 0.15	0.57 ± 0.11 x	8.95 ± 5.05
	12 m VT	0.29 ± 0.04	0.24 ± 0.02	0.04 ± 0	0.09 ± 0.01	0.16 ± 0.03	7.89 ± 2.02
	12 m CT	0.28 ± 0.04	0.38 ± 0.04	3.34 ± 0.36	0.48 ± 0.06	1.12 ± 0.34 x,y	12.89 ± 2.63 y
	24 m VT	0.43 ± 0.09	0.21 ± 0.03	0.24 ± 0.02	0.09 ± 0.01	0.24 ± 0.04 y	5.46 ± 1.59
	24 m CT	1.54 ± 0.16	0.28 ± 0.02	0.51 ± 0.04	1.61 ± 0.23	0.99 ± 0.17 x,y	5.65 ± 0.54
<i>rCry1</i>	3 m VT	0.24 ± 0.02	0.21 ± 0.01	0.12 ± 0.02	0.18 ± 0.01	0.19 ± 0.01	1.96 ± 0.14
	3 m CT	0.07 ± 0.01	0.07 ± 0.01	0.14 ± 0.02	0.22 ± 0.03	0.12 ± 0.02 x	3.19 ± 0.62
	12 m VT	0.32 ± 0.02	0.17 ± 0.02	0.11 ± 0.01	0.23 ± 0.02	0.21 ± 0.02	3.15 ± 0.58
	12 m CT	0.06 ± 0.01	0.03 ± 0	0.07 ± 0.01	0.09 ± 0.01	0.06 ± 0.01 x,y	3.3 ± 0.39 y
	24 m VT	0.29 ± 0.05	0.17 ± 0.01	0.23 ± 0.02	0.17 ± 0.01	0.21 ± 0.02	1.76 ± 0.27
	24 m CT	0.18 ± 0.01	0.05 ± 0.01	0.17 ± 0.01	0.2 ± 0.02	0.15 ± 0.02 x	4.9 ± 1.3
<i>rCry2</i>	3 m VT	0.83 ± 0.15	0.57 ± 0.03	0.23 ± 0.01	0.34 ± 0.02	0.49 ± 0.07	3.57 ± 0.64
	3 m CT	0.14 ± 0.01	0.17 ± 0.06	0.31 ± 0.03	0.27 ± 0.03	0.22 ± 0.02 x	2.25 ± 0.24
	12 m VT	1.15 ± 0.08	0.9 ± 0.01	0.14 ± 0.01	0.38 ± 0.01	0.64 ± 0.11	8.47 ± 1.01 y
	12 m CT	0.15 ± 0.02	0.19 ± 0.05	0.21 ± 0.01	0.19 ± 0.02	0.18 ± 0.01 x,y	1.42 ± 0.2 x,y
	24 m VT	1.21 ± 0.14	0.74 ± 0.04	0.56 ± 0.03	0.41 ± 0.02	0.73 ± 0.08 y	3.03 ± 0.53
	24 m CT	0.47 ± 0.01	0.11 ± 0.01	0.3 ± 0.02	0.52 ± 0.03	0.35 ± 0.04 x	4.71 ± 0.29 x
<i>rRev-erba</i>	3 m VT	0.98 ± 0.06	1.35 ± 0.04	0.71 ± 0.09	0.63 ± 0.04	0.92 ± 0.08	2.17 ± 0.1
	3 m CT	0.24 ± 0.01	0.14 ± 0.01	0.26 ± 0.01	0.27 ± 0.05	0.23 ± 0.02 x	1.95 ± 0.42
	12 m VT	0.9 ± 0.05	1.08 ± 0.04	0.21 ± 0.03	0.53 ± 0.01	0.68 ± 0.09	5.53 ± 0.67 y
	12 m CT	0.12 ± 0.01	0.29 ± 0.02	0.23 ± 0.03	0.1 ± 0.02	0.18 ± 0.02 x,y	3.16 ± 0.58 x
	24 m VT	0.91 ± 0.14	1.71 ± 0.09	0.86 ± 0.03	0.49 ± 0.03	0.99 ± 0.12	3.56 ± 0.3 y
	24 m CT	0.46 ± 0.04	0.15 ± 0	0.39 ± 0.02	0.28 ± 0.04	0.32 ± 0.03 x,y	2.95 ± 0.3 x
<i>rRora</i>	3 m VT	1.41 ± 0.06	1.15 ± 0.06	0.43 ± 0.04	0.66 ± 0.04	0.91 ± 0.1	3.4 ± 0.43
	3 m CT	0.46 ± 0.03	0.48 ± 0.07	0.32 ± 0.04	0.73 ± 0.06	0.49 ± 0.05 x	2.38 ± 0.3
	12 m VT	1.54 ± 0.1	0.89 ± 0.02	0.36 ± 0.02	0.68 ± 0	0.87 ± 0.11	4.36 ± 0.48
	12 m CT	0.41 ± 0.06	0.27 ± 0.06	1.76 ± 0.1	0.47 ± 0.02	0.73 ± 0.16	7.62 ± 1.79
	24 m VT	1.29 ± 0.21	1.13 ± 0.15	0.67 ± 0.06	0.66 ± 0.04	0.93 ± 0.09	2.01 ± 0.41
	24 m CT	0.61 ± 0.05	0.43 ± 0.01	0.16 ± 0.02	1.11 ± 0.1	0.58 ± 0.09 x,y	6.86 ± 0.38 x,y

mRNA expression of clock genes at ZT-0,6, 12 and 18. $p_x \leq 0.05$, $p_y \leq 0.05$ where ‘x’ refers to significant difference with the respective age-matched vehicle group. ‘y’ refers to significant difference with 3 m vehicle-treated group.

Table 7: Effect of curcumin on age-induced alterations of immune and microglia resting genes

Gene		ZT-0	ZT-6	ZT-12	ZT-18	Mean 24 h levels	Max/min ratio
<i>rNf-κb1</i>	3 m VT	0.74 ± 0.03	2.77 ± 0.45	0.91 ± 0.05	0.64 ± 0.08	1.26 ± 0.25	4.65 ± 1.22
	3 m CT	0.86 ± 0.06	0.22 ± 0.03	1.17 ± 0.09	1.52 ± 0.11	0.94 ± 0.13	7.08 ± 0.58
	12 m VT	4.33 ± 0.65	2.33 ± 0.06	0.27 ± 0.02	0.66 ± 0.04	1.9 ± 0.44	15.93 ± 2.65 _y
	12 m CT	0.59 ± 0.06	1.04 ± 0.08	0.53 ± 0.03	0.5 ± 0.07	0.66 ± 0.06 _{x,y}	2.15 ± 0.16 _x
	24 m VT	3.2 ± 0.42	2.03 ± 0.04	1.19 ± 0.1	0.95 ± 0.06	1.84 ± 0.25	3.49 ± 0.65
	24 m CT	1.85 ± 0.13	0.35 ± 0.01	0.98 ± 0.05	1.6 ± 0.14	1.2 ± 0.16 _x	5.32 ± 0.54
<i>rTnfa</i>	3 m VT	0.16 ± 0.01	0.55 ± 0.01	0.19 ± 0.01	0.24 ± 0.02	0.29 ± 0.04	3.49 ± 0.22
	3 m CT	0.15 ± 0.01	0.04 ± 0.01	0.1 ± 0.01	0.27 ± 0.02	0.14 ± 0.02 _x	7.91 ± 0.87 _x
	12 m VT	1.03 ± 0.1	0.37 ± 0.02	0.07 ± 0	0.2 ± 0.01	0.42 ± 0.1	14.27 ± 2.02 _y
	12 m CT	0.08 ± 0.01	0.17 ± 0.02	0.14 ± 0.02	0.06 ± 0.01	0.11 ± 0.01 _{x,y}	2.93 ± 0.37 _x
	24 m VT	0.59 ± 0.07	0.37 ± 0.05	0.09 ± 0	0.1 ± 0.01	0.29 ± 0.06	6.25 ± 0.75 _y
	24 m CT	0.16 ± 0.02	0.08 ± 0.01	0.22 ± 0.04	0.16 ± 0.02	0.16 ± 0.02 _{x,y}	3.19 ± 0.96 _x
<i>rIl6</i>	3 m VT	0.19 ± 0.04	0.14 ± 0.01	0.14 ± 0.03	0.15 ± 0.02	0.15 ± 0.01	1.59 ± 0.53
	3 m CT	0.13 ± 0.03	0.01 ± 0	0.03 ± 0.01	0.05 ± 0.01	0.06 ± 0.01 _x	13.22 ± 4.83
	12 m VT	0.61 ± 0.09	0.15 ± 0	0.02 ± 0	0.06 ± 0.01	0.21 ± 0.06	37.25 ± 6.8 _y
	12 m CT	0.02 ± 0	0.03 ± 0.01	0.04 ± 0.01	0.01 ± 0	0.02 ± 0 _{x,y}	2.86 ± 1.1 _x
	24 m VT	0.4 ± 0.07	0.15 ± 0.02	0.03 ± 0.01	0.09 ± 0.01	0.17 ± 0.04	36.96 ± 27.87
	24 m CT	0.07 ± 0.01	0.05 ± 0	0.14 ± 0.01	0.04 ± 0	0.08 ± 0.01 _{x,y}	3.63 ± 0.43 _y
<i>rTlr4</i>	3 m VT	1.82 ± 0.03	3.65 ± 0.26	2.43 ± 0.07	2.46 ± 0.11	2.59 ± 0.18	2.01 ± 0.16
	3 m CT	0.98 ± 0.05	0.69 ± 0.02	0.82 ± 0.05	1.37 ± 0.02	0.96 ± 0.07 _x	2 ± 0.04
	12 m VT	4.63 ± 0.18	3.29 ± 0.09	2.43 ± 0.19	2.01 ± 0.06	3.09 ± 0.27	2.31 ± 0.14
	12 m CT	2.13 ± 0.09	0.42 ± 0.04	1.56 ± 0.06	1.31 ± 0.08	1.36 ± 0.16 _{x,y}	5.18 ± 0.45 _{x,y}
	24 m VT	3.51 ± 0.38	2.12 ± 0.07	1.76 ± 0.11	2.18 ± 0.06	2.39 ± 0.19	2.03 ± 0.26
	24 m CT	0.8 ± 0.05	0.86 ± 0.02	1.51 ± 0.08	1.56 ± 0.11	1.18 ± 0.1 _{x,y}	1.96 ± 0.13
<i>rTlr9</i>	3 m VT	0.04 ± 0.01	1.54 ± 0.08	0.28 ± 0.03	0.15 ± 0.02	0.5 ± 0.16	42.45 ± 4.65
	3 m CT	0.91 ± 0.16	0.25 ± 0.05	0.38 ± 0.05	1 ± 0.09	0.63 ± 0.09	4.79 ± 1.34 _x
	12 m VT	2.3 ± 0.15	2.37 ± 0.05	0.21 ± 0.02	0.51 ± 0.07	1.35 ± 0.26 _y	11.71 ± 1.15 _y
	12 m CT	0.85 ± 0.06	0.24 ± 0.07	0.55 ± 0.04	0.29 ± 0.01	0.48 ± 0.07 _x	5.48 ± 2.45 _y
	24 m VT	1.6 ± 0.26	1.07 ± 0.07	0.29 ± 0.06	0.48 ± 0.12	0.86 ± 0.15	6.29 ± 1.49 _y
	24 m CT	1.05 ± 0.06	0.49 ± 0.02	1.07 ± 0.13	0.51 ± 0.04	0.78 ± 0.08	2.55 ± 0.2 _{x,y}
<i>rCx3cr1</i>	3 m VT	10.83 ± 0.25	54.9 ± 2.07	27.17 ± 0.65	27.94 ± 0.63	30.21 ± 4.11	5.07 ± 0.1
	3 m CT	10.08 ± 0.52	14 ± 1.28	19.8 ± 0.47	68.51 ± 3	28.1 ± 6.14	6.87 ± 0.57 _x
	12 m VT	69.21 ± 2.64	108.65 ± 3.01	20.09 ± 1.42	24.77 ± 0.75	55.68 ± 9.37 _y	5.46 ± 0.24
	12 m CT	41.34 ± 2.39	14.65 ± 0.17	13.28 ± 0.17	10.84 ± 0.54	20.03 ± 3.24 _x	3.81 ± 0.15 _{x,y}
	24 m VT	47.91 ± 3.85	55.2 ± 3.62	29.91 ± 1.77	35.25 ± 1.47	42.07 ± 2.89 _y	1.85 ± 0.09 _y
	24 m CT	35.31 ± 1.25	22.02 ± 0.41	29.55 ± 0.82	32.68 ± 2.06	29.89 ± 1.41 _x	1.6 ± 0.03 _{x,y}
<i>rCd172</i>	3 m VT	5.73 ± 0.08	17.11 ± 1.22	5.03 ± 0.12	5.62 ± 0.41	8.37 ± 1.34	3.41 ± 0.28
	3 m CT	1.43 ± 0.07	3.39 ± 0.12	3.69 ± 0.16	9.34 ± 0.32	4.46 ± 0.77 _x	6.56 ± 0.17 _x
	12 m VT	11.94 ± 0.83	7.94 ± 0.17	2.45 ± 0.2	5.63 ± 0.08	6.99 ± 0.91	4.96 ± 0.54 _y
	12 m CT	2.7 ± 0.3	3.05 ± 0.18	1.81 ± 0.04	2.34 ± 0.16	2.48 ± 0.15 _{x,y}	1.68 ± 0.09 _{x,y}
	24 m VT	16.51 ± 2.05	6.06 ± 0.32	5.57 ± 0.26	5.02 ± 0.19	8.29 ± 1.32	3.27 ± 0.3
	24 m CT	5.73 ± 0.24	1.56 ± 0.04	3.35 ± 0.22	5.06 ± 0.4	3.92 ± 0.43 _{x,y}	3.68 ± 0.13
<i>rCd45</i>	3 m VT	24.49 ± 1.25	51.88 ± 1.23	24.59 ± 1.15	17.05 ± 2.05	29.5 ± 3.49	3.25 ± 0.59
	3 m CT	22.27 ± 0.76	8.19 ± 0.57	19.71 ± 0.52	52.34 ± 2.98	25.63 ± 4.27	6.49 ± 0.57 _x
	12 m VT	57.61 ± 7.89	81.96 ± 1.44	27.27 ± 1.62	21.15 ± 1.44	47 ± 6.58 _y	3.92 ± 0.2
	12 m CT	37.26 ± 3.11	12.44 ± 0.96	13.16 ± 0.89	12.88 ± 0.19	18.93 ± 2.83 _{x,y}	3.02 ± 0.24 _x
	24 m VT	29.62 ± 2.55	42.48 ± 2.87	22.04 ± 0.95	36.69 ± 1.06	32.71 ± 2.18	1.94 ± 0.19
	24 m CT	26.99 ± 1.65	40.11 ± 1.02	34.22 ± 2.45	48.88 ± 2.77	37.55 ± 2.27	1.82 ± 0.07

mRNA expression of immune and microglia resting genes at ZT-0,6, 12, and 18. $p_x \leq 0.05$, $p_y \leq 0.05$ where 'x' refers to significant difference with the respective age-matched vehicle group. 'y' refers to significant difference with 3 m vehicle-treated group.

In 24 m LP of CT animals, curcumin restored the negative correlation between *rBmal1* and *rTlr4*; *rPer2* and *rTlr4*. In 24 m DP of CT animals, curcumin restored the negative correlation between *rBmal1* and *rTnfa*; *rBmal1* and *rTlr4*; *rPer1* and *rIl6*; *rPer2* and *rIl6*; *rCry1* and *rTnfa*; *rCry2* and *rTnfa*; *rCry1* and *rTlr9*; *rCry2* and *rTlr9*; *rRev-erba* and *rTlr4*; *rRora* and *rTnfa*; *rRora* and *rTlr9* (Fig. 38).

In 3 m LP of CT animals, *rCx3cr1* and *rCd172* showed positive correlation with *rPer1*, *rPer2*, *rCry1* and *rCry2*. *rCx3cr1* and *rCd172* showed negative correlation with *rBmal1* and *rRora*. *rCd45* showed positive correlation with *rBmal1* and *rRev-erba*. In 3 m DP of CT animals, *rCx3cr1* and *rCd172* showed positive correlation with *rCry1*, *rRev-erba* and *rRora*. *rCd45* showed positive correlation with *rCry1* and *rRora*. In 12 m LP of CT animals, curcumin restored negative correlation of *rCx3cr1*, *rCd172* and *rCd45* with *rPer2*. Also curcumin restored negative correlation between *rCd172* and *rCry1*; *rCx3cr1* and *rCry2*. In 12 m DP of CT animals, curcumin restored negative correlation between *rPer1* and *rCd45*; *rPer2* and *rCd172*; *rCry1* and *rCx3cr1*; *rCry2* and *rCx3cr1*; *rRev-erba* and *rCx3cr1*; *rRora* and *rCx3cr1*. In 24 m LP of CT animals, *rCx3cr1* and *rCd172* showed positive correlation and *rCd45* showed negative correlation with all clock genes. In 24 m DP of CT animals, curcumin partially restored positive correlation between *rCry2* and *rCd45*; *rRora* and *rCd45* (Fig. 38).

WGCNA analysis among clock, immune and microglia resting genes with curcumin treatment

In 3 m CT, *rNf- κ b1* showed weak interaction with *rRev-erba*, but *rBmal1* showed interactions with other immune genes. *rCry1* showed weak interactions with microglia resting genes. In 12 m CT, *rTnfa* showed interaction with *rRev-erba*; *rBmal1* showed interaction with *rTlr9*. *rCx3cr1* and *rCd45* showed interactions with *rBmal1*, *rPer1* and *rCry2*. In 24 m CT, only *rNf- κ b1* showed interactions with clock genes and microglia resting genes (Fig. 39).

II. A (i). Age-induced alterations of clock and immune genes mRNA expression in liver

Effect of aging on the daily rhythms of clock genes in liver

There was no change in the expression of all the genes between C and VT animal groups. In the liver of 3 m animals, *rBmal1* showed maximum expression at ZT-0 and minimum expression at ZT-12. *rPer1* and *rRev-erba* showed maximum expression at ZT-6 and minimum expression at ZT-18. *rPer2* showed maximum expression at ZT-12 and minimum expression at ZT-6. *rCry1*, *rCry2*, and *rRora* showed maximum expression at ZT-18 and minimum expression at ZT-6. With aging, *rBmal1*, *rPer2*, *rCry1*, *rRev-erba* did not show variation in the maximum expression. However, *rPer1* showed 6 h phase delay in 12 and 24 m animals. *rCry2* and *rRora* showed 6 h phase advance and 6 h phase delay in 12 and 24 m respectively (Fig. 40) (Table 8).

Effect of aging on the daily rhythms of immune genes expression in liver

In the liver of 3 m animals, *rNf- κ b1* and *rTlr4* showed maximum expression at ZT-6 and minimum expression at ZT-12. *rTnfa*, *rIl6*, and *rTlr9* showed maximum expression at ZT-12 and minimum expression at ZT-6. With aging, *rNf- κ b1* showed 6 h phase advance in 12 and 24 m in comparison to 3 m. *rTnfa* rhythmicity was abolished in 12 m but showed 6 h phase advance in 24 m in comparison to 3 m. *rIl6* showed 6 h phase delay in 12 m in comparison to 3 m. *rTlr4* and *rTlr9* showed 6 h phase delay in 12 m and 6 h phase advance in 24 m in comparison to 3 m (Fig. 41) (Table 9).

Effect of aging on mean 24 h levels and daily pulse of clock genes in liver

Mean 24 h levels of *rBmal1*, *rCry1*, *rRev-erba*, and *rRora* did not vary significantly with aging. *rPer1* showed increased expression in 12 m and decreased expression in 24 m in comparison to 3 m animals. *rPer2* and *rCry2* showed decreased mean levels in 24 m animals in comparison to 3 m animals (Fig. 42). Daily pulse of *rBmal1* was decreased in 12 m but did not alter in 24 m. *rPer1* and *rPer2* showed increased daily pulse in 12 m but did not alter in 24 m. *rCry1* and *rRora* showed decreased daily pulse, whereas *rCry2* showed increased daily pulse in 12 and 24 m. *rRev-erba* showed did not alter in 12 m but increased in 24 m (Fig. 43) (Table 8).

Effect of aging on mean 24 h levels and daily pulse of immune genes expression

With aging, *rNf- κ b1* and *rIl6* showed increased expression in 12 m but did not alter in 24 m in comparison to 3 m. *rTnfa* and *rTlr9* showed increased mean levels in 12 and 24 m in comparison to 3 m. *rTlr4* showed decreased in 12 m but did not alter in 24 m in comparison to 3 m (Fig. 42). Daily pulse of *rNf- κ b1* showed an increase and *rTlr4* showed a decrease in 12 and 24 m in comparison to 3 m. *rIl6* and *rTlr9* showed an increase in 12 and 24 m respectively in comparison to 3 m. *rTnfa* showed a decrease in 12 m and an increase in 24 m in comparison to 3 m (Fig. 43).

Effect of aging on correlation among clock genes expression

In 3 m LP, *rBmall* and *rRev-erba*; *rBmall* and *rPer1*; *rPer1* and *rPer2*; *rPer1* and *rCry1*; *rPer1* and *rCry2*; *rPer1* and *rRora*; *rPer2* and *rRev-erba*; *rCry1* and *rRev-erba*; *rCry2* and *rRev-erba*; *rRev-erba* and *rRora* showed negative correlation. *rBmall* and *rCry1*; *rBmall* and *rCry2*; *rBmall* and *rRora*; *rPer1* and *rRev-erba*; *rCry1* and *rCry2*; *rCry1* and *rRora*; *rCry2* and *rRora* showed positive correlation. In 3 m DP, *rBmall* and *rPer1*; *rBmall* and *rPer2*; *rBmall* and *rRev-erba*; *rPer1* and *rCry1*; *rPer1* and *rCry2*; *rPer1* and *rRora*; *rCry1* and *rRev-erba*; *rCry2* and *rRev-erba*; *rRev-erba* and *rRora* showed negative correlation. *rBmall* and *rCry1*; *rBmall* and *rCry2*; *rBmall* and *rRora*; *rPer1* and *rPer2*; *rPer1* and *rRev-erba*; *rPer2* and *rRev-erba*; *rCry1* and *rCry2*; *rCry1* and *rRora*; *rCry2* and *rRora* showed positive correlation (Fig. 44).

In 12 m LP, negative correlation was persisted between *rBmall* and *rPer1*; *rBmall* and *rRev-erba*; *rCry1* and *rRev-erba*; *rRev-erba* and *rRora*. Positive correlation was persisted between *rCry1* and *rRora*. But *rBmall* turned to negative correlation with *rPer2* and *rCry2*. Similarly, *rPer1* and *rPer2*; *rPer1* and *rCry1*; *rPer1* and *rCry2*; *rPer2* and *rCry1*; *rPer2* and *rCry2*; *rCry2* and *rRev-erba*; *rPer2* and *rRora*; *rCry1* and *rRora* turned to positive correlation. In 12 m DP, negative correlation persisted between *rBmall* and *rPer1*; *rBmall* and *rPer2*. Similarly, positive correlation between *rPer1* and *rPer2*; *rPer1* and *rRev-erba*; *rPer2* and *rRev-erba*; *rCry2* and *rRora*. However, *rBmall* and *rCry1*; *rCry1* and *rCry2*; *rCry1* and *rRora* turned to negative correlation. *rPer1* and *rCry2*; *rPer1* and *rRora*; *rPer2* and *rCry2*; *rPer2* and *rRora*; *rCry2* and *rRev-erba*; *rRev-erba* and *rRora* turned to positive correlation (Fig. 44).

In 24 m LP, negative correlation persisted between *rBmall* and *rPer1*; *rBmall* and *rRev-erba*; *rPer1* and *rCry2*; *rCry2* and *rRev-erba*; *rRev-erba* and *rRora*; *rPer1* and *rRora*. Similarly, positive correlation was persisted between *rBmall* and *rCry2*; *rBmall* and *rRora*; *rPer1* and *rRev-erba*; *rCry2* and *rRora*. But *rPer2* and *rCry1* turned to positive correlation. In 24 m DP,

negative correlation persisted between *rBmall* and *rPer1*; *rBmall* and *rPer2*; *rBmall* and *rRev-erba*; *rPer1* and *rRora*; *rRev-erba* and *rRora*. Similarly, positive correlation persisted between *rBmall* and *rCry2*; *rBmall* and *rRora*; *rPer1* and *rPer2*; *rPer1* and *rRev-erba*; *rPer2* and *rRev-erba*; *rCry2* and *rRora*. However, *rBmall* and *rCry1*; *rPer2* and *rRora*; *rCry1* and *rCry2*; *rCry1* and *rRora* turned to negative correlation (Fig. 44).

Effect of aging on the correlation among immune genes expression in liver

In 3 m LP, *rTnfa*, *rIl6*, and *rTlr9* showed a positive correlation with each other but showed a negative correlation with *rNf- κ b1* and *rTlr4* where these genes showed a positive correlation between each other. In 3 m DP, *rTnfa*, *rIl6* and *rTlr9* showed a positive correlation with each other but showed a negative correlation with *rNf- κ b1*. *rTnfa* showed a positive correlation with *rTlr4*. Correlation of *rTlr4* with *rIl6* and *rTlr9* was abolished (Fig. 44).

In 12 m LP, a negative correlation between *rTnfa* and *rTlr4* was persisted. Positive correlation between *rIl6* and *rTlr9* was persisted. However, *rTnfa* and *rIl6*; *rTnfa* and *rTlr9* turned to negative correlation. *rNf- κ b1* and *rTnfa*; *rIl6* and *rTlr4*; *rTlr4* and *rTlr9* to positive correlation. In 12 m DP, negative correlation between *rNf- κ b1* and *rIl6*; *rNf- κ b1* and *rTlr9* persisted. Positive correlation between *rIl6* and *rTlr9* persisted. But, *rTnfa* and *rIl6*; *rTnfa* and *rTlr9* turned to negative correlation. *rNf- κ b1* and *rTnfa* turned to a positive correlation (Fig. 44).

In 24 m LP, negative correlation persisted between *rNf- κ b1* and *rIl6*; *rIl6* and *rTlr6*. Positive correlation persisted between *rNf- κ b1* and *rTlr4*; *rTnfa* and *rTlr9*. However, *rTnfa* and *rIl6*; *rIl6* and *rTlr9* turned to negative correlation. *rNf- κ b1* and *rTnfa*; *rNf- κ b1* and *rTlr9*; *rTnfa* and *rTlr4*; *rTlr4* and *rTlr9* turned to positive correlation. In 24 m DP, the correlation among the inflammatory genes remained similar to 24 m LP (Fig. 44).

Effect of aging on the correlation between clock and immune genes in liver

In 3 m LP, *rNf- κ b1* and *rPer2*; *rPer1* and *rIl6* showed a negative correlation. *rNf- κ b1* and *rPer1*; *rPer2* and *rTnfa*; *rPer2* and *rIl6* showed positive correlation. *rPer2*, *rCry1*, *rCry2* and *rRora* showed negative correlation with *rTlr4* and positive correlation with *rTlr9*. *rPer1* and *rRev-erba* showed a negative correlation with *rTlr9* and positive correlation with *rTlr4*. In 3 m DP, *rBmall*, *rCry1*, *rCry2*, and *rRora* showed a positive correlation with *rNf- κ b1* but showed a negative correlation with *rTnfa*, *rIl6* and *rTlr9*. *rPer1* and *rRev-erba* showed a negative correlation with *rNf- κ b1* but showed a positive correlation with *rTnfa*, *rIl6* and *rTlr9*. *rPer2* and *rNf- κ b1*; *rPer1*

and *rTlr4*; *rPer2* and *rTlr4*; *rRev-erba* and *rTlr4* showed negative correlation. *rPer2* and *rTnfa*; *rBmall* and *rTlr4* showed a positive correlation (Fig. 44).

In 12 m LP, *rBmall* showed positive correlation with *rTnfa*, but showed negative correlation with *rIl6*, *rTlr4* and *rTlr9*. *rPer1*, *rPer2* and *rCry2* showed negative correlation with *rTnfa*, but showed positive correlation with *rIl6*, *rTlr4* and *rTlr9*. *rBmall* and *rNf- κ b1*; *rCry1* and *rNf- κ b1*; *rCry1* and *rIl6*; *rRora* and *rNf- κ b1*; *rRora* and *rIl6* showed positive correlation. *rCry2* and *rNf- κ b1*; *rRev-erba* and *rNf- κ b1*; *rRev-erba* and *rTnfa* showed negative correlation. In 12 m DP, *rBmall* and *rIl6*; *rBmall* and *rTlr9*; *rCry1* and *rNf- κ b1*; *rCry1* and *rTnfa* showed negative correlation. *rPer1* and *rTlr4*; *rPer2* and *rTlr4*; *rCry1* and *rIl6*; *rCry1* and *rTlr9*; *rCry2* and *rNf- κ b1*; *rCry2* and *rTnfa*; *rCry2* and *rTlr4*; *rRev-erba* and *rTnfa*; *rRev-erba* and *rTlr4*; *rRora* and *rNf- κ b1*; *rRora* and *rTnfa*; *rRora* and *rTlr4* showed positive correlation (Fig. 44).

In 24 m LP, *rBmall*, *rCry2* and *rRora* showed positive correlation, but *rPer1* showed negative correlation with *rNf- κ b1*, *rTnfa*, *rTlr4* and *rTlr9*. *rBmall* and *rIl6*; *rPer2* and *rTnfa*; *rCry1* and *rTnfa*; *rCry2* and *rIl6*; *rRev-erba* and *rNf- κ b1*; *rRora* and *rIl6* showed negative correlation. *rPer1* and *rIl6*; *rPer2* and *rIl6*; *rCry1* and *rIl6* showed positive correlation. In 24 m DP, *rTnfa*, *rTlr4* and *rTlr9* showed positive correlation with *rBmall*, *rCry2* and *rRora* but showed negative correlation with *rPer1*, *rPer2*, *rCry1* and *rRev-erba*. *rNf- κ b1* and *rBmall*; *rNf- κ b1* and *rCry2*; *rNf- κ b1* and *rRora*; *rIl6* and *rPer1*; *rIl6* and *rPer2*; *rIl6* and *rRev-erba* showed positive correlation. *rNf- κ b1* and *rPer1*; *rNf- κ b1* and *rCry1*; *rIl6* and *rBmall*; *rIl6* and *rRora* showed negative correlation (Fig. 44).

WGCNA analysis between clock and immune genes with aging

In 3 m, only clock genes showed interaction with each other but not with immune genes. In 12 m, interactions between clock genes were reduced but *rTlr9* showed interaction with *rIl6*. In 24 m, *rTnfa* and *rTlr4* showed interaction, whereas *rCry2* showed interaction with *rNf- κ b1* (Fig. 45).

II. A (ii). Age-induced alterations of clock and immune genes mRNA expression in kidney

Effect of aging on the daily rhythms of clock genes in kidney

In all the age groups studied, *rBmal1* showed significant daily rhythms with a peak at ZT-0 and trough at ZT-12. *rPer1* did not alter its expression pattern in all the age groups with maximum expression at ZT-12 and minimum expression at ZT-0. *rPer2* also expressed maximum at ZT-12 in all age groups but minimum at ZT-6 in 3 m and ZT-0 in both 12 and 24 m rat kidney. In 3 and 12 m animals, *rCry1* showed maximum expression at ZT-18 and minimum at ZT-6. But in 24 m, maximum expression was at ZT-12 with phase advance of 6 hours (h), minimum expression was at ZT-6. *rCry2* showed maximum expression at ZT-12 in all age groups but minimum at ZT-6 in 3 m and at ZT-0 in 12 and 24 m animals. *rRev-erba* expressed maximum at ZT-6 and minimum at ZT-18 in all the age groups. *rRora* showed maximum expression at ZT-18, minimum at ZT-6 in 3 m. Interestingly, in 12 m rhythmicity was abolished. In 24 m, maximum expression was observed at ZT-12 and minimum at ZT-0 (Fig. 46) (Table 10).

Effect of aging on the daily rhythms of immune genes in kidney

rNf- κ b1 showed maximum expression at ZT-12 and minimum expression at ZT-6 in 3 m animals. In 12 m, maximum expression was at ZT-6 and minimum at ZT-18 with 6 h phase advance in comparison to 3 m animals. In 24 m, maximum expression was at ZT-12 and minimum expression at ZT-18. *rTnfa* showed maximum expression at ZT-12 and minimum expression ZT-6 in 3 m animals. In 12 and 24 m, maximum expression was at ZT-6 i.e. 6 h phase advance with respect to 3 m, but the minimum expression was at ZT-12 and ZT-0 respectively. *rIl6* expressed maximum at ZT-12 and minimum at ZT-0 in 3 m animals. In 12 m, maximum expression was observed at ZT-6 with phase advance of 6 h and minimum at ZT-18. In 24 m, maximum and minimum expressions were at ZT-12 and ZT-0 respectively. *rTlr4* showed rhythmic expression with maximum at ZT-12 and minimum at ZT-6 in 3 m animals. In 12 m, maximum expression showed a phase advance of 6 h and minimum expression was observed at ZT-12. In 24 m, maximum expression was at ZT-12 and minimum expression at ZT-18. *rTlr9* showed maximum expression at ZT-12 and minimum at ZT-6 in 3 m animals. In 12 m, maximum expression was at ZT-6 with phase advance of 6 h and minimum at ZT-18. In 24 m, maximum expression was at ZT-12 and minimum at ZT-0 (Fig. 47) (Table 11).

Effect of aging on the mean 24 h levels and daily pulse of clock genes in kidney

Mean 24 h levels of all clock genes did not show significant change among age groups studied (Fig. 48). Daily pulse of *rBmal1* and *rPer1* did not show a significant change in 12 m but showed a significant decrease ($p<0.05$) and significant increase respectively in 24 m in comparison to 3 m rat kidney. Daily pulse of *rPer2*, *rCry2* and *rRev-erba* was significantly increased ($p<0.05$), but *rCry1* showed a decrease in 12 and 24 m in comparison to 3 m animals. Daily pulse of *rRora* showed a significant decrease ($p<0.05$) in 12 m but significantly increased ($p<0.05$) in 24 m with respect to 3 m animals (Fig. 49) (Table 10).

Effect of aging on the mean 24 h levels and daily pulse of immune genes in kidney

Mean 24 h levels of all immune genes except *rIl6* showed a significant increase in 12 and 24 m with respect to 3 m animals (Fig. 48). Daily pulse of *rNf- κ b1* was significantly decreased ($p<0.05$) in 12 m but increased in 24 m in comparison to 3 m animals. Daily pulse of *rTnfa* and *rTlr4* showed a significant increase ($p<0.05$), but *rIl6* showed a decrease in 12 and 24 m in comparison to 3 m. Daily pulse of *rTlr9* did not show significant change among age groups studied (Fig. 49) (Table 11).

Effect of aging on the correlation among clock genes expression

In the light phase of 3 m, a significant negative correlation between *rBmal1* and *rRev-erba* ($p<0.001$) was observed. Also, a negative correlation was observed between *rBmal1* and *rPer1* ($p<0.01$). Within the *rPer1,2* genes and within the *rCry1,2* genes there was a significant positive correlation ($p<0.001$). However, *rPer1,2* showed significant positive correlation with *rCry2* ($p<0.001$). *rRev-erba* showed negative correlation ($p<0.05$) with *rRora*. We also observed that *rRora* showed a positive correlation ($p<0.001$) with *rCry1,2*. In the dark phase of 3 m, negative correlation persisted between *rBmal1* and *rRev-erba* and the negative correlation between *rBmal1* and *rPer1,2* genes became more significant ($p<0.001$). Positive correlation ($p<0.001$) persisted between *rPer1,2* genes but positive correlation between *rCry1,2* was abolished. Positive correlation between *rPer1,2* and *rCry2* genes persisted. The negative correlation between *rRora* and *rRev-erba* was abolished. But positive correlation between *rRora* and *rCry1,2* genes persisted. Moreover, there was a positive correlation between *rRev-erba* and *rPer1,2* genes ($p<0.001$) (Fig. 50).

In the light phase of 12 m, the correlation between *rBmall* and *rRev-erba* was abolished. However, the negative correlation between *rBmall* and *rPer1* genes persisted ($p < 0.001$). Also, a positive correlation between *rPer1,2* genes persisted ($p < 0.001$), whereas the correlation between *rCry1,2* genes was abolished. Interestingly, a significant positive correlation appeared between *rPer1,2* and *rCry1* and positive correlation with *rCry2* ($p < 0.001$) persisted. Negative correlation between *rRora* and *rRev-erba* was abolished but positive correlation between *rRora* and *rCry2* persisted ($p < 0.001$). In dark phase of 12 m, there was no correlation between *rBmall* and *rRev-erba*, but negative correlation between *rBmall* and *rPer1* genes persisted ($p < 0.001$). Positive correlation between *rPer1,2* genes persisted ($p < 0.001$) but between *rCry1,2* genes correlation was abolished. Positive correlation persisted between *rPer1,2* and *rCry2* ($p < 0.001$). A positive correlation appeared between *rRora* and *rRev-erba* ($p < 0.01$). *rRora* also showed a positive correlation with *rCry2* ($p < 0.001$) (Fig. 50).

In the light phase of 24 m, the negative correlation between *rBmall* and *rRev-erba* persisted ($p < 0.001$). Significant negative correlation persisted between *rBmall* and *rPer1* genes ($p < 0.001$). Significant positive correlation persisted within and in between *rPer1,2* and *rCry1,2* genes ($p < 0.001$). *rRora* did not show correlation with *rRev-erba*, but showed positive correlation with *rCry1,2* ($p < 0.001$). In the dark phase of 24 m, correlations between clock genes were significantly affected where *rBmall* showed a significant negative correlation ($p < 0.001$) with all the other clock genes. A significant positive correlation ($p < 0.001$) appeared among all the clock genes (Fig. 50).

Effect of aging on the correlation among immune genes expression

Pairwise correlations among immune genes in light phase (LP) and dark phase (DP) were analyzed in 3, 12 and 24 m animals (Fig. 5). In the light phase of 3 m, *rNf- κ b1* showed a significant positive correlation ($p < 0.001$; $p < 0.01$) with all other immune genes except *rIl6*. In the dark phase of 3 m, *rNf- κ b1* showed a positive correlation ($p < 0.001$) with all the immune genes except *rTlr4*. In the light phase of 12 m, *rNf- κ b1* showed significant positive correlation ($p < 0.001$) with all other immune genes. In dark phase of 12 m, *rNf- κ b1* showed negative correlation with *rTnf α* and *rTlr4* ($p < 0.001$; $p < 0.01$) but significant positive correlation with *rTlr9* ($p < 0.001$) persisted and correlation with *rIl6* was abolished. In the light phase of 24 m, a positive correlation of *rNf- κ b1* with all the immune genes ($p < 0.001$; $p < 0.05$) persisted. In the dark phase of 24 m, *rNf- κ b1* showed a significant positive correlation ($p < 0.001$) with all the immune genes.

Effect of aging on correlation between clock and immune genes expression

Pairwise correlation between clock and immune genes in light phase (LP) and dark phase (DP) were analyzed in 3, 12 and 24 m animals (Fig. 5). In light phase of 3 m, *rNf- κ b1* and *rTnfa* showed significant positive correlation with *rRora* and *rCry1,2* ($p < 0.001$; $p < 0.01$) and negative correlation with *rRev-erba* ($p < 0.05$). *rIl6* showed significant positive correlation ($p < 0.001$) with *rPer1,2* genes. *rTlr4* and *rTlr9* showed significant positive correlation with *rRora* and *rCry1,2* genes ($p < 0.001$; $p < 0.01$; $p < 0.05$). *rTlr9* also showed positive correlation with *rPer1,2* genes. In dark phase of 3 m, *rNf- κ b1*, *rTnfa*, *rIl6*, *rTlr4* and *rTlr9* showed significant positive correlation with *rRev-erba* and *rPer1,2* genes ($p < 0.001$; $p < 0.01$; $p < 0.05$) (Fig. 50).

In light phase of 12 m, *rNf- κ b1* and *rTnfa* changed to negative correlation ($p < 0.001$) with *rCry1*, but significant positive correlation ($p < 0.001$) with *rRev-erba* was appeared. *rIl6*, *rTlr4*, *rTlr9* changed to negative correlation with *rCry1* and *rPer1,2* genes ($p < 0.001$; $p < 0.01$; $p < 0.05$). In dark phase of 12 m, *rTnfa* showed positive correlation with *rCry1* ($p < 0.01$). *rIl6* and *rTlr4* showed negative correlation with *rPer1,2* genes ($p < 0.01$; $p < 0.05$). *rTlr4* changed to negative correlation ($p < 0.001$) with *rRev-erba*, but positive correlation between *rRev-erba* and *rTlr9* persisted ($p < 0.05$) (Fig. 50).

In the light phase of 24 m, a positive correlation between *rNf- κ b1* and *rCry1,2* genes persisted ($p < 0.001$). Positive correlation of *rIl6*, *rTlr4* and *rTlr9* with *rPer1,2* and *rCry1,2* genes persisted ($p < 0.001$; $p < 0.05$). In dark phase of 24 m, all immune genes showed significantly altered correlations with all the clock genes where significant positive correlation appeared with all clock genes but showed a negative correlation with *rBmal1* ($p < 0.001$) (Fig. 50).

WGCNA analysis between the clock and immune genes with aging

In 3 m, *rCry2* and *rRora* showed interactions with *rTlr4*; *rPer1* showed interaction with *rIl6* and *rTlr9*. In 12 m, *rRev-erba* showed interactions with all immune genes except *rTlr4*. In 24 m, the interaction between *rRev-erba* and *rTnfa* persisted; *rPer1,2* showed interaction with all immune genes except *rTnfa*, whereas, *rBmal1* showed interaction with *rNf- κ b1* and *rIl6* (Fig. 51).

II. A (iii). Age-induced alterations of clock and immune genes mRNA expression in spleen

Effect of aging on the daily rhythms of clock genes in spleen

In 3 m spleen, *rBmal1* showed maximum expression at ZT-0 and minimum at ZT-12. *rPer1*, *rPer2*, and *rCry2* showed maximum expression at ZT-12 and minimum expression at ZT-6. *rCry1* showed maximum expression at ZT-0 and minimum expression at ZT-6. *rRev-erba* showed maximum expression at ZT-6 and minimum expression at ZT-18. *rRora* did not show any significant rhythm. With aging *rBmal1* showed 6 h phase delay in 12 m, but did not alter in 24 m in comparison to 3 m. *rPer1* showed 6 h phase advance in 12 and 24 m in comparison to 3 m. The *rPer2* maximum expression did not alter in 12 m but showed 6 h phase delay in 24 m. *rCry1* showed 12 h phase delay and 6 h phase advance in 12 and 24 m respectively in comparison to 3 m. *rCry2* showed 6 h phase delay and 6 h phase advance in 12 and 24 m respectively in comparison to 3 m. *rRev-erba* did not alter in 12 and 24 m in comparison to 3 m. *rRora* showed rhythmic expression in 12 m with maximum expression at ZT-6 and minimum expression at ZT-12. In 24 m, *rRora* showed maximum expression at ZT-0 and minimum expression at ZT-12 (Fig. 52) (Table 12).

Effect of aging on daily rhythms of immune genes in spleen

In 3 m spleen, *rNf- κ b1* and *rTlr9* showed maximum expression at ZT-0 and minimum at ZT-6. *rTnfa* and *rIl6* showed maximum expression at ZT-12 and minimum at ZT-6. *rTlr4* showed maximum expression at ZT-0 and minimum at ZT-18. With aging, *rNf- κ b1* showed 6 h phase advance and 6 h phase delay in 12 and 24 m respectively in comparison to 3 m. *rTnfa* showed 12 h phase advance and 6 h phase delay in comparison to 3 m. *rIl6* showed 6 h phase advance in 12 and 24 m in comparison to 3 m. *rTlr4* showed 6 h phase delay in 12 m but did not alter in 24 m in comparison to 3 m. *rTlr9* rhythmicity was abolished in 12 m but showed 6 h phase delay in 24 m in comparison to 3 m (Fig. 53) (Table 13).

Effect of aging on mean 24 h levels of clock genes in spleen

With aging *rBmal1* and *rCry1* showed increased expression in 12 m but did not alter in 24 m in comparison to 3 m. *rPer1*, *rPer2*, *rCry2* showed increased expression in 12 and 24 m in comparison to 3 m. *rRev-erba* showed no alteration in mean levels with aging. *rRora* expression showed no variation in 12 m but showed increased expression in 24 m in comparison to 3 m (Fig.

54). The daily pulse of *rBmal1* decreased in 12 m and increased in 24 m in comparison to 3 m. Daily pulse of *rPer1*, *rPer2* and *rRev-erba* showed a decrease in 12 and 24 m. Daily pulse of *rCry1* showed an increase in 12 m but decreased in 24 m. Daily pulse of *rCry2* and *rRora* showed an increase in 12 and 24 m in comparison to 3 m (Fig. 55) (Table 12).

Effect of aging on mean 24 h levels and daily pulse in spleen

rNf- κ b1, *rIl6*, and *rTlr4* showed increased expression in 12 and 24 m in comparison to 3 m. *rTnfa* did not alter in 12 m but showed increased expression in 24 m in comparison to 3 m. *rTlr9* showed increased expression in 12 m but did not alter in 24 m in comparison to 3 m (Fig. 54). Daily pulse of *rNf- κ b1* decreased in 12 m but did not alter in 24 m in comparison to 3 m. Daily pulse of *rTnfa* and *rIl6* did not alter in 12 m but showed an increase in 24 m in comparison to 3 m. Daily pulse of *rTlr4* showed an increase in 12 and 24 m in comparison to 3 m. Daily pulse of *rTlr9* decreased in 12 m but increased ion 24 m in comparison to 3 m (Fig. 55) (Table 13).

Effect of aging on the correlation among clock genes in spleen

In 3 m LP, *rBmal1* and *rPer2*; *rBmal1* and *rRev-erba*; *rPer1* and *rRora*; *rPer2* and *rRora*; *rCry1* and *rRora*; *rCry2* and *rRora*; *rCry1* and *rRev-erba* showed negative correlation. *rPer1* and *rPer2*; *rPer1* and *rCry1*; *rPer1* and *rCry2*; *rPer2* and *rCry2*; *rRev-erba* and *rRora* showed positive correlation. In 3 m DP, *rBmal1* and *rRora* showed negative correlation with *rPer1*, *rPer2*, *rCry2*, *rRev-erba*. Similarly, *rCry1* showed negative correlation with *rPer1*, *rPer2* and *rCry2*. *rBmal1* showed positive correlation with *rCry1* and *rRora*. *rPer1*, *rPer2*, *rCry2* and *rRev-erba* showed positive correlation with each other (Fig. 56).

In 12 m LP, *rBmal1* and *rPer2*; *rBmal1* and *rCry1*; *rBmal1* and *rCry2* showed negative correlation. *rPer1* and *rRev-erba*; *rPer1* and *rRora*; *rPer2* and *rCry1*; *rPer2* and *rCry2*; *rCry1* and *rCry2*; *rRev-erba* and *rRora* showed positive correlation. In 12 m DP, *rBmal1* and *rPer1*; *rPer1* and *rCry2*; *rPer2* and *rCry1*; *rPer2* and *rCry2*; *rCry1* and *rCry2*; *rPer2* and *rRev-erba*; *rBmal1* and *rRev-erba*; *rPer1* and *rRora*; *rCry2* and *rRora* showed positive correlation. *rBmal1* and *rRev-erba*; *rPer1* and *rRev-erba*; *rRev-erba* and *rRora* showed negative correlation (Fig. 56).

In 24 m LP, *rBmal1* and *rPer2*; *rPer2* and *rCry1*; *rBmal1* and *rRev-erba* showed negative correlation. *rBmal1* and *rCry1*; *rBmal1* and *rCry2*; *rBmal1* and *rRora*; *rPer1* and *rPer2*; *rPer1* and *rRev-erba*; *rCry1* and *rCry2*; *rCry1* and *rRora*; *rCry2* and *rRora* showed positive

correlation. In 24 m DP, *rBmal1* and *rPer2*; *rPer1* and *rPer2*; *rPer1* and *rCry1*; *rPer2* and *rRora*; *rCry1* and *rRev-erba*; *rCry2* and *rRev-erba* showed negative correlation. *rBmal1* and *rPer1*; *rBmal1* and *rCry2*; *rBmal1* and *rRora*; *rPer1* and *rRora*; *rPer2* and *rCry1*; *rCry1* and *rCry2*; *rCry2* and *rRora* showed positive correlation (Fig. 56).

Effect of aging on the correlation among immune genes in spleen

In 3 m LP, *rNf- κ b1* showed a positive correlation with *rTlr4* and *rTlr9*. *rTnfa* and *rIl6*; *rTlr4* and *rTlr9* showed a positive correlation. *rTnfa* and *rTlr4*; *rIl6* and *rTlr4* showed a negative correlation. *rNf- κ b1* showed a negative correlation with *rTnfa* and *rIl6*, positive correlation with *rTlr4* and *rTlr9*. *rTnfa* and *rIl6*; *rTlr4* and *rTlr9* showed a positive correlation. *rTnfa* and *rIl6* showed a negative correlation with *rTlr4* and *rTlr9* (Fig. 56).

In 12 m LP, *rNf- κ b1* and *rTnfa*; *rNf- κ b1* and *rTlr4*; *rTnfa* and *rTlr4* showed a positive correlation. *rNf- κ b1* and *rTnfa* showed a negative correlation with *rIl6* and *rTlr9*. *rTlr4* showed a negative correlation with *rTlr9*. In 12 m DP, *rNf- κ b1* and *rTnfa*; *rNf- κ b1* and *rTlr9*; *rTnfa* and *rTlr4*; *rTnfa* and *rTlr9* showed positive correlation. *rNf- κ b1* and *rIl6*; *rTnfa* and *rIl6*; *rIl6* and *rTlr9* showed a negative correlation (Fig. 56).

In 24 m LP, *rNf- κ b1* and *rIl6*; *rNf- κ b1* and *rTlr4*; *rNf- κ b1* and *rTlr9*; *rTnfa* and *rIl6*; *rIl6* and *rTlr9* showed positive correlation. In 24 m DP, *rNf- κ b1* and *rIl6*; *rNf- κ b1* and *rTlr4*; *rNf- κ b1* and *rTlr9*; *rTnfa* and *rTlr9*; *rIl6* and *rTlr4*; *rIl6* and *rTlr9* showed positive correlation (Fig. 56).

Effect of aging on the correlation between clock and immune genes in spleen

In 3 m LP, *rTnfa* and *rIl6* showed negative correlation with *rBmal1* and *rRora*, but showed positive correlation with *rPer1*, *rPer2* and *rCry2*. *rRev-erba* and *rNf- κ b1*; *rPer2* and *rTlr4*; *rCry2* and *rTlr4*; *rRev-erba* and *rTlr9* showed negative correlation. *rBmal1* and *rNf- κ b1*; *rCry1* and *rNf- κ b1*; *rBmal1* and *rTlr4*; *rBmal1* and *rTlr9*; *rCry1* and *rTlr9* showed positive correlation. In 3 m DP, *rTnfa* and *rIl6* showed negative correlation with *rBmal1* and *rRora*, but showed positive correlation with *rPer1*, *rPer2*, *rCry2* and *rRev-erba*. *rNf- κ b1*, *rTlr4* and *rTlr9* showed positive correlation with *rBmal1* and *rCry1*, but showed negative correlation with *rPer1*, *rPer2* and *rCry2*. *rCry1* and *rIl6*; *rRev-erba* and *rTlr9* showed negative correlation (Fig. 56).

In 12 m LP, *rPer2*, *rCry1*, and *rCry2* showed a negative correlation with *rNf- κ b1*, *rTnfa* and *rTlr4*, but showed a positive correlation with *rTlr9*. *rBmal1* showed a positive correlation with *rNf- κ b1*, *rTnfa*, and *rTlr4*, but showed a negative correlation with *rTlr9*. *rPer1* and *rRora* showed

a positive correlation with *rIl6* and *rTlr4*. *rRev-erba* showed a positive correlation with *rIl6*. In 12 m DP, *rNf- κ b1* and *rTnfa* showed a positive correlation with *rBmal1*, *rPer*, and *rRora*, but showed a negative correlation with *rRev-erba*. *rIl6* showed a negative correlation with *rBmal1*, *rPer1* and *rRora*, but showed a positive correlation with *rRev-erba*. *rTlr4* showed negative correlation with *rPer1*, *rCry1* and *rRev-erba*. *rTlr9* showed positive correlation with *rBmal1*, *rPer1*, *rCry2* and *rRora*. *rBmal1* showed a positive correlation with *rTlr4* (Fig. 56).

In 24 m LP, *rBmal1* and *rTlr4*; *rPer1* and *rTnfa*; *rPer2* and *rTnfa*; *rCry1* and *rTlr4*; *rCry2* and *rNf- κ b1*; *rCry2* and *rIl6*; *rCry2* and *rTlr4*; *rCry2* and *rTlr9*; *rRev-erba* and *rTnfa*; *rRora* and *rNf- κ b1*; *rRora* and *rTlr4*; *rRora* and *rTlr9* showed positive correlation. *rPer2* and *rTlr4* showed negative correlation. In 24 m DP, *rBmal1* and *rNf- κ b1*; *rBmal1* and *rIl6*; *rBmal1* and *rTlr4*; *rPer1* and *rNf- κ b1*; *rPer1* and *rTlr4*; *rPer2* and *rTnfa*; *rCry1* and *rTnfa*; *rCry1* and *rTlr9*; *rCry2* and *rNf- κ b1*; *rCry2* and *rIl6*; *rCry2* and *rTlr9*; *rRora* and *rNf- κ b1*; *rRora* and *rIl6*; *rRora* and *rTlr4* showed positive correlation. *rPer1* and *rTnfa*; *rPer2* and *rTlr4*; *rRev-erba* and *rTnfa*; *rRev-erba* and *rIl6*; *rRev-erba* and *rTlr9* showed negative correlation (Fig. 56).

WGCNA analysis between clock and immune genes with aging

In 3 m, clock and immune genes showed interaction with each other in two separate modules. In 12 m, the interactions between clock and immune genes were decreased, where only *rBmal1* showed interaction with *rNf- κ b1* and *rTnfa*. However, in 24 m, *rCry2* and *rRora* showed interaction with *rNf- κ b1*, *rIl6*, and *rTlr9* (Fig. 57).

II. A (iv). Age-induced alterations of 5-HT in liver, kidney, and spleen

Effect of aging on daily rhythms, mean 24 h levels, and daily pulse of 5-HT in liver

In 3 m liver, 5-HT showed rhythmicity with maximum levels at ZT-0 and minimum at ZT-12. In 12 m, the maximum levels did not vary but the minimum levels were observed at ZT-6. In 24 m, 6 h phase advance was observed with maximum levels at ZT-18 and minimum at ZT-0 (Fig. 58). Mean 24 h levels of 5-HT showed a significant reduction in 12 m but did not alter in 24 m in comparison to 3 m animals (Fig. 59a). Daily pulse of 5-HT showed a significant increase in 12 m but did not alter in 24 m animals (Fig. 59b) (Table 14).

Effect of aging on daily rhythms, mean 24 h levels, and daily pulse of 5-HT in kidney

In 3 m kidney, 5-HT showed significant daily rhythm with maximum levels at ZT-18 and minimum at ZT-0. In 12 m, 6 h phase delay was observed with maximum levels at ZT-0 and minimum at ZT-12. In 24 m, the maximum level was persisted at ZT-18 and minimum at ZT-0 (Fig. 58). Mean 24 h levels showed a significant increase in 12 and 24 m in comparison to 3 m (Fig. 59a). Daily pulse showed a significant increase in 12 m but did not vary in 24 m in comparison to 3 m (Fig. 59b) (Table 14).

Effect of aging on daily rhythms, mean 24 h levels, and daily pulse of 5-HT in spleen

In 3 m spleen, 5-HT showed rhythmicity with maximum levels at ZT-18 and minimum at ZT-12. In 12 m, 6 h phase delay was observed with maximum levels at ZT-0 and minimum at ZT-18. In 24 m, 6 h phase advance was observed with maximum levels at ZT-12 and minimum at ZT-0 (Fig. 58). Mean 24 h levels showed a significant decrease in 12 and 24 m in comparison to 3 m (Fig. 59a). Daily pulse of 5-HT did not alter with the aging (Fig. 59b) (Table 14).

II. B (i). Effect of curcumin on the age-induced alterations of clock and immune genes mRNA expression in liver

Effect of curcumin on daily rhythms of clock genes in liver

With curcumin administration, *rBmal1*, *rPer1*, *rPer2*, and *rRev-erba* expression pattern did not vary in all the age groups studied in comparison to age-matched vehicle group. In 3 m, curcumin phase advanced *rCry1* by 6 h with maximum expression being at ZT-0 and minimum expression at ZT-6. In 12 and 24 m, curcumin did not alter the phase of *rCry1* with respect to age-matched vehicle group. With curcumin administration, *rCry2* showed 12 h and 6 h phase advance in 3 and 12 m respectively but showed 12 h phase delay in 24 m in comparison to age-matched vehicle group. *rRora* showed no variation in 3 m CT but showed 12 h phase advance in 12 m CT in comparison to age-matched vehicle group. In 24 m curcumin restored the phase of *rRora* in comparison to 3 m VT (Fig. 40) (Table 8).

Effect of curcumin on daily rhythms of immune genes in liver

Curcumin administration did not alter the phase of *rNf- κ b1* in 3 m, however, in 12 m curcumin restored the phase of *rNf- κ b1* with maximum expression at ZT-6 in comparison to 3 m VT. In 24 m, *rNf- κ b1* showed 12 h phase delay with curcumin administration. Curcumin phase advanced *rTnfa* by 6 h in 3 m, but restored the rhythmicity in 12 m with maximum expression at ZT-0 in 12 m. In 24 m, curcumin restored the phase of *rTnfa* with maximum expression at ZT-12 in comparison to 3 m VT. Curcumin resulted in 6 h phase advance of *rIl6* in 3 m but did not alter in 12 and 24 m in comparison to age-matched vehicle group. Curcumin did not alter the phase of *rTlr4* in 3 m but restored the phase in 12 m with maximum expression at ZT-6 in comparison to 3 m VT. In 24 m, *rTlr4* showed 12 h phase delay with curcumin treatment in comparison to 3 m VT. Curcumin resulted in 6 h phase delay of *rTlr9* in 3 m but did not alter in 12 m in comparison to age-matched vehicle group. However, curcumin restored the phase of *rTlr9* in 24 m with maximum expression at ZT-12 in comparison to 3 m VT (Fig. 41) (Table 9).

Effect of curcumin on mean levels and daily pulse of clock genes in liver

Curcumin administration did not alter the mean levels of *rBmal1*, *rPer1*, *rPer2*, *rCry1* and *rRev-erba* in comparison to age-matched vehicle group. Curcumin decreased the levels of *rCry2* in 3 and 24 m in comparison to respective age-matched vehicle group. Curcumin reduced the levels of *rRora* in comparison to age-matched vehicle group (Fig. 42) (Table 8).

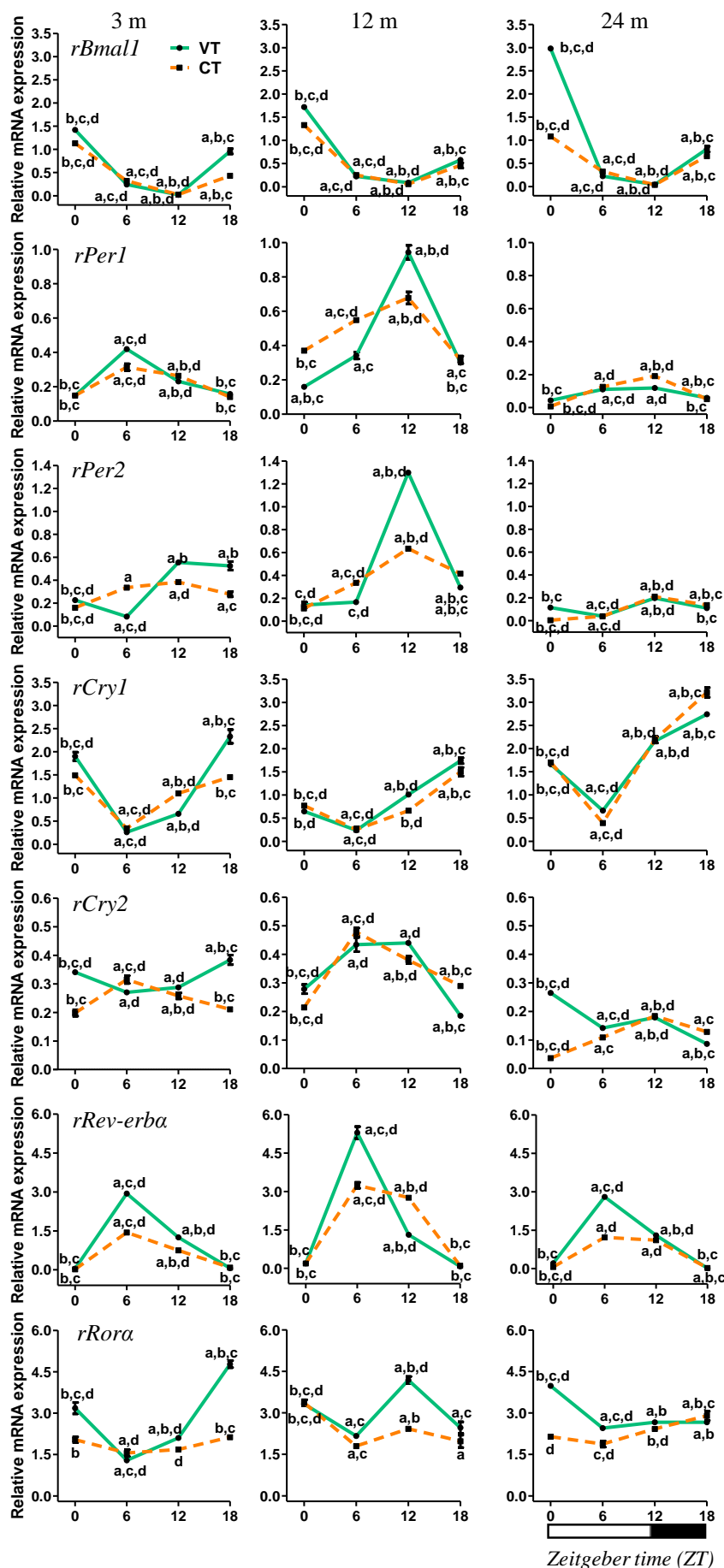


Fig. 40: Effect of curcumin administration on daily rhythms of clock genes mRNA expression in 3, 12 and 24 months (m) old rat liver. Each value is mean \pm SEM (n = 4), $p \leq 0.05$ and expressed as relative mRNA expression. $p_a \leq 0.05$; $p_b \leq 0.05$, $p_c \leq 0.05$ and $p_d \leq 0.05$ (where ‘a’, ‘b’, ‘c’ and ‘d’ refers to comparison with ZT-0, ZT-6, ZT-12, and ZT-18 respectively within the group).

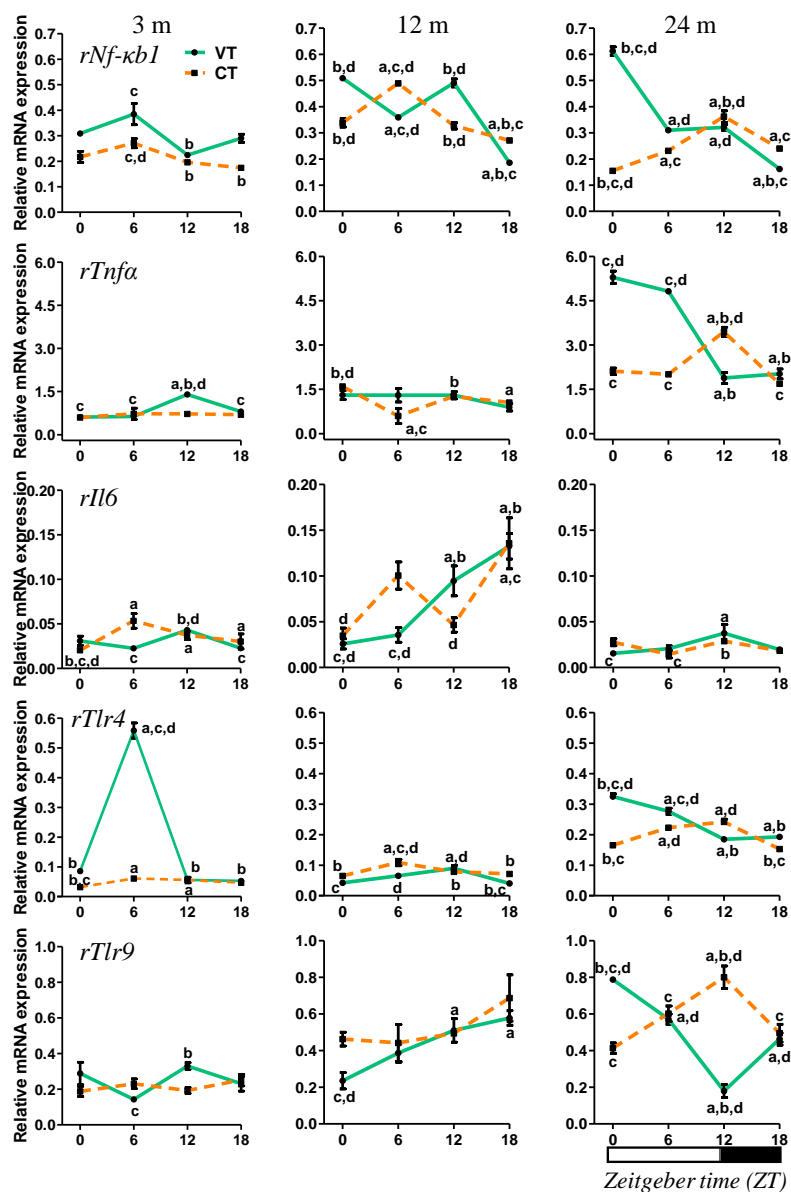


Fig. 41: Effect of curcumin administration on daily rhythms of immune genes mRNA expression in 3, 12 and 24 months (m) old rat liver. Each value is mean \pm SEM ($n = 4$), $p \leq 0.05$ and expressed as relative mRNA expression. $p_a \leq 0.05$; $p_b \leq 0.05$, $p_c \leq 0.05$ and $p_d \leq 0.05$ (where ‘a’, ‘b’, ‘c’ and ‘d’ refers to comparison with ZT-0, ZT-6, ZT-12, and ZT-18 respectively within the group).

With curcumin treatment, daily pulse of *rBmal1* showed a decrease in 3 m, did not alter in 12 m and decreased in 24 m in comparison to age-matched vehicle group. Curcumin decreased the daily pulse of *rPer1* in 3 and 12 m but increased in 24 m in comparison to age-matched vehicle group. Curcumin reduced the daily pulse in 3 m, but restored in 12 m in comparison to 3 m VT, in 24 m curcumin increased the daily pulse in comparison to 24 m VT. Curcumin decreased the daily pulse in 3 m, did not alter in 12 m, but increased in 24 m in comparison to age-matched vehicle group. Curcumin did not alter the daily pulse of *rRev-erba* in 3 m but decreased in 12 and

24 m in comparison to age-matched vehicle group. Curcumin decreased the daily pulse of *rRora* in 3 m but did not alter in 12 and 24 m in comparison to age-matched vehicle group (Fig. 43).

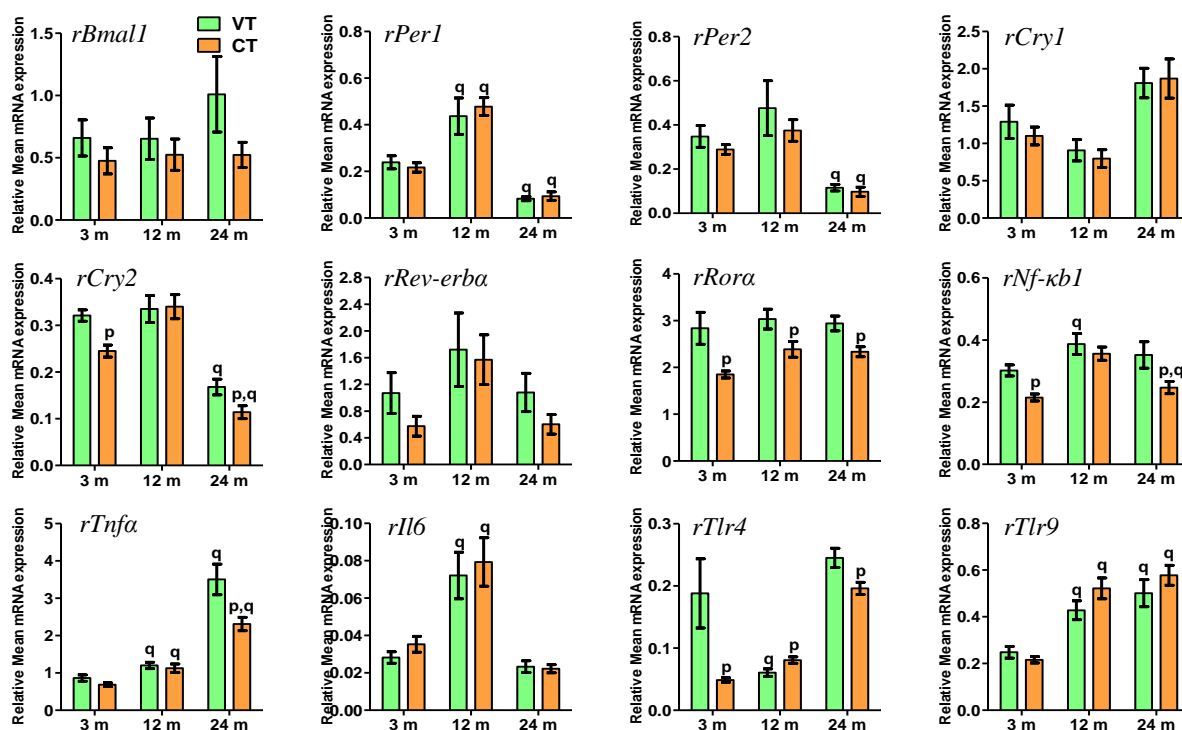


Fig. 42: Effect of curcumin administration on Mean 24 hour (h) levels of clock and immune genes expression in 3, 12 and 24 months (m) old rat liver. Each value is mean \pm SEM ($n = 4$), $p \leq 0.05$ and expressed as mean relative gene expression. $p_p \leq 0.05$ (where 'p' refers to comparison with the age-matched vehicle-treated group). $p_q \leq 0.05$ (where 'q' refers to comparison with 3 m vehicle-treated group).

Effect of curcumin on the mean 24 h levels and daily pulse of immune genes in liver

Curcumin administration resulted in the reduction of mean 24 h levels of *rNf-κb1* in all age groups, where curcumin has restored the levels in 12 m in comparison to 3 m VT. Curcumin did not alter the levels of *rTnfa* in 3 and 12 m but significantly reduced in 24 m in comparison to age-matched vehicle group. The levels of *rIl6* and *rTlr9* were not altered with curcumin administration in all age groups in comparison to age-matched vehicle group. Curcumin reduced the levels of *rTlr4* in 3 and 24 m in comparison to the age-matched vehicle group but restored the levels in 12 m in comparison to 3 m VT (Fig. 42). Curcumin did not alter the daily pulse of *rNf-κb1* in 3 m but restored in 12 m in comparison to 3 m VT group. In 24 m, curcumin decreased the daily pulse of *rNf-κb1* in comparison to 24 m VT group. Curcumin reduced the daily pulse of *rTnfa* in 3 and 24 m in comparison to age-matched vehicle group. However, in 12 m, curcumin

restored the daily pulse in comparison to 3 m VT group. Curcumin did not alter the daily pulse of *rIl6* in 3 and 24 m but decreased in 12 m in comparison to age-matched vehicle group. *rTlr4* showed decreased daily pulse in 3 and 24 m but did not alter in 12 m with curcumin treatment in comparison to age-matched vehicle group. Curcumin did not alter *rTlr9* daily pulse in 3 m but decreased in 12 and 24 m in comparison to age-matched vehicle group (Fig. 43) (Table 9).

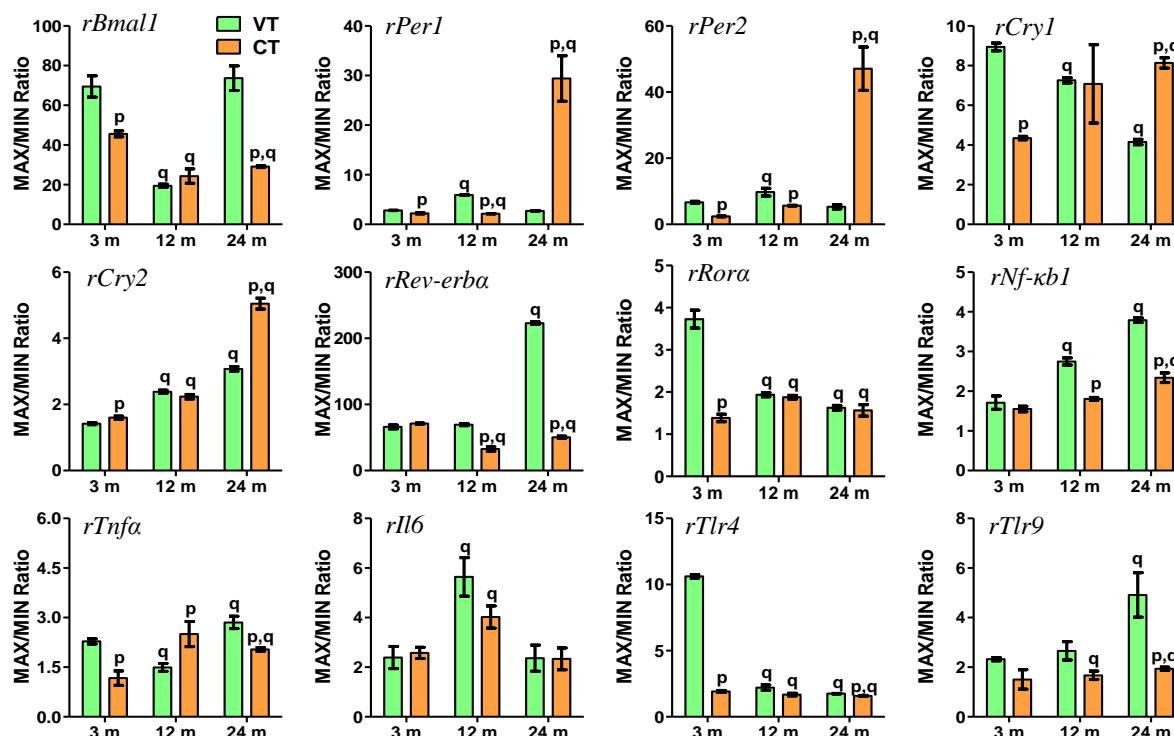


Fig. 43: Effect of curcumin administration on daily pulse of clock and immune genes expression in 3, 12 and 24 months (m) old rat liver. Each value is mean \pm SEM ($n = 4$), $p \leq 0.05$ and expressed as mean relative gene expression. $p_p \leq 0.05$ (where ‘p’ refers to comparison with the age-matched vehicle-treated group). $p_q \leq 0.05$ (where ‘q’ refers to comparison with 3 m vehicle-treated group).

Effect of curcumin on correlations among clock genes in liver

In LP and DP of 3 m CT, *rBmall* and *rPer1*; *rBmall* and *rPer2*; *rBmall* and *rCry2*; *rBmall* and *rRev-erba*; *rPer1* and *rCry1*; *rPer1* and *rRora*; *rPer2* and *rCry1*; *rPer2* and *rRora*; *rCry1* and *rCry2*; *rCry1* and *rRev-erba*; *rCry2* and *rRora*; *rRev-erba* and *rRora* showed negative correlation. *rBmall* and *rCry1*; *rBmall* and *rRora*; *rPer1* and *rPer2*; *rPer1* and *rCry2*; *rPer1* and *rRev-erba*; *rPer2* and *rCry2*; *rPer2* and *rRev-erba*; *rCry1* and *rRora*; *rCry2* and *rRev-erba* showed positive correlation (Fig. 44).

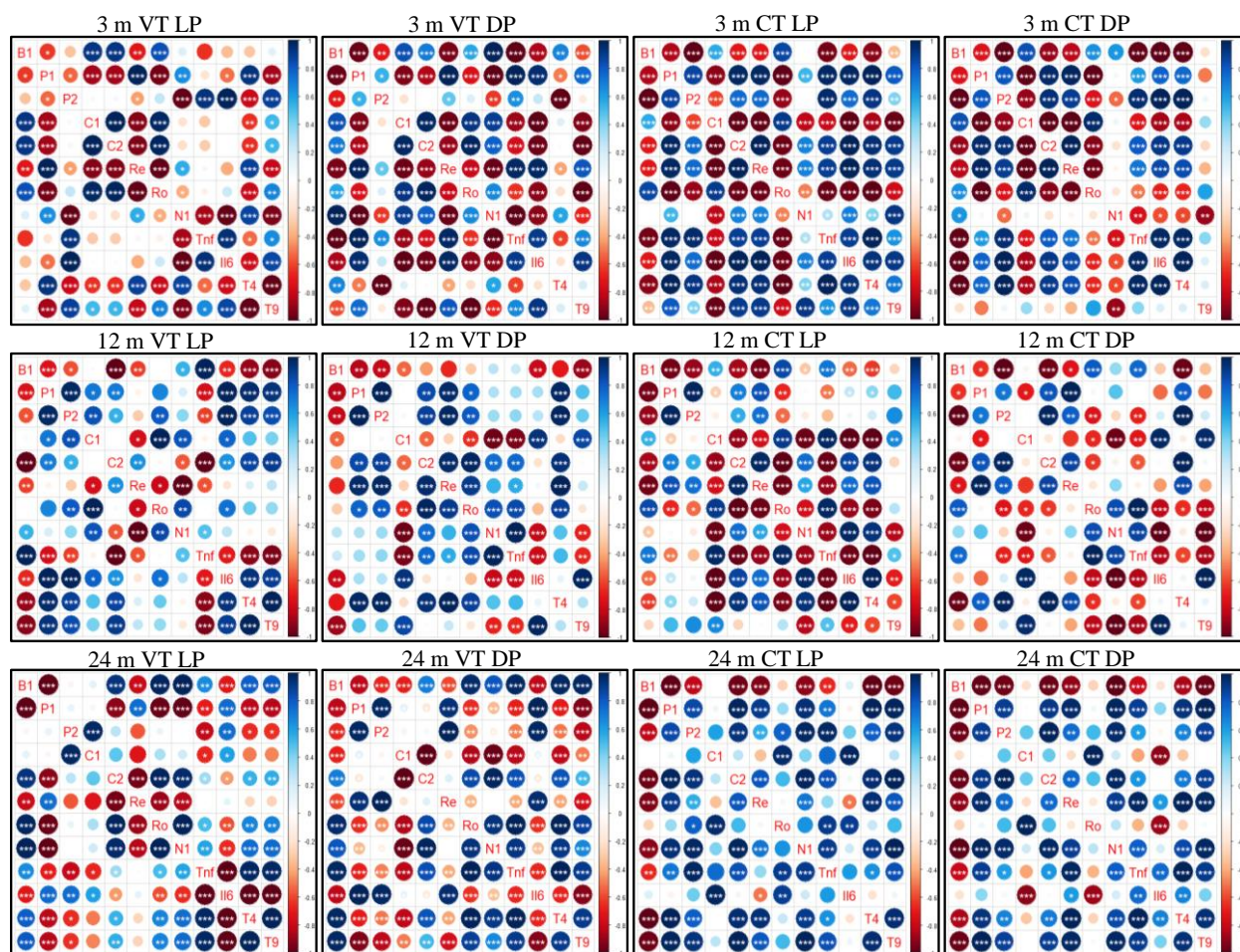


Fig. 44: Effect of curcumin administration on Pair wise correlations between clock and immune genes expression in light (ZT-0, 6, 12) and dark (ZT-12, 18, 24/0) phase of 3, 12 and 24 months (m) old rat liver (LP - light phase; DP - dark phase; VT - vehicle-treated; CT - curcumin treated). Intensity of color and size of circle represents correlation coefficient values between the genes. Where, positive correlations are indicated by shades of blue, negative correlations by shades of red and white indicates no correlation. ‘*’, ‘**’, ‘***’ indicates statistically significant correlations ($p \leq 0.05$), ($p \leq 0.01$), ($p \leq 0.001$) respectively. (B1- *rBmall*; P1 - *rPer1*; P2 - *rPer2*; C1 - *rCry1*; C2 - *rCry2*; Re - *rRev-erba*; Ro – *rRora*; N1 - *rNfkb1*; Tnf – *rTnfa*; Il6 - *rIl6*; T4 - *rTlr4*; T9 - *rTlr9*).

In LP of 12 m CT, curcumin restored the positive correlation between *rBmall* and *rCry1*; *rBmall* and *rRora*; *rPer1* and *rRev-erba* in comparison to 3 m VT group. Curcumin also restored the negative correlation between *rPer1* and *rCry1*; *rPer1* and *rRora* in comparison to 3 m VT group. *rBmall* and *rPer1*; *rBmall* and *rPer2*; *rBmall* and *rCry2*; *rBmall* and *rRev-erba*; *rPer2* and *rRora*; *rCry1* and *rCry2*; *rCry1* and *rRev-erba*; *rCry2* and *rRora*; *rRev-erba* and *rRora* showed negative correlation with curcumin treatment. *rPer1* and *rPer2*; *rPer1* and *rCry2*; *rPer1* and *rRev-erba*; *rPer2* and *rCry2*; *rPer2* and *rRev-erba*; *rCry1* and *rRora*; *rCry2* and *rRev-erba* showed positive correlation with curcumin treatment. In DP of 3 m CT, curcumin restored the

negative correlation between *rBmall* and *rRev-erba*; *rPer1* and *rCry1* in comparison to 3 m VT group. Curcumin restored positive correlation between *rBmall* and *rRora* in comparison to 3 m VT group. *rBmall* and *rPer1*; *rBmall* and *rPer2*; *rBmall* and *rCry2*; *rPer2* and *rRora*; *rCry1* and *rRora*; *rCry2* and *rRora* showed negative correlation with curcumin treatment. *rPer1* and *rPer2*, *rPer1* and *rCry2*; *rPer1* and *rRev-erba*; *rPer2* and *rCry2*; *rPer2* and *rRev-erba*; *rCry2* and *rRev-erba* showed positive correlation with curcumin treatment. In LP and DP of 24 m CT, curcumin resulted in negative correlation between *rBmall* and *rPer1*; *rBmall* and *rPer2*; *rBmall* and *rCry2*; *rBmall* and *rRev-erba*. Curcumin showed positive correlation between *rPer1* and *rPer2*; *rPer1* and *rCry2*; *rPer1* and *rRev-erba*; *rPer2* and *rCry2*; *rPer2* and *rRev-erba*; *rCry1* and *rRora*; *rCry2* and *rRev-erba* (Fig. 44).

Effect of curcumin on correlations among immune genes in liver

In LP of 3 m CT, all the immune genes showed a positive correlation with each other. In DP of 3 m CT, *rNf- κ b1* showed a negative correlation with all the other immune genes. *rTnfa*, *rIl6*, and *rTlr4* showed a positive correlation with each other. In LP of 12 m CT, curcumin restored the negative correlation between *rNf- κ b1* and *rTnfa*; *rNf- κ b1* and *rTlr9*; *rTlr4* and *rTlr9* in comparison to 3 m VT group. Curcumin also restored the positive correlation between *rNf- κ b1* and *rTlr4*; *rTnfa* and *rTlr9* in comparison to 3 m VT group. Curcumin showed a positive correlation between *rNf- κ b1* and *rIl6*; *rIl6* and *rTlr4*, but negative correlation between *rTnfa* and *rIl6*; *rTnfa* and *rTlr4*; *rIl6* and *rTlr9*. In DP of 12 m CT, curcumin restored the negative correlation between *rTnfa* and *rTlr4*. Curcumin resulted in a positive correlation between *rNf- κ b1* and *rTnfa*; *rIl6* and *rTlr9*, and negative correlation between *rNf- κ b1* and *rIl6*; *rNf- κ b1* and *rTlr9*; *rTnfa* and *rIl6*; *rTnfa* and *rTlr9*. In LP of 24 m CT, curcumin resulted in positive correlation between *rNf- κ b1* and *rTnfa*; *rNf- κ b1* and *rTlr4*; *rNf- κ b1* and *rTlr9*; *rTnfa* and *rTlr4*; *rTnfa* and *rTlr9*; *rTlr4* and *rTlr9*. In DP of 24 m CT, curcumin restored the positive correlation between *rTnfa* and *rIl6* in comparison to 3 m VT group. Curcumin showed positive correlation between *rNf- κ b1* and *rTnfa*; *rNf- κ b1* and *rTlr4*; *rNf- κ b1* and *rTlr9*; *rTnfa* and *rTlr4*; *rTnfa* and *rTlr9*; *rIl6* and *rTlr4*; *rTlr4* and *rTlr9* (Fig. 44).

Effect of curcumin on correlations between clock and immune genes in liver

In LP of 3 m CT, *rTnfa*, *rIl6*, *rTlr4* and *rTlr9* showed negative correlation with *rBmall*, *rCry1* and *rRora*, but showed positive correlation with *rPer1*, *rPer2*, *rCry2* and *rRev-erba*. *rNf- κ b1* and *rCry1*; *rNf- κ b1* and *rRora* showed a negative correlation. *rNf- κ b1* and *rPer1*; *rNf- κ b1* and *rCry2*;

rNf- κ b1 and *rRev-erba* showed positive correlation. In DP of 3 m CT, *rTnfa*, *rIl6* and *rTlr4* showed negative correlation with *rBmal1*, *rCry1* and *rRora*, but showed positive correlation with *rPer1*, *rPer2*, *rCry2* and *rRev-erba*. *rNf- κ b1* and *rPer2* showed a negative correlation. *rNf- κ b1* and *rBmal1* showed a positive correlation (Fig. 44).

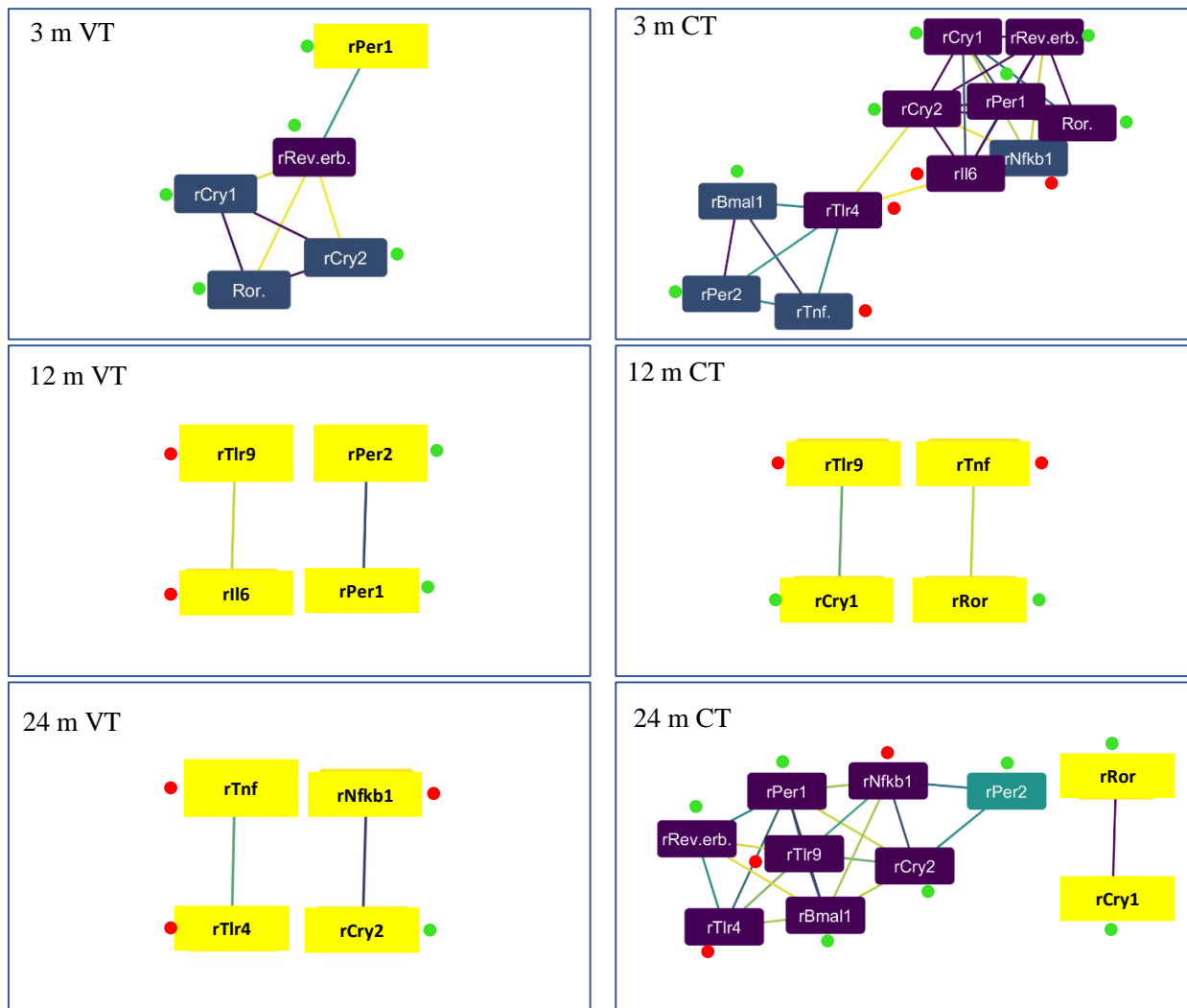


Fig. 45: WGCNA analysis between clock and immune gene clusters: effect aging on gene to gene network in 3, 12 and 24 m old rat liver (left panel) and effect of curcumin administration (right panel). Color of the node indicates no. of interactions (highest—purple; intermediate—cyan and least—yellow). Color of an edge indicates the strength of interaction (strongest—purple; cyan—intermediate and weakest—yellow). Green and red dots indicate clock, immune and microglia resting genes respectively.

In LP of 12 m CT, curcumin restored the negative correlation between *rCry1* and *rTlr4*; *rRora* and *rNf- κ b1*; *rRora* and *rTlr4*, positive correlation between *rCry1* and *rTlr9*; *rRev-erba* and *rTlr4*. *rNf- κ b1*, *rIl6* and *rTlr4* showed negative correlation with *rRora* and *rCry1*, but showed positive correlation with *rCry2* and *rRev-erba*. *rTnfa* showed negative correlation with *rCry2* and

rRev-erba, but showed positive correlation with *rCry1* and *rRora*. Curcumin resulted in negative correlation between *rBmall* and *rNf- κ b1*; *rBmall* and *rIl6*; *rBmall* and *rTlr4*; *rPer1* and *rTnfa*, but positive correlation between *rBmall* and *rTnfa*; *rPer1* and *rIl6*; *rPer1* and *rTlr4*; *rCry1* and *rTlr9*. In DP of 12 m CT, curcumin restored the negative correlation between *rCry2* and *rTnfa*; *rRora* and *rIl6*; *rRora* and *rTlr9*. Curcumin resulted in positive correlation between *rNf- κ b1* and *rRora*; *rTnfa* and *rRora*; *rTnfa* and *rBmall*; *rCry1* and *rIl6*; *rTlr4* and *rPer1*; *rTlr4* and *rPer2*; *rTlr4* and *rCry2*; *rTlr4* and *rRev-erba*; *rCry1* and *rTlr9*. Curcumin resulted in negative correlation between *rNf- κ b1* and *rCry1*; *rTnfa* and *rPer2*; *rTnfa* and *rCry1*; *rTlr4* and *rRora*; *rTlr4* and *rBmall*. In LP of 24 m CT, curcumin restored the positive correlation between *rPer1* and *rNf- κ b1*; *rPer1* and *rTlr4*; *rPer2* and *rTnfa*; *rPer2* and *rTlr9*; *rRev-erba* and *rNf- κ b1*. Curcumin resulted in positive correlation between *rBmall* and all immune genes except *rIl6*. Also, curcumin resulted in negative correlation between *rCry2* with all immune genes except *rIl6*. Curcumin showed positive correlation between *rPer1* and *rTnfa*; *rPer1* and *rTlr9*; *rPer2* and *rNf- κ b1*; *rPer2* and *rTlr4*; *rCry1* and *rIl6*; *rRev-erba* and *rTlr4*; *rRev-erba* and *rTlr9*; *rRora* and *rTnfa*; *rRora* and *rIl6*. In DP of 24 m CT, curcumin restored the negative correlation between *rBmall* and *rTnfa*; *rBmall* and *rTlr9*; *rCry1* and *rIl6*, and positive correlation between *rPer1* and *rTnfa*; *rPer1* and *rTlr9*; *rPer2* and *rTnfa*; *rRev-erba* and *rTnfa*; *rRev-erba* and *rTlr9*. Curcumin resulted in negative correlation between *rBmall* and *rNf- κ b1*; *rBmall* and *rTlr4*; *rRora* and *rIl6*, and positive correlation between *rPer1* and *rNf- κ b1*; *rPer1* and *rTlr4*; *rPer2* and *rNf- κ b1*; *rPer2* and *rTlr4*; *rPer2* and *rTlr9*; *rCry2* and *rNf- κ b1*; *rCry2* and *rTnfa*; *rCry2* and *rTlr4*; *rCry2* and *rTlr9*; *rRev-erba* and *rNf- κ b1*; *rRev-erba* and *rIl6*; *rRev-erba* and *rTlr4* (Fig. 44).

WGCNA analysis between clock and immune genes with curcumin treatment in liver

With curcumin administration, clock and immune genes showed strong interactions with each other in 3 m CT. However, in 12 m CT, these interactions were reduced with curcumin administration where *rCry1* and *rRora* showed interactions with *rTlr9* and *rTnfa* respectively. in 24 m CT, the interactions were increased between clock and immune genes (Fig. 45).

Table 8: Effect of curcumin on age-induced alterations of clock genes

Gene		ZT-0	ZT-6	ZT-12	ZT-18	Mean 24 h levels	Max/min ratio
<i>rBmal1</i>	3 m VT	1.42 ± 0.04	0.24 ± 0	0.02 ± 0	0.96 ± 0.05	0.66 ± 0.14	69.49 ± 5.4
	3 m CT	1.13 ± 0.03	0.32 ± 0.01	0.02 ± 0	0.43 ± 0.03	0.48 ± 0.1	45.6 ± 1.52 _x
	12 m VT	1.72 ± 0.02	0.22 ± 0.02	0.09 ± 0	0.58 ± 0.02	0.65 ± 0.17	19.48 ± 0.82 _y
	12 m CT	1.33 ± 0.04	0.25 ± 0.01	0.06 ± 0.01	0.46 ± 0.05	0.53 ± 0.13	24.33 ± 3.6 _y
	24 m VT	2.98 ± 0.04	0.22 ± 0.01	0.04 ± 0	0.81 ± 0.06	1.01 ± 0.3	73.7 ± 6.22
	24 m CT	1.08 ± 0.04	0.32 ± 0.01	0.04 ± 0	0.66 ± 0.02	0.52 ± 0.1	29.11 ± 0.47 _{x,y}
<i>rPer1</i>	3 m VT	0.15 ± 0	0.42 ± 0.01	0.23 ± 0	0.16 ± 0.01	0.24 ± 0.03	2.82 ± 0.04
	3 m CT	0.15 ± 0	0.31 ± 0.02	0.26 ± 0.01	0.14 ± 0	0.22 ± 0.02	2.23 ± 0.12 _x
	12 m VT	0.16 ± 0.01	0.34 ± 0.02	0.94 ± 0.04	0.3 ± 0.01	0.44 ± 0.08 _y	5.91 ± 0.07 _y
	12 m CT	0.37 ± 0.01	0.55 ± 0.01	0.68 ± 0.03	0.32 ± 0.02	0.48 ± 0.04 _y	2.15 ± 0.04 _{x,y}
	24 m VT	0.04 ± 0	0.11 ± 0	0.12 ± 0	0.06 ± 0.01	0.08 ± 0.01 _y	2.73 ± 0.04
	24 m CT	0.01 ± 0	0.13 ± 0.01	0.19 ± 0.01	0.05 ± 0	0.09 ± 0.02 _y	29.4 ± 4.57 _{x,y}
<i>rPer2</i>	3 m VT	0.23 ± 0	0.08 ± 0	0.55 ± 0.01	0.53 ± 0.04	0.35 ± 0.05	6.67 ± 0.33
	3 m CT	0.16 ± 0.01	0.34 ± 0.01	0.38 ± 0.01	0.28 ± 0.02	0.29 ± 0.02	2.41 ± 0.13 _x
	12 m VT	0.14 ± 0.02	0.17 ± 0.01	1.3 ± 0.02	0.29 ± 0.01	0.48 ± 0.12	9.76 ± 1.18 _y
	12 m CT	0.11 ± 0	0.34 ± 0.01	0.63 ± 0.02	0.42 ± 0.02	0.37 ± 0.05	5.66 ± 0.1 _x
	24 m VT	0.12 ± 0	0.04 ± 0	0.2 ± 0	0.11 ± 0.01	0.12 ± 0.01 _y	5.33 ± 0.65
	24 m CT	0 ± 0	0.04 ± 0	0.21 ± 0.01	0.14 ± 0.01	0.1 ± 0.02 _y	47.09 ± 6.55 _{x,y}
<i>rCry1</i>	3 m VT	1.9 ± 0.09	0.26 ± 0.01	0.66 ± 0.03	2.33 ± 0.15	1.29 ± 0.22	8.94 ± 0.2
	3 m CT	1.49 ± 0.03	0.34 ± 0.01	1.1 ± 0.03	1.45 ± 0.01	1.1 ± 0.12	4.35 ± 0.09 _x
	12 m VT	0.65 ± 0.01	0.24 ± 0.01	1.01 ± 0.05	1.74 ± 0.06	0.91 ± 0.14	7.26 ± 0.13 _y
	12 m CT	0.77 ± 0.01	0.25 ± 0.05	0.66 ± 0.02	1.5 ± 0.09	0.8 ± 0.12	7.08 ± 1.97
	24 m VT	1.66 ± 0.05	0.66 ± 0.02	2.16 ± 0.02	2.74 ± 0.02	1.81 ± 0.2	4.15 ± 0.14 _y
	24 m CT	1.7 ± 0.03	0.4 ± 0.01	2.19 ± 0.07	3.21 ± 0.1	1.87 ± 0.26	8.14 ± 0.26 _{x,y}
<i>rCry2</i>	3 m VT	0.34 ± 0.01	0.27 ± 0.01	0.29 ± 0.01	0.38 ± 0.02	0.32 ± 0.01	1.42 ± 0.03
	3 m CT	0.2 ± 0.01	0.32 ± 0.01	0.26 ± 0.01	0.21 ± 0	0.25 ± 0.01 _x	1.6 ± 0.05 _x
	12 m VT	0.28 ± 0.02	0.43 ± 0.02	0.44 ± 0	0.19 ± 0	0.33 ± 0.03	2.38 ± 0.05 _y
	12 m CT	0.21 ± 0.01	0.48 ± 0.01	0.38 ± 0.01	0.29 ± 0	0.34 ± 0.03	2.24 ± 0.07 _x
	24 m VT	0.27 ± 0.01	0.14 ± 0	0.18 ± 0	0.09 ± 0	0.17 ± 0.02 _y	3.07 ± 0.07
	24 m CT	0.04 ± 0	0.11 ± 0.01	0.18 ± 0.01	0.13 ± 0	0.11 ± 0.01 _{x,y}	5.05 ± 0.17 _{x,y}
<i>rRev-erba</i>	3 m VT	0.04 ± 0	2.94 ± 0.05	1.25 ± 0.02	0.06 ± 0	1.07 ± 0.31	66.05 ± 2.87
	3 m CT	0.02 ± 0	1.44 ± 0.05	0.75 ± 0.02	0.09 ± 0	0.57 ± 0.15	71.2 ± 0.72
	12 m VT	0.2 ± 0.01	5.3 ± 0.23	1.31 ± 0.01	0.08 ± 0	1.72 ± 0.55	69.43 ± 1.51
	12 m CT	0.19 ± 0.02	3.24 ± 0.12	2.76 ± 0.06	0.1 ± 0.01	1.57 ± 0.37	32.54 ± 3.29 _{x,y}
	24 m VT	0.21 ± 0	2.8 ± 0.07	1.3 ± 0.03	0.01 ± 0	1.08 ± 0.29	222.82 ± 2 _y
	24 m CT	0.06 ± 0	1.22 ± 0.07	1.11 ± 0.06	0.02 ± 0	0.6 ± 0.15	50.47 ± 1.59 _{x,y}
<i>rRora</i>	3 m VT	3.18 ± 0.21	1.29 ± 0.05	2.1 ± 0.03	4.77 ± 0.12	2.84 ± 0.34	3.73 ± 0.21
	3 m CT	2.04 ± 0.1	1.56 ± 0.12	1.68 ± 0.08	2.13 ± 0.08	1.85 ± 0.08 _x	1.39 ± 0.09 _x
	12 m VT	3.32 ± 0.03	2.16 ± 0.03	4.19 ± 0.13	2.46 ± 0.21	3.03 ± 0.21	1.94 ± 0.05 _y
	12 m CT	3.36 ± 0.11	1.79 ± 0.07	2.42 ± 0.07	1.97 ± 0.22	2.39 ± 0.17 _x	1.88 ± 0.04 _y
	24 m VT	3.98 ± 0.07	2.45 ± 0.05	2.66 ± 0.03	2.67 ± 0.02	2.94 ± 0.16	1.63 ± 0.06 _y
	24 m CT	2.15 ± 0.03	1.87 ± 0.11	2.42 ± 0.04	2.9 ± 0.16	2.33 ± 0.11 _x	1.56 ± 0.14 _y

mRNA expression of clock genes at ZT-0,6, 12 and 18. $p_x \leq 0.05$, $p_y \leq 0.05$ where, 'x' refers to significant difference with respective age-matched vehicle group. 'y' refers to significant difference with 3 m vehicle-treated group.

Table 9: Effect of curcumin on age-induced alterations of immune genes

Gene		ZT-0	ZT-6	ZT-12	ZT-18	Mean 24 h levels	Max/min ratio
<i>rNf-κb1</i>	3 m VT	0.31 ± 0.01	0.38 ± 0.04	0.22 ± 0	0.29 ± 0.02	0.3 ± 0.02	1.71 ± 0.17
	3 m CT	0.22 ± 0.02	0.27 ± 0.02	0.2 ± 0	0.17 ± 0	0.21 ± 0.01 _x	1.55 ± 0.07
	12 m VT	0.51 ± 0.01	0.36 ± 0.01	0.49 ± 0.02	0.19 ± 0.01	0.39 ± 0.03 _y	2.75 ± 0.09 _y
	12 m CT	0.34 ± 0.02	0.49 ± 0	0.33 ± 0.01	0.27 ± 0.01	0.36 ± 0.02	1.81 ± 0.04 _x
	24 m VT	0.61 ± 0.02	0.31 ± 0.01	0.32 ± 0.01	0.16 ± 0	0.35 ± 0.04	3.79 ± 0.06 _y
24 m CT	0.15 ± 0	0.23 ± 0.01	0.36 ± 0.02	0.24 ± 0	0.25 ± 0.02 _{x,y}	2.34 ± 0.12 _{x,y}	
<i>rTnfa</i>	3 m VT	0.61 ± 0.02	0.64 ± 0.03	1.4 ± 0.08	0.81 ± 0.08	0.86 ± 0.09	2.28 ± 0.08
	3 m CT	0.6 ± 0.05	0.73 ± 0.2	0.72 ± 0.08	0.69 ± 0.01	0.68 ± 0.05	1.17 ± 0.22 _x
	12 m VT	1.31 ± 0.15	1.3 ± 0.23	1.3 ± 0.13	0.9 ± 0.13	1.2 ± 0.09 _y	1.49 ± 0.12 _y
	12 m CT	1.6 ± 0.09	0.79 ± 0.18	1.26 ± 0.05	1.05 ± 0.06	1.16 ± 0.1 _y	2.5 ± 0.38 _x
	24 m VT	5.29 ± 0.21	4.82 ± 0.09	1.89 ± 0.19	2.02 ± 0.17	3.5 ± 0.41 _y	2.85 ± 0.19 _y
24 m CT	2.11 ± 0.11	2.01 ± 0.04	3.44 ± 0.16	1.69 ± 0.07	2.31 ± 0.18 _{x,y}	2.04 ± 0.05 _{x,y}	
<i>rIl6</i>	3 m VT	0.03 ± 0.01	0.02 ± 0	0.04 ± 0	0.02 ± 0	0.03 ± 0	2.39 ± 0.45
	3 m CT	0.02 ± 0	0.05 ± 0.01	0.04 ± 0	0.03 ± 0.01	0.04 ± 0	2.58 ± 0.23
	12 m VT	0.03 ± 0.01	0.04 ± 0.01	0.09 ± 0.02	0.13 ± 0.01	0.07 ± 0.01 _y	5.64 ± 0.78 _y
	12 m CT	0.03 ± 0.01	0.1 ± 0.01	0.05 ± 0.01	0.14 ± 0.03	0.08 ± 0.01 _y	4.02 ± 0.45 _y
	24 m VT	0.02 ± 0	0.02 ± 0	0.04 ± 0.01	0.02 ± 0	0.02 ± 0	2.36 ± 0.52
24 m CT	0.03 ± 0	0.01 ± 0	0.03 ± 0	0.02 ± 0	0.02 ± 0	2.34 ± 0.44	
<i>rTlr4</i>	3 m VT	0.09 ± 0	0.56 ± 0.03	0.06 ± 0	0.05 ± 0	0.19 ± 0.06	10.62 ± 0.13
	3 m CT	0.03 ± 0	0.06 ± 0	0.06 ± 0.01	0.05 ± 0	0.05 ± 0 _x	1.92 ± 0.07 _x
	12 m VT	0.04 ± 0.01	0.07 ± 0	0.09 ± 0.01	0.04 ± 0	0.06 ± 0.01 _y	2.21 ± 0.2 _y
	12 m CT	0.06 ± 0.01	0.11 ± 0.01	0.08 ± 0	0.07 ± 0	0.08 ± 0.01 _x	1.68 ± 0.1 _y
	24 m VT	0.32 ± 0.01	0.28 ± 0.01	0.19 ± 0	0.19 ± 0.01	0.25 ± 0.02	1.75 ± 0.02 _y
24 m CT	0.17 ± 0	0.22 ± 0	0.24 ± 0.01	0.15 ± 0	0.2 ± 0.01 _x	1.58 ± 0.03 _{x,y}	
<i>rTlr9</i>	3 m VT	0.29 ± 0.06	0.14 ± 0.01	0.33 ± 0.02	0.23 ± 0.04	0.25 ± 0.03	2.32 ± 0.07
	3 m CT	0.19 ± 0.03	0.23 ± 0.03	0.19 ± 0.02	0.25 ± 0.03	0.22 ± 0.01	1.51 ± 0.39
	12 m VT	0.24 ± 0.04	0.39 ± 0.05	0.51 ± 0.06	0.58 ± 0.04	0.43 ± 0.04 _y	2.66 ± 0.37
	12 m CT	0.46 ± 0.04	0.44 ± 0.1	0.49 ± 0.01	0.69 ± 0.13	0.52 ± 0.04 _y	1.67 ± 0.17 _y
	24 m VT	0.79 ± 0.01	0.57 ± 0.03	0.18 ± 0.04	0.46 ± 0.03	0.5 ± 0.06 _y	4.91 ± 0.9 _y
24 m CT	0.41 ± 0.03	0.6 ± 0.04	0.8 ± 0.06	0.5 ± 0.05	0.58 ± 0.04 _y	1.93 ± 0.07 _{x,y}	

mRNA expression of immune genes at ZT-0,6, 12 and 18. $p_x \leq 0.05$, $p_y \leq 0.05$ where ‘x’ refers to significant difference with the respective age-matched vehicle group. ‘y’ refers to significant difference with 3 m vehicle-treated group.

II. B (ii). Effect of curcumin on the age-induced alterations of clock and immune genes mRNA expression in kidney

Effect of curcumin on daily rhythms of clock genes in kidney

With curcumin treatment, *rBmal1* showed maximum expression at ZT-18 i.e. 6 h phase advance in 3 m animals with respect to 3 m vehicle group and minimum expression was at ZT-6. In 12 and 24 m, maximum expression persisted at ZT-0 and minimum at ZT-12 with curcumin treatment in comparison to age-matched vehicle groups. *rPer1* showed maximum expression at ZT-6 in 3 m CT group with phase advance of 6 h in comparison to 3 m vehicle group, minimum expression was at ZT-0. In both 12 and 24 m, curcumin treatment showed similar expression as in age-matched vehicle groups. In 3 m, curcumin treatment did not alter *rPer2* maximum expression but the minimum expression was shifted from ZT-6 to ZT-0. In 12 and 24 m, curcumin administration did not change the expression pattern of *rPer2* with respect to age-matched vehicle groups. In 3 m, maximum expression of *rCry1* persisted at ZT-18 but the minimum expression was observed at ZT-0 with curcumin treatment. In 12 m, curcumin did not alter daily rhythm in comparison to the vehicle group. In 24 m, curcumin restored maximum expression at ZT-18 in comparison to 3 m vehicle group. *rCry2* showed maximum expression at ZT-6 and minimum expression at ZT-0 in 3 m CT group. However, in 12 and 24 m, expression patterns were similar to the age-matched vehicle groups. In the case of *rRev-erba*, curcumin treatment did not change daily rhythm pattern in all the age groups with respect to age-matched vehicle groups. *rRora* showed maximum expression at ZT-6 and minimum expression at ZT-0 in 3 m CT group. In 12 m, curcumin restored rhythmicity with maximum expression at ZT-12 and minimum expression at ZT-6. In 24 m, maximum expression persisted at ZT-12 but the minimum expression was at ZT-18 with curcumin administration (Fig. 46) (Table 10).

Effect of curcumin on daily rhythms of immune genes in kidney

Curcumin administration resulted in significant decrease in the expression of inflammatory genes in kidney. Curcumin administration phase delayed *rNf- κ b1* about 6 h with maximum expression at ZT-18 and minimum expression at ZT-0 in 3 m. In 12 m, *rNf- κ b1* showed the restoration in comparison with 3 m vehicle group with maximum expression at ZT-12 and minimum expression at ZT-6. In 24 m, *rNf- κ b1* was phase advanced by 6 h with maximum expression at ZT-6 and minimum expression at ZT-18 with respect to 24 m vehicle group (Fig. 47).

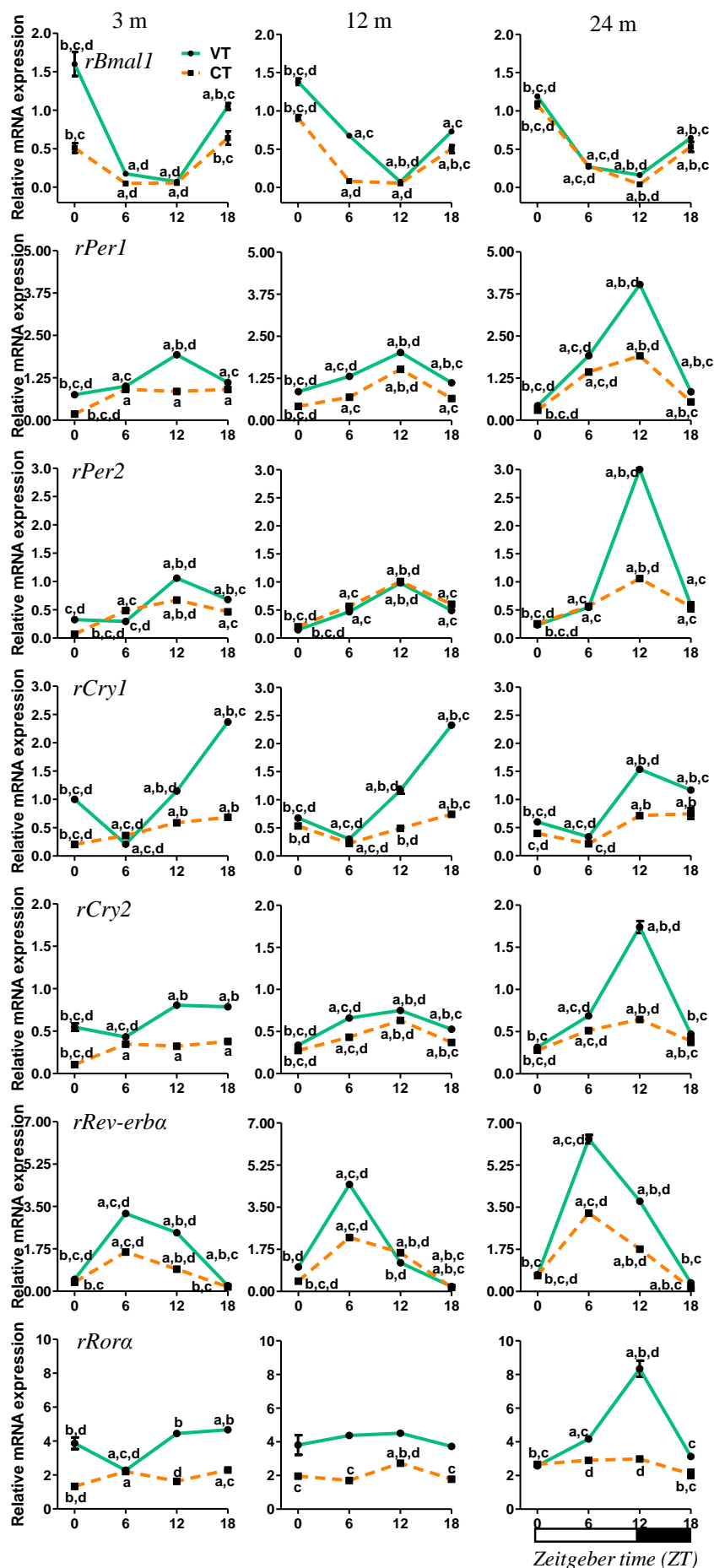


Fig. 46: Effect of curcumin administration on daily rhythms of clock genes mRNA expression in 3, 12 and 24 months (m) old rat kidney. Each value is mean \pm SEM ($n = 4$), $p \leq 0.05$ and expressed as relative mRNA expression. $p_a \leq 0.05$; $p_b \leq 0.05$, $p_c \leq 0.05$ and $p_d \leq 0.05$ (where ‘a’, ‘b’, ‘c’ and ‘d’ refers to comparison with ZT-0, ZT-6, ZT-12 and ZT-18 respectively within the group).

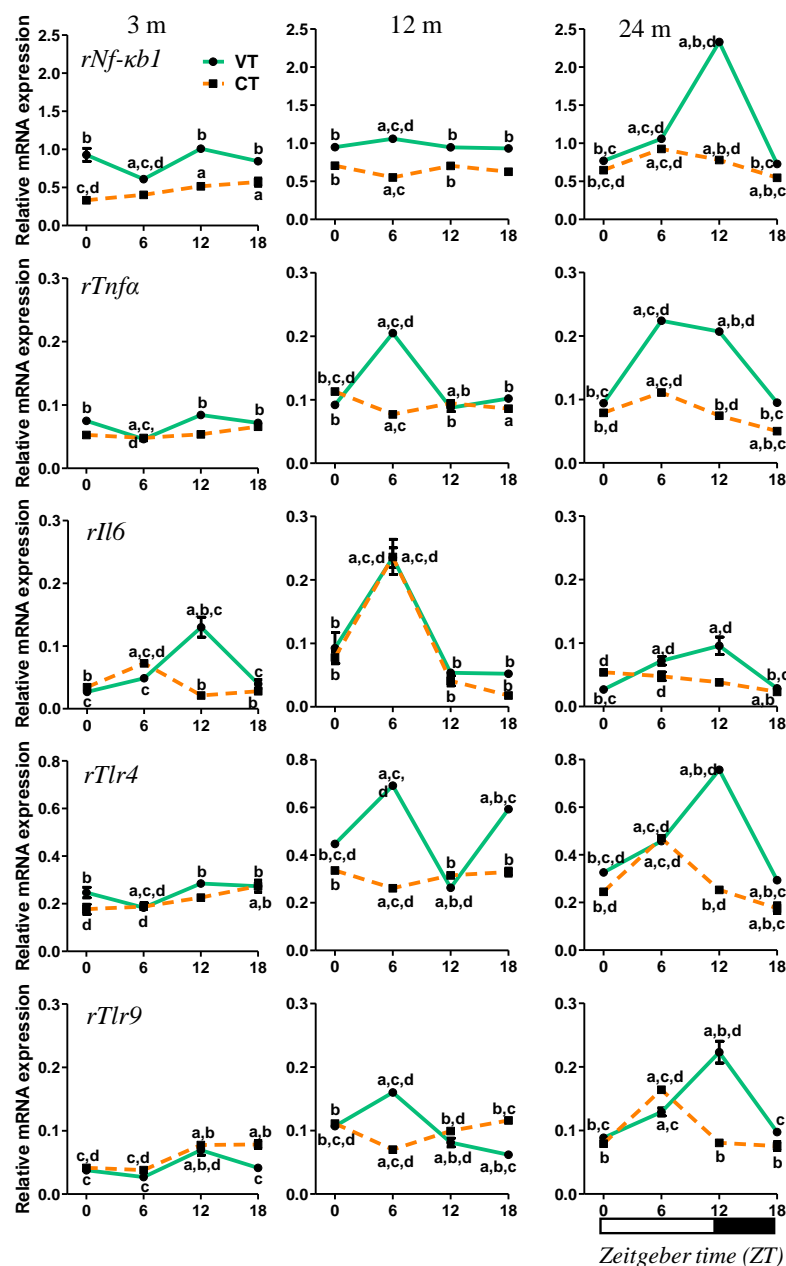


Fig. 47: Effect of curcumin administration on daily rhythms of *rNfκb1*, *rTnfa*, *rIl6*, *rTlr4* and *rTlr9* mRNA expression in 3, 12 and 24 months (m) old rat kidney. Each value is mean \pm SEM ($n = 4$), $p \leq 0.05$ and expressed as relative mRNA expression. $p_a \leq 0.05$; $p_b \leq 0.05$, $p_c \leq 0.05$ and $p_d \leq 0.05$ (where ‘a’, ‘b’, ‘c’ and ‘d’ refers to comparison with ZT-0, ZT-6, ZT-12, and ZT-18 respectively within the group).

rTnfa showed phase delay of 6 h with maximum expression at ZT-18, minimum expression at ZT-6 in 3 m CT. In 12 m, maximum expression was observed at ZT-0 which is 6 h phase advance with respect to 12 m vehicle group and minimum expression was at ZT-6. In 24 m, the expression pattern was not changed with respect to 24 m vehicle group. *rIl6* showed 6 h phase advance with maximum expression at ZT-6 and minimum expression at ZT-12 in 3 m CT group.

In 12 m, curcumin treatment did not change expression pattern with respect to 12 m vehicle group. But in 24 m, maximum expression was observed at ZT-0 which is 12 h phase advance in comparison to 24 m vehicle group and minimum expression at ZT-18. In 3 m curcumin-treated group, *rTlr4* showed maximum expression at ZT-18 with a phase delay of 6 h in comparison to 3 m vehicle group, and minimum expression was observed at ZT-0. In 12 m, maximum expression was observed at ZT-0 with the phase advance of 6 h and the minimum was observed at ZT-6. In 24 m, maximum expression was observed at ZT-6 with phase advance of 6 h and minimum expression was observed at ZT-18. With curcumin treatment, *rTlr9* showed rhythmic expression with a maximum at ZT-18 i.e. 6 hours phase delay with respect to 3 m vehicle group and minimum at ZT-6. In 12 m, maximum expression was observed at ZT-18 with a phase delay of 12 h and minimum expression at ZT-6. In 24 m, maximum expression was observed at ZT-6 with phase advance of 6 h and minimum expression was observed at ZT-18 (Fig. 47) (Table 11).

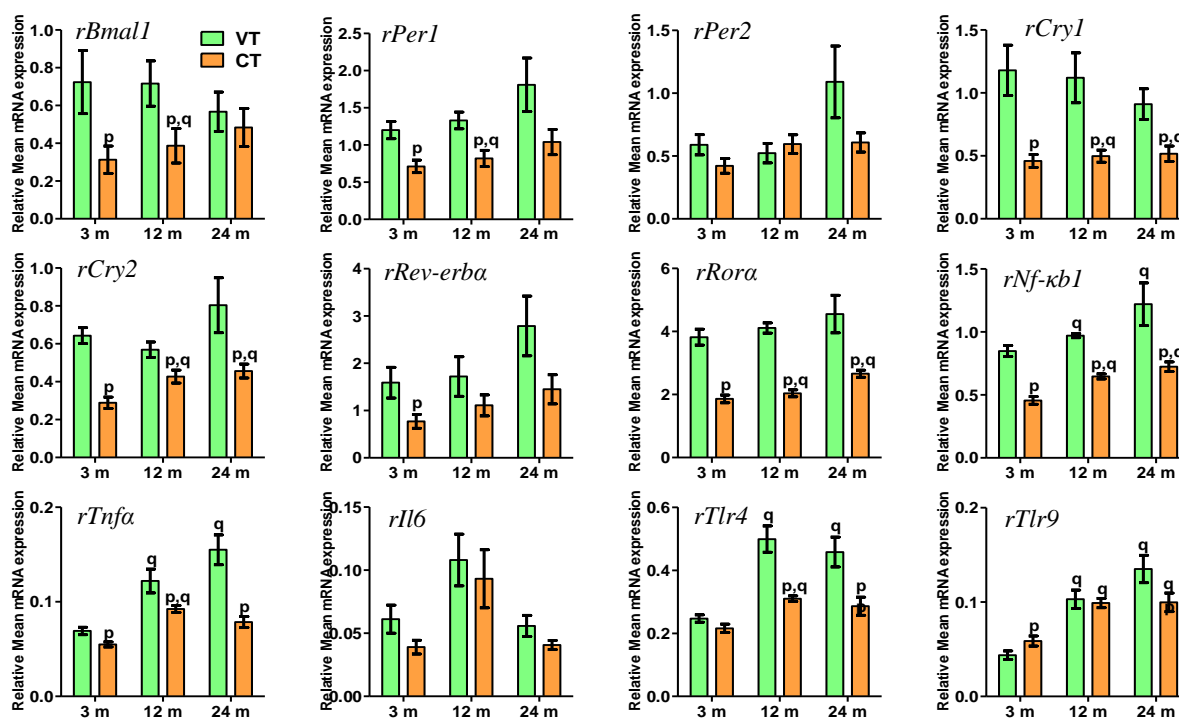


Fig. 48: Effect of curcumin administration on Mean 24 hour (h) levels of clock and immune genes expression in 3, 12 and 24 months (m) old rat kidney. Each value is mean \pm SEM ($n = 4$), $p \leq 0.05$ and expressed as mean relative gene expression. $p_p \leq 0.05$ (where 'p' refers to comparison with the age-matched vehicle-treated group). $p_q \leq 0.05$ (where 'q' refers to comparison with 3 m vehicle-treated group).

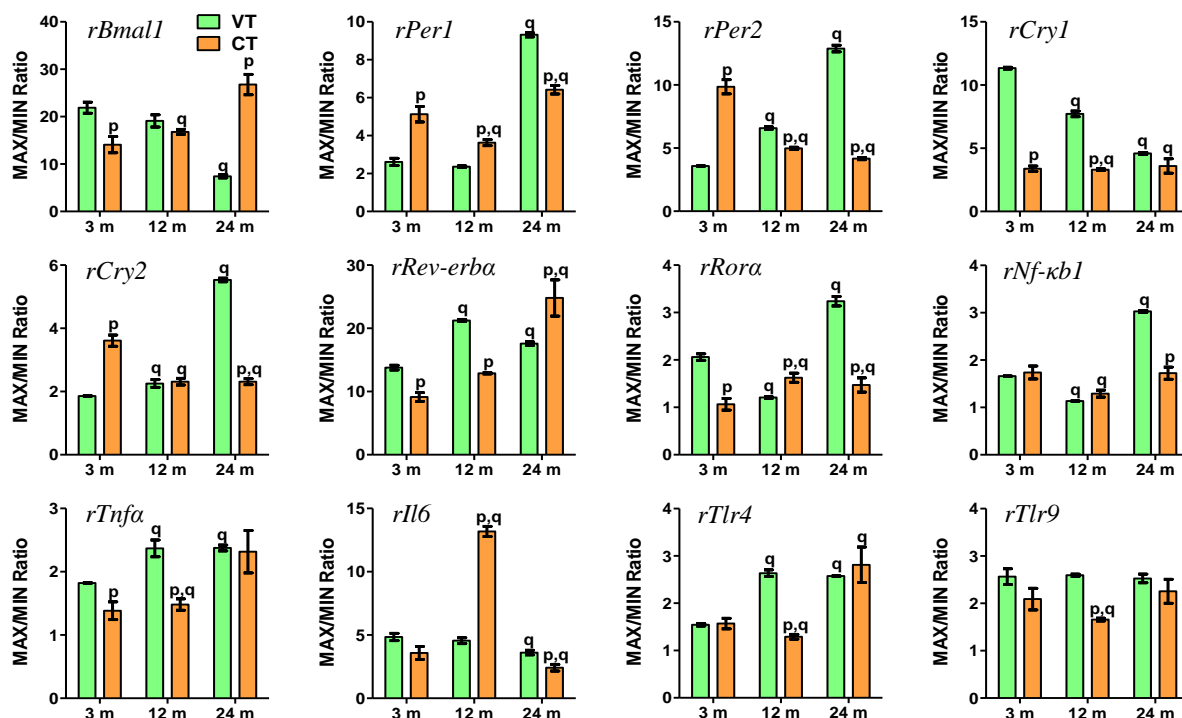


Fig. 49: Effect of curcumin administration on Daily pulse of clock and immune genes expression in 3, 12 and 24 months (m) old rat kidney. Each value is mean \pm SEM ($n = 4$), $p \leq 0.05$ and expressed as mean relative gene expression. $p_p \leq 0.05$ (where ‘p’ refers to comparison with the age-matched vehicle-treated group). $p_q \leq 0.05$ (where ‘q’ refers to comparison with 3 m vehicle-treated group).

Effect of curcumin on mean 24 h levels and daily pulse of clock genes in kidney

Curcumin administration reduced *rBmal1* and *rPer1* mean 24 h levels significantly ($p < 0.05$) in 3 and 12 m in comparison to age-matched vehicle groups, but did not show any change in 24 m. There was no significant change in mean 24 h levels of *rPer2* in 3, 12 and 24 m in comparison to age-matched vehicle groups. With curcumin administration mean 24 h levels of *rCry1*, *rCry2* and *rRora* were significantly decreased ($p < 0.05$) in all age groups with respect to age-matched VT. Mean 24 h levels showed a significant decrease in 3 m but did not show a significant change in 12 and 24 m group in comparison to age-matched vehicle groups (Fig. 48). Daily pulse of *rBmal1* showed a significant decrease in 3 m, did not vary in 12 m, but restored in 24 m animals with a significant increase ($p < 0.05$) in comparison to age-matched vehicle group. Daily pulse of *rPer1* showed a significant increase ($p < 0.05$) in 3 and 12 m with curcumin treatment in comparison to age-matched vehicle groups. In 24 m CT animals, a significant decrease ($p < 0.05$) was observed in comparison to 24 m vehicle group. Daily pulse of *rPer2* was significantly increased in 3 m but decreased in 12 and 24 m CT ($p < 0.05$) with respect to age-matched vehicle

groups. Daily pulse of *rCry1* reduced significantly ($p<0.05$) in all age groups. Daily pulse of *rCry2* increased in 3 m, unaltered in 12 m and decreased in 24 m ($p<0.05$) upon curcumin treatment. Curcumin treatment significantly decreased ($p<0.05$) daily pulse of *rRev-erba* in 3 and 12 m with respect to age-matched vehicle groups. However, curcumin restored daily pulse in 12 m in comparison to 3 m vehicle group. But in 24 m, daily pulse increased ($p<0.05$) in comparison to 24 m vehicle group. Curcumin decreased daily pulse of *rRora* in 3 and 24 m ($p<0.05$), however, increased ($p<0.05$) in 12 with respect to age-matched vehicle groups (Fig. 49) (Table 10).

Effect of curcumin on mean 24 h levels and daily pulse of immune genes in kidney

Being anti-oxidant curcumin significantly reduced the mean 24 h levels of *rNf- κ b1* and *rTnfa* in all age groups ($p<0.05$). But in 24 m, curcumin restored mean 24 h levels of *rTnfa* in comparison with 3 m vehicle group. Curcumin administration did not alter mean 24 h levels of *rIl6* in all age groups. Curcumin administration did not change mean 24 h levels of *rTlr4* in 3 m, but significantly reduced in 12 and 24 m ($p<0.05$) with respect to age-matched vehicle groups. Interestingly, in 24 m, curcumin restored the mean levels in comparison to 3 m vehicle group. With curcumin treatment, mean 24 h levels of *rTlr9* were significantly increased in 3 m ($p<0.05$), remained unaltered in 12 m and significantly decreased in 24 m ($p<0.05$) with respect to their age-matched vehicle groups (Fig. 48). Daily pulse of *rNf- κ b1* did not show a significant change in 3 and 12 m with respect to their age-matched vehicle groups. However, in 24 m, curcumin decreased ($p<0.05$) and restored daily pulse with respect to 3 m vehicle group. In 3 and 12 m, daily pulse of *rTnfa* was reduced significantly ($p<0.05$) in comparison to age-matched vehicle group. In 24 m, daily pulse remained unaltered with respect to 24 m vehicle group. Daily pulse of *rIl6* remained unaltered in 3 m, significantly increased in 12 m ($p<0.05$), and significantly decreased in 24 m ($p<0.05$) with curcumin administration. Daily pulse of *rTlr4* did not alter in 3 m and 24 m but significantly reduced in 12 m ($p<0.05$) with respect to age-matched vehicle groups. Daily pulse of *rTlr9* was unaltered in 3 and 24 m, significantly reduced in 12 m ($p<0.05$) with curcumin treatment (Fig. 49) (Table 11).

Effect of curcumin on the correlations among clock genes in kidney

In light phase of 3 m CT group, negative correlation of *rBmal1* with *rPer1* genes and *rRev-erba* ($p<0.001$) persisted. Within and between *rPer1,2* and *rCry1,2* genes positive correlation persisted ($p<0.001$; $p<0.01$). *rRora* changed to positive correlation with *rRev-erba* ($p<0.001$) but positive

correlation with *rCry2* ($p < 0.001$) persisted. In dark phase of 3 m CT group, negative correlation of *rBmall* with *rRev-erba* ($p < 0.001$) persisted. Positive correlation persisted between *rPer1,2* and *rCry1,2* genes ($p < 0.001$). *rRora* showed insignificant negative correlation with *rRev-erba* but significant positive correlation ($p < 0.001$) with *Cry1,2* genes persisted (Fig. 50).

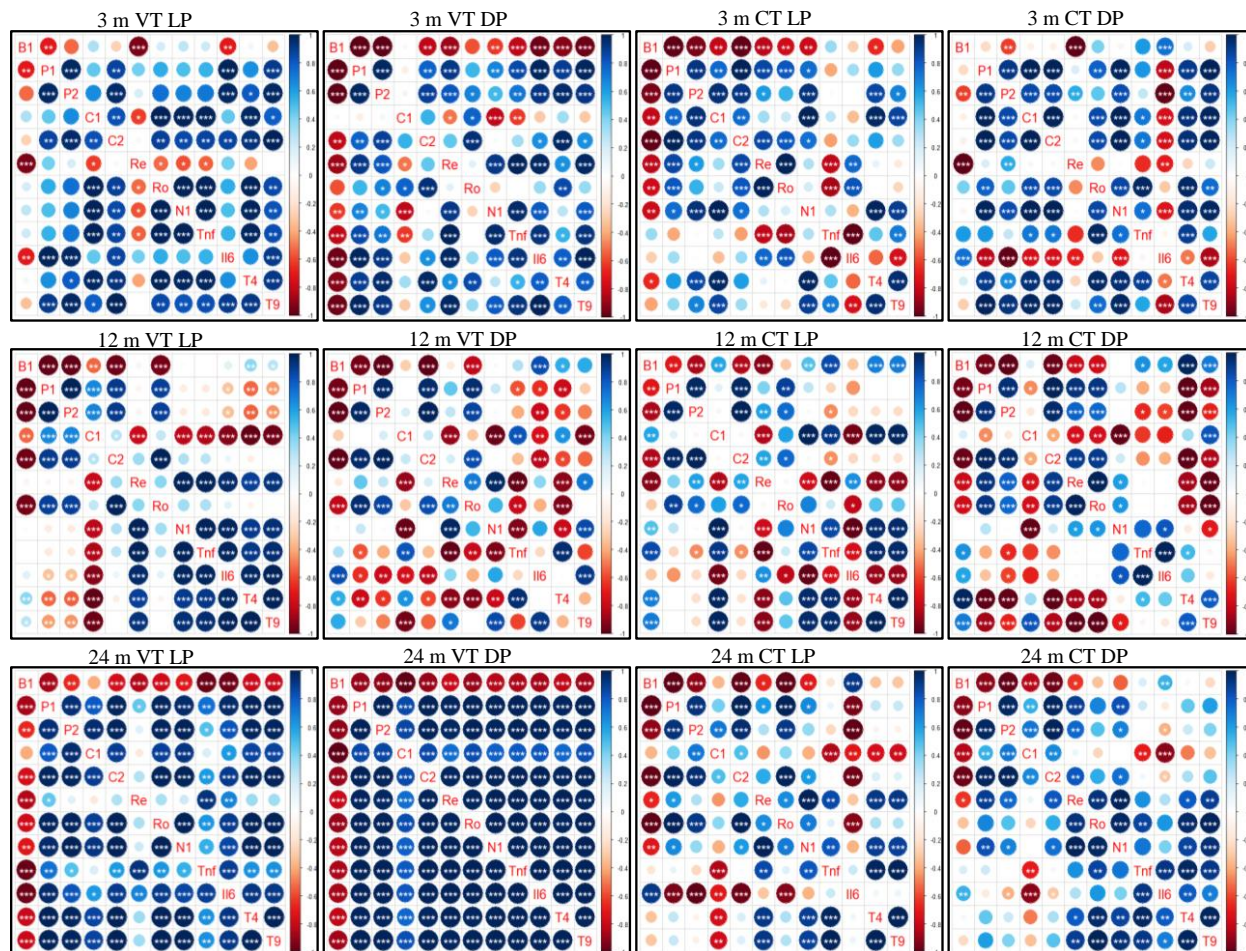


Fig. 50: Effect of curcumin administration on pairwise correlations between clock and immune genes in light (ZT-0, 6, 12) and dark (ZT-12, 18, 24/0) phase of 3, 12 and 24 months (m) old rat kidney (LP - light phase; DP - dark phase; VT - vehicle-treated; CT - curcumin treated). The intensity of color and size of the circle represents correlation coefficient values between the genes. Where, positive correlations are indicated by shades of blue, negative correlations by shades of red and white indicates no correlation. ‘*’, ‘**’, ‘***’ indicates statistically significant correlations ($p \leq 0.05$), ($p \leq 0.01$), ($p \leq 0.001$) respectively. (B1- *rBmall*; P1 - *rPer1*; P2 - *rPer2*; C1 - *rCry1*; C2 - *rCry2*; Re - *rRev-erba*; Ro - *rRora*; N1 - *rNfkb1*; Tnf - *rTnfa*; Il6 - *rIl6*; T4 - *rTlr4*; T9 - *rTlr9*).

In light phase of 12 m CT group, negative correlation of *rBmall* with *rRev-erba* was restored and negative correlation with *rPer1* gene ($p < 0.001$; $p < 0.01$) persisted. Positive correlation between *rPer1,2* genes persisted ($p < 0.001$). Curcumin administration abolished correlation between *rCry1,2* genes. *rRora* showed significant positive correlation with *rCry2* ($p < 0.05$) but not with

rRev-erba and *rCry1*. In dark phase of 12 m CT group, negative correlation of *rBmal1* with *rRev-erba* was restored and negative correlation with *rPer1* gene ($p < 0.001$) persisted. Positive correlation between *rPer1,2* genes ($p < 0.001$) persisted. Interestingly, *rCry1* showed negative correlation with *rCry2* ($p < 0.05$). *rRora* showed positive correlation with *rCry2*, *rRev-erba* ($p < 0.001$) and negative correlation with *rCry1* ($p < 0.01$) (Fig. 50).

In light phase of 24 m CT group, negative correlation of *rBmal1* with *rPer1* genes and *rRev-erba* ($p < 0.001$) persisted. Positive correlation within the *rPer1,2* and *rCry1,2* genes persisted ($p < 0.001$; $p < 0.05$). In dark phase of 24 m CT group, negative correlation of *rBmal1* with *rPer1* and *rRev-erba* ($p < 0.001$) persisted. Positive correlation within and between *rPer1,2* and *rCry1,2* genes persisted ($p < 0.001$; $p < 0.01$) (Fig. 50).

Effect of curcumin on the correlations among immune genes in kidney

In the light phase of 3 m CT group, curcumin administration abolished correlation between *rNf- κ b1* and *rTnfa* but showed a significant negative correlation between *rTnfa* and *Il6* ($p < 0.001$). The positive correlation of *rNf- κ b1* with *Tlr9* and *Tlr4* ($p < 0.001$) persisted. In the dark phase of 3 m CT group, a positive correlation of *rNf- κ b1* with *rTnfa*, *rTlr9* and *rTlr4* ($p < 0.001$; $p < 0.05$) persisted. But *rNf- κ b1* changed to negative correlation with *rIl6* ($p < 0.001$) (Fig. 50).

In the light phase of 12 m CT group, a positive correlation of *rNf- κ b1* with *rTnfa*, *rTlr4* and *rTlr9* ($p < 0.001$) persisted. A significant negative correlation was observed between *rTnfa* and *rIl6* ($p < 0.001$). A significant negative correlation was observed between *rIl6* and *rTlr4,9* ($p < 0.001$). In the dark phase of 12 m CT group, curcumin treatment resulted in the abolition of correlation of *rNf- κ b1* with *rTnfa* and *rTlr4*. However, a positive correlation was restored between *rNf- κ b1* and *rIl6* ($p < 0.05$); *rTnfa* and *rIl6* ($p < 0.001$). Interestingly, negative correlation appeared between *rNf- κ b1* and *rTlr9* ($p < 0.05$). A positive correlation between *rTnfa* and *rIl6* ($p < 0.001$) was restored, and the positive correlation between *rTlr4* and *rTlr9* ($p < 0.001$) was restored (Fig. 50).

In the light phase of 24 m CT group, a positive correlation of *rNf- κ b1* with *rTnfa* and *rTlr4,9* ($p < 0.001$; $p < 0.01$) persisted. Curcumin administration resulted in the abolition of the correlation between *rNf- κ b1* and *rIl6* and resulted in restoration in comparison to LP of 3 m vehicle group. Correlation between *rIl6* and *rTlr4,9* abolished. In the dark phase of 24 m CT group significant correlation of *rNf- κ b1* with *rTnfa* abolished, but positive correlation with *rTlr4,9* ($p < 0.001$; $p < 0.01$) persisted. Positive correlation of *rIl6* with *rTlr4,9* ($p < 0.01$; $p < 0.05$) persisted (Fig. 50).

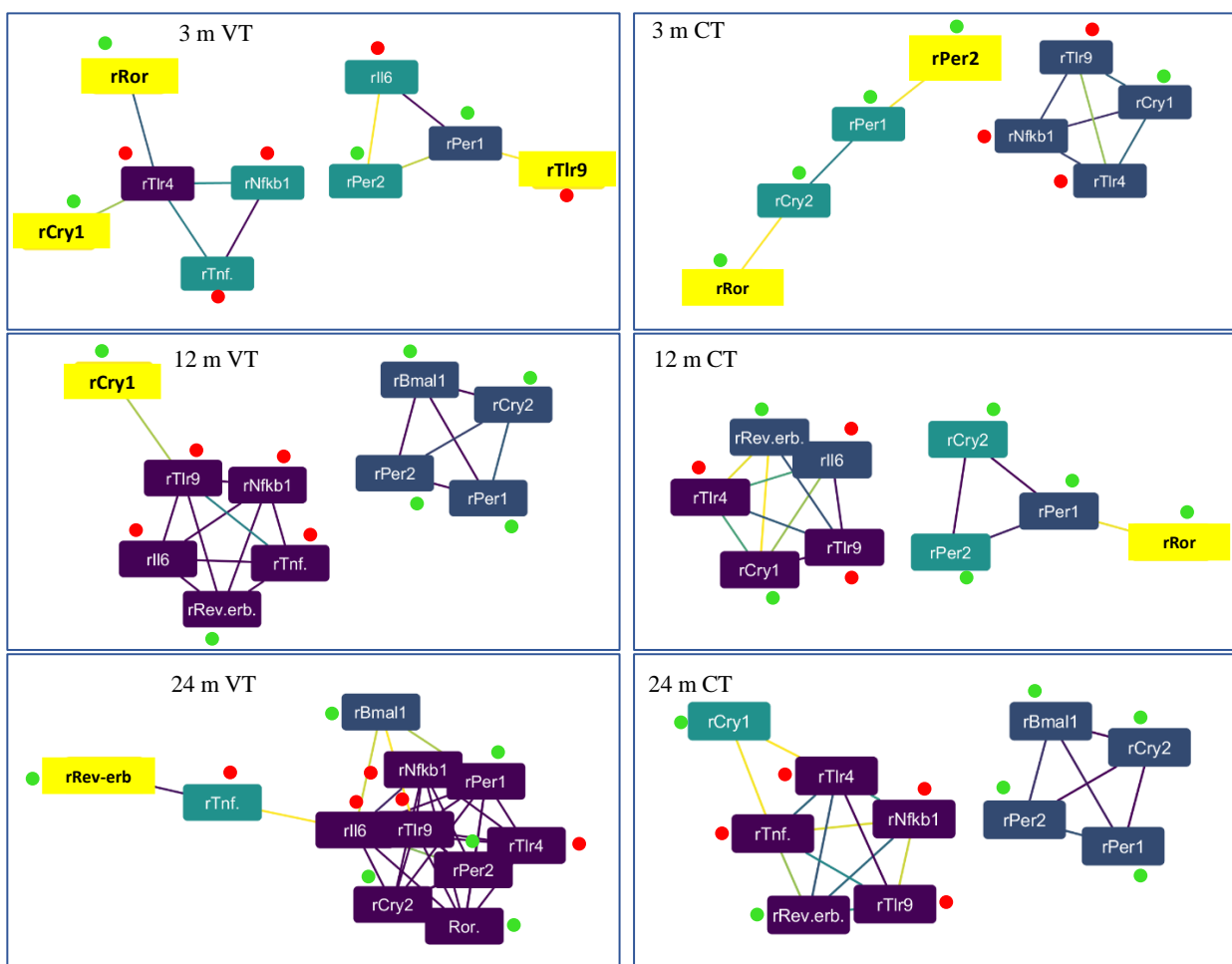


Fig. 51: WGCNA analysis between clock and immune gene clusters: effect aging on gene to gene network in 3, 12 and 24 m old rat kidney (left panel) and effect of curcumin administration (right panel). Color of the node indicates no. of interactions (highest—purple; intermediate—cyan and least—yellow). Color of an edge indicates the strength of interaction (strongest—purple; cyan—intermediate and weakest—yellow). Green and red dots indicate clock and immune genes respectively.

Effect of curcumin on the correlations between clock and immune genes in kidney

In the light phase of 3 m CT group, positive correlation of *rCry1,2* genes with *rNf- κ b1* ($p < 0.001$; $p < 0.05$) persisted but abolished with *rTnfa*. The positive correlation of *rTlr4* and *rTlr9* with *Cry1* ($p < 0.001$) persisted. Curcumin resulted in the abolition of the correlation between *rIl6* and *rPer1,2* genes. In the dark phase of 3 m CT group, a significant positive correlation of *rPer1,2* genes with *rNf- κ b1* ($p < 0.001$) persisted. Positive correlation of *rPer1,2* with *Tlr4* and *Tlr9* persisted ($p < 0.001$; $p < 0.01$) (Fig. 50).

In the light phase of 12 m CT group, *rNf- κ b1*, *rTnfa* and *rTlr4,9* changed to a positive correlation with *rCry1* and *rRev-erba*. The positive correlation of *rTlr4* and *rTlr9* with *rPer1,2* genes abolished. In the dark phase of 12 m CT group, *rTlr9* showed a significant negative correlation with *rPer1,2* genes ($p < 0.001$). Correlation of *rCry1* with *rTnfa*, *rIl6* and *rTlr4* abolished. Correlation between *rRev-erba* and *rTnfa* abolished (Fig. 50).

In the light phase of 24 m CT group, the correlation between *rTlr4,9* and *rPer1,2* genes abolished. *rIl6* showed negative correlation with *rPer1,2* genes ($p < 0.001$). Correlation between *rNf- κ b1* and *rCry1* abolished. *rIl6* and *rTlr4,9* changed to negative correlation with *rCry1*. In the dark phase of 24 m CT group, there was the abolition of the correlation between *rTlr4,9* and *rPer1,2* genes. *rTnfa*, *rIl6* changed to negative correlation with *rCry1*. Correlation between *rCry1* and *rNf- κ b1* abolished with curcumin treatment (Fig. 50).

WGCNA analysis between clock and immune genes with curcumin treatment in kidney

In 3 m CT, *rCry1* showed interactions with *rNf- κ b1*, *rTlr4,9*. In 12 m CT, interactions of *rRev-erba* with *rIl6* and *rTlr9* persisted and *rBmal1* lost the interactions with other clock genes. In 24 m CT, the interactions between clock and immune genes showed similarity with the interactions observed in 12 m VT, where *rRev-erba* showed interactions with all immune genes except *rIl6*; *rBmal1*, *rPer1,2*, *rCry2* showed interactions with each other (Fig. 51).

Table 10: Effect of curcumin on age-induced alterations of clock genes expression

Gene		ZT-0	ZT-6	ZT-12	ZT-18	Mean 24 h levels	Max/min ratio
<i>rBmal1</i>	3 m VT	1.6 ± 0.16	0.17 ± 0.01	0.07 ± 0.01	1.05 ± 0.04	0.72 ± 0.17	21.89 ± 1.16
	3 m CT	0.51 ± 0.06	0.05 ± 0.01	0.06 ± 0.01	0.64 ± 0.09	0.31 ± 0.07 _x	14.1 ± 1.71 _x
	12 m VT	1.38 ± 0.04	0.68 ± 0.02	0.07 ± 0.01	0.73 ± 0.02	0.72 ± 0.12	19.1 ± 1.28
	12 m CT	0.91 ± 0.04	0.08 ± 0.01	0.05 ± 0	0.5 ± 0.05	0.39 ± 0.09 _{x,y}	16.8 ± 0.53 _y
	24 m VT	1.19 ± 0.02	0.27 ± 0.01	0.16 ± 0.01	0.65 ± 0.02	0.57 ± 0.1	7.43 ± 0.33 _y
	24 m CT	1.08 ± 0.04	0.28 ± 0.01	0.04 ± 0	0.53 ± 0.06	0.48 ± 0.1	26.77 ± 2.16 _x
<i>rPer1</i>	3 m VT	0.75 ± 0.06	1 ± 0.01	1.93 ± 0.03	1.11 ± 0.02	1.2 ± 0.11	2.61 ± 0.19
	3 m CT	0.18 ± 0.02	0.91 ± 0.07	0.85 ± 0.07	0.91 ± 0.09	0.71 ± 0.08 _x	5.13 ± 0.41 _x
	12 m VT	0.86 ± 0.02	1.31 ± 0.03	2.02 ± 0.07	1.12 ± 0.01	1.33 ± 0.11	2.36 ± 0.04
	12 m CT	0.42 ± 0	0.69 ± 0.03	1.52 ± 0.05	0.65 ± 0.03	0.82 ± 0.11 _{x,y}	3.63 ± 0.16 _{x,y}
	24 m VT	0.43 ± 0.01	1.92 ± 0.03	4.03 ± 0.05	0.84 ± 0.01	1.81 ± 0.36	9.32 ± 0.11 _y
	24 m CT	0.3 ± 0	1.43 ± 0.01	1.91 ± 0.07	0.54 ± 0.06	1.04 ± 0.17	6.42 ± 0.22 _{x,y}
<i>rPer2</i>	3 m VT	0.33 ± 0.03	0.3 ± 0	1.06 ± 0.01	0.68 ± 0.02	0.59 ± 0.08	3.58 ± 0.02
	3 m CT	0.07 ± 0.01	0.48 ± 0.03	0.67 ± 0.05	0.46 ± 0.04	0.42 ± 0.06	9.86 ± 0.57 _x
	12 m VT	0.15 ± 0	0.47 ± 0.01	0.98 ± 0.04	0.49 ± 0.01	0.52 ± 0.08	6.59 ± 0.1 _y
	12 m CT	0.2 ± 0	0.57 ± 0.03	1.01 ± 0.02	0.6 ± 0.02	0.6 ± 0.07	4.99 ± 0.09 _{x,y}
	24 m VT	0.23 ± 0.01	0.55 ± 0.01	3 ± 0.02	0.59 ± 0.01	1.09 ± 0.29	12.88 ± 0.27 _y
	24 m CT	0.25 ± 0.01	0.57 ± 0	1.06 ± 0	0.56 ± 0.08	0.61 ± 0.08	4.17 ± 0.09 _{x,y}
<i>rCry1</i>	3 m VT	1 ± 0.05	0.21 ± 0	1.15 ± 0.03	2.37 ± 0.03	1.18 ± 0.2	11.34 ± 0.07
	3 m CT	0.2 ± 0.02	0.36 ± 0.02	0.59 ± 0.05	0.68 ± 0.05	0.46 ± 0.05 _x	3.38 ± 0.21 _x
	12 m VT	0.68 ± 0.01	0.3 ± 0.01	1.17 ± 0.06	2.33 ± 0.06	1.12 ± 0.2	7.72 ± 0.23 _y
	12 m CT	0.53 ± 0.02	0.22 ± 0.01	0.49 ± 0.01	0.74 ± 0.03	0.5 ± 0.05 _{x,y}	3.31 ± 0.06 _{x,y}
	24 m VT	0.6 ± 0.02	0.34 ± 0.01	1.54 ± 0.02	1.17 ± 0.02	0.91 ± 0.12	4.59 ± 0.07 _y
	24 m CT	0.4 ± 0.01	0.21 ± 0.01	0.71 ± 0.02	0.75 ± 0.09	0.52 ± 0.06 _{x,y}	3.6 ± 0.57 _y
<i>rCry2</i>	3 m VT	0.55 ± 0.04	0.43 ± 0.01	0.8 ± 0.01	0.79 ± 0.01	0.64 ± 0.04	1.86 ± 0.01
	3 m CT	0.11 ± 0.01	0.35 ± 0.03	0.32 ± 0.02	0.38 ± 0.03	0.29 ± 0.03 _x	3.61 ± 0.18 _x
	12 m VT	0.34 ± 0.02	0.66 ± 0.02	0.75 ± 0.01	0.53 ± 0.01	0.57 ± 0.04	2.25 ± 0.12 _y
	12 m CT	0.27 ± 0.01	0.43 ± 0.01	0.63 ± 0.02	0.37 ± 0.01	0.43 ± 0.03 _{x,y}	2.31 ± 0.11 _y
	24 m VT	0.31 ± 0.01	0.69 ± 0.02	1.74 ± 0.07	0.47 ± 0.01	0.8 ± 0.14	5.53 ± 0.06 _y
	24 m CT	0.28 ± 0.01	0.51 ± 0.01	0.64 ± 0.02	0.39 ± 0.04	0.46 ± 0.04 _{x,y}	2.31 ± 0.09 _{x,y}
<i>rRev-erba</i>	3 m VT	0.5 ± 0.04	3.21 ± 0.03	2.42 ± 0.04	0.23 ± 0.01	1.59 ± 0.33	13.79 ± 0.38
	3 m CT	0.38 ± 0.04	1.62 ± 0.12	0.91 ± 0.05	0.18 ± 0.01	0.77 ± 0.15 _x	9.14 ± 0.7 _x
	12 m VT	1.02 ± 0.01	4.45 ± 0.1	1.19 ± 0.05	0.21 ± 0	1.72 ± 0.42	21.25 ± 0.17 _y
	12 m CT	0.43 ± 0.01	2.24 ± 0.09	1.61 ± 0.02	0.17 ± 0.01	1.11 ± 0.22	12.89 ± 0.09 _x
	24 m VT	0.7 ± 0.01	6.33 ± 0.17	3.75 ± 0.06	0.36 ± 0.01	2.79 ± 0.63	17.58 ± 0.28 _y
	24 m CT	0.66 ± 0.01	3.25 ± 0.06	1.76 ± 0.07	0.14 ± 0.01	1.45 ± 0.31	24.81 ± 2.86 _{x,y}
<i>rRora</i>	3 m VT	3.87 ± 0.34	2.28 ± 0.1	4.45 ± 0.05	4.67 ± 0.07	3.82 ± 0.26	2.06 ± 0.07
	3 m CT	1.33 ± 0.13	2.2 ± 0.15	1.63 ± 0.11	2.3 ± 0.17	1.86 ± 0.12 _x	1.07 ± 0.12 _x
	12 m VT	3.81 ± 0.58	4.38 ± 0.11	4.51 ± 0.08	3.73 ± 0.08	4.11 ± 0.16	1.21 ± 0.02 _y
	12 m CT	1.96 ± 0.06	1.7 ± 0.1	2.73 ± 0.02	1.78 ± 0.05	2.04 ± 0.11 _{x,y}	1.62 ± 0.1 _{x,y}
	24 m VT	2.57 ± 0.07	4.17 ± 0.06	8.34 ± 0.48	3.13 ± 0.1	4.55 ± 0.59	3.24 ± 0.1 _y
	24 m CT	2.66 ± 0.04	2.9 ± 0.15	2.98 ± 0.11	2.09 ± 0.24	2.66 ± 0.11 _{x,y}	1.47 ± 0.15 _{x,y}

mRNA expression of clock genes at ZT-0,6, 12 and 18. $p_x \leq 0.05$, $p_y \leq 0.05$ where, 'x' refers to significant difference with respective age-matched vehicle group. 'y' refers to significant difference with 3 m vehicle-treated group.

Table 11: Effect of curcumin on age-induced alterations of immune genes expression

Gene		ZT-0	ZT-6	ZT-12	ZT-18	Mean 24 h levels	Max/min ratio
<i>rNf-κb1</i>	3 m VT	0.93 ± 0.08	0.61 ± 0.01	1.01 ± 0.01	0.84 ± 0.01	0.85 ± 0.04	1.66 ± 0
	3 m CT	0.33 ± 0.04	0.4 ± 0.03	0.52 ± 0.04	0.57 ± 0.05	0.46 ± 0.03 _x	1.74 ± 0.14
	12 m VT	0.95 ± 0.02	1.06 ± 0.01	0.95 ± 0.03	0.93 ± 0.01	0.97 ± 0.02 _y	1.13 ± 0 _y
	12 m CT	0.71 ± 0.01	0.55 ± 0.03	0.7 ± 0.01	0.63 ± 0.04	0.65 ± 0.02 _{x,y}	1.29 ± 0.07 _y
	24 m VT	0.77 ± 0	1.06 ± 0.03	2.33 ± 0.03	0.73 ± 0.01	1.22 ± 0.17 _y	3.03 ± 0.02 _y
	24 m CT	0.65 ± 0.01	0.93 ± 0.01	0.78 ± 0.02	0.55 ± 0.04	0.72 ± 0.04 _{x,y}	1.72 ± 0.13 _x
<i>rTnfa</i>	3 m VT	0.07 ± 0	0.05 ± 0	0.08 ± 0	0.07 ± 0	0.07 ± 0	1.82 ± 0.01
	3 m CT	0.05 ± 0.01	0.05 ± 0	0.05 ± 0	0.07 ± 0.01	0.05 ± 0 _x	1.38 ± 0.14 _x
	12 m VT	0.09 ± 0	0.2 ± 0	0.09 ± 0.01	0.1 ± 0	0.12 ± 0.01 _y	2.37 ± 0.13 _y
	12 m CT	0.11 ± 0	0.08 ± 0	0.09 ± 0	0.09 ± 0	0.09 ± 0 _{x,y}	1.48 ± 0.09 _{x,y}
	24 m VT	0.09 ± 0	0.22 ± 0.01	0.21 ± 0	0.09 ± 0	0.15 ± 0.02 _y	2.38 ± 0.05 _y
	24 m CT	0.08 ± 0	0.11 ± 0.01	0.07 ± 0	0.05 ± 0.01	0.08 ± 0.01 _x	2.32 ± 0.33
<i>rIl6</i>	3 m VT	0.03 ± 0	0.05 ± 0	0.13 ± 0.02	0.04 ± 0.01	0.06 ± 0.01	4.84 ± 0.29
	3 m CT	0.03 ± 0	0.07 ± 0	0.02 ± 0	0.03 ± 0	0.04 ± 0.01	3.58 ± 0.51
	12 m VT	0.09 ± 0.02	0.24 ± 0.02	0.05 ± 0	0.05 ± 0	0.11 ± 0.02	4.55 ± 0.23
	12 m CT	0.08 ± 0.01	0.24 ± 0.03	0.04 ± 0.01	0.02 ± 0	0.09 ± 0.02	13.19 ± 0.4 _{x,y}
	24 m VT	0.03 ± 0	0.07 ± 0.01	0.1 ± 0.01	0.03 ± 0	0.06 ± 0.01	3.61 ± 0.18 _y
	24 m CT	0.05 ± 0	0.05 ± 0.01	0.04 ± 0	0.02 ± 0	0.04 ± 0	2.42 ± 0.26 _{x,y}
<i>rTlr4</i>	3 m VT	0.25 ± 0.02	0.18 ± 0	0.28 ± 0.01	0.27 ± 0.01	0.25 ± 0.01	1.55 ± 0.03
	3 m CT	0.18 ± 0.02	0.19 ± 0.02	0.23 ± 0.01	0.27 ± 0.02	0.22 ± 0.01	1.57 ± 0.11
	12 m VT	0.45 ± 0.01	0.69 ± 0	0.26 ± 0.01	0.59 ± 0	0.5 ± 0.04 _y	2.64 ± 0.07 _y
	12 m CT	0.34 ± 0	0.26 ± 0.01	0.32 ± 0.01	0.33 ± 0.02	0.31 ± 0.01 _{x,y}	1.29 ± 0.05 _{x,y}
	24 m VT	0.33 ± 0	0.46 ± 0.01	0.76 ± 0.01	0.29 ± 0	0.46 ± 0.05 _y	2.57 ± 0.01 _y
	24 m CT	0.25 ± 0	0.47 ± 0.01	0.25 ± 0.01	0.18 ± 0.02	0.29 ± 0.03 _x	2.81 ± 0.38 _y
<i>rTlr9</i>	3 m VT	0.04 ± 0	0.03 ± 0	0.07 ± 0.01	0.04 ± 0	0.04 ± 0	2.57 ± 0.17
	3 m CT	0.04 ± 0	0.04 ± 0	0.08 ± 0.01	0.08 ± 0.01	0.06 ± 0.01 _x	2.09 ± 0.23
	12 m VT	0.11 ± 0	0.16 ± 0	0.08 ± 0.01	0.06 ± 0	0.1 ± 0.01 _y	2.6 ± 0.02
	12 m CT	0.11 ± 0	0.07 ± 0	0.1 ± 0	0.12 ± 0.01	0.1 ± 0 _y	1.66 ± 0.03 _{x,y}
	24 m VT	0.09 ± 0.01	0.13 ± 0.01	0.22 ± 0.02	0.1 ± 0	0.13 ± 0.01 _y	2.53 ± 0.09
	24 m CT	0.08 ± 0	0.16 ± 0	0.08 ± 0	0.08 ± 0.01	0.1 ± 0.01 _y	2.26 ± 0.25

mRNA expression of immune genes at ZT-0,6, 12 and 18. $p_x \leq 0.05$, $p_y \leq 0.05$ where 'x' refers to significant difference with the respective age-matched vehicle group. 'y' refers to significant difference with 3 m vehicle-treated group.

II. B (iii). Effect of curcumin on the age-induced alterations of clock and immune genes mRNA expression in spleen

Effect of curcumin on daily rhythms of clock genes in spleen

With curcumin administration, *rBmal1* did not show variation in the phase of rhythmicity in all age groups in comparison to age-matched vehicle group. *rPer1* showed 6 h phase delay in 3 m, did not alter in 12 m in comparison to the age-matched vehicle group, but phase was restored in 24 m with maximum expression at ZT-12 in comparison to 3 m VT group. Curcumin did not alter the phase of *rPer2* in 3 and 24 m, but phase delayed by 6 h in 12 m in comparison to age-matched vehicle group. Curcumin resulted in 12 h and 6 h phase delay of *rCry1* in 3 and 12 m respectively but did not alter in 24 m in comparison to age-matched vehicle group. Curcumin resulted in 6 h phase delay of *rCry2* in 3 m but restored the phase in 12 m with maximum expression at ZT-12 in comparison to 3 m VT group. Curcumin did not alter the phase of *rCry2* in 24 m in comparison to 24 m VT group. Curcumin did not show alteration in the phase of *rRev-erba* in all the age groups in comparison to age-matched vehicle group. *rRora* showed rhythmicity in 3 m with maximum expression at ZT-18, but in 12 and 24 m, *rRora* showed 6 h phase delay with curcumin administration in comparison to age-matched vehicle group (Fig. 52).

Effect of curcumin on daily rhythms of immune genes in spleen

With curcumin administration, *rNf- κ b1* did not show alteration in all the age groups in comparison to age-matched vehicle group. Curcumin phase delayed *rTnfa* by 6 h in 3 m, but phase advanced by 6 h and 12 h in 12 and 24 m in comparison to age-matched vehicle group. Curcumin resulted in 6 h and 12 h phase delay of *rIl6* in 3 and 12 m respectively but did not alter in 24 m in comparison to age-matched vehicle group. *rTlr4* showed 6 h phase advance in 3 m but showed 12 h and 6 h phase delay in 12 and 24 m in comparison to age-matched vehicle group. Curcumin phase advanced *rTlr9* by 6 h in 3 m, but restored the phase in 12 m with maximum expression at ZT-18 and phase delayed by 12 h in 24 m in comparison to age-matched vehicle group (Fig. 53) (Table 13).

Effect of curcumin on mean 24 h levels and daily pulse of clock genes in spleen

Curcumin administration did not alter the levels of *rBmal1* in 3 and 24 m in comparison to age-matched vehicle group but restored the levels in 12 m in comparison to 3 m VT group. Curcumin resulted in increased levels in 3 m, decreased in 12 m and did not alter in 24 m in comparison to

age-matched vehicle group. Curcumin increased the levels of *rPer2* in 3 m, but restored in 12 and 24 m in comparison to 3 m VT group. Curcumin did not alter the levels in 3 m, decreased the levels in 24 m in comparison to the age-matched vehicle group, but restored the levels in 12 m in comparison to 3 m VT group. *rCry2* levels showed an increase in 3 m, decrease in 12 m but did not alter in 24 m in comparison to age-matched vehicle group. Curcumin did not alter the levels of *rRev-erba* in all age groups in comparison to age-matched vehicle group. Curcumin increased the levels of *rRora* in 3 m but did not alter in 12 and 24 m in comparison to age-matched vehicle group (Fig. 54). Curcumin decreased the daily pulse of *rBmal1* in 3 and 24 m but did not alter in 12 m in comparison to age-matched vehicle group. *rPer1* did not alter in 3 m but restored in 12 m in comparison to 3 m VT group. In 24 m, curcumin increased the mean levels in 24 m in comparison to 24 m VT group. Curcumin decreased the levels of *rCry1* in 3 m, did not alter in 12 m but increased in 24 m in comparison to age-matched vehicle group. *rCry2* levels were increased but *rRev-erba* levels are decreased with curcumin administration in all age groups in comparison to age-matched vehicle group. *rRora* levels were not altered in 3 and 24 m but decreased in 12 m in comparison to age-matched vehicle group (Fig. 55) (Table 12).

Effect of curcumin on mean 24 h levels and daily pulse of immune genes in spleen

Curcumin administration did not alter the levels of *rNf- κ b1* in 3 m but restored the levels in 12 and 24 m in comparison to 3 m VT group. Curcumin reduced the levels of *rTnfa* in all age groups in comparison to age-matched vehicle group. Curcumin increased the levels of *rIl6* in 3 m, did not alter in 12 m, but decreased in 24 m in comparison to age-matched vehicle group. The mean 24 h levels of *rTlr4* were increased in 3 m but did not later in 12 and 24 m with curcumin treatment in comparison age-matched vehicle group. Curcumin increased the levels of *rTlr9* in 3 m but restored the levels in 12 m in comparison to 3 m VT group. In 24 m, curcumin decreased the levels of *rTlr9* with curcumin administration (Fig. 54). Curcumin decreased the daily pulse of *rNf- κ b1* in 3 m but restored in 12 m in comparison to 3 m VT group. In 24 m, curcumin did not alter the daily pulse in comparison to 24 m VT group. Daily pulse of *rTnfa* decreased in 3 and 24 m but did not alter in 24 m with curcumin treatment in comparison to age-matched vehicle group. Curcumin increased the daily pulse of *rIl6* in 3 and 12 m but did not alter in 24 m in comparison to age-matched vehicle group. Curcumin increased the daily pulse of *rTlr4* in 3 and 12 m but decreased in 24 m in comparison to age-matched vehicle group. Daily pulse of *rTlr9* did not alter in 3 m, increased in 12 m, but decreased in 24 m in comparison to age-matched vehicle group (Fig. 55) (Table 13).

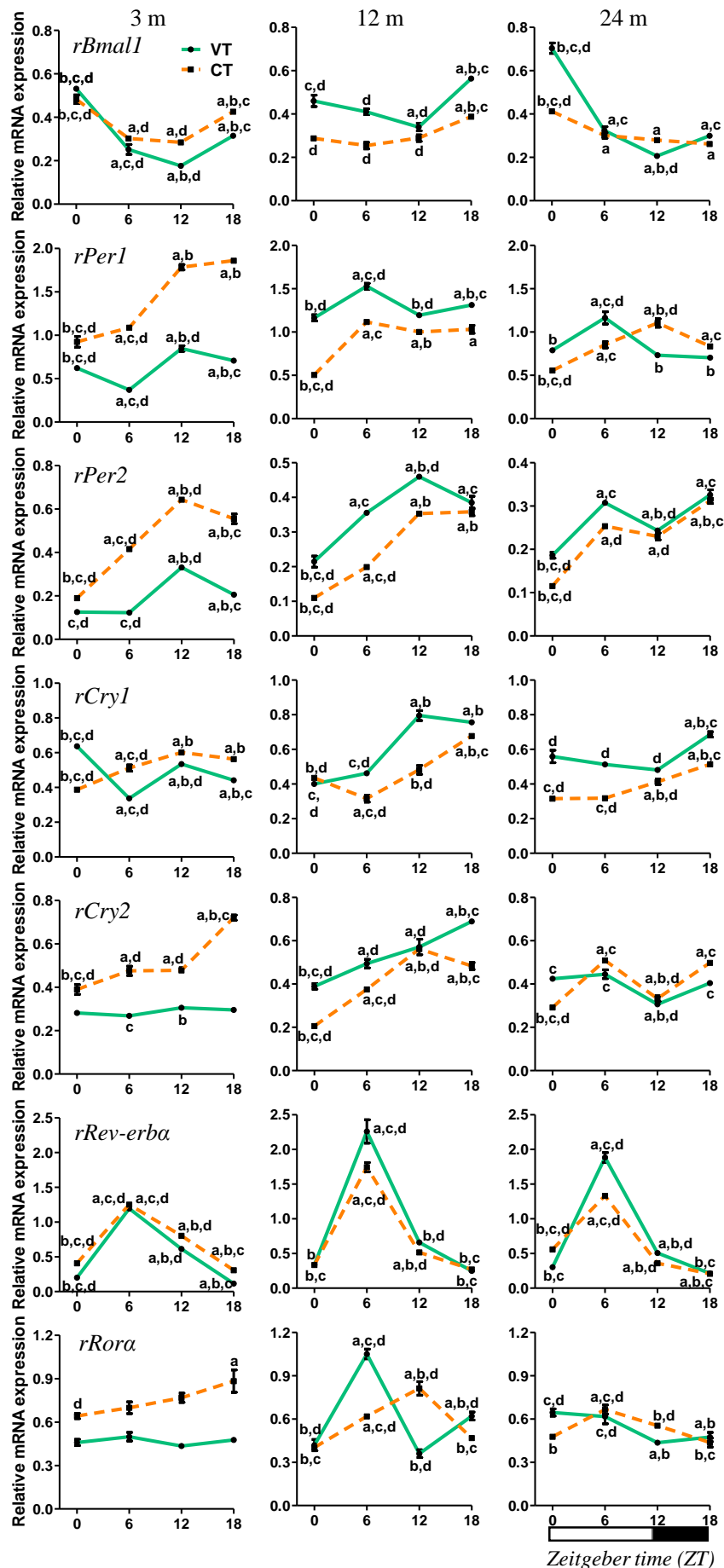


Fig. 52: Effect of curcumin administration on daily rhythms of clock genes mRNA expression in 3, 12 and 24 months (m) old rat spleen. Each value is mean \pm SEM ($n = 4$), $p_a \leq 0.05$; $p_b \leq 0.05$, $p_c \leq 0.05$ and $p_d \leq 0.05$ (where 'a', 'b', 'c' and 'd' refers to comparison with ZT-0, ZT-6, ZT-12, and ZT-18 respectively within the group).

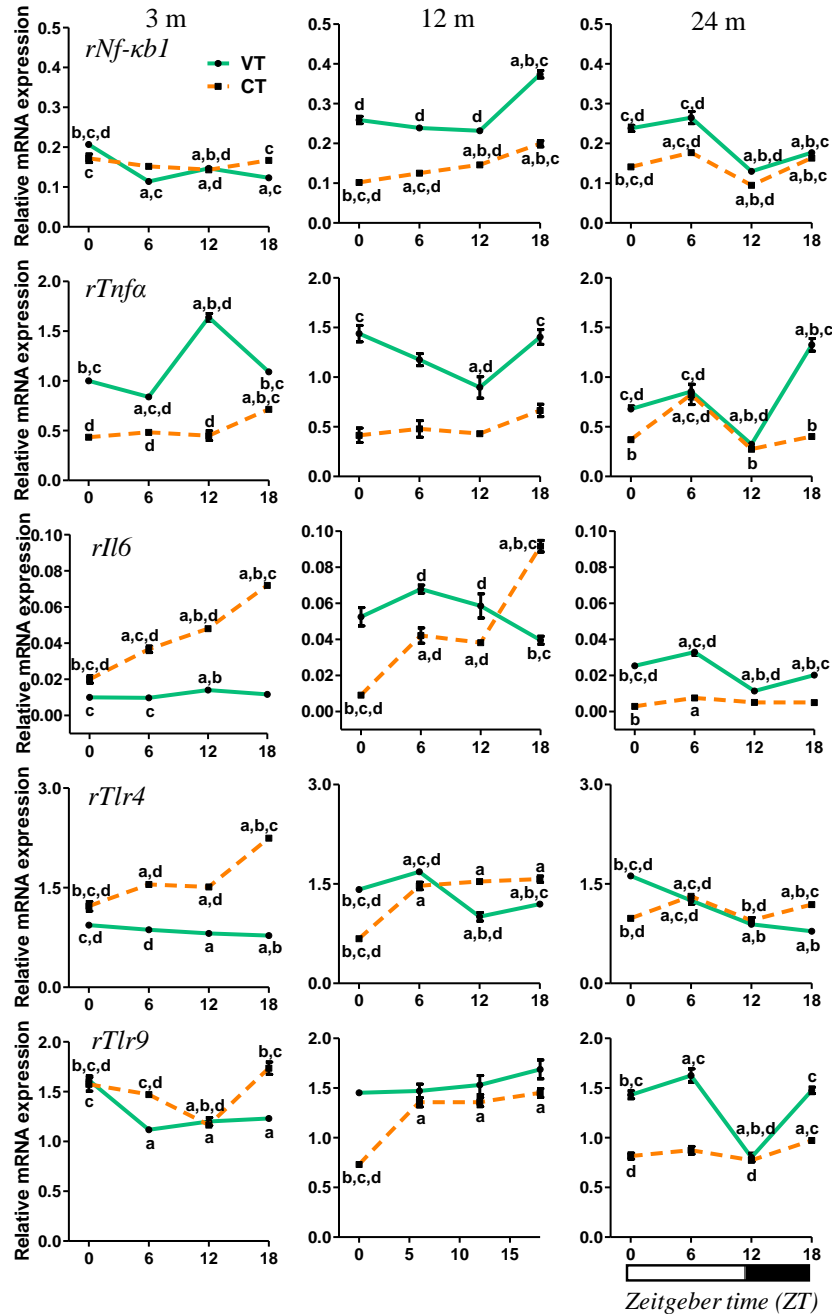


Fig. 53: Effect of curcumin administration on daily rhythms of *rNfκb1*, *rTnfa*, *rIl6*, *rTlr4* and *rTlr9* mRNA expression in 3, 12 and 24 months (m) old rat spleen. Each value is mean \pm SEM ($n = 4$), $p \leq 0.05$ and expressed as relative mRNA expression. $p_a \leq 0.05$; $p_b \leq 0.05$, $p_c \leq 0.05$ and $p_d \leq 0.05$ (where ‘a’, ‘b’, ‘c’ and ‘d’ refers to comparison with ZT-0, ZT-6, ZT-12, and ZT-18 respectively within the group).

Effect of curcumin on the correlations of clock genes in spleen

In LP of 3 m CT, *rPer1*, *rPer2*, *rCry1*, *rCry2*, *rRev-erba*, and *rRora* showed a positive correlation with each other but showed a negative correlation with *rBmall*. In DP of 3 m CT, *rBmall* showed negative correlation with *rPer1*, *rPer2*, *rCry1* and *rRev-erba*, whereas, *rRora*

showed positive correlation with *rPer1*, *rPer2*, *rCry1* and *rCry2*. *rPer1*, *rPer2*, and *rCry1* showed a positive correlation with each other. *rPer1* showed a positive correlation with *rCry2*, but *rRev-erba* showed a positive correlation with *rPer2* and *rCry1* (Fig. 56).

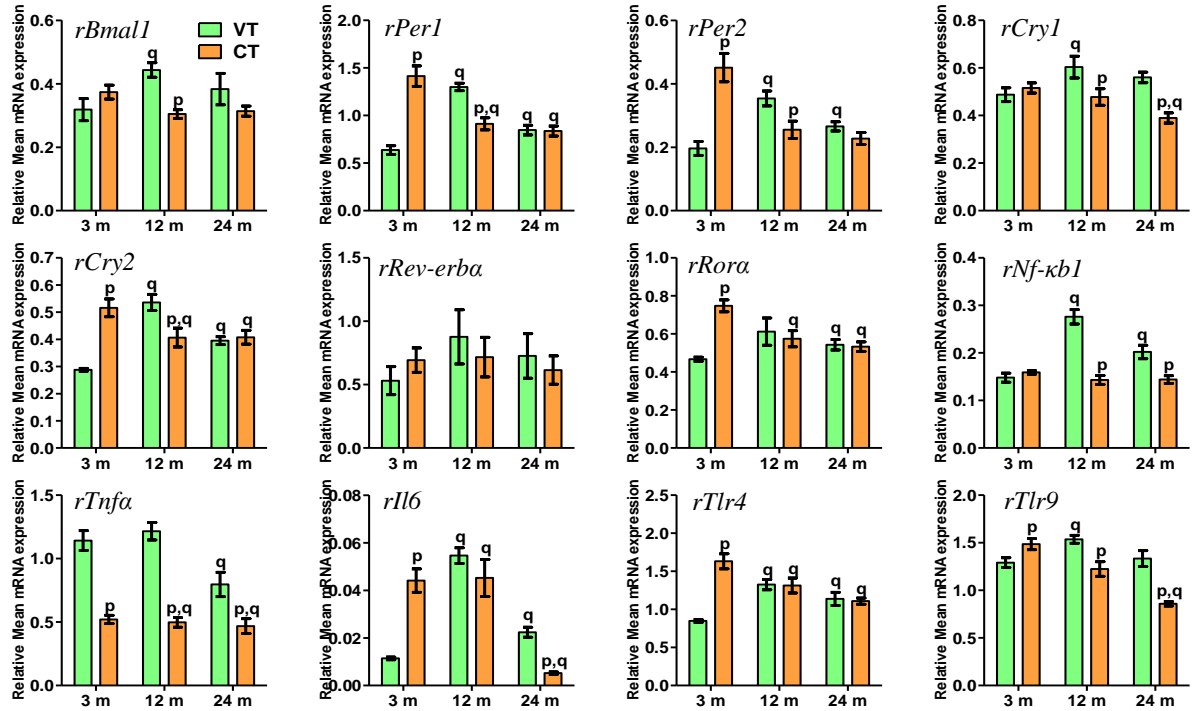


Fig. 54: Effect of curcumin administration on Mean 24 hour (h) levels of clock and immune genes expression in 3, 12 and 24 months (m) old rat spleen. Each value is mean \pm SEM ($n = 4$), $p \leq 0.05$ and expressed as mean relative gene expression. $p_p \leq 0.05$ (where ‘p’ refers to comparison with age-matched vehicle-treated group). $p_q \leq 0.05$ (where ‘q’ refers to comparison with 3 m vehicle-treated group).

In LP of 12 m CT, curcumin restored the negative correlation between *rBmall* and *rRev-erba*; *rCry1* and *rRev-erba*, and restored the positive correlation between *rPer1* and *rCry2*. Curcumin resulted in positive correlation between *rBmall* and *rCry1*; *rPer1* and *rCry2*; *rPer1* and *rRev-erba*; *rPer1* and *rRora*; *rPer2* and *rCry2*; *rPer2* and *rRora*; *rCry2* and *rRora*, and negative correlation between *rBmall* and *rPer1*; *rPer1* and *rCry1*. In DP of 12 m CT, curcumin restored positive correlation between *rBmall* and *rCry1*; *rPer1* and *rPer2*. Curcumin resulted in positive correlation between *rPer1* and *rCry2*; *rPer2* and *rCry2*; *rCry2* and *rRora*; *rRev-erba* and *rRora*, but negative correlation between *rBmall* and *rRev-erba*; *rBmall* and *rRora*; *rCry1* and *rRev-erba*. In LP of 24 m CT, curcumin restored the positive correlation between *rPer1* and *rCry1*; *rPer2* and *rCry2*; *rRev-erba* and *rRora*, and restored negative correlation between *rCry1* and *rRev-erba*. Curcumin resulted in negative correlation between *rBmall* and *rPer1*; *rBmall* and

rPer2; *rBmall* and *rCry1*; *rBmall* and *rRora*, and positive correlation between *rPer1* and *rPer2*; *rPer2* and *rRora*; *rCry2* and *rRev-erba*; *rCry2* and *rRora*. In DP of 24 m CT, curcumin restored the negative correlation between *rBmall* and *rPer1*; *rBmall* and *rCry2*; *rPer2* and *rCry2*; *rCry2* and *rRora*, and restored the positive correlation between *rPer1* and *rPer2*. Curcumin resulted in negative correlation between *rBmall* and *rPer2*; *rBmall* and *rCry1*; *rPer1* and *rRev-erba*; *rPer2* and *rRev-erba*; *rCry1* and *rRev-erba*; *rCry2* and *rRev-erba*, and positive correlation between *rBmall* and *rRev-erba*; *rPer1* and *rRora*; *rPer2* and *rCry1*; *rCry1* and *rCry2* (Fig. 56).

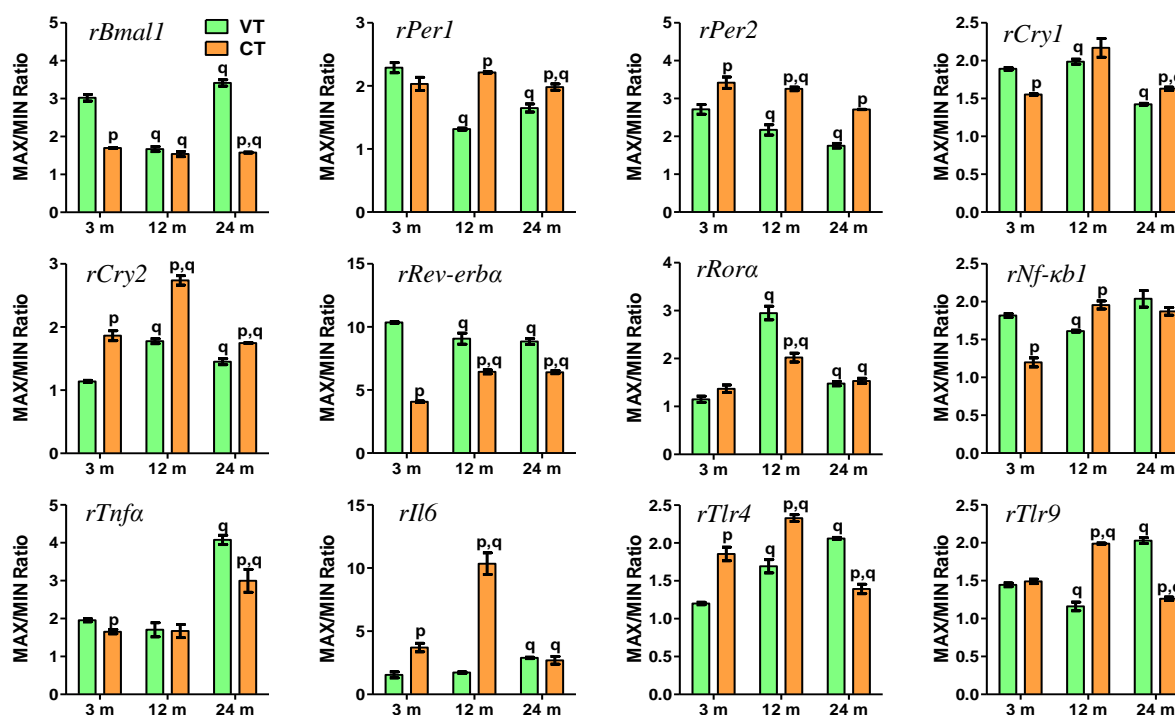


Fig. 55: Effect of curcumin administration on Daily pulse of clock and immune genes expression in 3, 12 and 24 months (m) old rat spleen. Each value is mean \pm SEM ($n = 4$), $p \leq 0.05$ and expressed as mean relative gene expression. $p_p \leq 0.05$ (where 'p' refers to comparison with age matched vehicle-treated group). $p_q \leq 0.05$ (where 'q' refers to comparison with 3 m vehicle-treated group).

Effect of curcumin on the correlation among immune genes in spleen

In LP of 3 m CT, curcumin resulted in negative correlation between *rNf-kb1* and *rTnfa*; *rNf-kb1* and *rIl6*; *rNf-kb1* and *rTlr4*; *rNf-kb1* and *rTlr9*; *rTlr4* and *rTlr9*, and positive correlation between *rNf-kb1* and *rTlr9*; *rTnfa* and *rIl6*; *rTnfa* and *rTlr4*; *rIl6* and *rTlr4*. In DP of 3 m CT, curcumin resulted in a positive correlation between *rNf-kb1* and *rTlr9*; *rTnfa* and *rIl6*; *rTnfa* and *rTlr4*; *rIl6* and *rTlr4* (Fig. 56).

Table 12: Effect of curcumin on age-induced alterations of clock genes expression

<i>Gene</i>		ZT-0	ZT-6	ZT-12	ZT-18	Mean 24 h levels	Max/min ratio
<i>rBmal1</i>	3 m VT	0.53 ± 0.01	0.25 ± 0.02	0.18 ± 0.01	0.31 ± 0.01	0.32 ± 0.03	3.02 ± 0.09
	3 m CT	0.48 ± 0.02	0.3 ± 0.01	0.28 ± 0.01	0.43 ± 0.01	0.37 ± 0.02	1.7 ± 0.01 x
	12 m VT	0.46 ± 0.03	0.41 ± 0.01	0.34 ± 0.02	0.56 ± 0.01	0.44 ± 0.02 y	1.67 ± 0.07 y
	12 m CT	0.29 ± 0.01	0.25 ± 0.02	0.29 ± 0.01	0.39 ± 0.01	0.3 ± 0.01 x	1.54 ± 0.07 y
	24 m VT	0.7 ± 0.02	0.32 ± 0.02	0.21 ± 0.01	0.3 ± 0.01	0.38 ± 0.05	3.41 ± 0.08 y
	24 m CT	0.41 ± 0.01	0.3 ± 0.01	0.28 ± 0.01	0.26 ± 0.01	0.31 ± 0.02	1.58 ± 0.01 x,y
<i>rPer1</i>	3 m VT	0.62 ± 0.01	0.37 ± 0	0.85 ± 0.03	0.71 ± 0.02	0.64 ± 0.05	2.29 ± 0.08
	3 m CT	0.92 ± 0.06	1.09 ± 0.01	1.78 ± 0.03	1.86 ± 0.02	1.41 ± 0.11 x	2.03 ± 0.1
	12 m VT	1.16 ± 0.04	1.53 ± 0.03	1.19 ± 0.02	1.31 ± 0.01	1.3 ± 0.04 y	1.32 ± 0.02 y
	12 m CT	0.5 ± 0	1.12 ± 0.01	1 ± 0.02	1.03 ± 0.05	0.91 ± 0.06 x,y	2.21 ± 0.01 x
	24 m VT	0.79 ± 0.01	1.16 ± 0.07	0.73 ± 0.01	0.7 ± 0.02	0.85 ± 0.05 y	1.65 ± 0.06 y
	24 m CT	0.56 ± 0.01	0.85 ± 0.03	1.1 ± 0.05	0.83 ± 0.01	0.84 ± 0.05 y	1.98 ± 0.05 x,y
<i>rPer2</i>	3 m VT	0.13 ± 0	0.12 ± 0.01	0.33 ± 0.01	0.21 ± 0	0.2 ± 0.02	2.71 ± 0.13
	3 m CT	0.19 ± 0.01	0.42 ± 0.01	0.64 ± 0.01	0.55 ± 0.02	0.45 ± 0.04 x	3.42 ± 0.15 x
	12 m VT	0.21 ± 0.02	0.36 ± 0	0.46 ± 0.01	0.38 ± 0.02	0.35 ± 0.02 y	2.17 ± 0.14 y
	12 m CT	0.11 ± 0	0.2 ± 0	0.35 ± 0.01	0.36 ± 0.01	0.26 ± 0.03 x	3.25 ± 0.05 x,y
	24 m VT	0.19 ± 0.01	0.31 ± 0	0.24 ± 0	0.33 ± 0.01	0.27 ± 0.01 y	1.75 ± 0.06 y
	24 m CT	0.12 ± 0	0.25 ± 0.01	0.23 ± 0.01	0.31 ± 0.01	0.23 ± 0.02	2.71 ± 0 x
<i>rCry1</i>	3 m VT	0.64 ± 0.01	0.34 ± 0	0.53 ± 0.01	0.44 ± 0.01	0.49 ± 0.03	1.89 ± 0.02
	3 m CT	0.39 ± 0	0.51 ± 0.02	0.6 ± 0.01	0.56 ± 0.01	0.52 ± 0.02	1.55 ± 0.01 x
	12 m VT	0.4 ± 0.01	0.46 ± 0.01	0.8 ± 0.03	0.76 ± 0.01	0.6 ± 0.05 y	1.99 ± 0.03 y
	12 m CT	0.44 ± 0.01	0.32 ± 0.02	0.48 ± 0.03	0.68 ± 0.01	0.48 ± 0.03 x	2.17 ± 0.12
	24 m VT	0.56 ± 0.04	0.51 ± 0.01	0.48 ± 0.01	0.69 ± 0.02	0.56 ± 0.02	1.42 ± 0.01 y
	24 m CT	0.32 ± 0.01	0.32 ± 0.01	0.41 ± 0.02	0.51 ± 0	0.39 ± 0.02 x,y	1.63 ± 0.02 x,y
<i>rCry2</i>	3 m VT	0.28 ± 0.01	0.27 ± 0.01	0.31 ± 0.01	0.3 ± 0	0.29 ± 0.01	1.14 ± 0.02
	3 m CT	0.39 ± 0.02	0.48 ± 0.02	0.48 ± 0.01	0.72 ± 0.01	0.52 ± 0.03 x	1.86 ± 0.08 x
	12 m VT	0.39 ± 0.01	0.49 ± 0.02	0.57 ± 0.04	0.69 ± 0.01	0.54 ± 0.03 y	1.78 ± 0.04 y
	12 m CT	0.21 ± 0.01	0.37 ± 0.01	0.56 ± 0.01	0.48 ± 0.02	0.41 ± 0.03 x,y	2.74 ± 0.07 x,y
	24 m VT	0.42 ± 0.01	0.45 ± 0.02	0.31 ± 0.01	0.4 ± 0.01	0.4 ± 0.01 y	1.45 ± 0.05 y
	24 m CT	0.29 ± 0.01	0.51 ± 0.01	0.33 ± 0.01	0.5 ± 0.01	0.41 ± 0.03 y	1.75 ± 0.01 x,y
<i>rRev-erba</i>	3 m VT	0.2 ± 0.01	1.19 ± 0.01	0.61 ± 0.01	0.12 ± 0	0.53 ± 0.11	10.35 ± 0.06
	3 m CT	0.41 ± 0.02	1.25 ± 0.01	0.8 ± 0.02	0.31 ± 0.01	0.69 ± 0.1	4.07 ± 0.06 x
	12 m VT	0.34 ± 0.02	2.26 ± 0.17	0.66 ± 0.02	0.25 ± 0.01	0.88 ± 0.21	9.07 ± 0.44 y
	12 m CT	0.33 ± 0.03	1.75 ± 0.07	0.52 ± 0.01	0.27 ± 0	0.72 ± 0.16	6.44 ± 0.16 x,y
	24 m VT	0.3 ± 0.02	1.88 ± 0.07	0.51 ± 0.01	0.21 ± 0	0.73 ± 0.18	8.84 ± 0.23 y
	24 m CT	0.56 ± 0.03	1.33 ± 0.02	0.36 ± 0.01	0.21 ± 0.01	0.61 ± 0.11	6.41 ± 0.12 x,y
<i>rRora</i>	3 m VT	0.46 ± 0.02	0.5 ± 0.03	0.43 ± 0.01	0.48 ± 0.01	0.47 ± 0.01	1.15 ± 0.07
	3 m CT	0.64 ± 0.02	0.7 ± 0.04	0.77 ± 0.03	0.88 ± 0.08	0.75 ± 0.03 x	1.37 ± 0.08
	12 m VT	0.42 ± 0.04	1.05 ± 0.03	0.36 ± 0.03	0.62 ± 0.03	0.61 ± 0.07	2.95 ± 0.14 y
	12 m CT	0.4 ± 0.01	0.62 ± 0.01	0.81 ± 0.05	0.47 ± 0.01	0.57 ± 0.04 y	2.02 ± 0.09 x,y
	24 m VT	0.64 ± 0.03	0.62 ± 0.05	0.44 ± 0.01	0.47 ± 0.03	0.54 ± 0.03 y	1.48 ± 0.04 y
	24 m CT	0.48 ± 0.01	0.66 ± 0.03	0.55 ± 0.01	0.44 ± 0.03	0.53 ± 0.02 y	1.53 ± 0.06 y

mRNA expression of clock genes at ZT-0, 6, 12 and 18. $p_x \leq 0.05$, $p_y \leq 0.05$ where, 'x' refers to significant difference with respective age-matched vehicle group. 'y' refers to significant difference with 3 m vehicle-treated group.

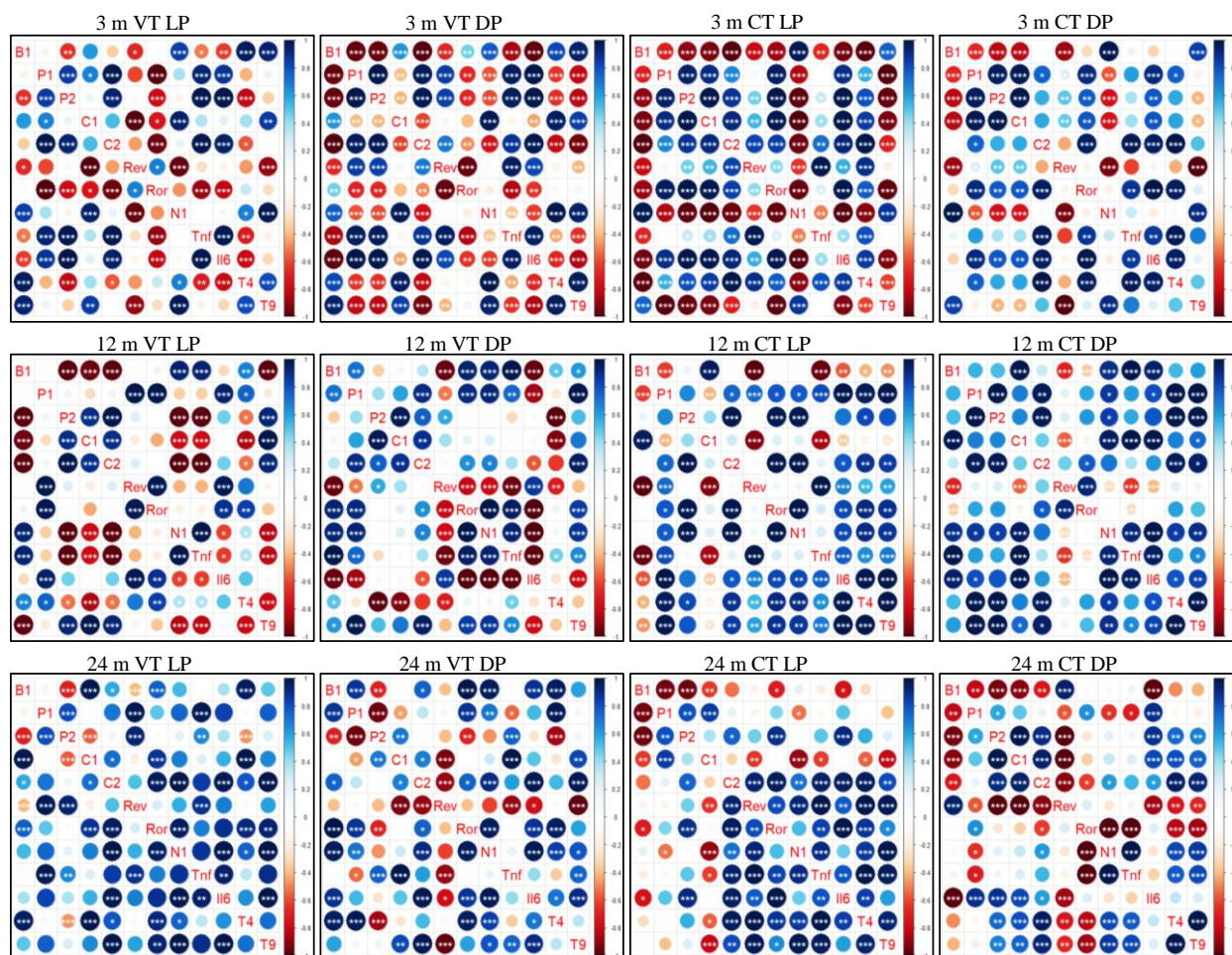


Fig. 56: Effect of curcumin administration on Pair wise correlations between clock and immune genes in light (ZT-0, 6, 12) and dark (ZT-12, 18, 24/0) phase of 3, 12 and 24 months (m) old rat spleen (LP - light phase; DP - dark phase; VT - vehicle-treated; CT - curcumin treated). Intensity of color and size of circle represents correlation coefficient values between the genes. Where, positive correlations are indicated by shades of blue, negative correlations by shades of red and white indicates no correlation. ‘*’, ‘**’, ‘***’ indicates statistically significant correlations ($p \leq 0.05$), ($p \leq 0.01$), ($p \leq 0.001$) respectively. (B1- *rBmall1*; P1 - *rPer1*; P2 - *rPer2*; C1 - *rCry1*; C2 - *rCry2*; Re - *rRev-erba*; Ro - *rRora*; N1 - *rNfkb1*; Tnf - *rTnfa*; Il6 - *rIl6*; T4 - *rTlr4*; T9 - *rTlr9*).

In LP of 12 m CT, curcumin restored the positive correlation between *rNf-kb1* and *rTlr9*; *rTnfa* and *rIl6*; *rTlr4* and *rTlr9*. Curcumin resulted in a positive correlation between *rNf-kb1* and *rIl6*; *rNf-kb1* and *rTlr4*. *rTnfa* and *rIl6* showed a positive correlation with *rTlr4* and *rTlr9*. In DP of 12 m CT, curcumin restored the positive correlation between *rNf-kb1* and *rTlr4*; *rTnfa* and *rIl6*; *rTlr4* and *rTlr9*. Curcumin resulted in positive correlation of *rNf-kb1* and *rTnfa*; *rNf-kb1* and *rIl6*; *rNf-kb1* and *rTlr9*; *rTnfa* and *rTlr9*; *rIl6* and *rTlr4*; *rIl6* and *rTlr9*. In LP of 24 m CT, curcumin restored the positive correlation between *rTlr4* and *rTlr9*. Curcumin resulted in positive correlation between *rNf-kb1* and *rTnfa*; *rNf-kb1* and *rTlr4*; *rNf-kb1* and *rTlr9*; *rTnfa* and *rIl6*;

rTnfa and *rTlr4*; *rTnfa* and *rTlr9*; *rIl6* and *rTlr4*. In DP of 24 m CT, curcumin restored the positive correlation between *rTlr4* and *rTlr9*. Curcumin resulted in positive correlation between *rNf- κ b1* and *rTnfa*; *rNf- κ b1* and *rTlr4*; *rNf- κ b1* and *rTlr9*; *rTnfa* and *rTlr4*; *rTnfa* and *rTlr9* (Fig. 56).

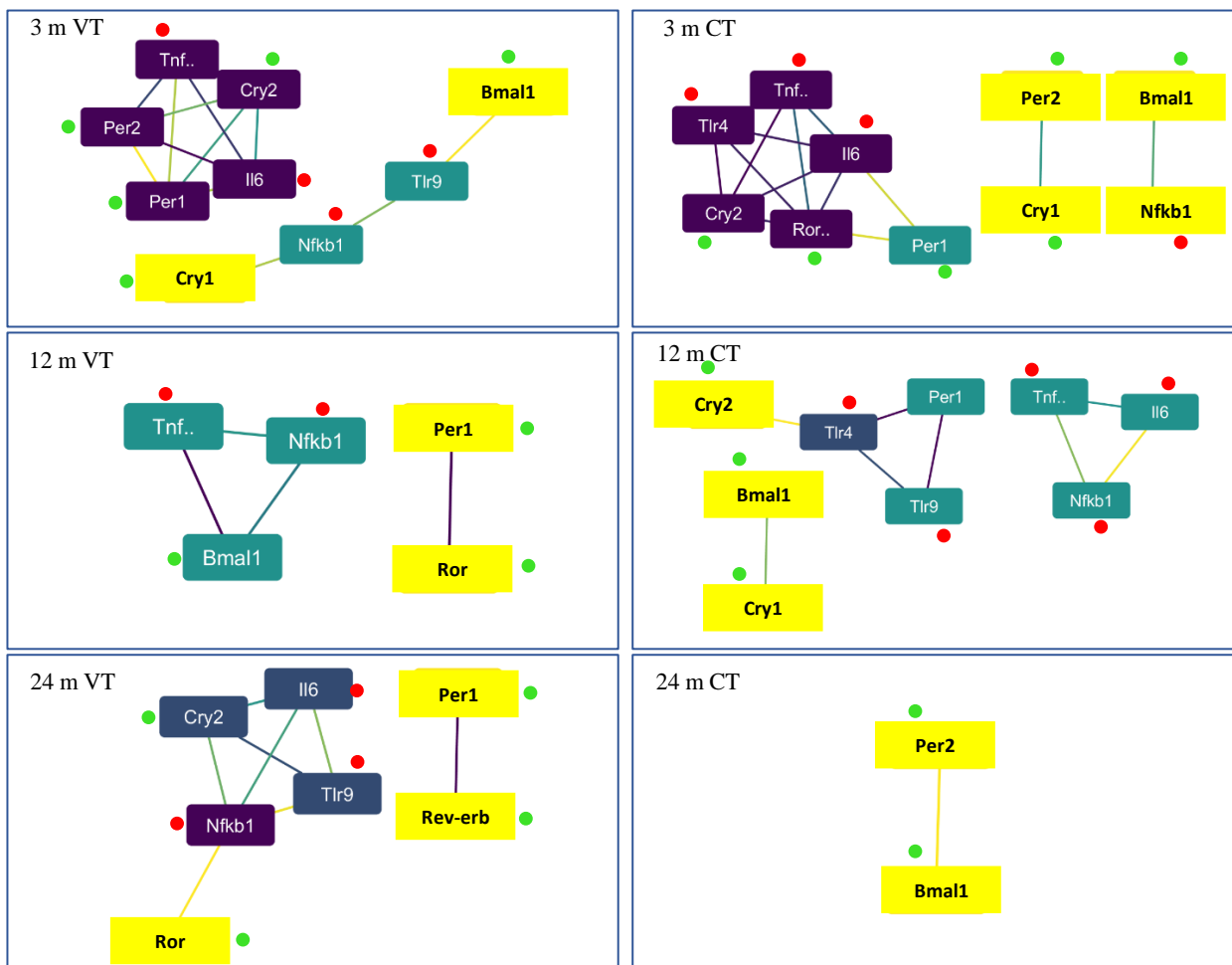


Fig. 57: WGCNA analysis between clock and immune gene clusters: effect aging on gene to gene network in 3, 12 and 24 m old rat kidney (left panel) and effect of curcumin administration (right panel). Color of the node indicates no. of interactions (highest—purple; intermediate—cyan and least—yellow). Color of an edge indicates the strength of interaction (strongest—purple; cyan—intermediate and weakest—yellow). Green and red dots indicate clock and immune genes respectively.

Effect of curcumin on the correlation between clock and immune genes in spleen

In LP of 3 m CT, *rPer1*, *rPer2*, *rCry1*, *rCry2*, *rRev-erba* and *rRora* showed negative correlation with *rNf- κ b1*, but showed positive correlation with *rIl6* and *rTlr4*. *rBmal1* showed positive correlation with *rNf- κ b1* and *rTlr9*. *rBmal1* showed negative correlation with *rTnfa*, *rIl6* and

rTlr4, *rPer1*, *rPer2*, *rCry1*, *rCry2* and *rRora* showed negative correlation with *rTlr9*. *rPer2*, *rCry1*, *rCry2*, *rRev-erba* showed positive correlation with *rTnfa*. In DP of 3 m CT, *rPer1*, *rPer2*, *rCry1* and *rRev-erba* showed negative correlation with *rNf- κ b1*. *rPer2*, *rCry1* and *rRev-erba* showed negative correlation with *rTlr9*. *rTnfa* showed positive correlation with *rCry2* and *rRora*. *rIl6* showed positive correlation with *rPer1*, *rPer2*, *rCry1*, *rCry2* and *rRora*. *rTlr4* showed positive correlation with *rPer1*, *rCry2* and *rRora*. *rBmall* showed positive correlation with *rNf- κ b1* and *rTlr9*. In LP of 12 m CT, curcumin restored the negative correlation between *rBmall* and *rTnfa*; *rBmall* and *rIl6*, and positive correlation between *rPer1* and *rTnfa*; *rCry2* and *rIl6*. *rCry2* with *rNf- κ b1*, *rTlr4*, *rTlr9*; *rRev-erba* with *rTnfa*, *rIl6*, *rTlr4*, *rTlr9*; *rRora* with *rNf- κ b1*, *rIl6*, *rTlr4*, *rTlr9* showed positive correlation. In DP of 12 m CT, curcumin restored positive correlation between *rCry1* and *rNf- κ b1*; *rCry1* and *rTlr9*. *rNf- κ b1* with *rBmall*, *rPer1*, *rPer2*, *rCry1*; *rTnfa* with *rBmall*, *rCry1*; *rIl6* with *rBmall*, *rPer1*, *rCry1*; *rTlr4* with *rPer1*, *rPer2*, *rCry2*; *rTlr9* with *rPer1*, *rPer2*, *rCry1*, *rCry2* showed positive correlation. *rRev-erba* showed negative correlation with *rTnfa* and *rIl6*. In LP of 24 m CT, curcumin restored the negative correlation between *rBmall* and *rIl6*, and positive correlation between *rPer2* and *rIl6*; *rCry2* and *rTnfa*. *rPer1* with *rNf- κ b1*; *rCry1* with *rNf- κ b1*, *rTnfa*, *rTlr4*, *rTlr9* showed negative correlation. *rCry2*, *rRev-erba* and *rRora* showed positive correlation with all immune genes. In DP of 24 m CT, curcumin restored negative correlation between *rBmall* and *rIl6*; *rPer1* and *rNf- κ b1*; *rRora* and *rTnfa*, and positive correlation between *rPer1* and *rIl6*; *rPer2* and *rIl6*; *rCry1* and *rTlr4*. *rPer1* with *rTnfa*; *rRev-erba* with *rIl6*, *rTlr4*, *rTlr9*; *rRora* with *rNf- κ b1*, *rTlr4*, *rTlr9* showed negative correlation. *rPer2* with *rTlr4*, *rTlr9*; *rCry1* with *rIl6*, *rTlr9*; *rCry2* with *rNf- κ b1*, *rIl6*, *rTlr4*, *rTlr9* showed positive correlation (Fig. 56).

WGCNA analysis between clock and immune genes with curcumin treatment in spleen

In 3 m CT, curcumin administration did not alter the interaction between clock and immune genes. In 12 m CT, immune genes showed interactions within themselves but not with clock genes. In 24 m CT, immune genes lost interaction with each other and *rBmall* showed interaction with *rPer2* (Fig. 57).

Table 13: Effect of curcumin on age-induced alterations of immune genes

Gene		ZT-0	ZT-6	ZT-12	ZT-18	Mean 24 h levels	Max/min ratio
<i>rNf-κb1</i>	3 m VT	0.21 \pm 0	0.11 \pm 0	0.15 \pm 0	0.12 \pm 0	0.15 \pm 0.01	1.82 \pm 0.02
	3 m CT	0.17 \pm 0.01	0.15 \pm 0	0.14 \pm 0	0.17 \pm 0	0.16 \pm 0	1.2 \pm 0.06 x
	12 m VT	0.26 \pm 0.01	0.24 \pm 0	0.23 \pm 0.01	0.37 \pm 0.01	0.28 \pm 0.02 y	1.61 \pm 0.01 y
	12 m CT	0.1 \pm 0	0.13 \pm 0	0.15 \pm 0.01	0.2 \pm 0.01	0.14 \pm 0.01 x	1.96 \pm 0.05 x
	24 m VT	0.24 \pm 0.01	0.27 \pm 0.02	0.13 \pm 0	0.18 \pm 0	0.2 \pm 0.01 y	2.04 \pm 0.11
	24 m CT	0.14 \pm 0	0.18 \pm 0	0.09 \pm 0	0.16 \pm 0	0.14 \pm 0.01 x	1.87 \pm 0.05
<i>rTnfa</i>	3 m VT	1 \pm 0.02	0.84 \pm 0.01	1.64 \pm 0.04	1.09 \pm 0.02	1.14 \pm 0.08	1.96 \pm 0.04
	3 m CT	0.43 \pm 0.02	0.48 \pm 0.01	0.45 \pm 0.05	0.71 \pm 0.02	0.52 \pm 0.03 x	1.65 \pm 0.05 x
	12 m VT	1.44 \pm 0.08	1.18 \pm 0.06	0.9 \pm 0.11	1.4 \pm 0.07	1.22 \pm 0.07	1.7 \pm 0.19
	12 m CT	0.41 \pm 0.07	0.48 \pm 0.08	0.43 \pm 0.01	0.66 \pm 0.06	0.5 \pm 0.04 x,y	1.67 \pm 0.17
	24 m VT	0.68 \pm 0.03	0.86 \pm 0.07	0.32 \pm 0.01	1.33 \pm 0.06	0.8 \pm 0.1 y	4.08 \pm 0.12 y
	24 m CT	0.37 \pm 0.01	0.83 \pm 0.1	0.27 \pm 0.01	0.4 \pm 0.01	0.47 \pm 0.06 x,y	3 \pm 0.3 x,y
<i>rIl6</i>	3 m VT	0.01 \pm 0	1.54 \pm 0.24				
	3 m CT	0.02 \pm 0	0.04 \pm 0	0.05 \pm 0	0.07 \pm 0	0.04 \pm 0 x	3.71 \pm 0.34 x
	12 m VT	0.05 \pm 0.01	0.07 \pm 0	0.06 \pm 0.01	0.04 \pm 0	0.05 \pm 0 y	1.73 \pm 0.06
	12 m CT	0.01 \pm 0	0.04 \pm 0	0.04 \pm 0	0.09 \pm 0	0.05 \pm 0.01 y	10.35 \pm 0.85 x,y
	24 m VT	0.03 \pm 0	0.03 \pm 0	0.01 \pm 0	0.02 \pm 0	0.02 \pm 0 y	2.89 \pm 0.06 y
	24 m CT	0 \pm 0	0.01 \pm 0	0.01 \pm 0	0 \pm 0	0.01 \pm 0 x,y	2.7 \pm 0.31 y
<i>rTlr4</i>	3 m VT	0.94 \pm 0.02	0.87 \pm 0.01	0.81 \pm 0.02	0.78 \pm 0.01	0.85 \pm 0.02	1.2 \pm 0.02
	3 m CT	1.22 \pm 0.07	1.55 \pm 0.02	1.51 \pm 0.03	2.25 \pm 0.01	1.63 \pm 0.1 x	1.85 \pm 0.09 x
	12 m VT	1.42 \pm 0.01	1.68 \pm 0.03	1.01 \pm 0.06	1.19 \pm 0.03	1.33 \pm 0.07 y	1.69 \pm 0.09 y
	12 m CT	0.67 \pm 0.01	1.47 \pm 0.06	1.54 \pm 0.02	1.57 \pm 0.05	1.31 \pm 0.1 y	2.33 \pm 0.04 x,y
	24 m VT	1.62 \pm 0.03	1.25 \pm 0.05	0.89 \pm 0.01	0.79 \pm 0.02	1.14 \pm 0.09 y	2.06 \pm 0.01 y
	24 m CT	0.98 \pm 0.02	1.31 \pm 0.01	0.95 \pm 0.04	1.19 \pm 0.02	1.11 \pm 0.04 y	1.39 \pm 0.06 x,y
<i>rTlr9</i>	3 m VT	1.62 \pm 0.04	1.12 \pm 0.01	1.2 \pm 0.04	1.23 \pm 0.02	1.29 \pm 0.05	1.44 \pm 0.02
	3 m CT	1.57 \pm 0.07	1.47 \pm 0.01	1.16 \pm 0.02	1.74 \pm 0.06	1.49 \pm 0.06 x	1.49 \pm 0.03
	12 m VT	1.45 \pm 0.01	1.47 \pm 0.07	1.53 \pm 0.1	1.69 \pm 0.1	1.54 \pm 0.04 y	1.16 \pm 0.06 y
	12 m CT	0.73 \pm 0.02	1.36 \pm 0.05	1.36 \pm 0.05	1.45 \pm 0.04	1.22 \pm 0.08 x	1.99 \pm 0.01 x,y
	24 m VT	1.43 \pm 0.04	1.63 \pm 0.07	0.8 \pm 0.04	1.48 \pm 0.03	1.33 \pm 0.08	2.03 \pm 0.04 y
	24 m CT	0.82 \pm 0.03	0.87 \pm 0.04	0.77 \pm 0.03	0.97 \pm 0.02	0.86 \pm 0.02 x,y	1.26 \pm 0.02 x,y

mRNA expression of immune genes at ZT-0,6, 12 and 18. $p_x \leq 0.05$, $p_y \leq 0.05$ where ‘x’ refers to significant difference with the respective age-matched vehicle group. ‘y’ refers to significant difference with 3 m vehicle-treated group.

II. B (iv). Effect of curcumin on the age-induced alterations of 5-HT in liver, kidney, and spleen

Effect of curcumin on age-induced alterations of daily rhythms, mean 24 h levels, and daily pulse of 5-HT in liver

With curcumin administration in 3 m, 6 h phase delay was observed in comparison to 3 m VT with maximum levels at ZT-6 and minimum at ZT-12. In 12 m CT, maximum levels were observed at ZT-6 with 6 h phase delay in comparison to 12 m VT. In 24 m, 6 h phase delay was observed with maximum levels at ZT-0 in comparison with 24 m VT (Fig. 58). Mean 24 h levels did not alter in 3 and 12 m CT but decreased in 24 m CT in comparison with age-matched VT groups (Fig. 59a). Daily pulse was not altered in 3 and 24 m CT but showed an increase in 12 m CT in comparison to age-matched VT groups (Fig. 59b) (Table 14).

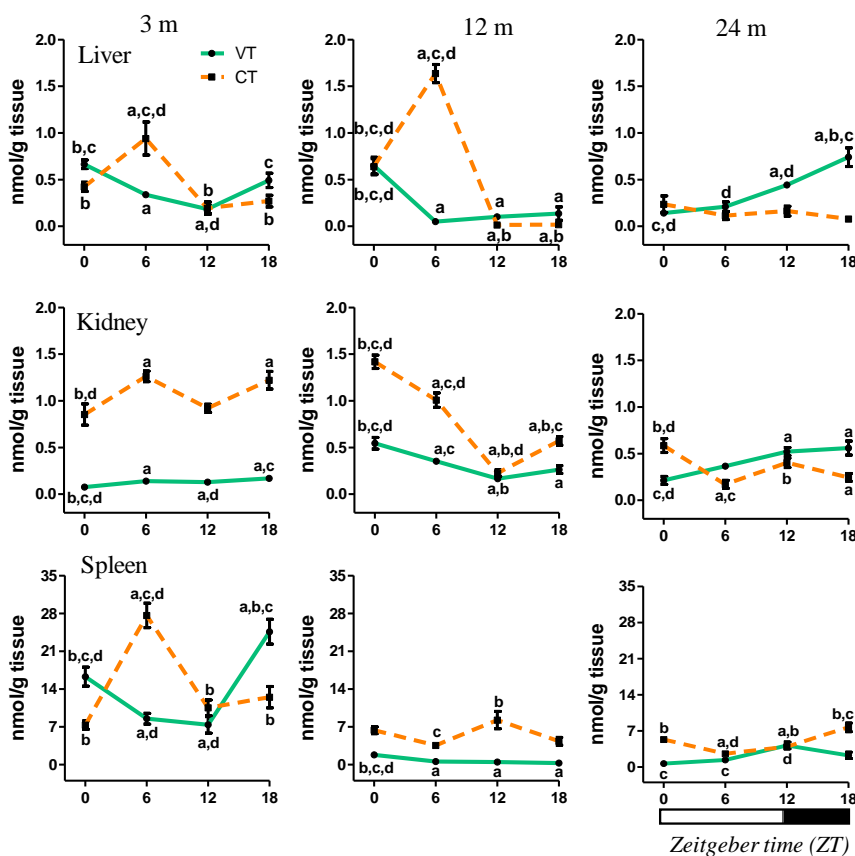


Fig. 58: Effect of curcumin administration on daily rhythms of 5-HT in 3, 12 and 24 months (m) old rat liver, kidney, and spleen. Each value is mean \pm SEM ($n = 4$), $p \leq 0.05$ and expressed as relative mRNA expression. $p_a \leq 0.05$; $p_b \leq 0.05$, $p_c \leq 0.05$ and $p_d \leq 0.05$ (where ‘a’, ‘b’, ‘c’ and ‘d’ refers to comparison with ZT-0, ZT-6, ZT-12, and ZT-18 respectively within the group).

Effect of curcumin on age-induced alterations of daily rhythms, mean 24 h levels, and daily pulse of 5-HT in kidney

With curcumin treatment, 5-HT showed 12 h phase advance in 3 m CT with maximum levels at ZT-6 in comparison to 3 m VT group. In 12 m CT, the phase was not altered with maximum levels at ZT-0 and minimum at ZT-12 in comparison to 12 m VT group. In 24 m CT, 6 h phase delay was observed with maximum levels at ZT-0 in comparison with 24 m VT group (Fig. 58). Mean 24 h levels were increased in 3 and 12 m CT, but did not vary in 24 m CT in comparison to age-matched VT groups (Fig. 59a). Daily pulse was not altered in 3 and 24 m CT but increased in 12 m CT in comparison to age-matched VT groups (Fig. 59b) (Table 14).

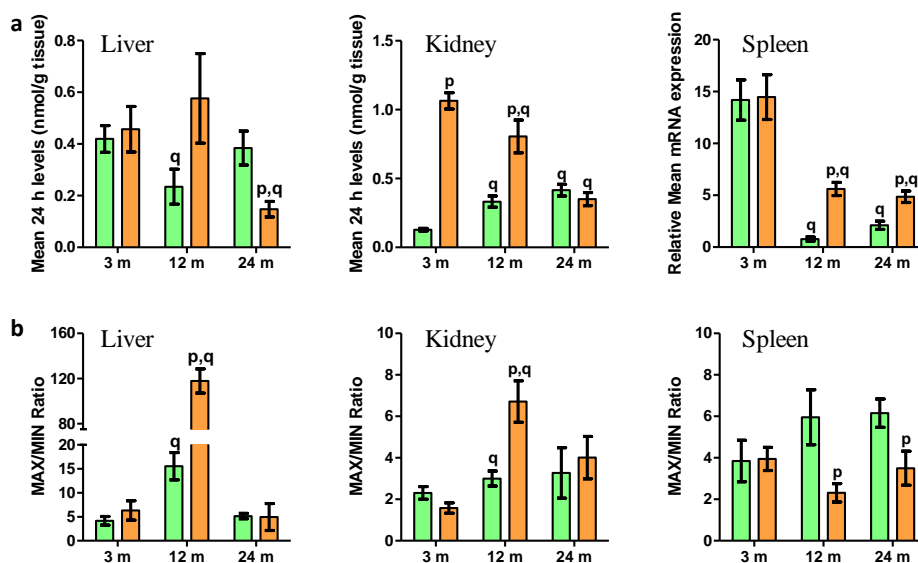


Fig. 59: Effect of curcumin administration on (a) Mean 24 hour (h) levels and (b) Daily pulse of 5-HT in 3, 12 and 24 months (m) old rat liver, kidney, and spleen. Each value is mean \pm SEM ($n = 4$), $p \leq 0.05$ and expressed as mean relative gene expression. $p_p \leq 0.05$ (where 'p' refers to comparison with the age-matched vehicle-treated group). $p_q \leq 0.05$ (where 'q' refers to comparison with 3 m vehicle-treated group).

Effect of curcumin on age-induced alterations of daily rhythms, mean 24 h levels, and daily pulse of 5-HT in spleen

In spleen, with curcumin treatment, 12 h phase advance was observed in 5-HT levels in 3 m CT with maximum levels at ZT-6 in comparison to 3 m VT group. In 12 m CT, 12 h phase delay was observed with maximum levels at ZT-12 in comparison to 12 m VT group. In 24 m CT, 6 h phase delay was observed with maximum expression at ZT-18 in comparison to 24 m VT group (Fig. 58). Mean 24 h levels did not alter in 3 m CT but showed a significant increase in 12 and 24

m CT in comparison to age-matched VT groups (Fig. 59a). Daily pulse did not alter in 3 m CT but showed a significant decrease in 12 and 24 m CT in comparison to age-matched VT groups (Fig. 59b) (Table 14).

Table 14: Effect of curcumin on age-induced alterations of 5-HT levels

Tissue		ZT-0	ZT-6	ZT-12	ZT-18	Mean 24 h levels	Max/min ratio
Liver	3M VT	0.66 ± 0.05	0.34 ± 0.03	0.18 ± 0.04	0.49 ± 0.08	0.42 ± 0.05	4.16 ± 0.9
	3M CT	0.42 ± 0.05	0.94 ± 0.18	0.19 ± 0.07	0.27 ± 0.06	0.46 ± 0.09	6.33 ± 2.01
	12M VT	0.65 ± 0.09	0.05 ± 0.02	0.1 ± 0.03	0.14 ± 0.07	0.23 ± 0.07 _y	15.56 ± 2.85 _y
	12M CT	0.64 ± 0.09	1.64 ± 0.1	0.01 ± 0	0.02 ± 0	0.58 ± 0.17	117.8 ± 10.68 _{x,y}
	24M VT	0.14 ± 0	0.21 ± 0.05	0.44 ± 0.01	0.74 ± 0.1	0.38 ± 0.07	5.15 ± 0.57
	24 CT	0.24 ± 0.09	0.11 ± 0.04	0.16 ± 0.05	0.08 ± 0.03	0.15 ± 0.03 _{x,y}	4.96 ± 2.82
Kidney	3M VT	0.08 ± 0.01	0.14 ± 0	0.13 ± 0	0.17 ± 0.01	0.13 ± 0.01	2.31 ± 0.3
	3M CT	0.85 ± 0.11	1.26 ± 0.06	0.92 ± 0.04	1.22 ± 0.09	1.06 ± 0.06 _x	1.58 ± 0.25
	12M VT	0.54 ± 0.06	0.35 ± 0.03	0.17 ± 0.02	0.26 ± 0.04	0.33 ± 0.04 _y	3 ± 0.36 _y
	12M CT	1.42 ± 0.07	1.01 ± 0.08	0.23 ± 0.03	0.57 ± 0.05	0.81 ± 0.12 _{x,y}	6.71 ± 1 _{x,y}
	24M VT	0.21 ± 0.04	0.37 ± 0.03	0.52 ± 0.04	0.56 ± 0.08	0.42 ± 0.04 _y	3.27 ± 1.22
	24 CT	0.59 ± 0.07	0.17 ± 0.04	0.4 ± 0.05	0.25 ± 0.04	0.35 ± 0.05 _y	4.01 ± 1.02
Spleen	3M VT	16.28 ± 1.75	8.5 ± 0.99	7.36 ± 1.54	24.61 ± 2.3	14.19 ± 1.95	3.85 ± 1
	3M CT	7.29 ± 0.77	27.62 ± 2.27	10.5 ± 1.47	12.47 ± 1.98	14.47 ± 2.16	3.94 ± 0.56
	12M VT	1.79 ± 0.5	0.55 ± 0.12	0.47 ± 0.07	0.29 ± 0.04	0.78 ± 0.19 _y	5.96 ± 1.32
	12M CT	6.35 ± 0.63	3.53 ± 0.19	8.23 ± 1.6	4.32 ± 0.72	5.61 ± 0.63 _{x,y}	2.31 ± 0.44 _y
	24M VT	0.66 ± 0.05	1.36 ± 0.16	4.16 ± 0.67	2.26 ± 0.61	2.11 ± 0.4 _y	6.16 ± 0.68
	24 CT	5.3 ± 0.5	2.55 ± 0.54	3.91 ± 0.29	7.68 ± 0.85	4.86 ± 0.55 _{x,y}	3.5 ± 0.82 _y

Levels of 5-HT at ZT-0,6, 12 and 18. $p_x \leq 0.05$, $p_y \leq 0.05$ where 'x' refers to significant difference with the respective age-matched vehicle group. 'y' refers to significant difference with 3 m vehicle-treated group.

III. A (i). Effect of LPS on clock, immune and microglia resting genes mRNA expression in microglia

Effect of LPS on daily rhythms of clock, immune and microglia resting genes in microglia

With LPS treatment, *rBmall* showed 6 h phase delay with maximum expression at ZT-6 and minimum at ZT-18. *rPer1*, *rPer2* and *rRev-erba* showed 6 h phase delay with maximum expression at ZT-12 and minimum at ZT-0. *rCry1*, *rCry2* and *rRora* lost the rhythmicity. *rNf- κ b1* and *rTnfa* showed 6 h phase delay with maximum expression at ZT-12. *rIl6* showed rhythmic expression with maximum expression at ZT-6 and minimum at ZT-0. *rTlr4* and *rTlr9* did not show variation in phase with maximum expression at ZT-6 and minimum expression at ZT-0. The phase of *rCx3cr1* did not vary with maximum expression at ZT-6 and minimum expression at ZT-18. *rCd172* and *rCd45* lost rhythmicity with LPS treatment in comparison to VT group (Fig. 60) (Table 15, 16).

Effect of LPS on mean 24 h levels and daily pulse of clock, immune and microglia resting genes in microglia

With LPS administration, *rBmall*, *rRora*, *rCry2* showed significant increase in mean 24 h levels. *rRev-erba* and *rCry1* showed significant decrease in mean 24 h levels. *rNf- κ b1*, *rTnfa*, *rIl6* and *rTlr4* showed significant increase, whereas *rTlr9* did not show variation in mean 24 h levels. *rCx3cr1* did not vary in mean 24 h levels but *rCd172* and *rCd45* showed significant decrease in mean 24 h levels in comparison to VT group (Fig. 61). With LPS treatment, daily pulse did not alter for *rBmall*, *rPer2*, *rCry1*, *rCry2* and *rRora*. But *rPer1* and *rRev-erba* showed significant increase. *rIl6* showed increased daily pulse and *rTlr9* showed decreased daily pulse. *rCx3cr1* showed increase in daily pulse, but *rCd172* showed no variation and *rCd45* showed reduction in comparison to VT group (Fig. 62) (Table 15, 16).

Effect of LPS on correlation among clock, immune and microglia resting genes in microglia

In the light phase with the LPS treatment, *rBmall* and *rRora*; *rPer1* and *rPer2*; *rPer1* and *rCry1*; *rPer1* and *rCry2*; *rPer1* and *rRev-erba*; *rPer2* and *rCry1*; *rPer2* and *rCry2*; *rPer2* and *rRev-erba*; *rCry1* and *rCry2*; *rCry1* and *rRev-erba*; *rCry2* and *rRev-erba* were positively correlated. *rBmall* and *rPer1*; *rBmall* and *rCry1*; *rBmall* and *rCry2*; *rBmall* and *rRev-erba*; *rPer1* and *rRora*; *rPer2* and *rRora*; *rCry1* and *rRora*; *rCry2* and *rRora*; *rRev-erba* and *rRora* showed negative correlation. *rNf- κ b1* and *rTnfa*; *rNf- κ b1* and *rIl6*; *rNf- κ b1* and *rTlr9*; *rIl6* and *rTlr9*; *rTlr4* and

rTlr9 showed positive correlation whereas *rTnfa* and *rTlr4* showed negative correlation. All the microglial resting genes showed positive correlation with each other. Between clock gene and immune gene *rBmall* and *rNf- κ b1*; *rBmall* and *rTlr4*; *rPer1* and *rNf- κ b1*; *rPer1* and *rTnfa*; *rPer1* and *rTlr9*; *rPer2* and *rIl6*; *rPer2* and *rTlr9*; *rCry1* and *rNf- κ b1*; *rCry1* and *rTnfa*; *rCry1* and *rTlr9*; *rCry2* and *rNf- κ b1*; *rCry2* and *rTnfa*; *rCry2* and *rTlr9*; *rRev-erba* and *rNf- κ b1*; *rRev-erba* and *rTnfa*; *rRora* and *rTlr4* showed positive correlation whereas *rBmall* and *rTnfa*; *rPer1* and *rTlr4*; *rPer2* and *rTlr4*; *rCry1* and *rTlr4*; *rCry2* and *rTlr4*; *rRev-erba* and *rTlr4*; *rRora* and *rNf- κ b1*; *rRora* and *rTnfa*; *rRora* and *rTlr9* were negatively correlated. The microglial resting genes and clock genes showed positive correlation between *rBmall* and *rCx3cr1*; *rBmall* and *rCd172*; *rBmall* and *rCd45*. We found negative correlation between *rPer1* and *rCd172*; *rPer2* and *rCd172*; *rCry1* and *rCd172*; *rCry1* and *rCd45*; *rCry2* and *rCd172*; *rCry2* and *rCd45*; *rRev-erba* and *rCd172*; *rRev-erba* and *rCd45* (Fig. 63).

In dark phase the clock genes *rBmall* and *rRora*; *rPer1* and *rPer2*; *rPer1* and *rCry2*; *rPer1* and *rRev-erba*; *rPer2* and *rCry2*; *rPer2* and *rRev-erba*; *rCry1* and *rCry2*; *rCry1* and *rRev-erba*; *rCry2* and *rRev-erba* showed positive correlation whereas *rBmall* and *rCry1*; *rBmall* and *rCry2*; *rBmall* and *rRev-erba*; *rPer1* and *rRora*; *rPer2* and *rRora*; *rCry1* and *rRora*; *rCry2* and *rRora*; *rRev-erba* and *rRora* showed negative correlation. Amongst the immune genes *rNf- κ b1* and *rTnfa*; *rNf- κ b1* and *rIl6*; *rNf- κ b1* and *rTlr9*; *rTnfa* and *rIl6*; *rIl6* and *rTlr9* showed positive correlation while *rIl6* and *rTlr4* showed negative correlation. In microglial resting genes *rCd172* and *rCd45* were positively correlated. Upon correlating clock genes with immune genes we found *rBmall* and *rTlr4*; *rPer1* and *rNf- κ b1*; *rPer1* and *rTnfa*; *rPer1* and *rIl6*; *rPer1* and *rTlr9*; *rPer2* and *rNf- κ b1*; *rPer2* and *rTnfa*; *rPer2* and *rIl6*; *rPer2* and *rIl6*; *rPer2* and *rTlr9*; *rCry1* and *rIl6*; *rCry2* and *rNf- κ b1*; *rCry2* and *rTnfa*; *rCry2* and *rTnfa*; *rCry2* and *rIl6*; *rCry2* and *rTlr9*; *rRev-erba* and *rNf- κ b1*; *rRev-erba* and *rTnfa*; *rRev-erba* and *rIl6*; *rRev-erba* and *rTlr9* showed positive correlation. *rBmall* and *rIl6*; *rRora* and *rNf- κ b1*; *rRora* and *rTnfa*; *rRora* and *rIl6*, *rRora* and *rTlr9* showed negative correlation. Microglia resting genes and clock genes showed *rBmall* and *rCx3cr1*; *rBmall* and *rCd172*; *rBmall* and *rCd45*; *rPer1* and *rCx3cr1*; *rRora* and *rCd172*; *rRora* and *rCd45* were positively correlated whereas *rPer1* and *rCd172*; *rPer1* and *rCd45*; *rPer2* and *rCd172*; *rPer2* and *rCd45*; *rCry1* and *rCx3cr1*; *rCry2* and *rCd172*; *rCry1* and *rCd45*; *rCry2* and *rCd172*; *rCry2* and *rCd45*; *rRev-erba* and *rCd172*; *rRev-erba* and *rCd45* showed negative correlation (Fig. 63).

WGCNA analysis among clock, immune and microglia resting genes with LPS treatment in microglia

With LPS treatment, clock and immune genes showed decreased interactions with each other. *rCd45* showed interaction with *rBmall*. *rTnfa* showed interaction with *rPer1* and *rPer2*. *rTlr4* showed interaction with *rCry1* (Fig. 64).

III. A (ii). Effect of LPS on clock and immune genes mRNA expression in liver

Effect of LPS on daily rhythms of clock and immune genes in liver

With the LPS administration *rBmall* did not show change in maximum expression but minimum expression shifted to ZT-18. However, *rPer1*, *rCry1*, *rCry2* and *rRora* showed phase shift with maximum expression at ZT-0 and minimum at ZT-12. *rPer2* showed 12 h phase advance with maximum expression at ZT-0 and minimum at ZT-6. *rRev-erba* showed 12 h phase delay with maximum expression at ZT-18 and minimum at ZT-6. *rNf- κ b1*, *rIl6*, *rTlr4* and *rTlr9* showed phase shift with maximum expression at ZT-0 and minimum at ZT-12. But *rTnfa* expressed maximum at ZT-6 with 6 h phase advance and minimum at ZT-12 (Fig. 65) (Table 17).

Effect of LPS on mean 24 h levels and daily pulse in liver

Mean 24 h levels of *rBmall* showed no significant variation in LPS treated and PDTC treated groups *rPer1* did not show significant variation in LPS in comparison to VT. *rPer2* did not show significant variation among the groups studied. *rCry1* and *rCry2* did not vary in LPS group in comparison to VT. *rRev-erba* showed significant decrease in LPS group in comparison to VT. *rRora* did not show variation between VT and LPS. *rNf- κ b1* showed significant increase in LPS in comparison to VT. *rTnfa*, *rIl6* and *rTlr4* also showed significant increase in LPS group in comparison of VT group. *rTlr9* did not show variation between LPS and VT group (Fig. 66).

Daily pulse of *rBmall* and *rRev-erba* showed significant decrease in LPS in comparison to VT. *rPer1* showed significant increase in LPS in comparison to VT. *rPer2* and *rCry2* showed significant increase in LPS in comparison to VT. *rCry1* did not show variation between VT and LPS groups. *rRora* showed increase in LPS group in comparison to VT. *rNf- κ b1*, *rTnfa*, *rTlr9* showed increase in LPS in comparison to VT. *rIl6* showed increase in LPS group in comparison to VT. *rTlr4* showed decrease in LPS in comparison to VT (Fig. 67) (Table 17).

Effect of LPS on correlation between clock and immune genes in liver

In LPS group, all the clock genes showed significant positive correlation between each other ($p < 0.001$; $p < 0.01$). *rNf- κ b1* showed positive correlation with *rTlr4* and *rTlr9* ($p < 0.001$; $p < 0.01$). *rTnfa* and *rIl6*; *rIl6* and *rTlr9*; *rTlr4* and *rTlr9* showed positive correlation ($p < 0.01$; $p < 0.05$). *rTlr4* showed positive correlation with all the clock genes ($p < 0.001$). *rBmal1*, *rPer1*, *rCry2* and *rRora* showed positive correlation with *rTlr9* ($p < 0.01$; $p < 0.05$). In dark phase, all the clock and immune genes showed positive correlation with each other ($p < 0.001$) (Fig. 68).

WGCNA analysis between clock and immune genes with LPS treatment in liver

In LPS group, clock and immune genes showed strong interactions with each other (Fig. 69).

III. A (iii). Effect of LPS on clock and immune genes mRNA expression in kidney

Effect of LPS on daily rhythms of clock and immune genes in Kidney

rBmal1 showed maximum expression at ZT-0 and minimum at ZT-12 in VT group. With LPS treatment, maximum expression did not alter but minimum expression observed at ZT-6. *rPer1* showed maximum expression at ZT-12 and minimum at ZT-0 in VT, with LPS treatment 12 h phase advance was observed. *rPer2* and *rCry2* showed maximum expression at ZT-12 and minimum at ZT-6 in VT, but with LPS treatment 6 h phase delay was observed with maximum expression at ZT-18. *rCry1* and *rRora* expressed maximum at ZT-18 in VT, with LPS treatment, *rRora* maximum expression did not vary but *rCry1* showed 6 h phase delay with maximum expression at ZT-0. *rRev-erba* showed maximum expression at ZT-6 and minimum at ZT-18 in VT, but with LPS treatment 12 h phase delay was observed with maximum expression at ZT-18. *rNf- κ b1*, *rTnfa*, *rIl6*, *rTlr4* and *rTlr9* showed peak at ZT-12 and minimum expression at ZT-6 except for *rIl6* which showed minimum expression at ZT-0. LPS treatment did not vary the expression of *rNf- κ b1*, but resulted in 6 h phase advance in case of *rTnfa* and *rIl6*, 12 h phase advance in case of *rTlr4* and *rTlr9* (Fig. 70) (Table 18).

Effect of LPS on mean 24 h levels and daily pulse in kidney

Mean 24 h levels of *rBmal1* significantly increased in LPS in comparison to VT. *rPer1* showed significant decrease in LPS in comparison to VT group. *rPer2* showed significant decrease in LPS group in comparison to VT. *rCry1* mean 24 h levels did not alter in the groups studied.

rCry2 levels decreased in LPS in comparison to VT. *rRev-erba* and *rRora* showed significantly increased levels in LPS in comparison to VT. With the LPS treatment, *rNf- κ b1*, *rTnfa*, *rIl6* and *rTlr4* showed significantly increased levels in comparison to VT. *rTlr9* expressions levels significantly not altered in LPS group in comparison to LPS group (Fig. 71). Daily pulse of *rBmal1* showed significant decrease in LPS in comparison to VT group. Daily pulse of *rPer1*, *rPer2*, *rCry2* and *rRora* did not vary in the groups studied. *rCry1* showed decreased daily pulse in LPS in comparison to VT. Daily pulse of *rRev-erba* decreased with LPS treatment in comparison to VT. Daily pulse of *rNf- κ b1* did not alter in the groups studied. In case of *rTnfa*, daily pulse significantly increased in LPS. Daily pulse of *rIl6* increased in LPS group in comparison to VT group. Daily pulse of *rTlr4* significantly increased in LPS in comparison to VT group. Daily pulse of *rTlr9* did not show significant change in LPS in comparison to VT group (Fig. 72) (Table 18).

Effect of LPS on correlation between clock and immune genes in kidney

In LPS group light phase, *rBmal1* and *rPer1*; *rBmal1* and *rCry1*; *rPer1* and *rCry1*; *rPer2* and *rCry1*; *rCry2* and *rRev-erba*; *rRev-erba* and *rRora* showed positive correlation ($p < 0.001$; $p < 0.01$; $p < 0.05$). *rPer1* and *rCry2*; *rPer2* and *rRora* showed negative correlation ($p < 0.001$; $p < 0.05$). *rRev-erba* and *rRora* showed negative correlation with *rBmal1*, *rPer1* and *rCry1* ($p < 0.001$; $p < 0.01$). *rNf- κ b1* showed negative correlation with all immune genes except *rTlr4* ($p < 0.001$; $p < 0.05$). *rTnfa* and *rIl6* showed positive correlation ($p < 0.001$). *rTlr4* showed negative correlation with *rTnfa* and *rIl6* ($p < 0.001$; $p < 0.05$). *rTnfa* and *rIl6* showed negative correlation with *rBmal1*, *rPer1*, *rPer2* and *rCry1* ($p < 0.001$; $p < 0.01$; $p < 0.05$), but showed positive correlation with *rRev-erba* and *rRora* ($p < 0.001$; $p < 0.05$). *rNf- κ b1* showed positive correlation with *rPer2* and *rCry1*, while *rTlr4* showed positive correlation with *rBmal1*, *rPer1* and *rCry1* ($p < 0.001$; $p < 0.05$). In dark phase, *rBmal1* showed negative correlation with *rPer2*, *rCry2*, *rRev-erba* and *rRora* ($p < 0.001$; $p < 0.01$), but showed positive correlation with *rPer1* and *rCry1* ($p < 0.001$). *rPer1* and *rCry1*; *rPer2* and *rCry2*; *rPer2* and *rRev-erba*; *rPer2* and *rRora*; *rCry2* and *rRev-erba*; *rCry2* and *rRora*; *rRev-erba* and *rRora* showed positive correlation ($p < 0.001$; $p < 0.01$). *rPer1* and *rPer2*; *rPer1* and *rCry2*; *rPer1* and *rRev-erba*; *rCry1* and *rCry2*; *rCry1* and *rRev-erba* ($p < 0.001$). *rNf- κ b1* and *rTnfa*; *rNf- κ b1* and *rTlr4*; *rNf- κ b1* and *rTlr9*; *rTnfa* and *rIl6*; *rTlr4* and *rIl6*; *rTlr9* and *rIl6* showed negative correlation ($p < 0.001$). *rNf- κ b1* and *rIl6*; *rTnfa* and *rTlr4*; *rTnfa* and *rTlr9*; *rTlr4* and *rTlr9* showed positive correlation ($p < 0.001$). *rNf- κ b1* and *rIl6* showed positive correlation with *rPer2*, *rCry2* and *rRev-erba*, but showed negative

correlation with *rBmall*, *rPer1* and *rCry1*. *rTnfa*, *rTlr4* and *rTlr9* showed positive correlation with *rBmall*, *rPer1* and *rCry1*, and showed negative correlation with *rPer2*, *rCry2* and *rRev-erba* ($p < 0.001$).

WGCNA analysis between clock and immune genes with LPS treatment in kidney

With LPS administration, the interactions between clock and immune genes decreased in comparison to VT (Fig. 74).

III. A (iv). Effect of LPS on clock and immune genes mRNA expression in spleen

Effect of LPS on daily rhythms of clock and immune genes in spleen

In spleen, *rBmall* showed maximum expression at ZT-0 and minimum at ZT-12 in VT group, with LPS treatment, maximum expression did not alter but minimum expression observed at ZT-6. *rPer1*, *rPer2*, *rCry2* showed similar pattern with maximum expression at ZT-12 and minimum at ZT-6 in VT group. Interestingly, LPS treatment resulted in 6 h phase delay with maximum expression at ZT18 in *rPer1*, *rPer2* and abolished rhythm in *rCry2*. *rCry1* showed maximum expression at ZT-0 and minimum at ZT-6, but with LPS treatment 12 h phase delay was observed with maximum expression at ZT-12. *rRev-erba* showed maximum expression at ZT-6 and minimum at ZT-18, with LPS treatment maximum expression observed at ZT-12 with 6 h phase delay. *rRora* did not show rhythmicity in VT and LPS treated groups. *rNf- κ b1*, *rTlr4* and *rTlr9* showed maximum expression at ZT-0 in VT, with LPS administration the maximum expression of *rNf- κ b1* did not vary but *rTlr4* and *rTlr9* showed maximum expression at ZT-18. *rTnfa* and *rIl6* expressed maximum at ZT-12 and minimum at ZT-6 in VT group, with LPS treatment, *rTnfa* showed 6 h phase advance and *rIl6* showed 6 h phase delay (Fig. 75) (Table 19).

Effect of LPS on mean 24 h levels and daily pulse in spleen

Mean 24 h levels of *rBmall* did not show significant change among the groups studied. *rPer1* levels showed no significant variation in LPS in comparison to VT. *rPer2* levels did not vary in LPS group. *rCry1* showed no variation in LPS group. *rCry2* levels showed no variation in LPS group. *rRev-erba* levels significantly decreased in LPS in comparison to VT group. *rRora* showed significantly decreased levels in LPS in comparison to VT. With the LPS administration all the immune genes showed increased levels of expression (Fig. 76). Daily pulse of *rBmall* and

rRora significantly did not alter in LPS in comparison to VT group. Daily pulse of *rPer1* did not vary in the groups studied. *rPer2* showed significant increase in LPS group in comparison to VT group. Daily pulse of *rCry1* showed significant increase in LPS in comparison to VT group. *rCry2* showed increased daily pulse in LPS group in comparison to VT group. *rRev-erba* showed no variation in LPS group in comparison to VT group. *rNf- κ b1*, *rTnfa*, *rIl6* and *rTlr4* showed no significant variation in daily pulse among the groups studied. *rTlr9* showed increased daily pulse in LPS group (Fig. 77) (Table 19).

Effect of LPS on correlation between clock and immune genes in spleen

In LPS group light phase, *rBmal1* showed negative correlation with *rPer1*, *rPer2* and *rCry2* ($p < 0.001$; $p < 0.01$). *rPer1* and *rPer2*; *rPer1* and *rCry2*; *rPer1* and *rRev-erba*; *rPer2* and *rCry2*; *rPer2* and *rRev-erba*; *rCry1* and *rRev-erba*; *rCry2* and *rRev-erba* showed positive correlation ($p < 0.001$; $p < 0.05$). *rNf- κ b1* and *rTnfa*; *rNf- κ b1* and *rIl6*; *rTnfa* and *rTlr4*; *rIl6* and *rTlr4*; *rIl6* and *rTlr9* showed negative correlation ($p < 0.001$; $p < 0.01$; $p < 0.05$). *rTnfa* and *rIl6*; *rNf- κ b1* and *rTlr9* showed positive correlation ($p < 0.001$). *rNf- κ b1* and *rTlr9* showed positive correlation with *rBmal1* but showed negative correlation with *rPer1*, *rPer2* and *rCry2* ($p < 0.001$; $p < 0.01$). *rTnfa* and *rIl6* showed positive correlation with *rRora* and *rCry2*, but showed negative correlation with *rBmal1* and *rCry1* ($p < 0.001$; $p < 0.01$; $p < 0.05$). *rTlr4* and *rCry1*; *rTlr4* and *rRev-erba* showed positive correlation, while *rTlr4* and *rRora*; *rTlr9* and *rRev-erba* showed negative correlation ($p < 0.001$; $p < 0.05$). In dark phase, *rBmal1* showed negative correlation with *rPer1*, *rCry2* and *rRev-erba* ($p < 0.001$; $p < 0.01$; $p < 0.05$). *rPer1* and *rPer2*; *rPer1* and *rCry2*; *rPer2* and *rCry2*; *rCry2* and *rRev-erba* showed positive correlation ($p < 0.001$; $p < 0.05$). *rPer1* and *rCry1*; *rPer2* and *rCry1*; *rCry1* and *rCry2*; *rCry1* and *rRora* showed negative correlation ($p < 0.001$; $p < 0.01$; $p < 0.05$). *rNf- κ b1* and *rTnfa* showed negative correlation, while *rNf- κ b1* and *rTlr9*; *rTnfa* and *rIl6*; *rTnfa* and *rTlr4*; *rIl6* and *rTlr4*; *rIl6* and *rTlr9* showed positive correlation ($p < 0.001$; $p < 0.01$; $p < 0.05$). *rNf- κ b1* and *rBmal1*; *rNf- κ b1* and *rRora*; *rTnfa* and *rCry2*; *rTnfa* and *rRev-erba*; *rIl6* and *rCry2*; *rTlr4* and *rCry2*; *rTlr9* and *rRora* showed positive correlation ($p < 0.001$; $p < 0.01$). *rTnfa*, *rIl6*, *rTlr4* and *rTlr9* showed positive correlation with *rPer1* and *rPer2* ($p < 0.001$; $p < 0.01$; $p < 0.05$) (Fig. 78).

WGCNA analysis between clock and immune genes with LPS treatment in spleen

With LPS treatment, the interactions between clock and immune genes decreased in comparison to VT (Fig. 79).

III. B (i). Role of NF- κ B inhibitor on the LPS induced alterations of clock, immune, and microglia resting genes mRNA expression in microglia

Effect of NF- κ B inhibitor on the daily rhythms of clock, immune and microglia resting genes in microglia

rBmall and *rPer2* showed 6 h phase delay in LPS+PDTC group which is similar to LPS group, but did not show variation in PDTC group in comparison to VT group. *rPer1* and *rRev-erba* showed similar expression in LPS+PDTC and PDTC groups in comparison to VT group. *rCry1* and *rCry2* showed 6 and 12 h phase delay respectively in LPS+PDTC group but did not show variation in PDTC group in comparison to VT group. *rRora* showed 6 h phase delay in LPS+PDTC and PDTC groups in comparison to VT group. *rNf- κ b1*, *rTnfa*, *rTlr4* and *rTlr9* showed 6 h phase advance in LPS+PDTC and PDTC groups in comparison to VT group. *rIl6* showed maximum expression at ZT-12 in LPS+PDTC, where rhythmicity was lost in PDTC group. *rCx3cr1* and *rCd45* showed 6 h phase advance in LPS+PDTC and PDTC groups in comparison to VT group. *rCd172* showed no alteration in LPS+PDTC group, but showed 6 h phase advance in comparison to VT group (Fig. 60) (Table 15, 16).

Effect of NF- κ B inhibitor on mean 24 h levels and daily pulse of clock, immune and microglia resting genes in microglia

rBmall showed significant increased mean 24 h levels in LPS+PDTC group which is similar to LPS group, but did not show variation in PDTC group in comparison to VT group. *rPer1*, *rPer2* and *rRev-erba* did not show variation in LPS+PDTC and PDTC groups in comparison to VT and LPS groups. *rCry1* showed decreased levels in LPS+PDTC group which is significantly higher than LPS group, but did not show variation in PDTC group in comparison to VT group. *rCry2* showed no variation in LPS+PDTC and PDTC group in comparison to VT group. *rRora* showed no variation in LPS+PDTC and PDTC group in comparison to VT group. *rNf- κ b1*, *rTnfa*, *rIl6*, and *rTlr4* showed significantly reduced levels in LPS+PDTC and PDTC groups in comparison to VT group. *rTlr9* did not show variation in LPS+PDTC and PDTC groups in comparison to VT group. *rCx3cr1* showed significantly increased levels in LPS+PDTC and PDTC groups in comparison to VT and LPS group. Whereas, *rCd45* showed decreased expression in LPS+PDTC and PDTC groups in comparison to VT group (Fig. 61). Daily pulse of *rBmall*, *rPer2*, *rCry1*, and *rCry2* showed an increase in PDTC group alone in comparison to VT and LPS group. *rPer1*, *rRev-erba* and *rRora* showed significant increase in LPS+PDTC and PDTC groups. Daily pulse

of *rNf- κ b1* showed an increase in PDTC group, but *rTnfa* and *rTlr4* did not alter in all groups in comparison to VT group. *rIl6* showed increased daily pulse in LPS+PDTC group, but did not alter in PDTC group, whereas, *rTlr9* showed decreased daily pulse in LPS+PDTC and PDTC group in comparison to VT group. *rCx3cr1* showed decreased daily pulse, but *rCd172* showed increased daily pulse in PDTC group, whereas, *rCd45* showed decreased daily pulse in LPS+PDTC group in comparison to VT group (Fig. 62) (Table 15, 16).

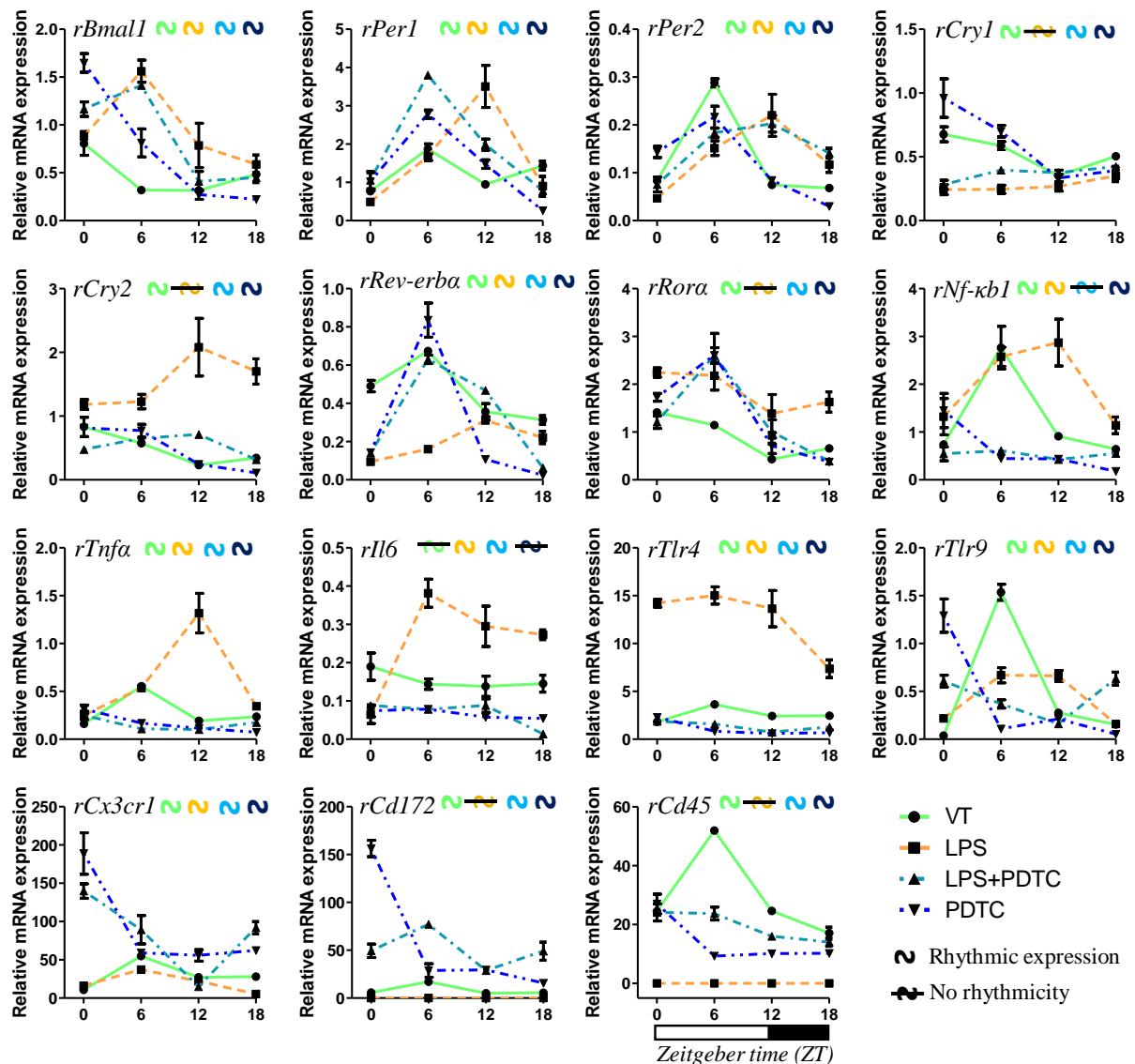


Fig. 60: Effect of PDTC (NF- κ B inhibitor) on LPS induced alterations of daily rhythms of *rBmal1*, *rPer1*, *rPer2*, *rCry1*, *rCry2*, *rRev-erba*, *rRora*, *rNf- κ b1*, *rTnfa*, *rIl6*, *rTlr4*, *rTlr9*, *rCx3cr1*, *rCd172* and *rCd45* mRNA expression in 3 m old rat microglia. Color of the rhythmic wave indicates the group: green – VT, yellow – LPS, cyan – LPS+PDTC, blue – PDTC.

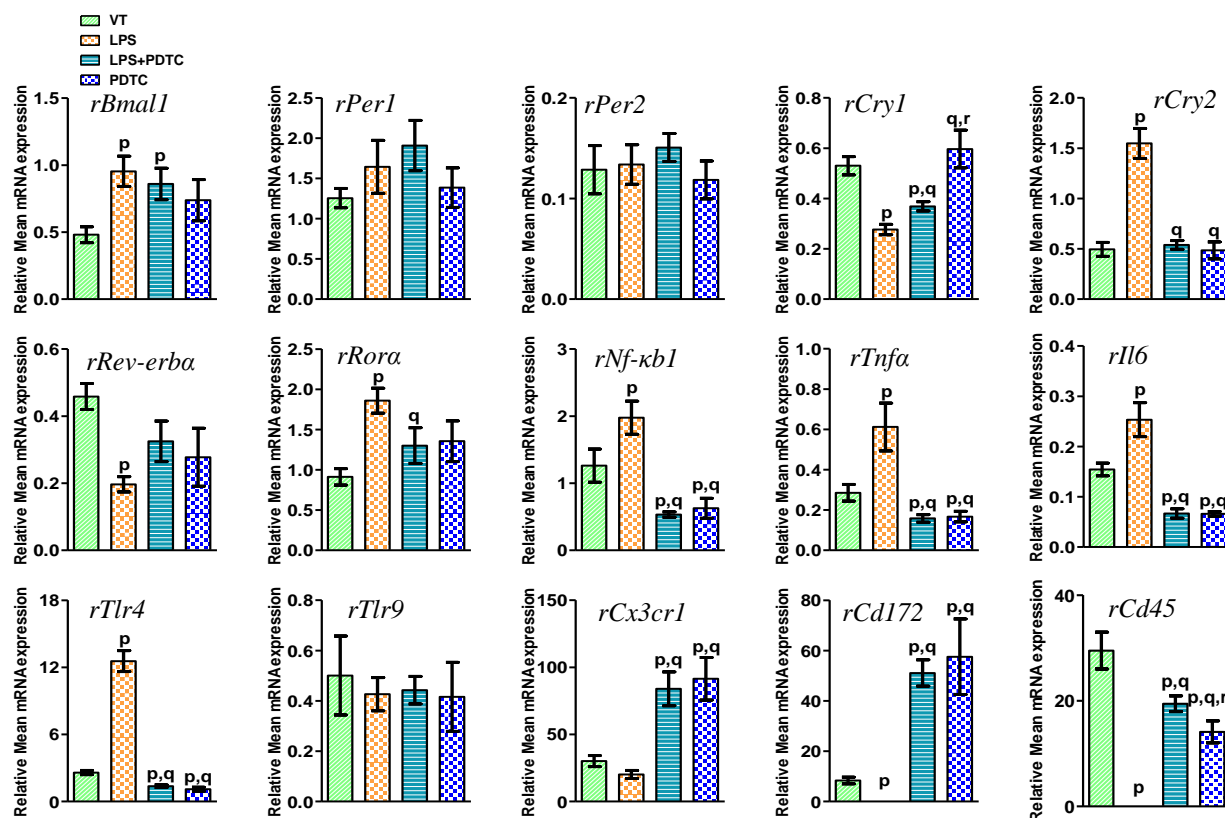


Fig. 61: Effect of PDTC (NF- κ B inhibitor) on LPS induced alterations of Mean 24 h levels of *rBmal1*, *rPer1*, *rPer2*, *rCry1*, *rCry2*, *rRev-erba*, *rRora*, *rNf-kb1*, *rTnfa*, *rIl6*, *rTlr4*, *rTlr9*, *rCx3cr1*, *rCd172* and *rCd45* mRNA expression in 3 m old rat microglia. Each value is mean \pm SEM (n = 4), $p \leq 0.05$ and expressed as mean relative gene expression. $p_p \leq 0.05$ (where 'p' refers to comparison with vehicle-treated group). $p_q \leq 0.05$ (where 'q' refers to comparison with LPS treated group). $p_r \leq 0.05$ (where 'r' refers to comparison with LPS+PDTC treated group).

Effect of NF- κ B inhibitor on correlation among clock, immune and microglia resting genes

In LPS+PDTC treatment Light Phase, amongst the clock genes *rBmal1* and *rROR*; *rPer1* and *rPer2*; *rPer1* and *rCry1*; *rPer1* and *rCry2*; *rPer1* and *rRor*; *rPer2* and *rCry1*; *rPer2* and *rCry2*; *rPer2* and *rRev-erba*; *rCry1* and *rCry2*; *rCry1* and *rRev-erba*; *rCry2* and *rRev-erba*; *rRev-erba* and *rRora* showed significant positive correlations whereas *rBmal1* and *rPer2*; *rBmal1* and *rCry2* showed negative correlation. The immune genes *rNf-kb1* and *rTlr4*; *rNf-kb1* and *rTlr9*; *rTnfa* and *rIl4*; *rTnfa* and *rTlr4*; *rTnfa* and *rTlr8*; *rTnfa* and *rTlr9*; *rTlr4* and *rTlr9* showed significant positive correlations while *rNf-kb1* and *rIl6* appeared to be negatively correlated. All the Microglial resting genes found to be positively correlated with each other. When we compared correlation between clock gene and immune genes we found *rBmal1* showing positive correlation with all the immune gene except *rIl6* on the other hand we found

all other clock genes like *rPer1* to be negatively correlated with all the immune genes except *rNf-kb1* and *rTlr4*. *rPer2* showed negative correlation with *rTnfa*, *rTlr4*, *rTlr9* whereas *rCry1* and *rCry2* were negatively correlated with all the immune genes except *rIl6* for *rCry2* and *rNf-kb1* for *rCry1*. *rRev-erba* and *rTnfa*; *rRev-erba* and *rIl6*; *rRev-erba* and *rTlr4*; *rRev-erba* and *rTlr9*; *rRora* and *rIl6* showed negative correlation in the LP of LPS+PTDC treatment. Most of the clock genes like *rPer2*, *rCry1*, *rCry2* showed negative correlation with microglia resting genes except *rPer1* and *rCd172*; *rRora* and *rCd172* which were positively correlated. We also found *rBmall* to be positive correlated with all the microglia resting genes (Fig. 63).

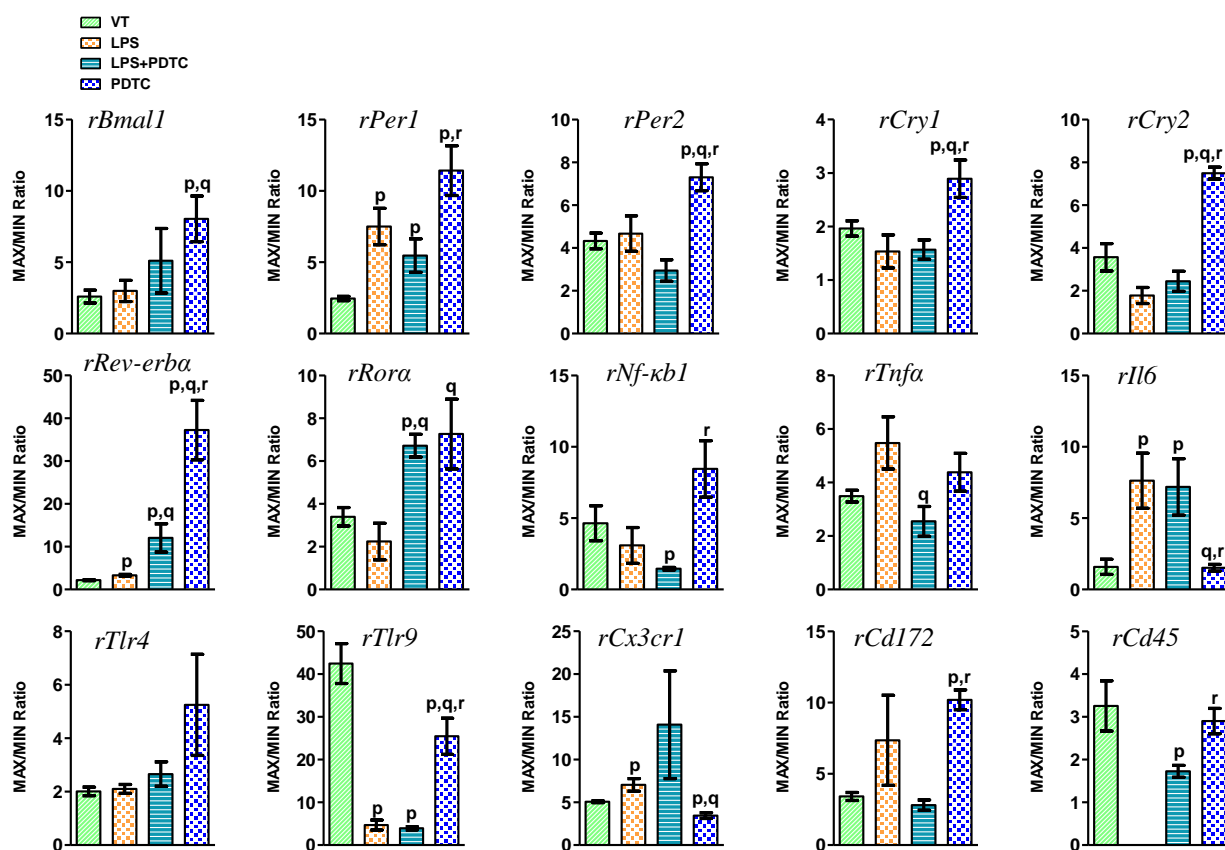


Fig. 62: Effect of PDTC (NF- κ B inhibitor) on LPS induced alterations of Daily pulse of *rBmall*, *rPer1*, *rPer2*, *rCry1*, *rCry2*, *rRev-erba*, *rRora*, *rNfkb1*, *rTnfa*, *rIl6*, *rTlr4*, *rTlr9*, *rCx3cr1*, *rCd172* and *rCd45* mRNA expression in 3 m old rat microglia. Each value is mean \pm SEM ($n = 4$), $p \leq 0.05$ and expressed as mean relative gene expression. $p_p \leq 0.05$ (where 'p' refers to comparison with vehicle-treated group). $p_q \leq 0.05$ (where 'q' refers to comparison with LPS treated group). $p_r \leq 0.05$ (where 'r' refers to comparison with LPS+PDTC treated group).

In dark phase of LPS+PDTC treatment the clock gene *rBmall* showed negative correlation with all other clock genes except *rCry2* and *rRora*. *rCry1* and *rRora* were negatively correlated. We found most of the other clock genes *rPer1* and *rPer2*; *rPer1* and *rCry2*; *rPer1* and *rRev-erba*; r

Per2 and *rCry1*; *rPer2* and *rCry2*; *rPer2* and *rRev-erba*; *rCry2* and *rRev-erba*; *rCry2* and *rRora* showed positive correlation. Amongst the immune genes *rNf- κ b1* showed positive correlation with *rTnfa*, *rTlr4*, *rTlr9* with the exception of *rIl6* which was negatively correlated. *rTnfa* and *rTlr4*; *rTnfa* and *rTlr9*; *rTlr4* and *rTlr9* showed positive correlation. Apart from this *rIl6* and *rTlr9* were negatively correlated. All the microglia resting molecules were positively correlated. When clock genes were correlated with immune genes *rBmal1* showed positive correlation with all the immune genes, whereas most of the clock genes *rPer1*, *rPer2*, *rCry1*, *rCry2*, *rRev-erba* showed negative correlation with most of the immune genes exception *rIl6* and *rPer1* positive correlation, *rIl6* for *rPer2*, *rNf- κ b1*, *rTlr9* for *rCry1*, *rCry2* and *rIl6* positive correlation, *rIl6* and *rRev-erba* positive correlation. *rBmal1* showed positive correlation with all the microglia resting molecules. *rPer1*, *rCry2*, *rRev-erba* showed negative correlation with *rCx3cr1*, *rCd172*. Along with this *rPer2* and *rCd172*; *rPer2* and *rCd45*; *rIl6* and *rCd172* showed negative correlation. *rRora* and *rCd45* were positively correlated (Fig. 63).

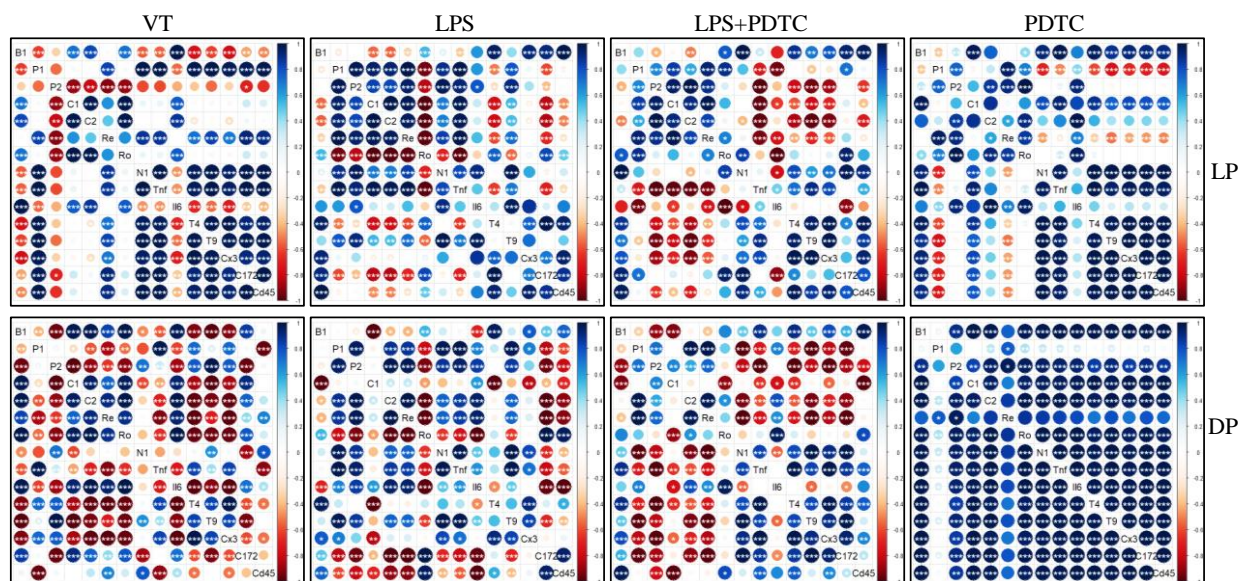


Fig. 63: Effect of PDTC (NF- κ B inhibitor) on LPS induced alterations of Pair wise correlations among *rBmal1*, *rPer1*, *rPer2*, *rCry1*, *rCry2*, *rRev-erba*, *rRora*, *rNfkb1*, *rTnfa*, *rIl6*, *rTlr4*, *rTlr9*, *rCx3cr1*, *rCd172* and *rCd45* in light (ZT-0, 6, 12) phase (LP) and dark (ZT-12, 18, 24/0) phase (DP) of 3, 12 and 24 months (m) old rat microglia. Intensity of color and size of circle represents correlation coefficient values between the genes. Where, positive correlations are indicated by shades of blue, negative correlations by shades of red, and white indicates no correlation. ‘*’, ‘**’, ‘***’ indicates statistically significant correlations ($p \leq 0.05$), ($p \leq 0.01$). ($p \leq 0.001$) respectively. (B1 - *rBmal1*; P1 - *rPer1*; P2 - *rPer2*; C1 - *rCry1*; C2 - *rCry2*; Re - *rRev-erba*; Ro - *rRora*; N1 - *rNfkb1*; Tnf - *rTnfa*; Il6 - *rIl6*; T4 - *rTlr4*; T9 - *rTlr9*; Cx3 - *rCx3cr1*; Cd1 - *rCd172*; Cd4 - *rCd45*).

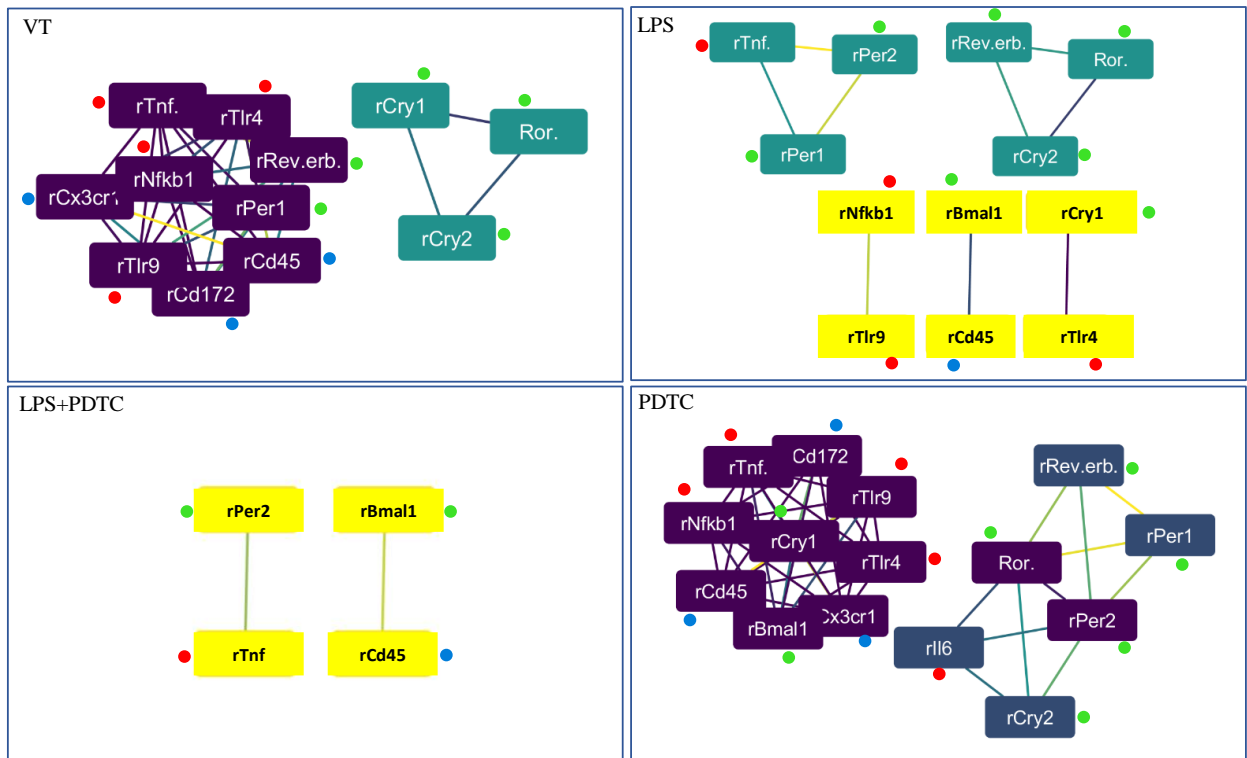


Fig. 64: WGCNA analysis between clock, immune and microglia resting genes clusters: effect of LPS on gene to gene network in 3 m old rat microglia and effect of PDTC (NF- κ B inhibitor) administration. Color of node indicates no. of interactions (highest—purple; intermediate—green and least—yellow). Color of edge indicates the strength of interaction (strongest—purple; intermediate—green and weakest—yellow). Green and red dots indicate clock and immune genes respectively.

Only with PDTC treatment Light phase *rBmal1* and *rPer2*; *rBmal1* and *rCry1*; *rBmal1* and *rRora*; *rPer1* and *rPer2*; *rPer1* and *rRev-erba*; *rPer1* and *rRora*; *rPer2* and *rCry2*; *rPer2* and *rRev-erba*; *rPer2* and *rRor*; *rCry1* and *rCry2*; *rCry1* and *rRora*; *rRev-erba* and *rRora* showed positive correlation, only *rBmal1* and *rPer1* showed negative correlation. All the immune genes were found to be positively correlated with the exception of *rNf- κ b1* and *rIl6*; *rTnfa* and *rIl6*; *rIl6* and *rTlr4* and *rIl6* and *rTlr9* which did not show any significant correlation. All the microglial resting genes were positively correlated. While clock genes were correlated with immune genes, we found *rBmal1* and *rNf- κ b1*; *rBmal1* and *rTnfa*; *rBmal1* and *rTlr4*; *rBmal1* and *rTlr9*; *rPer1* and *rIl6*; *rPer2* and *rIl6*; *rCry1* and *rNf- κ b1*; *rCry1* and *rTnfa*; *rCry1* and *rIl6*; *rCry1* and *rTlr4*; *rCry1* and *rTlr9*; *rCry2* and *rIl6*; *rRev-erba* and *rIl6*; *rRora* and *rIl6*; *rRora* and *rTnfa* showed positive correlations. In clock genes and microglial resting genes *rBmal1* and *rCx3cr1*; *rBmal1* and *rCd172*; *rCry1* and *rCx3cr1*; *rCry1* and *rCd45*; *rCry1* and *rCd172* showed positive correlation whereas *rPer1* and *rCx3cr1*; *rPer1* and *rCd172*; *rPer1* and *rCd172*; *rRev-erba* and

rCx3cr1; *rRev-erba* and *rCd172*; *rRev-erba* and *rCd45* were negatively correlated. Upon Dark phase all the clock genes, immune genes and microglial resting genes showed positive correlation. All the correlation between clock gene and Immune genes, clock gene and microglial resting genes were positively correlated (Fig. 63).

WGCNA analysis among clock, immune and microglia resting genes with PDTC treatment in microglia

In LPS+PDTC group, interactions between clock and immune genes decreased, where *rTnfa* showed interaction with *rPer2*. In PDTC group, clock and immune genes showed strong interaction with each other in two modules (Fig. 64).

Table 15: Effect of NF- κ B inhibitor on LPS induced alterations of clock genes expression

Gene		ZT-0	ZT-6	ZT-12	ZT-18	Mean 24 h levels	Max/min ratio
<i>rBmal1</i>	VT	0.81 ± 0.12	0.32 ± 0.02	0.32 ± 0.01	0.48 ± 0.03	0.48 ± 0.06	2.59 ± 0.45
	LPS	0.88 ± 0.02	1.56 ± 0.12	0.79 ± 0.23	0.59 ± 0.1	0.95 ± 0.11 _x	2.99 ± 0.74
	LPS+PDTC	1.17 ± 0.08	1.41 ± 0.03	0.41 ± 0.1	0.45 ± 0.05	0.86 ± 0.12 _x	5.1 ± 2.26
	PDTC	1.65 ± 0.1	0.81 ± 0.15	0.27 ± 0.05	0.22 ± 0.03	0.74 ± 0.15	8.03 ± 1.6 _{x,y}
<i>rPer1</i>	VT	0.77 ± 0.05	1.87 ± 0.14	0.95 ± 0.04	1.43 ± 0.12	1.26 ± 0.12	2.46 ± 0.15
	LPS	0.49 ± 0.06	1.67 ± 0.1	3.51 ± 0.55	0.9 ± 0.26	1.64 ± 0.33	7.5 ± 1.27 _x
	LPS+PDTC	1.06 ± 0.23	3.8 ± 0.01	1.99 ± 0.14	0.78 ± 0.14	1.91 ± 0.31	5.46 ± 1.17 _x
	PDTC	1.02 ± 0.24	2.78 ± 0.11	1.48 ± 0.11	0.26 ± 0.04	1.39 ± 0.25	11.42 ± 1.74 _{x,z}
<i>rPer2</i>	VT	0.08 ± 0	0.29 ± 0.01	0.07 ± 0.01	0.07 ± 0.01	0.13 ± 0.02	4.33 ± 0.37
	LPS	0.05 ± 0	0.15 ± 0.02	0.22 ± 0.04	0.12 ± 0.02	0.13 ± 0.02	4.67 ± 0.83
	LPS+PDTC	0.08 ± 0.02	0.18 ± 0.01	0.2 ± 0.02	0.14 ± 0.01	0.15 ± 0.01	2.94 ± 0.5
	PDTC	0.14 ± 0.01	0.22 ± 0.02	0.08 ± 0	0.03 ± 0	0.12 ± 0.02	7.3 ± 0.63 _{x,y,z}
<i>rCry1</i>	VT	0.68 ± 0.06	0.59 ± 0.03	0.35 ± 0.04	0.5 ± 0.03	0.53 ± 0.04	1.96 ± 0.14
	LPS	0.24 ± 0.04	0.25 ± 0.03	0.27 ± 0.04	0.35 ± 0.04	0.28 ± 0.02 _x	1.54 ± 0.31
	LPS+PDTC	0.28 ± 0.04	0.4 ± 0.02	0.38 ± 0.02	0.42 ± 0.02	0.37 ± 0.02 _{x,y}	1.57 ± 0.18
	PDTC	0.96 ± 0.15	0.7 ± 0.05	0.33 ± 0.03	0.39 ± 0.03	0.6 ± 0.07 _{y,z}	2.89 ± 0.35 _{x,y,z}
<i>rCry2</i>	VT	0.83 ± 0.15	0.57 ± 0.03	0.23 ± 0.01	0.34 ± 0.02	0.49 ± 0.07	3.57 ± 0.64
	LPS	1.18 ± 0.08	1.23 ± 0.11	2.08 ± 0.45	1.7 ± 0.2	1.55 ± 0.15 _x	1.77 ± 0.37
	LPS+PDTC	0.48 ± 0.04	0.65 ± 0.02	0.71 ± 0.05	0.32 ± 0.05	0.54 ± 0.04 _y	2.44 ± 0.47
	PDTC	0.81 ± 0.02	0.77 ± 0.1	0.24 ± 0.03	0.11 ± 0	0.48 ± 0.08 _y	7.49 ± 0.28
<i>rRev-erba</i>	VT	0.49 ± 0.03	0.67 ± 0.02	0.36 ± 0.04	0.31 ± 0.02	0.46 ± 0.04	2.17 ± 0.1
	LPS	0.09 ± 0.01	0.16 ± 0.01	0.31 ± 0.02	0.22 ± 0.03	0.2 ± 0.02 _x	3.33 ± 0.19 _x
	LPS+PDTC	0.14 ± 0.02	0.63 ± 0.02	0.47 ± 0.01	0.06 ± 0.01	0.32 ± 0.06	12.04 ± 3.3 _{x,y}
	PDTC	0.14 ± 0.02	0.84 ± 0.09	0.11 ± 0.01	0.02 ± 0	0.28 ± 0.09	37.22 ± 6.94 _{x,y,z}
<i>rRora</i>	VT	1.41 ± 0.06	1.15 ± 0.06	0.43 ± 0.04	0.66 ± 0.04	0.91 ± 0.1	3.4 ± 0.43
	LPS	2.24 ± 0.1	2.18 ± 0.3	1.39 ± 0.4	1.63 ± 0.21	1.86 ± 0.15 _x	2.24 ± 0.85
	LPS+PDTC	1.21 ± 0.13	2.6 ± 0.17	1 ± 0.26	0.39 ± 0.02	1.3 ± 0.22 _y	6.72 ± 0.53 _{x,y}
	PDTC	1.73 ± 0.08	2.6 ± 0.46	0.71 ± 0.16	0.38 ± 0.04	1.36 ± 0.25	7.26 ± 1.63 _y

mRNA expression of *rBmal1*, *rPer1*, *rPer2*, *rCry1*, *rCry2*, *rRev-erba*, and *rRora* at ZT-0, 6, 12 and 18. $p_x \leq 0.05$, $p_y \leq 0.05$, $p_z \leq 0.05$ where, 'x' refers to significant difference with vehicle group, 'y' refers to significant difference with LPS group, 'z' refers to significant difference with LPS+PDTC group.

Table 16: Effect of Effect of NF- κ B inhibitor on LPS induced alterations of immune and microglia resting genes expression

<i>Gene</i>		ZT-0	ZT-6	ZT-12	ZT-18	Mean 24 h levels	Max/min ratio
<i>rNf-κb1</i>	VT	0.74 \pm 0.03	2.77 \pm 0.45	0.91 \pm 0.05	0.64 \pm 0.08	1.26 \pm 0.25	4.65 \pm 1.22
	LPS	1.32 \pm 0.38	2.58 \pm 0.2	2.87 \pm 0.49	1.14 \pm 0.17	1.98 \pm 0.25 _x	3.09 \pm 1.25
	LPS+PDTC	0.54 \pm 0.15	0.61 \pm 0.02	0.42 \pm 0.03	0.55 \pm 0.05	0.53 \pm 0.04 _{x,y}	1.46 \pm 0.09 _x
	PDTC	1.45 \pm 0.36	0.45 \pm 0.03	0.43 \pm 0.02	0.18 \pm 0.02	0.63 \pm 0.15 _{x,y}	8.44 \pm 1.98 _z
<i>rTnfa</i>	VT	0.16 \pm 0.01	0.55 \pm 0.01	0.19 \pm 0.01	0.24 \pm 0.02	0.29 \pm 0.04	3.49 \pm 0.22
	LPS	0.25 \pm 0.04	0.53 \pm 0.04	1.32 \pm 0.21	0.34 \pm 0.03	0.61 \pm 0.12 _x	5.48 \pm 0.98
	LPS+PDTC	0.25 \pm 0.04	0.11 \pm 0	0.1 \pm 0.01	0.17 \pm 0.02	0.16 \pm 0.02 _{x,y}	2.55 \pm 0.56 _y
	PDTC	0.31 \pm 0.04	0.17 \pm 0.03	0.11 \pm 0.01	0.07 \pm 0	0.17 \pm 0.03 _{x,y}	4.38 \pm 0.71
<i>rIl6</i>	VT	0.19 \pm 0.04	0.14 \pm 0.01	0.14 \pm 0.03	0.15 \pm 0.02	0.15 \pm 0.01	1.59 \pm 0.53
	LPS	0.06 \pm 0.02	0.38 \pm 0.04	0.3 \pm 0.05	0.27 \pm 0.01	0.25 \pm 0.03 _x	7.62 \pm 1.93 _x
	LPS+PDTC	0.09 \pm 0.01	0.08 \pm 0.01	0.09 \pm 0.02	0.01 \pm 0	0.07 \pm 0.01 _{x,y}	7.18 \pm 1.98 _x
	PDTC	0.07 \pm 0.02	0.08 \pm 0	0.06 \pm 0	0.05 \pm 0.01	0.07 \pm 0 _{x,y}	1.52 \pm 0.24 _{y,z}
<i>rTlr4</i>	VT	1.82 \pm 0.03	3.65 \pm 0.26	2.43 \pm 0.07	2.46 \pm 0.11	2.59 \pm 0.18	2.01 \pm 0.16
	LPS	14.21 \pm 0.4	15.02 \pm 0.91	13.64 \pm 1.9	7.36 \pm 0.93	12.56 \pm 0.94 _x	2.1 \pm 0.16
	LPS+PDTC	1.87 \pm 0.18	1.58 \pm 0.2	0.75 \pm 0.1	1.28 \pm 0.07	1.37 \pm 0.13 _{x,y}	2.66 \pm 0.46
	PDTC	2.3 \pm 0.06	0.82 \pm 0.02	0.59 \pm 0.14	0.68 \pm 0.06	1.1 \pm 0.18 _{x,y}	5.25 \pm 1.89
<i>rTlr9</i>	VT	0.04 \pm 0.01	1.54 \pm 0.08	0.28 \pm 0.03	0.15 \pm 0.02	0.5 \pm 0.16	42.45 \pm 4.65
	LPS	0.22 \pm 0.02	0.67 \pm 0.08	0.66 \pm 0.06	0.16 \pm 0.03	0.43 \pm 0.07	4.69 \pm 1.16 _x
	LPS+PDTC	0.61 \pm 0.06	0.37 \pm 0.04	0.16 \pm 0	0.63 \pm 0.07	0.44 \pm 0.05	3.93 \pm 0.37 _x
	PDTC	1.29 \pm 0.17	0.11 \pm 0.01	0.21 \pm 0.02	0.05 \pm 0.01	0.42 \pm 0.14	25.44 \pm 4.24 _{x,y,z}
<i>rCx3cr1</i>	VT	10.83 \pm 0.25	54.9 \pm 2.07	27.17 \pm 0.65	27.94 \pm 0.63	30.21 \pm 4.11	5.07 \pm 0.1
	LPS	16.19 \pm 0.59	37.13 \pm 1.41	22 \pm 2.93	5.39 \pm 0.36	20.18 \pm 3.05	7.04 \pm 0.74 _x
	LPS+PDTC	139.8 \pm 9.52	89.28 \pm 18.45	14.85 \pm 3.73	91.94 \pm 8.05	83.97 \pm 12.59 _{x,y}	14.08 \pm 6.3
	PDTC	188.89 \pm 27.11	59.16 \pm 3.7	55.75 \pm 7.44	62.24 \pm 3.57	91.51 \pm 15.87 _{x,y}	3.45 \pm 0.34 _{x,y}
<i>rCd172</i>	VT	5.73 \pm 0.08	17.11 \pm 1.22	5.03 \pm 0.12	5.62 \pm 0.41	8.37 \pm 1.34	3.41 \pm 0.28
	LPS	0 \pm 0	0 \pm 0	0 \pm 0	0 \pm 0	0 \pm 0 _x	7.35 \pm 3.16
	LPS+PDTC	49.44 \pm 7.01	77.15 \pm 2.01	28.72 \pm 3.07	49.01 \pm 9.34	51.08 \pm 5.22 _{x,y}	2.8 \pm 0.36
	PDTC	156.31 \pm 8.59	28.8 \pm 7.05	29.41 \pm 3.26	15.59 \pm 1.46	57.53 \pm 15.02 _{x,y}	10.19 \pm 0.69 _{x,z}
<i>rCd45</i>	VT	24.49 \pm 1.25	51.88 \pm 1.23	24.59 \pm 1.15	17.05 \pm 2.05	29.5 \pm 3.49	3.25 \pm 0.59
	LPS	0 \pm 0	0 \pm 0	0 \pm 0	0 \pm 0	0 \pm 0 _x	0 \pm 0
	LPS+PDTC	24.09 \pm 2.92	23.7 \pm 2.21	15.98 \pm 0.81	14.01 \pm 1.42	19.45 \pm 1.47 _{x,y}	1.72 \pm 0.14 _x
	PDTC	26.96 \pm 3.34	9.25 \pm 0.29	10.09 \pm 0.75	10.17 \pm 1.05	14.12 \pm 2.08 _{x,y,z}	2.9 \pm 0.3 _y

mRNA expression of *rNfkb1*, *rTnfa*, *rIl6*, *rTlr4*, *rTlr9*, *rCx3cr1*, *rCd172* and *rCd45* at ZT-0, 6, 12 and 18. $p_x \leq 0.05$, $p_y \leq 0.05$, $p_z \leq 0.05$ where, 'x' refers to significant difference with vehicle group, 'y' refers to significant difference with LPS group, 'z' refers to significant difference with LPS+PDTC group.

III. B (ii). Role of NF- κ B inhibitor on the LPS induced alterations of clock and immune genes mRNA expression in liver

Effect of NF- κ B inhibitor on the daily rhythms of clock and immune genes in liver

In LPS+PDTC and PDTC groups, *rBmal1* did not show variation in expression pattern in comparison to VT and LPS group. In LPS+PDTC group, *rPer1* showed 6 h phase delay but showed 6 h phase advance in PDTC group in comparison to VT group. *rPer2* showed 6 h phase advance in LPS+PDTC group but did not change in PDTC in comparison to VT. *rCry1* showed 6 h phase delay in LPS+PDTC and PDTC groups. *rCry2* showed 6 h phase advance, but did not vary in PDTC in comparison to VT. *rRev-erba* showed 6 h phase delay in LPS+PDTC group but showed no variation with PDTC in comparison to VT. In LPS+PDTC group, *rRora* showed 6 h phase advance, but showed 6 h phase delay in PDTC group in comparison to VT. *rNf- κ b1* showed 6 h phase delay in LPS+PDTC group, but rhythmicity was abolished in PDTC group. *rTnfa* and *rTlr9* showed no variation in LPS+PDTC group, but showed 12 h phase advance in PDTC group in comparison to VT. *rIl6* showed 6 h phase advance in LPS+PDTC group. But, in PDTC group, rhythmicity was abolished. *rTlr4* showed 6 h phase advance in LPS+PDTC group, but in PDTC group, 6 h phase delay was observed in comparison to VT (Fig. 65) (Table 17).

Effect of NF- κ B inhibitor on mean 24 h levels and daily pulse of clock and immune genes in liver

Mean 24 h levels of *rBmal1* showed no significant variation in LPS+PDTC and PDTC treated groups in comparison to VT group. *rPer1* and *rCry1* showed significant increase in PDTC group alone in comparison to LPS and LPS+PDTC groups. *rPer2* and *rCry2* did not show significant variation among all the groups studied. *rRev-erba* showed significant decrease in LPS+PDTC group, but did not alter in PDTC group in comparison to VT. *rRora* did not show variation LPS+PDTC but showed significant decrease in PDTC in comparison to VT. *rNf- κ b1*, *rTnfa*, *rIl6*, *rTlr4* and *rTlr9* showed significant decrease in LPS+PDTC and PDTC groups in comparison to VT (Fig. 66). Daily pulse of *rBmal1* and *rRev-erba* showed significant decrease in LPS+PDTC and PDTC groups in comparison to VT. *rPer1* showed significant increase in PDTC, but did not show significant variation in LPS+PDTC group in comparison to VT. *rPer2* and *rCry2* showed significant increase in LPS+PDTC group but did not vary in PDTC group in comparison to VT. *rCry1* did not show variation in PDTC group but showed significant decrease in LPS+PDTC group in comparison to VT. Daily pulse of *rRora* did not vary in LPS+PDTC group, but

decreased in PDTC group in comparison to VT. *rNf- κ b1*, *rTnfa*, *rTlr9* showed increase in LPS+PDTC group, but did not vary in PDTC group in comparison to VT. Daily pulse of *rIl6* did not vary in LPS+PDTC and PDTC groups in comparison to VT. *rTlr4* showed decrease in PDTC group but did not vary in LPS+PDTC group in comparison to VT (Fig. 67) (Table 17).

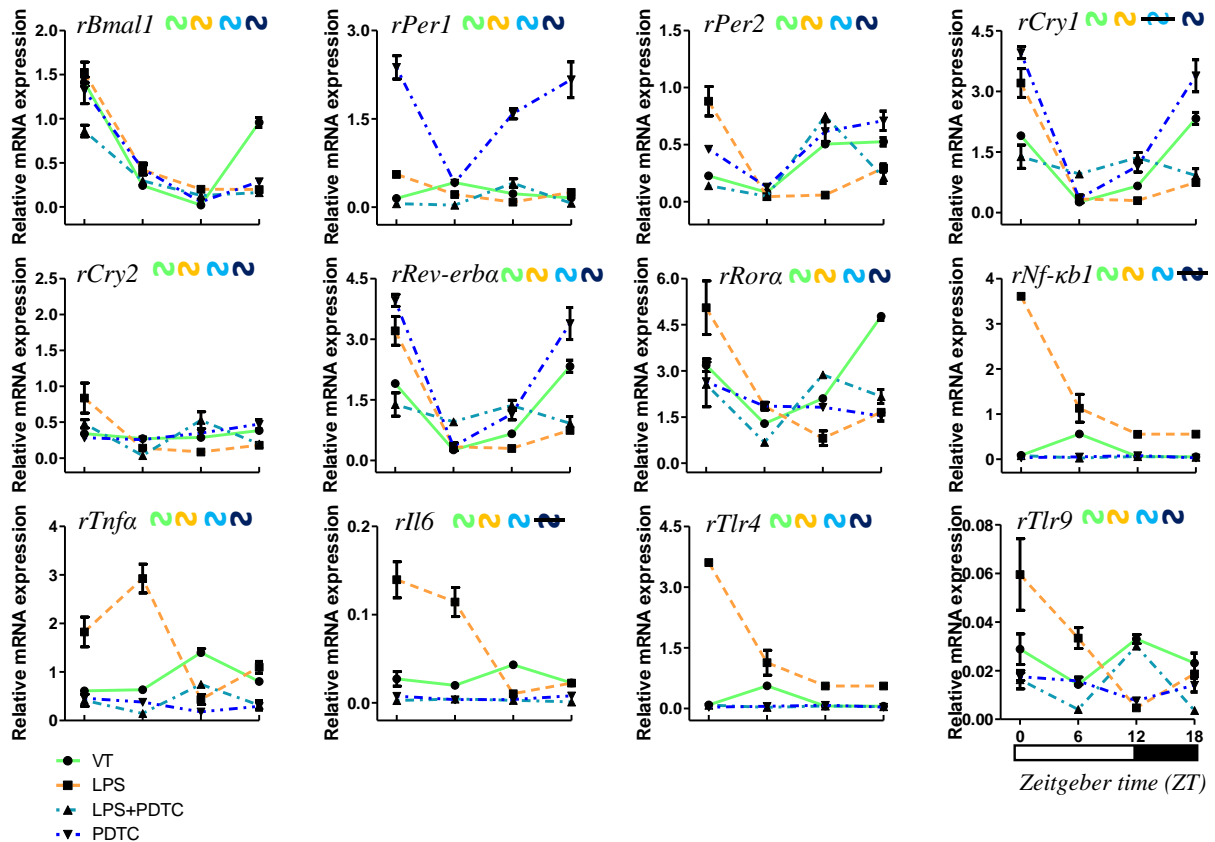


Fig. 65: Effect of PDTC (NF- κ B inhibitor) on LPS induced alterations of daily rhythms of *rBmal1*, *rPer1*, *rPer2*, *rCry1*, *rCry2*, *rRev-erba*, *rRora*, *rNf κ b1*, *rTnfa*, *rIl6*, *rTlr4*, and *rTlr9* mRNA expression in 3 m old rat liver. Color of the rhythmic wave indicates the group: black – VT, yellow – LPS, cyan – LPS+PDTC, blue – PDTC.

Role of NFKB Inhibitor on correlation between clock and immune genes

In LPS+PDTC group light phase, *rBmal1* showed negative correlation with *rPer1*; *rPer1* and *rCry1* showed insignificant positive correlation. All the other clock genes showed positive correlation between each other ($p < 0.001$; $p < 0.01$; $p < 0.05$). *rNf- κ b1* showed positive correlation with *rTnfa*, *rTlr4* and *rTlr9* ($p < 0.001$), and negative correlation with *rIl6* ($p < 0.001$). *rTnfa* and *rIl6*; *rIl6* and *rTlr4*; *rIl6* and *rTlr9* showed negative correlation ($p < 0.001$, 0.01). *rTnfa* showed positive correlation with *rTlr4* and *rTlr9* ($p < 0.001$; $p < 0.05$). *rNf- κ b1*,

rTnfa and *rTlr9* showed positive correlation with all clock genes except *rBmal1* ($p < 0.001$; $p < 0.01$; $p < 0.05$). *rIl6* showed negative correlation with *rCry1*, *rCry2*, *rRev-erba* and *rRora*, but *rTlr4* showed positive correlation with all those genes ($p < 0.001$, 0.05) (Fig. 68).

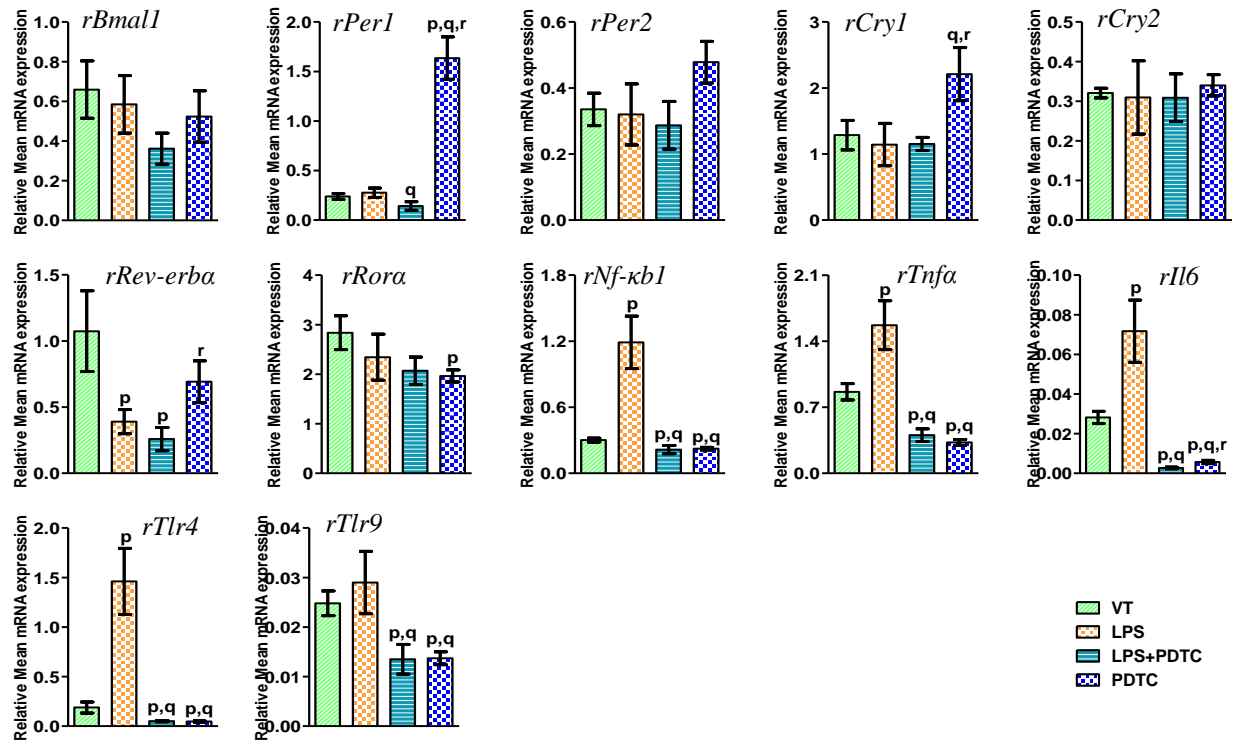


Fig. 66: Effect of PDTC (NF- κ B inhibitor) on LPS induced alterations of Mean 24 h levels of *rBmal1*, *rPer1*, *rPer2*, *rCry1*, *rCry2*, *rRev-erba*, *rRora*, *rNf- κ b1*, *rTnfa*, *rIl6*, *rTlr4*, and *rTlr9* mRNA expression in 3 m old rat liver. Each value is mean \pm SEM ($n = 4$), $p \leq 0.05$ and expressed as mean relative gene expression. $p_p \leq 0.05$ (where ‘p’ refers to comparison with vehicle-treated group). $p_q \leq 0.05$ (where ‘q’ refers to comparison with LPS treated group). $p_r \leq 0.05$ (where ‘r’ refers to comparison with LPS+PDTC treated group).

In dark phase, *rBmal1* showed negative correlation with *rPer1*, *rPer2* and *rRev-erba* ($p < 0.001$). *rPer1* and *rPer2*, *rCry1* and *rCry2*; *rCry2* and *rRora*; *rRev-erba* and *rRora* showed positive correlation ($p < 0.001$). *rPer1* and *rPer2* showed positive correlation with *rRev-erba* and *rRora* ($p < 0.001$). *rNf- κ b1* and *rIl6* showed positive correlation ($p < 0.001$). *rTlr9* showed positive correlation with *rNf- κ b1*, *rTnfa* and *rIl6* ($p < 0.001$; $p < 0.05$). *rTnfa* and *rTlr9* showed positive correlation with *rPer1*, *rPer2*, *rRev-erba* and *rRora* ($p < 0.001$). *rNf- κ b1* and *rIl6* showed positive correlation with *rCry1*, *rCry2* and *rRora* ($p < 0.001$; $p < 0.05$). In PDTC group light phase, *rBmal1* and *rPer1*; *rBmal1* and *rCry1*; *rBmal1* and *rRora*; *rPer1* and *rPer2*; *rPer1* and *rCry1*; *rPer1* and *rRora*; *rPer2* and *rCry2*; *rCry1* and *rRora* showed positive correlation ($p <$

0.001; $p < 0.01$; $p < 0.05$). *rBmal1* and *rCry2*; *rBmal1* and *rRev-erba*; *rPer1* and *rRev-erba*; *rRev-erba* and *rRora* showed negative correlation ($p < 0.001$; $p < 0.01$; $p < 0.05$) (Fig. 68).

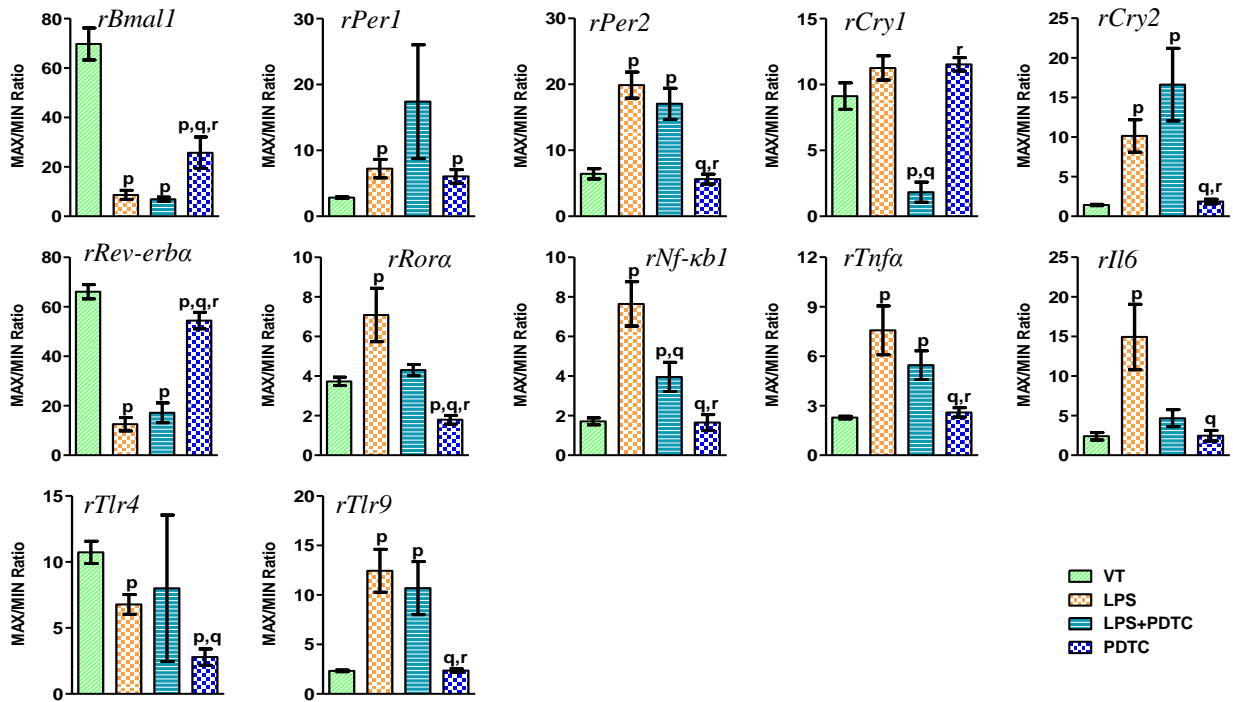


Fig. 67: Effect of PDTC (NF- κ B inhibitor) on LPS induced alterations of Daily pulse of *rBmal1*, *rPer1*, *rPer2*, *rCry1*, *rCry2*, *rRev-erba*, *rRora*, *rNf- κ b1*, *rTnfa*, *rIl6*, *rTlr4*, and *rTlr9* mRNA expression in 3 m old rat liver. Each value is mean \pm SEM ($n = 4$), $p \leq 0.05$ and expressed as mean relative gene expression. $p_p \leq 0.05$ (where ‘p’ refers to comparison with vehicle-treated group). $p_q \leq 0.05$ (where ‘q’ refers to comparison with LPS treated group). $p_r \leq 0.05$ (where ‘r’ refers to comparison with LPS+PDTC treated group).

rNf- κ b1 and *rTnfa*; *rTnfa* and *rIl6* showed positive correlation ($p < 0.001$; $p < 0.05$). *rTlr4* showed negative correlation with *rNf- κ b1*, *rTnfa* and *rIl6* ($p < 0.001$; $p < 0.01$), while *rTlr9* showed positive correlation with those genes ($p < 0.001$; $p < 0.05$). *rBmal1* and *rRora* showed positive correlation with *rTnfa*, *rIl6* and *rTlr9* but showed negative correlation with *rTlr4* ($p < 0.001$). *rBmal1* and *rNf- κ b1*; *rPer1* and *rIl6*; *rCry1* and *rIl6* showed positive correlation ($p < 0.001$; $p < 0.01$). *rPer2* showed negative correlation with *rNf- κ b1*, *rTnfa* and *rTlr9* ($p < 0.001$; $p < 0.05$). *rPer2* and *rCry2* showed negative correlation with *rNf- κ b1*, *rTnfa* and *rTlr9* ($p < 0.001$; $p < 0.05$). *rCry1* and *rTlr4*; *rRev-erba* and *rIl6*; *rRora* and *rTlr4* showed negative correlation ($p < 0.001$; $p < 0.01$). In dark phase, *rBmal1* showed positive correlation with *rPer1*, *rCry1* and *rRora* ($p < 0.001$), and showed negative correlation with other clock genes ($p < 0.001$). *rPer1* and *rCry1*; *rPer2* and *rCry2* showed positive correlation ($p < 0.001$). *rPer1* and *rPer2*; *rPer2* and *rCry1*; *rCry1* and *rCry2* showed negative correlation ($p < 0.05$). *rPer1* and *rCry1* showed

positive correlation with *rRora* and negative correlation with *rRev-erba* ($p < 0.001$; $p < 0.01$). *rPer2* and *rCry2* showed positive correlation with *rRev-erba* and negative correlation with *rRora* ($p < 0.001$; $p < 0.05$). *rNf-kb1* and *rTnfa*; *rNf-kb1* and *rIl6*; *rTnfa* and *rIl6* showed positive correlation ($p < 0.001$). *rTlr4* and *rTlr9* showed negative correlation ($p < 0.001$). *rTlr4* showed negative correlation with *rNf-kb1*, *rTnfa* and *rIl6*, while *rTlr9* showed positive correlation with those genes ($p < 0.001$). *rBmal1*, *rPer1* and *rCry1* showed positive correlation with all immune genes except *rTlr4* ($p < 0.001$; $p < 0.01$). *rRev-erba* showed negative correlation with all immune genes except *rTlr4* ($p < 0.001$). *rPer2* and *rCry2* showed negative correlation with *rTnfa* and *rTlr9*, while *rRora* showed positive correlation with those genes ($p < 0.001$; $p < 0.01$; $p < 0.05$) (Fig. 68).

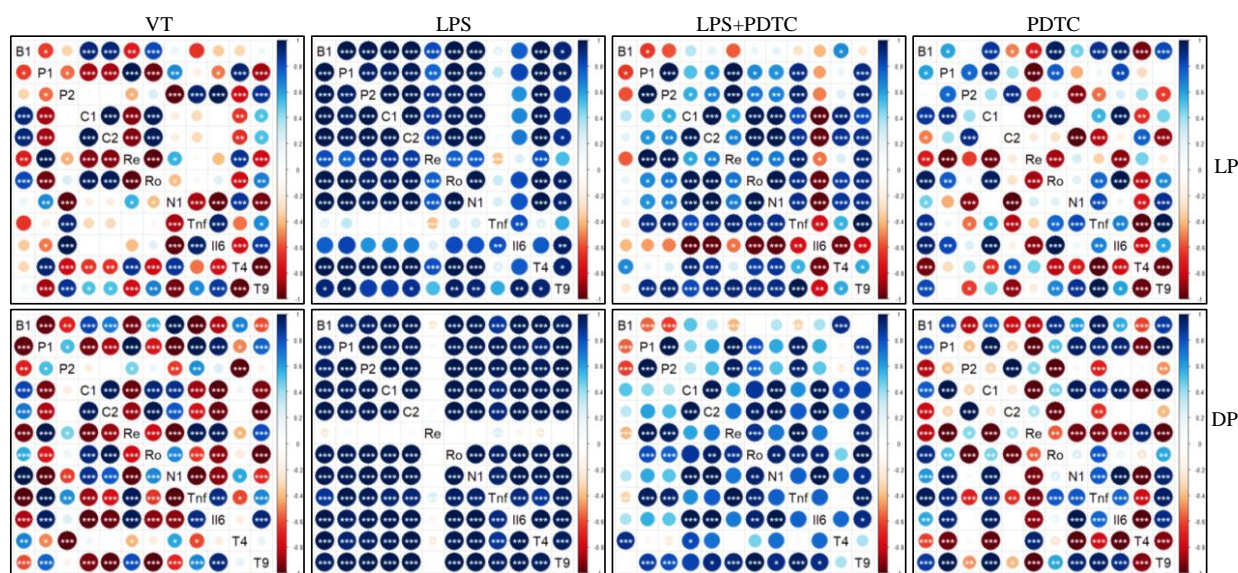


Fig. 68: Effect of PDTC (NF- κ B inhibitor) on LPS induced alterations of Pair wise correlations among clock and immune genes expression in light (ZT-0, 6, 12) phase (LP) and dark (ZT-12, 18, 24/0) phase (DP) of 3, 12 and 24 months (m) old rat liver. Intensity of color and size of circle represents correlation coefficient values between the genes. Where, positive correlations are indicated by shades of blue, negative correlations by shades of red, and white indicates no correlation. ‘*’, ‘**’, ‘***’ indicates statistically significant correlations ($p \leq 0.05$), ($p \leq 0.01$), ($p \leq 0.001$) respectively. (B1- *rBmal1*; P1 - *rPer1*; P2 - *rPer2*; C1 - *rCry1*; C2 - *rCry2*; Re - *rRev-erba*; Ro - *rRora*; N1 - *rNfkb1*; Tnf - *rTnfa*; Il6 - *rIl6*; T4 - *rTlr4*; T9 - *rTlr9*).

WGCNA analysis between clock and immune genes with PDTC treatment in liver

in LPS+PDTC group, clock and immune genes showed strong interaction with each other in two modules. In PDTC group, the interactions between clock and immune genes showed decrease (Fig. 69).

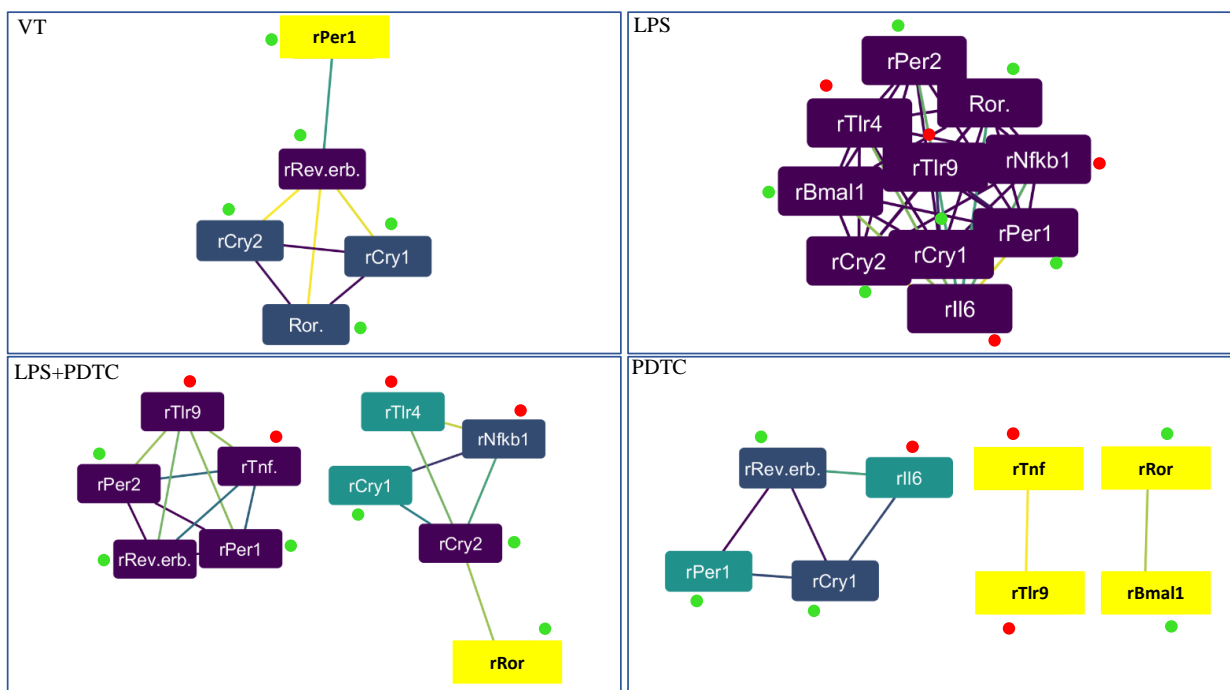


Fig. 69: WGCNA analysis between clock and immune genes clusters: effect of LPS on gene to gene network in 3 m old rat liver and effect of PDTC (NF- κ B inhibitor) administration. Color of node indicates no. of interactions (highest—purple; intermediate—blue and least—yellow). Color of edge indicates the strength of interaction (strongest—purple; intermediate—blue and weakest—yellow). Green and red dots indicate clock and immune genes respectively.

Table 17: Effect of NF- κ B inhibitor on LPS induced alterations of clock and immune genes

Gene		ZT-0	ZT-6	ZT-12	ZT-18	Mean 24 h levels	Max/min ratio
<i>rBmal1</i>	VT	1.42 ± 0.04	0.24 ± 0	0.02 ± 0	0.96 ± 0.05	0.66 ± 0.14	69.68 ± 6.46
	LPS	1.52 ± 0.12	0.42 ± 0.06	0.2 ± 0.01	0.2 ± 0.03	0.59 ± 0.15	8.65 ± 1.85 _x
	LPS+PDTC	0.61 ± 0.05	0.21 ± 0.03	0.09 ± 0.01	0.12 ± 0.02	0.26 ± 0.06	18.75 ± 6.22 _x
	PDTC	1.32 ± 0.15	0.43 ± 0.07	0.06 ± 0.01	0.29 ± 0.03	0.52 ± 0.13	25.7 ± 6.36 _{x,y,z}
<i>rPer1</i>	VT	0.15 ± 0	0.42 ± 0.01	0.23 ± 0	0.16 ± 0.01	0.24 ± 0.03	2.82 ± 0.1
	LPS	0.56 ± 0.03	0.21 ± 0.05	0.09 ± 0.02	0.25 ± 0.03	0.28 ± 0.05	7.24 ± 1.4 _x
	LPS+PDTC	0.06 ± 0	0.03 ± 0.01	0.41 ± 0.08	0.07 ± 0.01	0.14 ± 0.04 _y	17.39 ± 8.63
	PDTC	2.37 ± 0.2	0.41 ± 0.04	1.59 ± 0.09	2.16 ± 0.3	1.63 ± 0.21 _{x,y,z}	6.05 ± 1.04 _x
<i>rPer2</i>	VT	0.23 ± 0	0.08 ± 0	0.5 ± 0.01	0.53 ± 0.04	0.34 ± 0.05	6.42 ± 0.77
	LPS	0.88 ± 0.13	0.04 ± 0	0.06 ± 0.01	0.3 ± 0.03	0.32 ± 0.09	19.88 ± 1.97 _x
	LPS+PDTC	0.14 ± 0.03	0.05 ± 0.01	0.75 ± 0.03	0.21 ± 0.05	0.29 ± 0.07	17.04 ± 2.36 _x
	PDTC	0.46 ± 0.02	0.13 ± 0.01	0.61 ± 0.09	0.71 ± 0.09	0.48 ± 0.06	5.64 ± 0.75 _{y,z}
<i>rCry1</i>	VT	1.9 ± 0.09	0.26 ± 0.01	0.66 ± 0.03	2.33 ± 0.15	1.29 ± 0.22	9.12 ± 1.01
	LPS	3.2 ± 0.36	0.34 ± 0.1	0.29 ± 0.05	0.74 ± 0.04	1.14 ± 0.32	11.25 ± 0.92
	LPS+PDTC	1.38 ± 0.29	0.95 ± 0.08	1.36 ± 0.13	0.91 ± 0.17	1.15 ± 0.1	1.83 ± 0.76 _{x,y}
	PDTC	3.96 ± 0.15	0.35 ± 0.02	1.14 ± 0.14	3.39 ± 0.4	2.21 ± 0.4 _{y,z}	11.52 ± 0.51 _z
<i>rCry2</i>	VT	0.34 ± 0.01	0.27 ± 0.01	0.29 ± 0.01	0.38 ± 0.02	0.32 ± 0.01	1.42 ± 0.08
	LPS	1.67 ± 0.42	0.28 ± 0.05	0.17 ± 0.03	0.36 ± 0.07	0.62 ± 0.18	10.14 ± 2.05 _x
	LPS+PDTC	0.68 ± 0.08	0.05 ± 0.01	0.74 ± 0.17	0.28 ± 0.03	0.44 ± 0.08	16.62 ± 4.58 _x
	PDTC	0.57 ± 0.04	0.51 ± 0.02	0.7 ± 0.05	0.8 ± 0.13	0.64 ± 0.04	1.55 ± 0.22 _{y,z}
<i>rRev-erba</i>	VT	0.04 ± 0	2.94 ± 0.05	1.25 ± 0.02	0.06 ± 0	1.07 ± 0.31	66.02 ± 2.87
	LPS	0.41 ± 0.02	0.07 ± 0.01	0.22 ± 0.03	0.86 ± 0.22	0.39 ± 0.09 _x	12.54 ± 2.69 _x
	LPS+PDTC	0.16 ± 0.02	0.05 ± 0	0.78 ± 0.17	0.05 ± 0.01	0.26 ± 0.09 _x	17.16 ± 3.97 _x
	PDTC	0.03 ± 0	1.56 ± 0.14	0.88 ± 0.12	0.3 ± 0.04	0.69 ± 0.16 _z	54.41 ± 3.33 _{x,y,z}
<i>rRora</i>	VT	3.18 ± 0.21	1.29 ± 0.05	2.1 ± 0.03	4.77 ± 0.12	2.84 ± 0.34	3.73 ± 0.21
	LPS	5.05 ± 0.87	1.85 ± 0.05	0.81 ± 0.24	1.66 ± 0.09	2.34 ± 0.46	7.08 ± 1.35 _x
	LPS+PDTC	2.56 ± 0.73	0.68 ± 0.04	2.87 ± 0.05	2.17 ± 0.23	2.07 ± 0.28	4.3 ± 0.29
	PDTC	2.65 ± 0.07	1.86 ± 0.13	1.82 ± 0.11	1.54 ± 0.16	1.96 ± 0.12 _x	1.79 ± 0.22 _{x,y,z}
<i>rNf-κb1</i>	VT	0.31 ± 0.01	0.38 ± 0.04	0.22 ± 0	0.29 ± 0.02	0.3 ± 0.02	1.71 ± 0.17
	LPS	2.7 ± 0.09	0.87 ± 0.2	0.37 ± 0.05	0.82 ± 0.14	1.19 ± 0.24 _x	7.64 ± 1.12 _x
	LPS+PDTC	0.79 ± 0.1	0.21 ± 0.02	0.86 ± 0.19	0.26 ± 0.03	0.53 ± 0.09 _{x,y}	3.95 ± 0.74 _{x,y}
	PDTC	0.32 ± 0.01	0.36 ± 0.02	0.26 ± 0.06	0.33 ± 0.03	0.32 ± 0.02 _{x,y}	1.65 ± 0.4 _{y,z}
<i>rTnfa</i>	VT	0.61 ± 0.02	0.64 ± 0.03	1.4 ± 0.08	0.81 ± 0.08	0.86 ± 0.09	2.28 ± 0.08
	LPS	1.82 ± 0.31	2.92 ± 0.3	0.43 ± 0.1	1.1 ± 0.12	1.57 ± 0.26 _x	7.57 ± 1.48 _x
	LPS+PDTC	0.42 ± 0.13	0.14 ± 0.02	0.74 ± 0.04	0.31 ± 0.1	0.4 ± 0.07 _{x,y}	5.46 ± 0.87 _x
	PDTC	0.92 ± 0.09	0.76 ± 0.07	0.36 ± 0.03	0.58 ± 0.04	0.65 ± 0.06 _{x,y}	2.59 ± 0.29 _{y,z}
<i>rIl6</i>	VT	0.03 ± 0.01	0.02 ± 0	0.04 ± 0	0.02 ± 0	0.03 ± 0	2.4 ± 0.46
	LPS	0.14 ± 0.02	0.11 ± 0.02	0.01 ± 0	0.02 ± 0	0.07 ± 0.02 _x	14.93 ± 4.13 _x
	LPS+PDTC	0 ± 0	0 ± 0	0 ± 0	0 ± 0	0 ± 0 _{x,y}	4.68 ± 1.06
	PDTC	0.01 ± 0	0 ± 0	0 ± 0	0.01 ± 0	0.01 ± 0 _{x,y,z}	2.47 ± 0.67 _y
<i>rTlr4</i>	VT	0.09 ± 0	0.56 ± 0.03	0.06 ± 0	0.05 ± 0	0.19 ± 0.06	10.72 ± 0.84
	LPS	3.61 ± 0.04	1.13 ± 0.31	0.55 ± 0.06	0.55 ± 0.07	1.46 ± 0.33 _x	6.78 ± 0.75 _x
	LPS+PDTC	0.45 ± 0.05	0.14 ± 0.04	0.33 ± 0.08	0.25 ± 0.03	0.29 ± 0.04 _{x,y}	8 ± 5.55
	PDTC	0.12 ± 0.01	0.2 ± 0.02	0.31 ± 0.07	0.11 ± 0.02	0.19 ± 0.03 _{x,y}	2.79 ± 0.62 _{x,y}
<i>rTlr9</i>	VT	0.03 ± 0.01	0.01 ± 0	0.03 ± 0	0.02 ± 0	0.02 ± 0	2.32 ± 0.08
	LPS	0.24 ± 0.06	0.13 ± 0.02	0.02 ± 0	0.07 ± 0.01	0.12 ± 0.03	12.43 ± 2.17 _x
	LPS+PDTC	0.07 ± 0.02	0.02 ± 0	0.12 ± 0	0.01 ± 0	0.05 ± 0.01 _{x,y}	10.69 ± 2.68 _x
	PDTC	0.04 ± 0	0.03 ± 0	0.02 ± 0	0.03 ± 0.01	0.03 ± 0 _{x,y}	2.36 ± 0.16 _{y,z}

mRNA expression of clock and immune genes at ZT-0, 6, 12 and 18. $p_x \leq 0.05$, $p_y \leq 0.05$, $p_z \leq 0.05$ where, 'x' refers to significant difference with vehicle group, 'y' refers to significant difference with LPS group, 'z' refers to significant difference with LPS+PDTC group.

III. B (iii). Role of NF- κ B inhibitor on the LPS induced alterations of clock and immune genes mRNA expression in kidney

Effect of NF- κ B inhibitor on the daily rhythms of clock and immune genes in kidney

In LPS+PDTC and PDTC group, *rBmal1*, *rCry1* and *rRev-erba* did not alter the maximum expression in comparison to VT. *rPer2* and *rCry2* showed 6 h phase delay, but did not vary in PDTC in comparison to VT. In LPS+PDTC group, *rPer1* showed 6 h phase advance, however, did not change in PDTC group in comparison to VT. *rRora* showed 12 h phase advance in LPS+PDTC, but 6 h phase delay in PDTC group in comparison to VT. In LPS+PDTC group, *rNf- κ b1*, and *rTnfa* showed 6 h phase advance in comparison to VT. Interestingly, with PDTC treatment their rhythmicity was abolished. *rIl6* and *rTlr4* lost rhythmicity in LPS+PDTC and PDTC group. *rTlr9* rhythmicity was abolished in LPS+PDTC group, but in PDTC group *rTlr9* showed similar expression as in VT (Fig. 70) (Table 18).

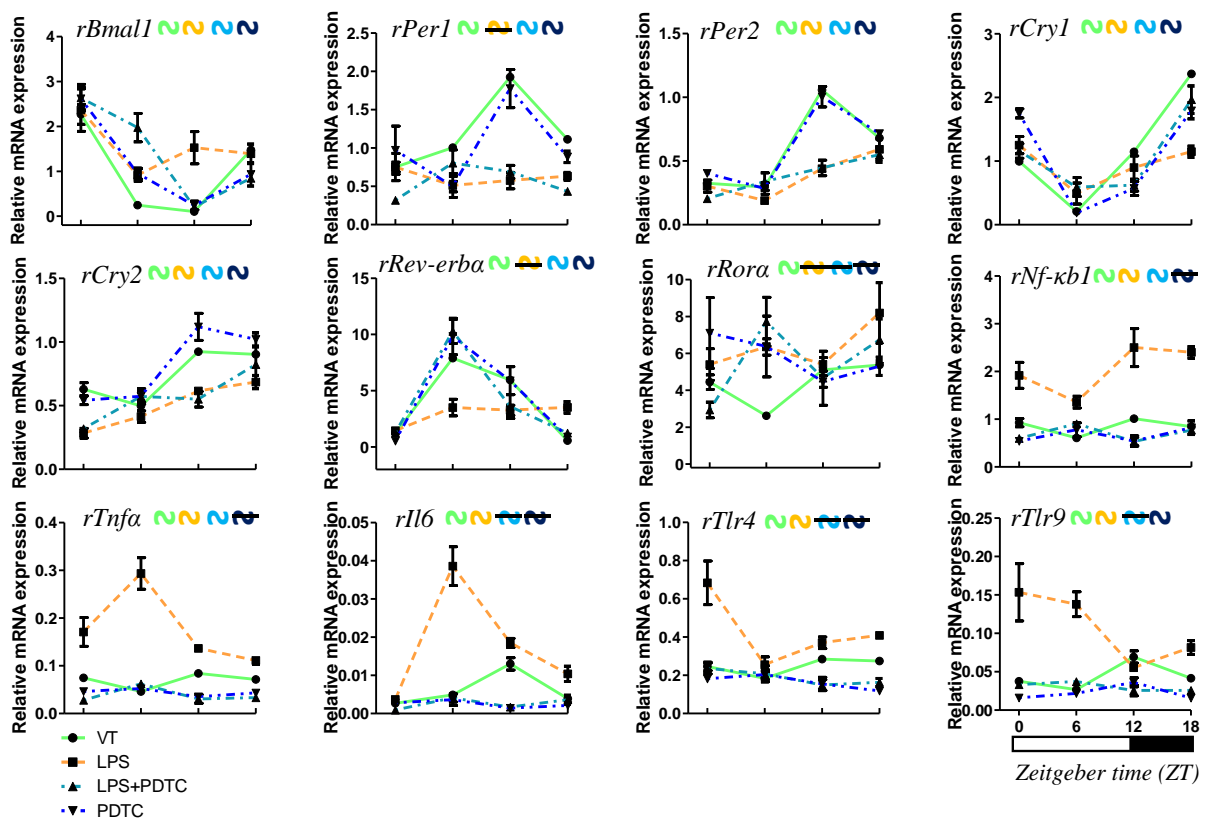


Fig. 70: Effect of PDTC (NF- κ B inhibitor) on LPS induced alterations of daily rhythms of *rBmal1*, *rPer1*, *rPer2*, *rCry1*, *rCry2*, *rRev-erba*, *rRora*, *rNf κ b1*, *rTnfa*, *rIl6*, *rTlr4*, and *rTlr9* mRNA expression in 3 m old rat kidney. Color of the rhythmic wave indicates the group: green – VT, yellow – LPS, cyan – LPS+PDTC, blue – PDTC.

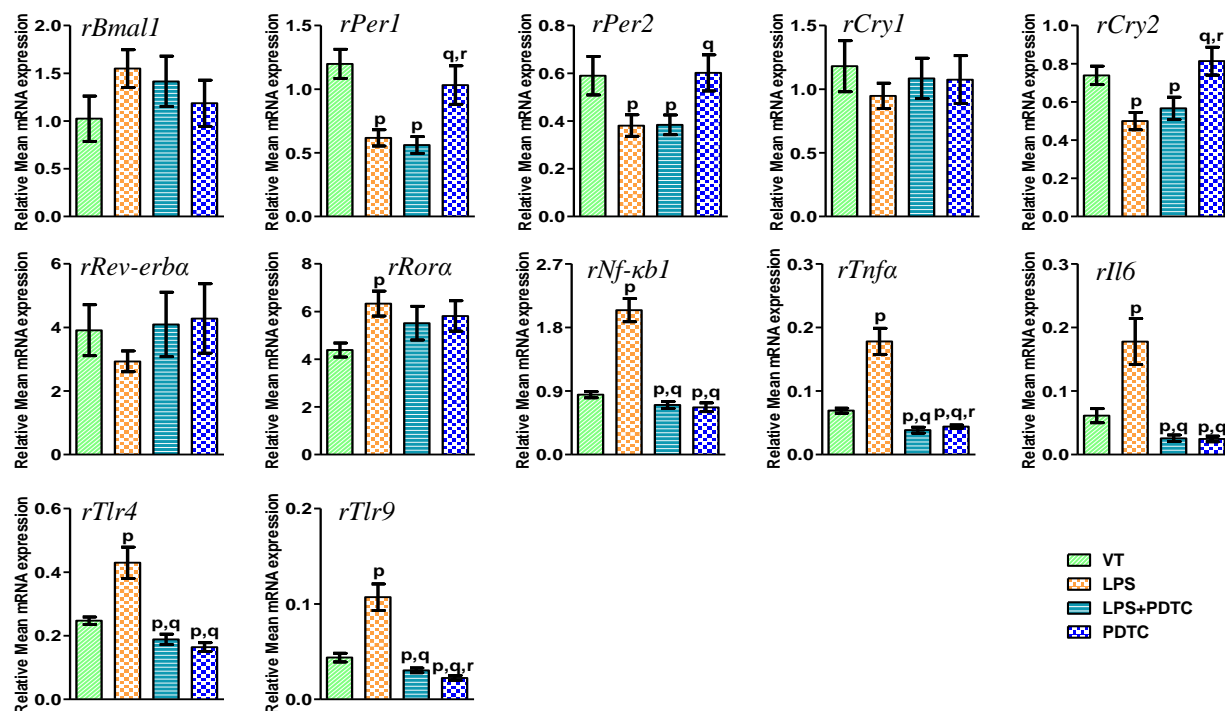


Fig. 71: Effect of PDTC (NF- κ B inhibitor) on LPS induced alterations of Mean 24 h levels of *rBmall*, *rPer1*, *rPer2*, *rCry1*, *rCry2*, *rRev-erba*, *rRora*, *rNfkb1*, *rTnfa*, *rIl6*, *rTlr4*, and *rTlr9* mRNA expression in 3 m old rat liver. Each value is mean \pm SEM (n = 4), $p \leq 0.05$ and expressed as mean relative gene expression. $p_p \leq 0.05$ (where 'p' refers to comparison with vehicle-treated group). $p_q \leq 0.05$ (where 'q' refers to comparison with LPS treated group). $p_r \leq 0.05$ (where 'r' refers to comparison with LPS+PDTC treated group).

Effect of NF- κ B inhibitor on mean 24 h levels and daily pulse of clock and immune genes in kidney

Mean 24 h levels of *rBmall*, *rCry1*, *rRev-erba* and *rRora* did not vary in LPS+PDTC and PDTC in comparison to VT. *rPer1*, *rPer2* and *rCry2* showed significant decrease in LPS+PDTC group, did not change in PDTC group in comparison to VT. With the LPS treatment, all the immune genes showed significant decrease in LPS+PDTC and PDTC groups in comparison to VT (Fig. 71). Daily pulse of *rBmall*, *rPer1*, *rPer2*, *rCry2*, *rRev-erba* and *rRora* showed no variation in LPS+PDTC and PDTC groups in comparison to VT. Daily pulse of all immune genes did not alter in LPS+PDTC and PDTC groups in comparison to VT (Fig. 72) (Table 18).

Effect of NF- κ B inhibitor on correlation between clock and immune genes in kidney

In LPS+PDTC group light phase, *rBmall* showed negative correlation with *rPer1*, *rPer2* and *rCry2*, but showed positive correlation with *rCry1* ($p < 0.001$; $p < 0.05$). *rPer1* and *rPer2*

showed positive correlation with *rCry2*, *rRev-erba* and *rRora*, but showed negative correlation with *rCry1* ($p < 0.001$; $p < 0.05$). *rCry2*, *rRev-erba* and *rRora* showed positive correlation with each other but showed negative correlation with *rCry1* ($p < 0.001$; $p < 0.01$). *rPer1* and *rPer2* showed positive correlation ($p < 0.001$) (Fig. 73).

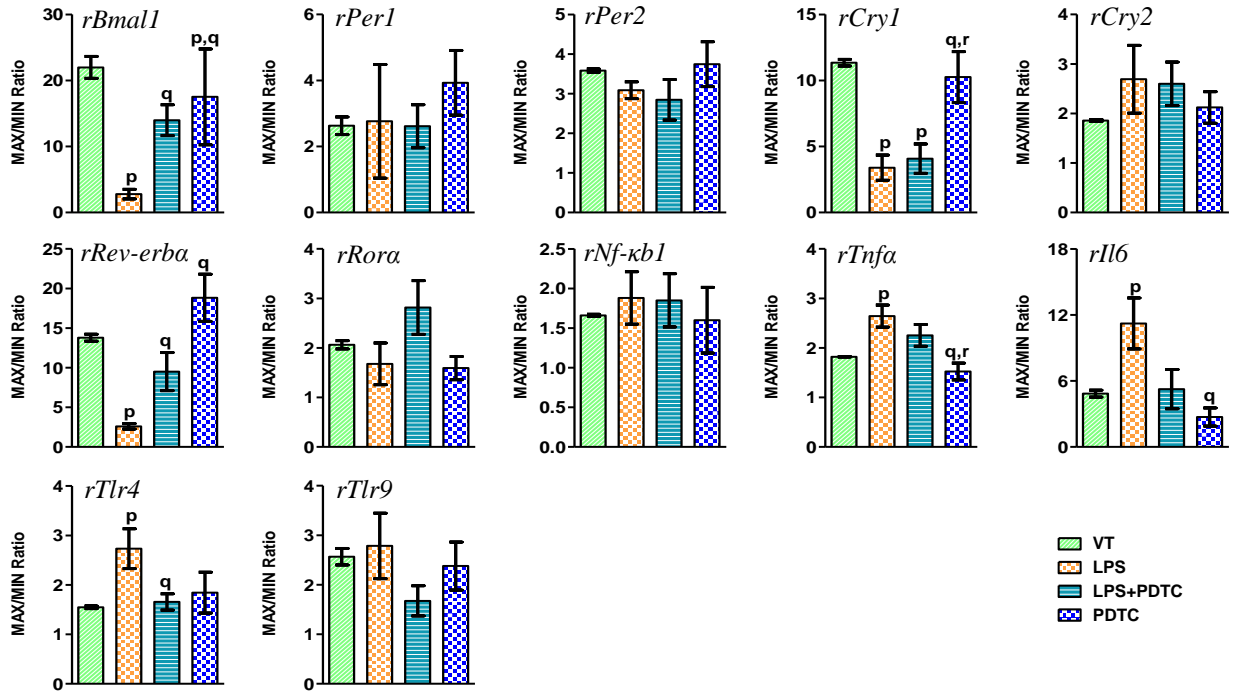


Fig. 72: Effect of PDTC (NF- κ B inhibitor) on LPS induced alterations of Daily pulse of *rBmall*, *rPer1*, *rPer2*, *rCry1*, *rCry2*, *rRev-erba*, *rRora*, *rNf-kb1*, *rTnfa*, *rIl6*, *rTlr4* and *rTlr9* mRNA expression in 3 m old rat kidney. Each value is mean \pm SEM ($n = 4$), $p \leq 0.05$ and expressed as mean relative gene expression. $p_p \leq 0.05$ (where 'p' refers to comparison with vehicle-treated group). $p_q \leq 0.05$ (where 'q' refers to comparison with LPS treated group). $p_r \leq 0.05$ (where 'r' refers to comparison with LPS+PDTC treated group).

rNf-kb1 showed positive correlation with all immune genes except *rTlr4* ($p < 0.001$; $p < 0.05$). *rTnfa* and *rIl6*; *rTlr4* and *rTlr9* ($p < 0.001$; $p < 0.01$). *rNf-kb1* and *rRev-erba*; *rNf-kb1* and *rRora*; *rTlr9* and *rBmall* showed positive correlation. *rTnfa* and *rIl6* showed positive correlation with *rPer1*, *rCry2*, *rRev-erba* and *rRora*, and negative correlation with *rCry1* ($p < 0.001$; $p < 0.01$; $p < 0.05$). *rTlr4* showed positive correlation with *rBmall* and *rCry1*, but showed negative correlation with *rPer1*, *rPer2* and *rCry2* ($p < 0.001$; $p < 0.01$). In dark phase, *rBmall* showed negative correlation with all clock genes except *rCry1*. *rPer1* and *rPer2*; *rPer1* and *rRev-erba*; *rPer2* and *rCry2*; *rPer2* and *rRora*; *rCry1* and *rCry2*; *rCry1* and *rRora*; *rCry2* and *rRora* showed positive correlation. *rCry1* and *rRev-erba* showed negative correlation ($p < 0.05$). *rNf-kb1* and *rTnfa*; *rNf-kb1* and *rIl6*; *rTnfa* and *rIl6*; *rTlr4* and *rTlr9* showed positive correlation ($p < 0.001$; $p < 0.05$). *rTnfa* and *rIl6* showed negative correlation with *rTlr4* and *rTlr9* ($p < 0.001$; $p < 0.01$). *rNf-kb1*

and *rRora*; *rNf- κ b1* and *rCry2*; *rNf- κ b1* and *rCry1*; *rTnfa* and *rRora*; *rTnfa* and *rCry2*; *rTnfa* and *rPer2*; *rIl6* and *rRora*; *rIl6* and *rCry2*; *rIl6* and *rCry1*; *rIl6* and *rPer2* showed positive correlation. *rTnfa* and *rIl6* showed negative correlation with *rBmal1* ($p < 0.001$; $p < 0.05$). *rTlr4* and *rTlr9* showed negative correlation with all clock genes except *rCry1* but showed positive correlation with *rBmal1* (Fig. 73).

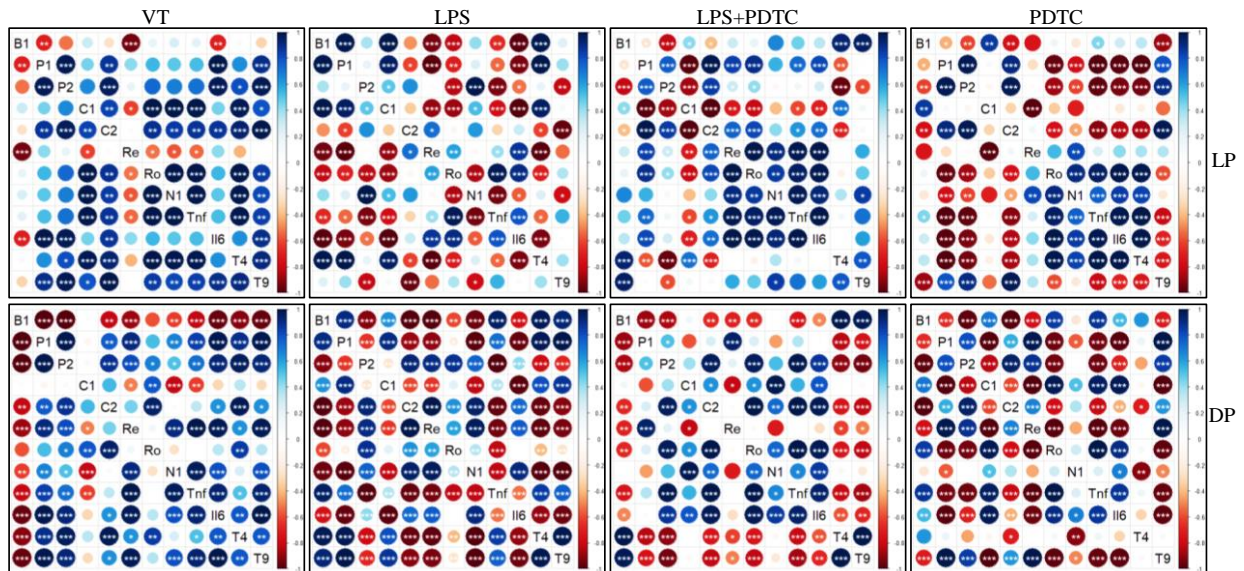


Fig. 73: Effect of PDTC (NF- κ B inhibitor) on LPS induced alterations of Pair wise correlations among clock and immune genes expression in light (ZT-0, 6, 12) phase (LP) and dark (ZT-12, 18, 24/0) phase (DP) of 3, 12 and 24 months (m) old rat kidney. Intensity of color and size of circle represents correlation coefficient values between the genes. Where, positive correlations are indicated by shades of blue, negative correlations by shades of red, and white indicates no correlation. ‘*’, ‘**’, ‘***’ indicates statistically significant correlations ($p \leq 0.05$), ($p \leq 0.01$), ($p \leq 0.001$) respectively. (B1- *rBmal1*; P1 - *rPer1*; P2 - *rPer2*; C1 - *rCry1*; C2 - *rCry2*; Re - *rRev-erba*; Ro - *rRora*; N1 - *rNf κ b1*; Tnf - *rTnfa*; Il6 - *rIl6*; T4 - *rTlr4*; T9 - *rTlr9*).

In PDTC group light phase, *rBmal1* and *rCry1*; *rPer1* and *rPer2*; *rPer1* and *rCry1*; *rPer2* and *rCry2* showed positive correlation ($p < 0.001$; $p < 0.01$). *rBmal1* and *rPer1*; *rBmal1* and *rPer2*; *rBmal1* and *rCry2*; *rCry1* and *rRev-erba*; *rCry2* and *rRora* showed negative correlation ($p < 0.001$; $p < 0.01$). All the immune genes except *rTlr9* showed positive correlation with each other ($p < 0.001$). *rTlr9* showed negative correlation with all clock genes except *rNf- κ b1* ($p < 0.001$). *rNf- κ b1*, *rTnfa*, *rIl6* and *rTlr4* showed positive correlation with *rRora*, but showed negative correlation with *rPer1*, *rPer2* and *rCry2* ($p < 0.001$; $p < 0.01$; $p < 0.05$). *rBmal1* and *rTnfa*; *rRev-erba* and *rRora* showed positive correlation ($p < 0.01$; $p < 0.05$). *rTlr9* showed negative correlation with *rBmal1* and *rRora*, but showed positive correlation with *rPer1*, *rPer2* and *rCry2*. In dark phase, *rBmal1* showed negative correlation with *rPer1*, *rPer2*, *rCry2* and *rRev-erba*, but showed positive correlation with *rCry1* and *rRora* ($p < 0.001$). *rPer1* and *rPer2* showed negative

correlation with *rCry1* and *rRora*, and positive correlation with *rCry2* and *rRev-erba*. *rCry1* and *rRora*; *rCry2* and *rRev-erba* showed positive correlation ($p < 0.001$). *rCry1* and *rCry2*; *rCry1* and *rRev-erba*; *rCry2* and *rRora*; *rRev-erba* and *rRora* showed negative correlation ($p < 0.001$). *rNf- κ b1* and *rIl6*; *rTnfa* and *rIl6* showed positive correlation, whereas *rNf- κ b1* and *rTlr4*; *rNf- κ b1* and *rTlr9*; *rTnfa* and *rTlr9*; *rIl6* and *rTlr9* showed negative correlation ($p < 0.01$; $p < 0.05$). *rTnfa* and *rIl6* showed positive correlation with *rBmal1*, *rCry1* and *rRora*, but showed negative correlation with *rPer1*, *rPer2*, *rCry2* and *rRev-erba* ($p < 0.001$; $p < 0.01$). *rNf- κ b1* and *rCry1* showed positive correlation ($p < 0.05$). *rNf- κ b1* and *rPer1*; *rTlr4* and *rCry2* showed negative correlation ($p < 0.05$). *rTlr9* showed negative correlation with *rBmal1*, *rCry1* and *rRora*, but showed positive correlation with *rPer1*, *rPer2*, *rCry2* and *rRev-erba* ($p < 0.001$) (Fig. 73).

WGCNA analysis between clock and immune genes with PDTC treatment in kidney

In LPS+PDTC group, clock and immune genes showed integrations with each other. In PDTC group, *rTnfa* and *rIl6* showed interaction with clock genes (Fig. 74).

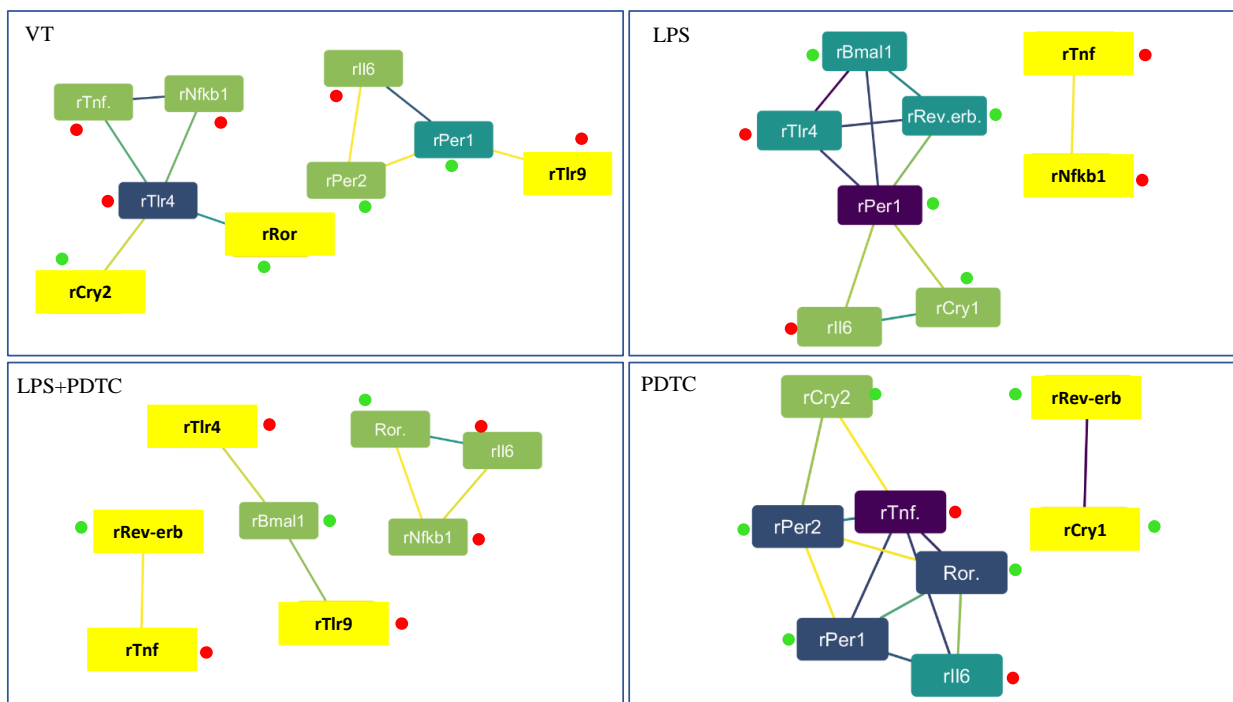


Fig. 74: WGCNA analysis between clock and immune genes clusters: effect of LPS on gene to gene network in 3 m old rat kidney and effect of PDTC (NF- κ B inhibitor) administration. Color of node indicates no. of interactions (highest—purple; intermediate—blue and least—yellow). Color of edge indicates the strength of interaction (strongest—purple; intermediate—blue and weakest—yellow). Green and red dots indicate clock and immune genes respectively.

Table 18: Effect of NF- κ B inhibitor on LPS induced alterations of clock and immune genes

<i>Gene</i>		ZT-0	ZT-6	ZT-12	ZT-18	Mean 24 h levels	Max/min ratio
<i>rBmal1</i>	VT	1.6 ± 0.16	0.17 ± 0.01	0.07 ± 0.01	1.05 ± 0.04	0.72 ± 0.17	21.98 ± 1.66
	LPS	2.36 ± 0.47	0.92 ± 0.13	1.53 ± 0.36	1.39 ± 0.22	1.55 ± 0.2	2.78 ± 0.72 _x
	LPS+PDTC	2.64 ± 0.3	2.75 ± 0.41	0.21 ± 0.03	0.84 ± 0.05	1.61 ± 0.31	13.99 ± 2.33 _y
	PDTC	2.62 ± 0.25	0.95 ± 0.12	0.24 ± 0.1	0.93 ± 0.26	1.19 ± 0.24	17.52 ± 7.26 _{x,y}
<i>rPer1</i>	VT	0.75 ± 0.06	1 ± 0.01	1.93 ± 0.03	1.11 ± 0.02	1.2 ± 0.11	2.63 ± 0.27
	LPS	0.75 ± 0.18	0.51 ± 0.16	0.58 ± 0.11	0.63 ± 0.05	0.62 ± 0.06 _x	2.76 ± 1.72
	LPS+PDTC	0.32 ± 0.03	0.8 ± 0.17	0.69 ± 0.09	0.44 ± 0.03	0.56 ± 0.07 _x	2.61 ± 0.65
	PDTC	0.97 ± 0.31	0.5 ± 0.07	1.78 ± 0.25	0.88 ± 0.07	1.03 ± 0.15 _{y,z}	3.93 ± 0.98
<i>rPer2</i>	VT	0.33 ± 0.03	0.3 ± 0	1.06 ± 0.01	0.68 ± 0.02	0.59 ± 0.08	3.58 ± 0.04
	LPS	0.74 ± 0.02	0.41 ± 0.03	0.94 ± 0.06	1.27 ± 0.17	0.84 ± 0.09 _x	3.09 ± 0.21
	LPS+PDTC	0.5 ± 0.07	0.96 ± 0.14	1.1 ± 0.15	1.35 ± 0.14	0.98 ± 0.1 _x	2.85 ± 0.51
	PDTC	0.86 ± 0.06	0.75 ± 0.16	2.15 ± 0.17	1.94 ± 0.44	1.43 ± 0.2 _y	3.37 ± 0.8
<i>rCry1</i>	VT	1 ± 0.05	0.21 ± 0	1.15 ± 0.03	2.37 ± 0.03	1.18 ± 0.2	11.35 ± 0.24
	LPS	1.25 ± 0.13	0.49 ± 0.17	0.9 ± 0.18	1.15 ± 0.09	0.95 ± 0.1	3.4 ± 0.95 _x
	LPS+PDTC	1.16 ± 0.11	0.59 ± 0.15	0.62 ± 0.09	1.97 ± 0.22	1.08 ± 0.16	4.08 ± 1.11 _x
	PDTC	1.75 ± 0.07	0.19 ± 0.02	0.57 ± 0.11	1.79 ± 0.13	1.07 ± 0.19	10.25 ± 1.92 _{y,z}
<i>rCry2</i>	VT	0.55 ± 0.04	0.43 ± 0.01	0.8 ± 0.01	0.79 ± 0.01	0.64 ± 0.04	1.86 ± 0.02
	LPS	0.28 ± 0.04	0.41 ± 0.05	0.62 ± 0.02	0.69 ± 0.05	0.5 ± 0.05 _x	2.69 ± 0.68
	LPS+PDTC	0.34 ± 0.01	0.61 ± 0.07	0.59 ± 0.07	0.88 ± 0.15	0.61 ± 0.06 _x	2.6 ± 0.44
	PDTC	0.54 ± 0.03	0.57 ± 0.04	1.12 ± 0.11	1.02 ± 0.05	0.81 ± 0.07 _{y,z}	2.12 ± 0.32
<i>rRev-erba</i>	VT	0.5 ± 0.04	3.21 ± 0.03	2.42 ± 0.04	0.23 ± 0.01	1.59 ± 0.33	13.79 ± 0.43
	LPS	1.44 ± 0.31	3.5 ± 0.74	3.26 ± 0.46	3.52 ± 0.52	2.93 ± 0.33	2.6 ± 0.35 _x
	LPS+PDTC	1.27 ± 0.28	10.27 ± 1.07	3.6 ± 1.06	1.24 ± 0.26	4.09 ± 1.01	9.51 ± 2.41 _y
	PDTC	0.52 ± 0.04	9.82 ± 1.62	5.89 ± 1.24	0.89 ± 0.12	4.28 ± 1.09	18.83 ± 2.98 _y
<i>rRora</i>	VT	3.87 ± 0.34	2.28 ± 0.1	4.45 ± 0.05	4.67 ± 0.07	3.82 ± 0.26	2.06 ± 0.08
	LPS	5.4 ± 0.86	6.35 ± 0.44	5.4 ± 0.37	8.19 ± 1.64	6.33 ± 0.52 _x	1.68 ± 0.42
	LPS+PDTC	2.93 ± 0.42	7.72 ± 1.32	4.65 ± 1.46	6.74 ± 1.13	5.51 ± 0.71	2.82 ± 0.54
	PDTC	5.53 ± 0.63	7.2 ± 1.31	4.47 ± 0.31	5.3 ± 0.49	5.63 ± 0.43	1.59 ± 0.24
<i>rNf-κb1</i>	VT	0.93 ± 0.08	0.61 ± 0.01	1.01 ± 0.01	0.84 ± 0.01	0.85 ± 0.04	1.66 ± 0.01
	LPS	1.92 ± 0.27	1.36 ± 0.12	2.5 ± 0.4	2.4 ± 0.12	2.04 ± 0.16 _x	1.88 ± 0.33
	LPS+PDTC	0.6 ± 0.02	0.9 ± 0.07	0.53 ± 0.09	0.77 ± 0.08	0.7 ± 0.05 _{x,y}	1.85 ± 0.34
	PDTC	0.54 ± 0.04	0.78 ± 0.15	0.54 ± 0.11	0.82 ± 0.14	0.67 ± 0.06 _{x,y}	1.6 ± 0.41
<i>rTnfa</i>	VT	0.07 ± 0	0.05 ± 0	0.08 ± 0	0.07 ± 0	0.07 ± 0	1.82 ± 0.01
	LPS	0.17 ± 0.03	0.29 ± 0.03	0.14 ± 0	0.11 ± 0.01	0.18 ± 0.02 _x	2.64 ± 0.22 _x
	LPS+PDTC	0.06 ± 0	0.12 ± 0.01	0.06 ± 0.02	0.07 ± 0.01	0.08 ± 0.01 _{x,y}	2.25 ± 0.22
	PDTC	0.05 ± 0.01	0.05 ± 0	0.03 ± 0	0.04 ± 0.01	0.04 ± 0 _{x,y}	1.52 ± 0.17 _{y,z}
<i>rIl6</i>	VT	0.03 ± 0	0.05 ± 0	0.13 ± 0.02	0.04 ± 0.01	0.06 ± 0.01	4.85 ± 0.31
	LPS	0.04 ± 0.01	0.39 ± 0.05	0.19 ± 0.01	0.1 ± 0.02	0.18 ± 0.04 _x	11.22 ± 2.32 _x
	LPS+PDTC	0.03 ± 0	0.17 ± 0.03	0.06 ± 0.01	0.15 ± 0.03	0.1 ± 0.02 _{x,y}	5.57 ± 1.56
	PDTC	0.05 ± 0.01	0.07 ± 0.01	0.03 ± 0.01	0.06 ± 0	0.05 ± 0.01 _{x,y,z}	2.52 ± 0.61 _y
<i>rTlr4</i>	VT	0.25 ± 0.02	0.18 ± 0	0.28 ± 0.01	0.27 ± 0.01	0.25 ± 0.01	1.55 ± 0.03
	LPS	0.68 ± 0.11	0.26 ± 0.04	0.37 ± 0.03	0.41 ± 0.02	0.43 ± 0.05 _x	2.73 ± 0.4 _x
	LPS+PDTC	0.36 ± 0.04	0.31 ± 0.06	0.23 ± 0.04	0.25 ± 0.03	0.29 ± 0.03 _{x,y}	1.66 ± 0.16 _y
	PDTC	0.29 ± 0.03	0.33 ± 0.04	0.25 ± 0.06	0.19 ± 0.02	0.27 ± 0.02 _{x,y}	1.84 ± 0.41
<i>rTlr9</i>	VT	0.04 ± 0	0.03 ± 0	0.07 ± 0.01	0.04 ± 0	0.04 ± 0	2.57 ± 0.17
	LPS	0.15 ± 0.04	0.14 ± 0.02	0.06 ± 0	0.08 ± 0.01	0.11 ± 0.01	2.78 ± 0.66
	LPS+PDTC	0.03 ± 0	0.04 ± 0	0.03 ± 0.01	0.03 ± 0	0.03 ± 0 _{x,y}	1.67 ± 0.3
	PDTC	0.02 ± 0	0.02 ± 0	0.04 ± 0.01	0.02 ± 0	0.02 ± 0 _{x,y}	2.38 ± 0.48

mRNA expression of clock and immune genes at ZT-0, 6, 12 and 18. $p_x \leq 0.05$, $p_y \leq 0.05$, $p_z \leq 0.05$ where, 'x' refers to significant difference with vehicle group, 'y' refers to significant difference with LPS group, 'z' refers to significant difference with LPS+PDTC group.

III. B (iv). Role of NF- κ B inhibitor on the LPS induced alterations of clock and immune genes mRNA expression in spleen

Effect of NF- κ B inhibitor on the daily rhythms of clock and immune genes in spleen

rBmal1, *rPer1* and *rRev-erba* showed no variation in phase in LPS+PDTC and PDTC group in comparison to VT. *rPer2* phase delay of 6 h in LPS+PDTC, but did not alter in PDTC in comparison to VT. *rCry1* showed 12 h phase delay in LPS+PDTC, but did not vary in PDTC in comparison to VT. *rCry2* showed no phase variation in LPS+PDTC, but showed 6 h phase delay in PDTC in comparison to VT. *rRora* did not show rhythmicity in LPS+PDTC group, however, *rRora* showed rhythmicity in PDTC group with maximum expression at ZT-0 and minimum at ZT-6. Interestingly, LPS+PDTC administration abolished rhythmicity of all the immune genes studied. *rNf- κ b1*, *rTlr4* and *rTlr9* showed similar pattern of expression in PDTC in comparison to VT group. *rTnfa* and *rIl6* showed 12 h phase advance with PDTC treatment in comparison to VT group (Fig. 75) (Table 19).

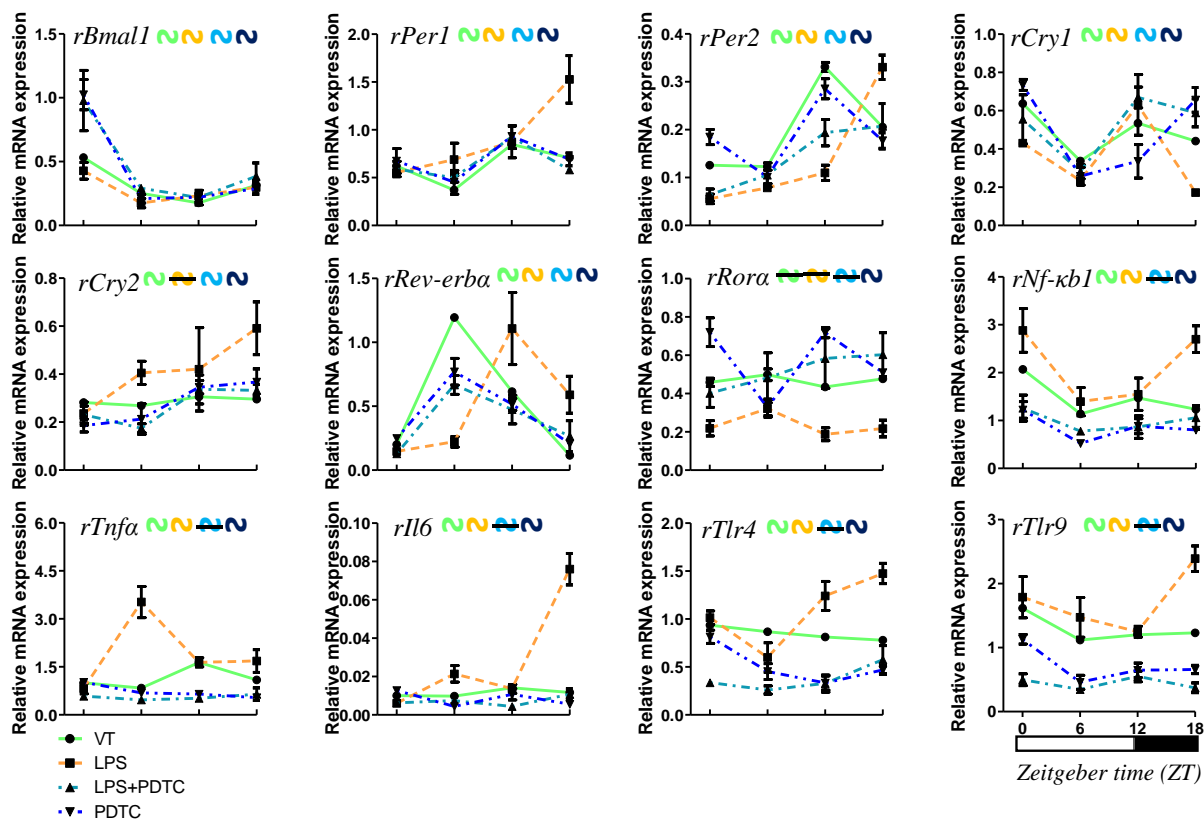


Fig. 75: Effect of PDTC (NF- κ B inhibitor) on LPS induced alterations of daily rhythms of clock and immune genes mRNA expression in 3 m old rat spleen. Color of the rhythmic wave indicates the group: black – VT, yellow – LPS, cyan – LPS+PDTC, blue – PDTC.

Effect of NF- κ B inhibitor on mean 24 h levels and daily pulse of clock and immune genes in spleen

Mean 24 h levels of all clock genes did not alter in LPS+PDTC and PDTC group in comparison to VT group. In LPS+PDTC and PDTC groups all the immune genes showed significantly decreased expression in comparison to VT group (Fig. 76). Daily pulse of *rBmall* and *rRora* did not alter in LPS+PDTC, but increased in PDTC in comparison to VT group. Daily pulse of *rPer1* and *rPer2* did not vary in LPS+PDTC and PDTC groups in comparison to VT group. Daily pulse of *rCry1* and *rCry2* showed significant increase in LPS+PDTC group, but did not alter in PDTC group in comparison to VT group. *rRev-erba* showed decreased daily pulse in LPS+PDTC and PDTC groups in comparison to VT group. Daily pulse of all immune genes did not alter in LPS+PDTC and PDTC groups in comparison to VT group (Fig. 77) (Table 19).

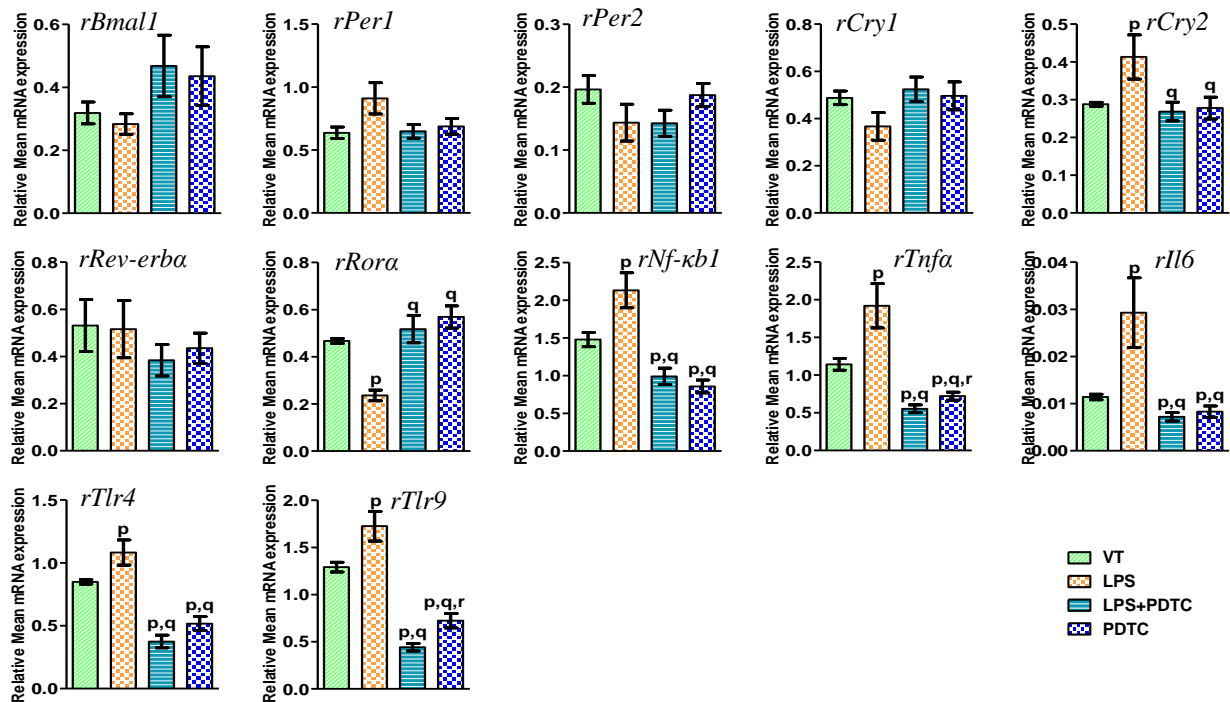


Fig. 76: Effect of PDTC (NF- κ B inhibitor) on LPS induced alterations of Mean 24 h levels of clock and immune genes mRNA expression in 3 m old rat spleen. Each value is mean \pm SEM ($n = 4$), $p \leq 0.05$ and expressed as mean relative gene expression. $p_p \leq 0.05$ (where ‘p’ refers to comparison with vehicle-treated group). $p_q \leq 0.05$ (where ‘q’ refers to comparison with LPS treated group). $p_r \leq 0.05$ (where ‘r’ refers to comparison with LPS+PDTC treated group).

Effect of NF- κ B inhibitor on correlation between clock and immune genes in spleen

In LPS+PDTC group light phase, *rBmall* showed negative correlation with *rPer2*, *rRev-erba* and *rRora* ($p < 0.001$). *rPer1* showed positive correlation with *rPer2*, *rCry1*, *rCry2* and *rRora*; *rRev-*

erba and *rRora* ($p < 0.001$; $p < 0.01$). *rNf- κ b1* and *rTnfa*; *rNf- κ b1* and *rTlr4*; *rTnfa* and *rTlr4*; *rTnfa* and *rTlr9*; *rTlr4* and *rTlr9* showed positive correlation ($p < 0.001$; $p < 0.01$; $p < 0.05$). *rIl6* and *rTlr4*; *rIl6* and *rTlr9* showed negative correlation ($p < 0.001$; $p < 0.05$). *rNf- κ b1* and *rTnfa* showed positive correlation with *rBmall*, but showed negative correlation with *rRev-erba* and *rRora* ($p < 0.001$; $p < 0.01$; $p < 0.05$). *rNf- κ b1* and *rPer2*; *rTlr4* and *rRev-erba* showed negative correlation ($p < 0.001$; $p < 0.05$). *rIl6* showed negative correlation with *rPer1*, *rPer2*, *rCry1*, *rCry2* and *rRora* ($p < 0.001$; $p < 0.01$; $p < 0.05$). *rTlr4* and *rTlr9* showed positive correlation with *rPer1*, *rCry1* and *rCry2* ($p < 0.001$; $p < 0.05$). In dark phase, *rBmall* showed negative correlation with all other clock genes, while the other clock genes showed positive correlation with each other ($p < 0.001$; $p < 0.01$). *rNf- κ b1* and *rTnfa*; *rTnfa* and *rIl6*; *rTnfa* and *rTlr4*; *rIl6* and *rTlr4* showed positive correlation ($p < 0.001$; $p < 0.01$; $p < 0.05$). *rTlr9* showed negative correlation with other immune genes except *rNf- κ b1* ($p < 0.001$). *rNf- κ b1* showed negative correlation with all clock genes except *rBmall* ($p < 0.001$). *rTnfa* showed negative correlation with ($p < 0.01$; $p < 0.05$) (Fig. 78).

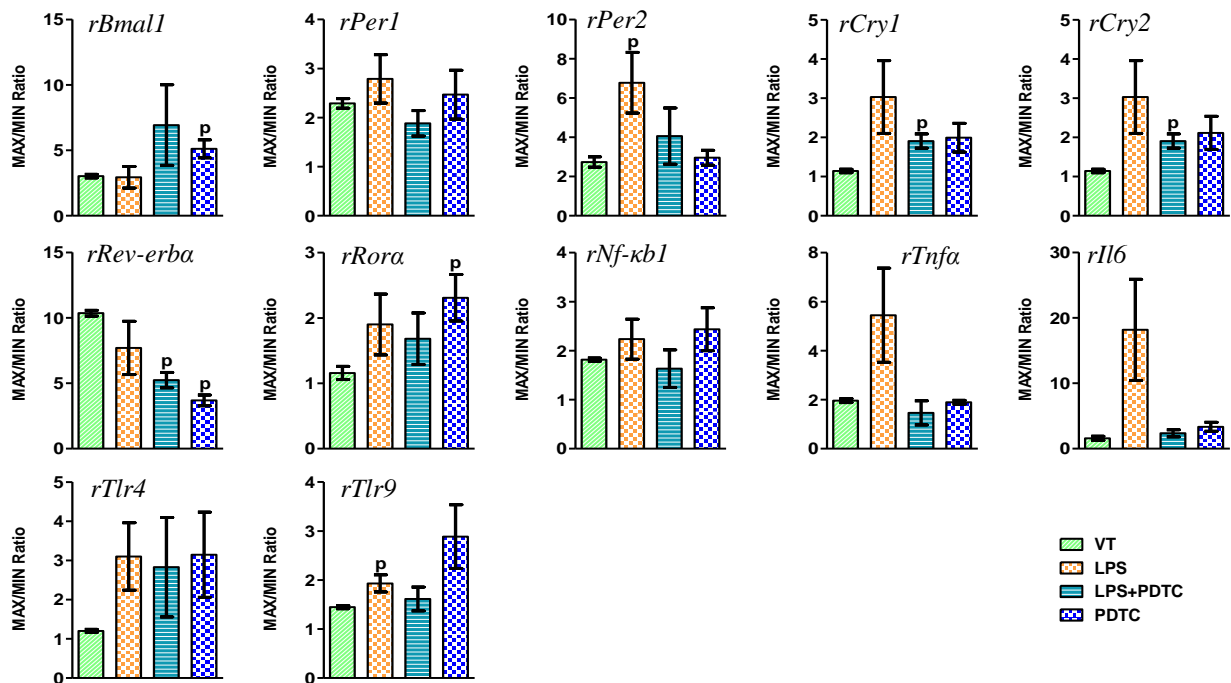


Fig. 77: Effect of PDTC (NF- κ B inhibitor) on LPS induced alterations of Daily pulse of clock and immune genes mRNA expression in 3 m old rat kidney. Each value is mean \pm SEM ($n = 4$), $p \leq 0.05$ and expressed as mean relative gene expression. $p_p \leq 0.05$ (where 'p' refers to comparison with vehicle-treated group). $p_q \leq 0.05$ (where 'q' refers to comparison with LPS treated group). $p_r \leq 0.05$ (where 'r' refers to comparison with LPS+PDTC treated group).

In PDTC group light phase, *rBmall* and *rCry1*; *rPer1* and *rPer2*; *rPer1* and *rCry2*; *rPer2* and *rCry2*; *rCry2* and *rRev-erba* showed positive correlation ($p < 0.001$). *rBmall* and *rCry2*; *rBmall* and *rRev-erba*; *rCry1* and *rCry2*; *rCry1* and *rRev-erba* showed negative correlation ($p < 0.001$). All the immune genes showed positive correlation with each other ($p < 0.001$; $p < 0.01$; $p < 0.05$). All the immune genes showed positive correlation with *rBmall*, *rCry1*, and showed negative correlation with *rRev-erba* ($p < 0.001$; $p < 0.01$; $p < 0.05$). *rNf- κ b1* and *rRora*; *rIl6* and *rRora* showed positive correlation, while *rTnfa* and *rCry2*; *rTlr4* and *rCry2*; *rTlr9* and *rCry2* showed negative correlation ($p < 0.001$; $p < 0.05$) (Fig. 78).

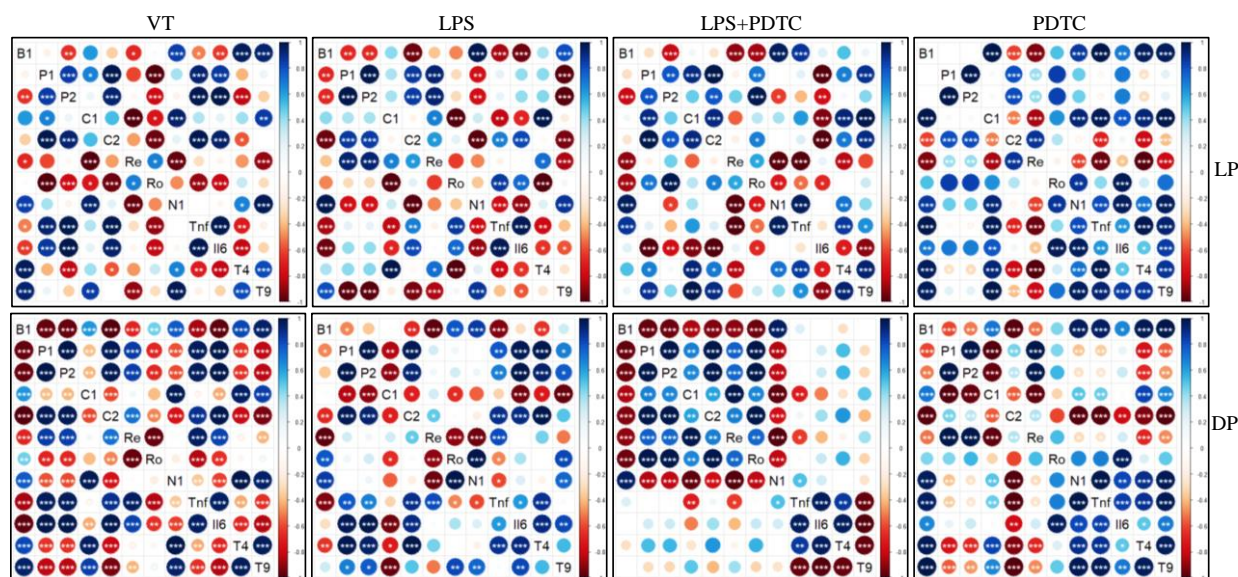


Fig. 78: Effect of PDTC (NF- κ B inhibitor) on LPS induced alterations of Pair wise correlations among clock and immune genes in light (ZT-0, 6, 12) phase (LP) and dark (ZT-12, 18, 24/0) phase (DP) of 3, 12 and 24 months (m) old rat spleen. Intensity of color and size of circle represents correlation coefficient values between the genes. Where, positive correlations are indicated by shades of blue, negative correlations by shades of red, and white indicates no correlation. ‘*’, ‘**’, ‘***’ indicates statistically significant correlations ($p \leq 0.05$), ($p \leq 0.01$), ($p \leq 0.001$) respectively. (B1- *rBmall*; P1 - *rPer1*; P2 - *rPer2*; C1 - *rCry1*; C2 - *rCry2*; Re - *rRev-erba*; Ro - *rRora*; N1 - *rNf κ b1*; Tnf - *rTnfa*; Il6 - *rIl6*; T4 - *rTlr4*; T9 - *rTlr9*).

In dark phase, *rBmall* showed negative correlation with all clock genes except *rCry1* and *rRora* ($p < 0.001$; $p < 0.01$). *rPer1* and *rPer2* showed positive correlation ($p < 0.001$). *rPer1* and *rPer2* showed positive correlation with *rCry2* and *rRev-erba*, but showed negative correlation with *rCry1* ($p < 0.001$; $p < 0.01$). *rCry1* and *rCry2*; *rCry1* and *rRev-erba* showed negative correlation ($p < 0.001$). *rBmall* and *rCry1*; *rCry2* and *rRev-erba* showed positive correlation ($p < 0.001$; $p < 0.01$). All the immune genes showed positive correlation with each other ($p < 0.001$; $p < 0.01$; $p < 0.05$). *rNf- κ b1*, *rTnfa*, *rTlr4* and *rTlr9* showed positive correlation with *rBmall* and *rCry1*, but

showed negative correlation with *rPer1*, *rPer2*, *rCry2* and *rRev-erba* ($p < 0.001$; $p < 0.01$; $p < 0.05$). *rIl6* showed positive correlation with *rBmal1* and *rRora*, but showed negative correlation with *rCry2* ($p < 0.001$; $p < 0.01$; $p < 0.05$) (Fig. 78).

WGCNA analysis between clock and immune genes with PDTC treatment in spleen

In LPS+PDTC group, the interaction between clock and immune genes reduced, only *rRev-erba* showed interaction with *rNf- κ b1*. In PDTC group, *rBmal1* showed interaction with *rTnfa*, *rTlr4* and *rTlr9* (Fig. 79).

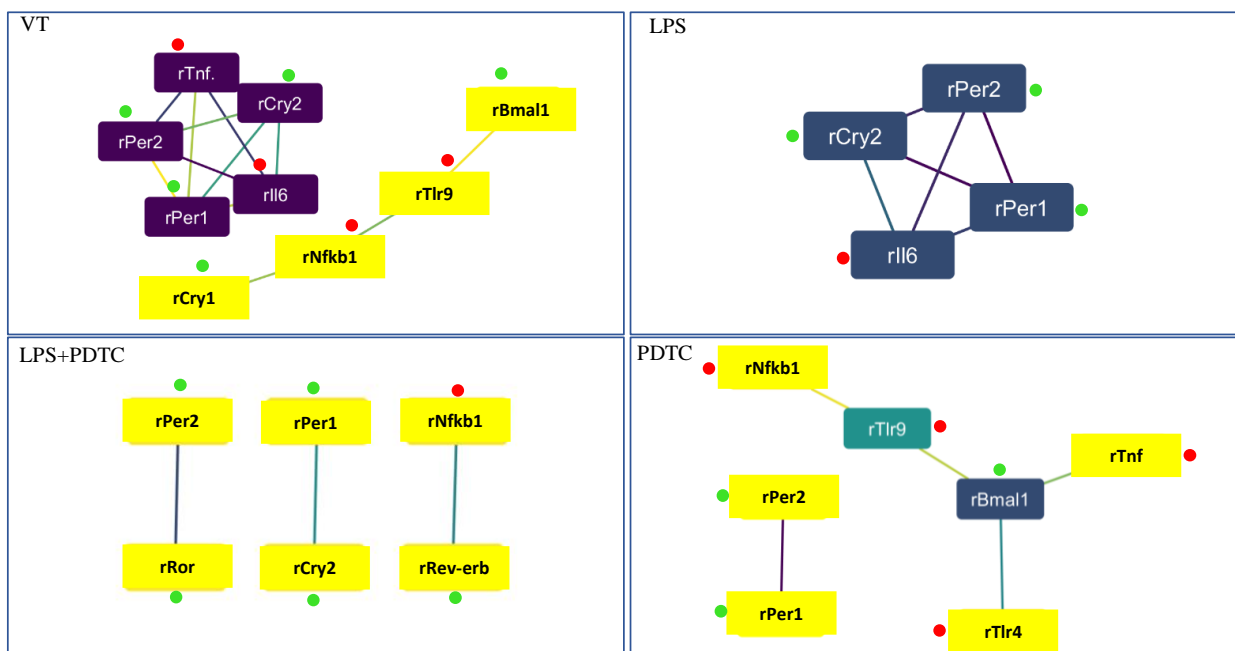


Fig. 79: WGCNA analysis between clock and immune genes clusters: effect of LPS on gene to gene network in 3 m old rat spleen and effect of PDTC (NF- κ B inhibitor) administration. Color of node indicates no. of interactions (highest—purple; intermediate—blue and least—yellow). Color of edge indicates the strength of interaction (strongest—purple; intermediate—blue and weakest—yellow). Green and red dots indicate clock and immune genes respectively.

Table 19:Effect of NF- κ B inhibitor on LPS induced alterations of clock and immune genes

<i>Gene</i>		ZT-0	ZT-6	ZT-12	ZT-18	Mean 24 h levels	Max/min ratio
<i>rBmall</i>	VT	0.53 ± 0.01	0.25 ± 0.02	0.18 ± 0.01	0.31 ± 0.01	0.32 ± 0.03	3.03 ± 0.14
	LPS	0.43 ± 0.07	0.18 ± 0.04	0.23 ± 0.03	0.3 ± 0.05	0.28 ± 0.03	2.94 ± 0.82
	LPS+PDTC	0.98 ± 0.24	0.29 ± 0.02	0.22 ± 0.06	0.38 ± 0.11	0.47 ± 0.1	6.93 ± 3.08
	PDTC	1.02 ± 0.12	0.21 ± 0.03	0.22 ± 0.02	0.29 ± 0.04	0.44 ± 0.09	5.11 ± 0.69 _x
<i>rPer1</i>	VT	0.62 ± 0.01	0.37 ± 0	0.85 ± 0.03	0.71 ± 0.02	0.64 ± 0.05	2.29 ± 0.1
	LPS	0.55 ± 0.04	0.69 ± 0.17	0.87 ± 0.17	1.53 ± 0.25	0.91 ± 0.12	2.79 ± 0.49
	LPS+PDTC	0.51 ± 0.07	0.43 ± 0.04	0.8 ± 0.1	0.51 ± 0.02	0.56 ± 0.05	1.88 ± 0.26
	PDTC	1.17 ± 0.23	0.79 ± 0.22	1.62 ± 0.06	1.2 ± 0.12	1.2 ± 0.11	2.47 ± 0.5
<i>rPer2</i>	VT	0.13 ± 0	0.12 ± 0.01	0.33 ± 0.01	0.21 ± 0	0.2 ± 0.02	2.74 ± 0.26
	LPS	0.06 ± 0.01	0.08 ± 0.01	0.11 ± 0.02	0.33 ± 0.03	0.14 ± 0.03	6.77 ± 1.55 _x
	LPS+PDTC	0.05 ± 0.01	0.07 ± 0.02	0.14 ± 0.02	0.15 ± 0.03	0.1 ± 0.01	4.06 ± 1.43
	PDTC	0.13 ± 0.01	0.07 ± 0.01	0.2 ± 0.01	0.13 ± 0.01	0.13 ± 0.01	2.96 ± 0.38
<i>rCry1</i>	VT	0.64 ± 0.01	0.34 ± 0	0.53 ± 0.01	0.44 ± 0.01	0.49 ± 0.03	1.89 ± 0.05
	LPS	0.43 ± 0.02	0.23 ± 0.02	0.63 ± 0.16	0.17 ± 0.02	0.37 ± 0.06	3.5 ± 0.56
	LPS+PDTC	0.64 ± 0.15	0.32 ± 0.04	0.77 ± 0.06	0.68 ± 0.08	0.6 ± 0.06	2.54 ± 0.5 _x
	PDTC	0.84 ± 0.03	0.3 ± 0.05	0.38 ± 0.1	0.75 ± 0.07	0.57 ± 0.07	3.08 ± 0.44
<i>rCry2</i>	VT	0.28 ± 0.01	0.27 ± 0.01	0.31 ± 0.01	0.3 ± 0	0.29 ± 0.01	1.14 ± 0.04
	LPS	0.24 ± 0.05	0.41 ± 0.05	0.42 ± 0.17	0.59 ± 0.11	0.41 ± 0.06 _x	3.03 ± 0.93
	LPS+PDTC	0.23 ± 0.04	0.17 ± 0.02	0.34 ± 0.06	0.36 ± 0.02	0.28 ± 0.03 _y	2.14 ± 0.25 _x
	PDTC	0.37 ± 0.05	0.32 ± 0.03	0.69 ± 0.06	0.51 ± 0.06	0.47 ± 0.04 _y	2.19 ± 0.29
<i>rRev-erba</i>	VT	0.2 ± 0.01	1.19 ± 0.01	0.61 ± 0.01	0.12 ± 0	0.53 ± 0.11	10.36 ± 0.22
	LPS	0.07 ± 0	0.11 ± 0.02	0.55 ± 0.14	0.29 ± 0.07	0.26 ± 0.06	7.7 ± 2.04
	LPS+PDTC	0.06 ± 0	0.33 ± 0.04	0.24 ± 0.06	0.13 ± 0.06	0.19 ± 0.03	5.24 ± 0.58 _x
	PDTC	0.12 ± 0.01	0.38 ± 0.05	0.54 ± 0.1	0.1 ± 0	0.29 ± 0.05	5.17 ± 0.9 _x
<i>rRora</i>	VT	0.46 ± 0.02	0.5 ± 0.03	0.43 ± 0.01	0.48 ± 0.01	0.47 ± 0.01	1.16 ± 0.1
	LPS	0.22 ± 0.04	0.32 ± 0.04	0.19 ± 0.03	0.22 ± 0.04	0.24 ± 0.02 _x	1.9 ± 0.47
	LPS+PDTC	0.4 ± 0.07	0.48 ± 0.13	0.58 ± 0.15	0.6 ± 0.11	0.52 ± 0.06 _y	1.68 ± 0.39
	PDTC	0.72 ± 0.08	0.33 ± 0.04	0.72 ± 0.03	0.51 ± 0.02	0.57 ± 0.05 _y	2.31 ± 0.36 _x
<i>rNf-κb1</i>	VT	2.07 ± 0.03	1.14 ± 0.01	1.47 ± 0.05	1.23 ± 0.02	1.48 ± 0.09	1.82 ± 0.03
	LPS	2.88 ± 0.46	1.39 ± 0.29	1.55 ± 0.34	2.7 ± 0.28	2.13 ± 0.23 _x	2.24 ± 0.41
	LPS+PDTC	1.26 ± 0.27	0.78 ± 0.03	0.86 ± 0.24	1.06 ± 0.25	0.99 ± 0.11 _{x,y}	1.63 ± 0.38
	PDTC	1.98 ± 0.28	0.85 ± 0.11	1.43 ± 0.25	1.3 ± 0.08	1.39 ± 0.14 _{x,y}	2.44 ± 0.44
<i>rTnfa</i>	VT	1 ± 0.02	0.84 ± 0.01	1.64 ± 0.04	1.09 ± 0.02	1.14 ± 0.08	1.96 ± 0.08
	LPS	0.82 ± 0.17	3.53 ± 0.49	1.64 ± 0.14	1.68 ± 0.36	1.92 ± 0.29 _x	5.45 ± 1.92
	LPS+PDTC	0.58 ± 0.06	0.47 ± 0.05	0.52 ± 0.06	0.64 ± 0.2	0.55 ± 0.05 _{x,y}	1.46 ± 0.49
	PDTC	1.02 ± 0.03	0.68 ± 0.09	0.65 ± 0.06	0.54 ± 0.02	0.72 ± 0.05 _{x,y,z}	1.9 ± 0.08
<i>rIl6</i>	VT	0.01 ± 0	0.01 ± 0	0.01 ± 0	0.01 ± 0	0.01 ± 0	1.58 ± 0.32
	LPS	0.01 ± 0	0.02 ± 0	0.01 ± 0	0.08 ± 0.01	0.03 ± 0.01 _x	18.16 ± 7.73
	LPS+PDTC	0.01 ± 0	0.01 ± 0	0 ± 0	0.01 ± 0	0.01 ± 0 _{x,y}	2.35 ± 0.55
	PDTC	0.01 ± 0	0 ± 0	0.01 ± 0	0.01 ± 0	0.01 ± 0 _{x,y}	3.34 ± 0.69
<i>rTlr4</i>	VT	0.94 ± 0.02	0.87 ± 0.01	0.81 ± 0.02	0.78 ± 0.01	0.85 ± 0.02	1.2 ± 0.04
	LPS	1.01 ± 0.07	0.6 ± 0.15	1.24 ± 0.15	1.47 ± 0.11	1.08 ± 0.1 _x	3.1 ± 0.86
	LPS+PDTC	0.34 ± 0.03	0.26 ± 0.04	0.33 ± 0.09	0.58 ± 0.15	0.37 ± 0.05 _{x,y}	2.83 ± 1.27
	PDTC	0.81 ± 0.07	0.45 ± 0.08	0.33 ± 0.07	0.47 ± 0.04	0.52 ± 0.06 _{x,y}	3.15 ± 1.09
<i>rTlr9</i>	VT	1.62 ± 0.04	1.12 ± 0.01	1.2 ± 0.04	1.23 ± 0.02	1.29 ± 0.05	1.45 ± 0.03
	LPS	1.79 ± 0.32	1.47 ± 0.31	1.25 ± 0.08	2.39 ± 0.2	1.73 ± 0.16 _x	1.93 ± 0.17 _x
	LPS+PDTC	0.5 ± 0.09	0.35 ± 0.04	0.55 ± 0.08	0.37 ± 0.08	0.44 ± 0.04 _{x,y}	1.61 ± 0.24
	PDTC	1.13 ± 0.07	0.46 ± 0.11	0.65 ± 0.11	0.66 ± 0.06	0.72 ± 0.08 _{x,y,z}	2.89 ± 0.65

mRNA expression of clock and immune genes at ZT-0, 6, 12 and 18. $p_x \leq 0.05$, $p_y \leq 0.05$, $p_z \leq 0.05$ where, 'x' refers to significant difference with vehicle group, 'y' refers to significant difference with LPS group, 'z' refers to significant difference with LPS+PDTC group.

Chapter IV Discussion

I. A. Age induced alterations on mRNA expression of various clock, immune and microglia resting genes

To understand the expression pattern of molecular clock genes and how they change with the aging we have studied the mRNA expression of various clock genes at different time points. Microglia exhibited rhythmic expression of circadian clock genes in young adult animals (3 m). Daily rhythm of *rBmal1* showed maximum expression at ZT-0 which is similar to the expression in cortical and hippocampal microglia of young adult mice and rat respectively (Hayashi et al. 2013; Fonken et al. 2016) (Fig. 33). In peritoneal macrophages, the maximum expression of *rBmal1* was observed at ZT-0 similar to microglia (Hayashi et al. 2007), interestingly, at ZT-18 the expression levels were elevated in macrophages but in microglia the levels were less. This probably explains the functional difference between the microglia and macrophages in relation to the differences in the intrinsic molecular mechanism. But in central clock SCN, the expression of *rBmal1* showed maximum at ZT-18 (Mattam and Jagota 2014) which is 6 h early to the microglia. This further proves that the master and slave clocks have similar circadian machinery yet their expression pattern varies (Schibler et al. 2015) depending on their physiological niche. The expression pattern of *rPer1* and *rPer2* (Fig. 33) is in agreement with the previous report on hippocampal microglia (Fonken et al. 2015). But macrophages exhibit different expression pattern of *rPer1* and *rPer2* as observed in the mice (Hayashi et al. 2007). Interestingly, in the central clock, *rPer1* showed similar pattern of expression but *rPer2* showed different expression pattern (Mattam and Jagota 2014). *rCry1* and *rCry2* showed maximum expression at ZT-0 which showed similarity with the expression observed in microglial BV-2 cell cultures (Nakazato et al. 2016). On contrary, *rCry1* and *rCry2* showed maximum expression at ZT-12 in SCN (Mattam and Jagota 2014). *rRev-erba* and *rRora* showed maximum expression at ZT-6 and ZT-0 respectively in our study (Fig. 33), whereas in peritoneal macrophages of mice, the maximum expression was observed at ZT-10 and ZT-14 respectively (Hayashi et al. 2007). All this studies suggests that though the microglia are resident macrophages of CNS, they exhibit several variations in the circadian parameters with the peritoneal macrophages, which may further lead to the physiological variations between these cell types.

With the aging, we did not observe phase change in the expression pattern of *rBmal1*, *rPer1*, *rCry1*, *rCry2*, *rRev-erba* and *rRora*, but there was change of expression of *rPer2* in both 12 and 24 m animals (Fig. 33). Interestingly, in hippocampal microglia, *rPer1* showed loss of rhythmicity but not *rBmal1*, *rPer2* and *rRev-erba* in 24 m animals (Fonken et al. 2016). This

disparity in the age related alterations of circadian clock could be because of the reason that we have taken the microglia from whole brain but not from any specific brain region. In the central clock, *rPer1* and *rBmal1* showed variation in both 12 and 24 m animals, whereas *rPer2*, *rCry1* and *rCry2* showed alterations in 12 m animals but not in 24 m animals (Mattam and Jagota 2014). This suggests that the central clock shows more age associated alterations in the circadian clock. Also central clock shows more middle age alterations than in microglia. Interestingly, in central clock *rRev-erba* did not show any variation in the expression pattern (Kukkemane and Jagota 2019). This is similar to the observed expression pattern in kidney as well (Thummadi and Jagota 2019). In kidney, *rCry1* and *rRora* showed alterations with aging (Thummadi and Jagota 2019). Only *rPer1* and *rPer2* showed increased expression in microglia in 24 m animals. Whereas in central clock, *rBmal1* and *rPer2* were decreased in 24 m animals, *rCry1* and *rCry2* showed increased expression in 12 m animals (Mattam and Jagota 2014). This also proves that the central clock is more sensitive to the age associated changes.

Further, we have also studied the gene expression pattern of various inflammatory genes and analysed how the pattern changes with the aging. Inflammatory genes exhibit circadian rhythms in several peripheral clocks but the expression pattern is highly tissue-specific based on their physiological functions of peripheral clocks. In microglia, *rNf- κ b1*, *rTnfa*, *rTlr4* and *rTlr9* showed rhythmic expression with maximum expression at ZT-6 (Fig. 34). Interestingly, in the hippocampal microglia, *Tnfa* showed maximum expression at ZT-6 (Fonken et al. 2016). In macrophages, these genes show rhythmic expression with similar expression pattern (Silver et al. 2012). However, we did not observe rhythmic expression of *rIl6* in microglia. But in macrophages *Il6* shows rhythmic expression (Keller et al. 2009). With aging, the expression pattern of inflammatory genes altered which suggests the change in the physiological conditions of the microglia (Fig. 34). In contrast to clock genes, we have observed the altered phases of the immune genes suggesting the desynchronization of clock and immune genes with the advancement in the age. Several studies showed an increase in the expression of inflammatory genes expression in the old aged microglia (Norden and Godbout 2013). Caldeira et al. (2014) showed that aged microglia i.e. microglia cultured for 16 days in vitro exhibited senescent phenotype with decreased expression of inflammatory genes. In contrast, it was shown that senescent microglia express increased inflammatory genes than the aged microglia (Stojiljkovic et al. 2019). Interestingly, with aging we did not observe any significant change in the expression levels of immune genes except *rTlr9* (Fig. 34). This disparity could be because most of the studies have considered only a single time point to understand the change in the expression of

genes with aging. In our study, considering four different time points have given better idea on how exactly immune genes vary with aging. However, a detailed study is required to further understand the variations in the expression of inflammatory genes with aging.

The physiological functions of microglia are maintained by chemokine receptor CX3CR1 and other receptors like CD45 and CD172. Therefore, we have studied the expression of these genes to know whether these genes show rhythmic expression and how they vary with the aging as they regulate the functional status of microglia. *Cx3cr1* in microglia is essential for the normal development of brain (Paolicelli et al. 2011). We observed a rhythmic expression of *rCx3cr1* at mRNA level (Fig. 35). Synaptic activity shows a diurnal variation in rodents with the help of cathepsin S (CatS), which is a microglia-specific lysosomal cysteine protease of brain (Hayashi et al. 2013). As *Cx3cr1* is essential for the synapse formation, it can be suggested that the rhythmic expression of *Cx3cr1* may also help in the diurnal variation of synaptic activity. In mature CD8+ cells, it was observed that *Cx3cr1* show circadian expression with the peak at CT-9 and nadir at CT-21 in humans (Dimitrov et al. 2009). *rCd45* showed maximum expression at ZT-6 i.e. at the middle of rest phase in young adults (Fig. 35). Interestingly, in rat lymphocytes, CD45 showed maximum expression at the end of the active phase (Pelegrí et al. 2003). *rCd172* showed maximum expression at ZT-6 in young adults. With aging, only *rCd172* showed altered phase in both 12 and 24 m animals (Fig. 35). Given the importance of *rCd172* in phagocytosis, it can be speculated that because of the altered rhythm of *rCd172* in microglia there could be a change in the phagocytic property of microglia in aged animals (Ritzel et al. 2015). The mean levels of *rCx3cr1* were increased significantly in 12 and 24 m animals (Fig. 36), whereas, in hippocampal microglia there was no change in the expression level of *Cx3cr1* (Fonken et al. 2016). But the levels of *Cx3cr1* was shown to be decreased in the aged microglia (Stojiljkovic et al. 2019). However, *Cx3cl1*, the fractalkine ligand for *Cx3cr1* was shown to reduce with aging in the brain regions (Bachstetter et al. 2011). This fractalkine signalling is essential to keep the microglia at steady state (Bachstetter et al. 2011). Though we observed increased expression of *rCx3cr1* mRNA levels, studying the protein expression and also *Cx3cl1* levels in these animals would have given a better understanding.

It is essential to understand how the clock genes correlate with each other and also with the immune and microglia resting genes to underpin the reasons behind the alterations of physiological functions of microglia. Correlation analysis among the clock genes showed that *rBmal1* and *rPer1* were negatively correlated in both light phase and dark phase of young adults.

Such interactions among the positive and negative limbs are essential for the proper maintenance of the physiologies in the animals (Solt et al. 2011). There was no correlation between *rBmal1* and *rRev-erba* in light phase of 3 m animals (Fig. 38). This further suggest that clock genes exhibit tissue-specific expression and interaction with each other. In *Per1* deficient macrophages, the expression of *Cx3cr1* was reduced in rodents (Wang et al. 2016). Interestingly, in our study we observed a positive correlation between *rPer1* and *rCx3cr1* in light and dark phase of young adult animals (Fig. 38). BMAL1 has shown to be required to induce the expression of *Il6* in the presence of an immunogen in microglia (Nakazato et al. 2017). Interestingly, in the present study, we observed positive correlation between *rBmal1* and *rIl6* in the light and dark phase of 3 m animals (Fig. 38). REV-ERB α was considered as the link between the circadian clock and immunity, where REV-ERB α can regulate the expression of *IL6* in macrophages (Gibbs et al. 2012). In our study, we observed no correlation between *rRev-erba* and *rIl6* in 3 m light phase, but a positive correlation was observed in dark phase of 3 m animals. REV-ERB α was also shown to inhibit the expression of *TLR4* in human macrophages (Fontaine et al. 2008), whereas, we observed significant positive correlation between *rRev-erba* and *rTlr4* in light phase and significant negative correlation in dark phase of 3 m animals (Fig. 38). CRY proteins can block the NF- κ B activity and ultimately shows repression on the expression of *IL6* (Narasimamurthy et al. 2012). In the present study, we observed the positive correlation between *rCry1,2* and *rIl6* genes expression. Further, *CRY1* was shown to repress the expression of *TLR4* in atherosclerosis mouse model (Yang et al. 2015). Interestingly, in our study, we observed negative correlation between *rCry1* and *rTlr4* in the light and dark phase of 3 m animals (Fig. 38). With aging the correlations between the genes studied were significantly altered in both light and dark phase of 12 and 24 m animals. This probably suggest that there is desynchrony among the clock, immune and microglia resting genes with aging in microglia. Gene to gene network analysis has shown that with aging the interactions between clock and immune genes increased (Fig. 39). This probably, suggest that the altered immune genes expression may be because of the subtle changes in the expression of clock genes.

I. B. Chronobiotic role of curcumin on the age induced alterations of clock, immune and microglia resting genes mRNA expression in microglia

Curcumin, an anti-inflammatory, anti-oxidant, anti-aging, anti-cancerous molecule, was known to interact with several biomolecules in the system. However, its potential as a chronobiotic was first explored from our laboratory. Recently, we have shown the chronobiotic role of curcumin

in restoring the clock genes expression in central clock SCN (Kukkemane and Jagota 2019). However, in the present study, we did not observe significant alterations in the pattern of clock genes with aging (Fig. 33). But curcumin administration had resulted in alterations of clock genes suggesting that circadian clock in microglia is sensitive to the curcumin. Also curcumin had restored the mean levels of *rCry2* in 24 m but altered the levels of other clock genes (Fig. 36) suggesting its differential role as chronobiotic. Being an anti-inflammatory molecule, curcumin was shown to modulate the inflammatory genes expression through Nrf2 activation (Wardyn et al. 2015). In the present study, curcumin restored the phase of *rNf- κ b1*, *rTnfa* in 12 m animals (Fig. 34). This further proves the potential of curcumin as chronobiotic in regulating the expression pattern of inflammatory genes expression. In microglia, the elevated levels of *rTlr9* with the aging were reduced and restored with the curcumin administration. Curcumin significantly reduced the levels of the immune genes expression (Fig. 36) which is in agreement with several studies (Xi et al. 2014). Also curcumin reduced the increased levels of *rCx3cr1* with aging. As the activity state of microglia is dependent on the expression of Cx3cr1, it is intriguing to understand the role of curcumin on the Cx3cr1 in a detailed manner to further establish curcumin as a potent therapeutic drug against the microglia associated pathologies. Curcumin also showed chronobiotic property by differentially restoring the correlations among the clock, immune and microglia resting genes (Fig. 38). Gene to gene network analysis showed that with curcumin the interaction between clock and immune genes decreased (Fig. 39), this may be because of the anti-inflammatory role of curcumin on immune genes expression.

II. A. Age induced alterations of clock and immune genes mRNA expression in liver, kidney and spleen

Circadian clock in liver has been linked to the metabolism (Reinke and Asher 2016). In the present study in liver, we observed significant daily rhythms of various clock genes in the young adult (3 m) (Fig. 40). *rBmall* and *rCry1* showed maximum expression in the dark phase which is similar to several previous reports (Sladek et al. 2007; Taraborrelli et al. 2011; Ribas-Latre et al. 2015; de Goede et al. 2018; de Goede et al. 2018). Similarly, *rPer1*, *rPer2*, *rCry2*, *rRev-erba*, *rRora* showed similar expression observed in previous report in liver (Canaple et al. 2006; Sladek et al. 2007; Taraborrelli et al. 2011; Takeda et al. 2012; de Goede et al. 2018; de Goede et al. 2018) (Fig. 40).

In the present study in kidney, all the clock genes studied showed significant daily rhythms in kidney of 3 m old animals. Elevated levels of *rBmall* at dark phase are corroborated with previous studies in different peripheral clocks across different species (Christiansen et al. 2016; Yang et al. 2016) (Fig. 46). Similarly, *rPer1* and *rPer2* showed offset at ZT-12 and is in agreement with previous studies in different tissues and species (Pizarro et al. 2013; Yang et al. 2016). Expression pattern of *rCry1*, *rCry2* and *rRev-erba* (Fig. 46) also corroborates to the previous studies (Takeda et al. 2012; Yang et al. 2016; Astafev et al. 2017). In spleen, there are no proper studies on the daily rhythms of clock genes. Similar to liver and kidney the maximum expression of *rBmall* was observed at ZT-0 (Fig. 52). Also, *rPer2* showed similar expression as in liver and kidney with maximum expression at ZT-12. *rRev-erba* also showed similar expression as in liver and kidney with maximum expression at ZT-6 (Fig. 52). The other genes showed variations in their expression pattern in different tissues which suggests the tissue-specific molecular mechanism of circadian clock.

Interestingly, in 3 m rat SCN, *rBmall* maximum expression was seen at ZT-18 (Mattam and Jagota 2014) which is 6 h earlier to liver, kidney, and spleen this further demonstrate the relation between master and slave clocks (Balsalobre et al. 2002). This emphasizes the importance of well organised synchrony between the clocks for a better survival of an organism (Hatori et al. 2017). Similar to peripheral clocks, SCN also exhibits *rPer2* peak expression at ZT-12 (Mattam and Jagota 2014). In kidney, *rPer1* did not show any change in expression with aging. Interestingly, mRNA levels of α ENaC (alpha subunit epithelial Na⁺ channel), essential for regulation of salt and water reabsorption was reported to be under PER1 regulation (Gumz et al. 2009), did not vary with aging (Haloui et al. 2013).

With aging, in liver *rPer1*, *rCry2*, and *rRora* showed alterations in the phase, whereas in kidney, *rCry1* and *rRora* showed variation, but in spleen all the clock genes except *rRev-erba* showed alterations in the phase of expression pattern (Fig. 40, 46, 52). However, in SCN all the clock genes showed variations in their phase as age progress (Mattam and Jagota 2014). This implies that central clock SCN and peripheral clock spleen are more sensitive towards the age-associated attritions than the peripheral clocks. Mean 24 h levels of *rPer1*, *rPer2* and *rCry2* in liver and all the clock genes except *rRev-erba* in spleen showed alterations with aging. However, in kidney clock genes did not show variation in levels. Interestingly, SCN displayed an increase in the mean 24 h levels of *rPer2*, *rCry1* and *rCry2* in 12 m (Mattam and Jagota 2014) further signifying the sensitivity of central clock in middle age.

rBmall showed significant negative correlation with *rPer1* and *rRev-erba* in both light phase and dark phase of 3 m in liver and kidney (Fig. 44, 50). These tightly regulated interactions are essential for the sustained metabolism in organisms (Solt et al. 2011). However, *rBmall* did not show any correlation with *Rora* in LP and DP of 3 m of kidney, which is in agreement with the minimal role of *Rora* on circadian clock in kidney (Takeda et al. 2012). Positive correlation between *rCry1* and *rCry2* in LP did not vary with aging in kidney and spleen in present study, but abolished in liver and SCN (Mattam and Jagota 2014). Negative correlation between *rBmall* and *rPer1* observed in liver and kidney was not observed in spleen and SCN (Mattam and Jagota 2014).

Time dependent immune responses are well documented in several immune cells; and there are remarkable evidences to show that they are cell and tissue specific circadian regulations (Curtis et al. 2014). NF- κ B1, an important regulatory transcription factor in inflammation, plays a central role in inducing transcription of *Tnfa*, *Il6* and several other cytokines and also involved in apoptosis, cellular growth and differentiation (Hoesel and Schmid 2013). Several studies showed that these inflammatory genes in immune cells show diurnal expression in rodents (Keller et al. 2009; Cermakian et al. 2013; Curtis et al. 2014). Interestingly, in our study, we observed that *rNf- κ b1*, *rTnf- α* and *rIl6* showing significant daily rhythms in 3 m liver, kidney and spleen and corroborates to the previous reports in immune cells (Curtis et al. 2014) (Fig. 41, 47, 53). In addition, LPS induced phase shift of circadian rhythms in SCN were observed to be through TNFR1 receptors (Paladino et al. 2014). In this context, it would be of greater importance to understand role of *Tnfa* on circadian rhythms in peripheral clocks to address renal chronoinflammatory aberrations. *Tlr9* contains canonical E-boxes at its promoter site where

CLOCK/BMAL1 complex can induce the expression, but its circadian rhythms are cell and tissue specific (Silver et al. 2012). In our study, we observed both *rTlr9* showing peak expression at ZT-12 in liver and kidney, which is similar to expression seen in inflammatory cells (Silver et al. 2012, 2018), but at ZT-0 in spleen. Interestingly, all the immune genes studied showed phase advance of 6 h in 12 m but remained unaltered in 24 m in kidney, but all the immune genes showed alterations with aging in liver and spleen. Further studies are essential in understanding the middle age perturbations in chrono-immune system.

Pairwise correlation analysis revealed the change of correlation of *rNf- κ b1* with other immune genes in liver in 12 m LP and DP, also the correlation of *rNf- κ b1* changed with *rTnf α* and *rTlr4* in DP of 12 m kidney, this suggests the deregulated interactions between inflammatory genes with aging. *rNf- κ b1* showed significant positive correlation with other immune genes in 24 m liver and kidney (Fig. 44, 50), this further suggests altered inflammatory status with aging.

Correlation analysis was performed between clock and immune genes in order to understand the possible interactions with each other. *rPer1* showed positive correlation with *rIl6* in LP and DP of 3 m kidney and spleen (Fig. 50, 56), but in liver there was a negative correlation between *rPer1* and *rIl6* (Fig. 44). Interestingly, it was shown that PER1 negatively regulates IL-6 expression in spinal astrocytes (Sugimoto et al. 2014). *Tlr9* shows *Per2* dependent circadian expression in macrophages (Silver et al. 2012), we also observed positive correlation between *rPer2* and *rTlr9* in LP and DP of 3 m liver and kidney (Fig. 44, 50). REV-ERB α shows inhibitory action on TLR4 expression in human macrophages (Fontaine et al. 2008), but in our study we observed insignificant negative correlation between *rRev-erba* and *rTlr4* in LP of 3 m kidney and spleen, but in liver significant positive correlation was observed between *rRev-erba* and *rTlr4*. In LP and DP of 12 m, the correlations were altered, suggesting desynchrony between immunity and circadian clock. CRY proteins were proposed to inhibit *Il6* expression by blocking NF κ B activity in fibroblasts and macrophages (Narasimamurthy et al. 2012). Interestingly, in our study we observed a positive correlation between *rCry2* and *rIl6* in kidney and spleen, whereas in liver there was no correlation between *rCry2* and *rIl6*. In another study, overexpression of CRY1 reduced the TLR4 expression in atherosclerosis mouse model (Yang et al. 2015). But, we observed a positive correlation between *rCry1* and *rTlr4* in LP of 3 m kidney (Fig. 50), but a negative correlation was observed between *rCry1* and *rTlr4* in liver (Fig. 44). As our study involves mRNA expression, study at protein level would yield a better understanding on their interactions. In DP of 24 m, all the immune genes showed significant positive correlation with all

clock genes except *rBmal1* in kidney, whereas in liver and spleen the correlations were altered, this provides significant basis for desynchronised clock and immune systems with aging.

Gene to gene network analysis showed that the interaction between clock and immune are very weak in liver and with aging the interactions reduced further in liver (Fig. 45). Gene to gene network analysis showed that in young age clock and immune genes exhibit interactions in two different groups with *rTlr4* and *rPer1* being the hub genes and intensity of the interactions are medium to weak. With aging the *rRev-erba* showed maximum interactions with immune and with increased strength of interactions. In 24 m, interactions between clock and immune genes were increased with increased intensity of strength (Fig. 51). This suggests that increased inflammatory status with aging might be because of subtle change in clock system. In spleen, in 12 m the clock and immune genes showed reduced interactions (Fig. 57) suggesting the desynchrony between clock and immune genes in spleen.

With aging, 5-HT daily rhythms were altered in liver, kidney and spleen (Fig. 58). In central clock also the daily rhythms were altered in 24 m (Reddy and Jagota 2015). Interestingly, the levels in SCN were increased (Reddy and Jagota 2015) which is similar in the case of peripheral clock kidney (Fig. 59a).

II. B Effect of curcumin on the age induced alterations of clock and immune genes mRNA expression in liver, kidney and spleen

Here we explored the chronobiotic properties of curcumin on peripheral clocks liver, kidney, and spleen for the first time. Curcumin administration did not show significant changes in expression pattern of clock genes in 3 m liver, but with aging curcumin altered the expression pattern of *rCry2* and *rRor-α* (Fig. 40). However, *rPer1*, *rCry1* and *rCry2* were altered with curcumin treatment in 3 m kidney but remained unaltered in 12 and 24 m animals with respect to their age-matched vehicle groups (Fig. 46). In spleen, curcumin altered expression of *rCry1*, *rCry2* and *rRor-α* and with aging almost all the clock genes were altered (Fig. 52). Further detailed study is required to understand the underlying mechanism of curcumin on these clock genes. Interestingly, only *rRor-α* showed sensitivity towards curcumin in all the tissues and all the age groups studied. The chronobiotic role of curcumin can be highlighted with restored phases of *rRor-α* in 24 m liver; *rCry1* in 24 m kidney; *rPer1* in 24 m and *rCry2* in 12 m spleen.

Curcumin administration had profound effect on daily rhythms of all the immune genes. Interestingly, curcumin had similar chronomodulatory effects on *rNf-κb1* and *rTnfa* in all age

groups in kidney (Fig. 47). This could be because of curcumin's regulation on *rTnfa* through NFκB1. Several researchers demonstrated the role of elevated pro-inflammatory molecules like NFκB1 and TNFα in various disorders (Tilstra et al. 2011; Wang et al. 2017). With aging, the levels of pro-inflammatory molecules increase in several tissues. Here we report that *rNf-κb1* and *rTnfa* expressions were significantly elevated with aging in liver and kidney (Fig. 42, 48), which corroborates to previous studies (Tilstra et al. 2011; Xi et al. 2014). Curcumin being an anti-inflammatory molecule reduced the expression of *rNf-κb1* and *rTnfa* in all age groups and restored *rNf-κb1* in 12 m liver; *rTnfa* in 24 m kidney; *rNf-κb1* in 12 and 24 m spleen (Fig. 42, 48, 54). Further, we also report the gradual increase in transcription of *rTlr4* and *rTlr9* with aging in kidney which supports previous studies (Xi et al. 2014). Curcumin reduced the mean 24 h levels of *rTlr4*, which is in agreement with previous studies (Zhu et al. 2014) and restored in 24 m kidney (Fig. 48). It has been reported that the anti-inflammatory action of curcumin could be through the activation of Nrf2 which was shown to attenuate inflammatory responses (Wardyn et al. 2015). Curcumin showed significant alterations in correlations among the immune genes in all the peripheral clocks studied as it reduced the expression of several immune genes (Fig. 44, 50, 56). Gene to gene interactions in liver showed that curcumin can alter the interactions between clock and immune genes in aging (Fig. 45). However, in kidney, with curcumin treatment in 24 m, interactions between clock and immune genes showed similarity with 12 m VT, suggesting the potential of curcumin as chronobiotic to regulate both clock and immune system (Fig. 51). In spleen, the interactions in 24 m were reduced highlighting the anti-inflammatory role of curcumin (Fig. 57). Curcumin administration restored the daily rhythm of 5-HT only in 24 m spleen (Fig. 58). However, curcumin partially restored the levels in 12 and 24 m spleen (Fig. 59a). This suggest that curcumin showed more beneficiary effect on spleen.

III. A. Effect of LPS on clock, and immune genes mRNA expression in microglia, liver, kidney and spleen

LPS, an endotoxin that is present on the outer membrane of gram negative bacteria, induces immune response through TLR4 receptor (Rosadini and Kagan, 2017). In our study, LPS administration elicited the expression levels of immune genes in all tissues studied, however, clock genes exhibited differential alterations in various tissues suggesting the tissue specific clock and immune interactions. *rBmal1* expressed maximum at ZT-0 in all the tissues studied, with LPS administration the maximum expression was altered in microglia, but did not alter in liver, kidney, spleen which suggests that clock shows response in tissue specific manner. BMAL1 being a core clock gene was showed to regulate the immune responses in macrophages (Oishi et al. 2017). Further, it has been proposed that increased inflammation with LPS administration at ZT-12 could be because of lower expression of *Bmal1* at that time point (Curtis et al. 2014). In our study, we observed increased expression of *rBmal1* and *rIl6* at ZT-6 with LPS treatment in microglia. But in the other peripheral clocks, though we did not observe any change in maximum expression time point, we observed significant change in the expression at other time points suggesting the altered rhythm of *rBmal1* expression with LPS treatment which is in agreement with previous report in liver (Shimizu et al. 2017). It has been shown that LPS downregulates the expression of *Bmal1* in macrophages (Wang et al. 2013). But in microglia, we observed significant increase in the expression of *rBmal1*. But in the other peripheral clocks we did not observe significant reduction in the levels of *rBmal1* with LPS treatment which is also in agreement with previous study in liver (Shimizu et al. 2017). PER1 has been attributed to regulate macrophage recruitment to prevent excessive immune response in liver (Wang et al. 2016). *rPer1* and *rPer2* showed altered phases with LPS administration in all the tissues. With the LPS administration *rPer1* and *rPer2* expression is blunted at the peak time point in microglia, liver and kidney but not in spleen. A similar result was observed in previous experiment in liver (Okada et al. 2008). Mean levels of *rPer1* and *rPer2* did not alter in microglia, liver and spleen which is in agreement with previous study where the levels were recovered on day2 after LPS administration in liver (Okada et al. 2008). Previous studies showed that several non-photic stimulations significantly suppress the expression of *Per1* and *Per2* mRNA expression (Moravcova et al. 2018) in various clocks. In our study we observed loss of rhythmicity of *rCry1* and *rCry2* in microglia with LPS treatment. But in other peripheral clocks alterations in *rCry1* and *rCry2* phases were observed with LPS administration. Mean 24 h levels of *rCry1* and *rCry2* showed tissue specific alterations. Interestingly, it was reported that overexpressing CRY1 could

protect from atherosclerosis through the modulation of TLR/NF- κ B pathway (Yang et al. 2015). Also CRY proteins show anti-inflammatory property by inhibiting the activation of TNF- α (Hashiramoto et al. 2010). *rRev-erba* showed altered rhythms in microglia, liver and spleen, whereas in kidney rhythmicity was completely lost. REV-ERB α serves as the link between the clock and immunity in macrophages (Gibbs et al. 2012). Also REV-ERB α can modulate the immune responses by altering the cytokines expression (Sato et al. 2014). In our study mean 24 h levels of *rRev-erba* showed significant decrease in microglia and liver but not showed significant variation in kidney and spleen. REV-ERB α was shown to negatively regulate IL-6 expression (Sato et al. 2014), it was also identified that *Rev-erba* promoter has NF- κ B binding site to repress its activation (Yang et al. 2014). In our study we observed increased *rNf- κ b1* and *rIl6* expression associated with reduced levels of *rRev-erba* in liver suggesting that increased *rNf- κ b1* might have played a role in reducing the levels of *rRev-erba*. We observed that *rRora* showed phase alteration in liver and rhythm abolition in microglia and kidney with LPS treatment. However, in spleen we did not observe significant daily rhythm in VT and LPS groups. In liver, we observed decreased expression at the ZT-18, the time point that corresponds to the maximum expression in VT group. In kidney though there was no rhythmicity, we observed increased expression at ZT-6, the time point that corresponds to the minimum expression In VT group. This suggests that LPS alters the expression of *rRora* in tissue specific manner. However, we observed increased expression levels of *rRora* in microglia and kidney and decreased levels in spleen. It was observed that *Rora* shows acute increase in its expression with LPS treatment in adipocytes (Liu et al. 2017) and in macrophages (Barish et al. 2005). In smooth muscle cells, overexpression of ROR α inhibited the levels of TNF- α and IL-6 (Delerive et al. 2001). In astrocytes, ROR α showed bidirectional regulation of IL-6 expression, where ROR α was required to maintain basal levels of IL-6. Whereas in the presence of immune stimulus ROR α negatively regulates the expression of IL-6 (Journiac et al. 2009). Taking together these studies suggest that ROR α is a negative regulator of pro-inflammatory molecules. Also studies have shown that ROR α does not involve NF- κ B to modulate immune responses (Stapleton et al. 2005). With LPS treatment immune genes showed phase alterations in all the tissues studied. In liver, all the immune genes except *rTnfa* showed peak at ZT-0. This probably could be because of acute increase in the levels of inflammatory molecules when LPS was administered. As the day progressed we observed the decrease in the levels of all the inflammatory genes. Interestingly, such increase of immune genes at ZT-0 were not observed in microglia, kidney and spleen suggesting that immune response varies from tissue to tissue. All the immune genes except *rTlr9* showed increase in

mean 24 h levels with LPS in microglia and liver which is in corroboration with previous studies (Nozaki et al. 2017; Hamesch et al. 2015; Liu et al. 2015). In microglia, with LPS treatment, the rhythmicity of *rCx3cr1* was not altered but rhythmicity was abolished for *rCd172* and *rCd45*. Further, the decreased levels of *rCd172* and *rCd45* suggests that microglia are activated upon LPS treatment.

The correlation analysis between the clock and the immune genes showed that altered expression of clock genes as immune response to the LPS treatment resulted in disrupted correlations with immune genes. Our results suggest that clock and immune genes response to LPS are indeed tissue specific as it is well reflected in correlation analysis. Gene to gene network analysis in microglia suggests that with the LPS treatment, clock and immune genes lost their interactions with each other. Gene to gene network analysis of liver with the LPS treatment shows that clock genes as immune response show strong interaction with immune genes. Our network analysis suggest that LPS induced alterations on clock genes expression could be through the NF- κ B pathway as we observed a strong interaction of *rNf- κ b1* with clock genes. In kidney we observed that with LPS treatment *rNf- κ b1* and *rTnfa* did not show interaction with clock genes suggesting NF- κ B independent pathway might be involved to induce inflammatory response from clock genes. Similarly in spleen, we found that with LPS treatment there was no *rNf- κ b1* interactions with any of the clock genes suggesting a NF- κ B independent pathway to induce response. However, further studies are needed to evaluate the role of NF- κ B on LPS induced alterations of clock genes. Gene to gene interaction studies showed that LPS can alter the response of clock and immune genes in tissue specific manner. Overall our results suggest that LPS induced clock and immune genes alterations are tissue specific.

III. B. Role of NF- κ B inhibitor on the LPS induced alterations of clock and immune genes mRNA expression in microglia, liver, kidney and spleen

PDTC is a potent inhibitor of NF- κ B activity. PDTC has been shown to reduce the NF- κ B mediated inflammation and associated pathologies. From our results we understood that LPS administration can modulate the clock genes expression in tissue specific manner in peripheral clocks. As LPS can trigger the activation of NF- κ B and elicits the inflammatory status, we wanted to understand whether NF- κ B is involved in the LPS induced alterations of clock genes. Therefore, we have administered PDTC to the animals to block the activity of NF- κ B. We also wanted to understand if NF- κ B is required for the basal expression of clock genes.

In microglia, with LPS+PDTC treatment, *rBmal1* and *rPer2* showed similar pattern as in LPS group, but with PDTC treatment, their expression pattern showed similarity with VT group. This suggests that LPS can act on these genes as NF- κ B independent manner. However, the unaltered expression pattern of *rPer1* and *rRev-erba* in LPS+PDTC and PDTC group in comparison to VT suggest that LPS act on these genes as NF- κ B dependent manner. It was shown that NF- κ B can alter the expression of *Rev-erba* by binding to its promoter region (Yang et al. 2014). In agreement with that we observed that LPS can regulate *Rev-erba* in the presence of immunogen. Altered phases of *rCry1* and *rCry2* in LPS+PDTC group suggest that LPS can act on these genes as NF- κ B dependent and independent manner. Altered phase of *rRora* in LPS+PDTC and PDTC group suggest that LPS act on this gene as NF- κ B dependent manner and also NF- κ B is required for the basal expression pattern (Fig. 60). The altered expression levels of *rBmal1* and *rCry1* in LPS+PDTC group suggest that LPS can alter the levels as NF- κ B independent manner. The unaltered levels of *rCry2* in LPS+PDTC group suggest that LPS can act as NF- κ B dependent manner (Fig. 61).

In liver, *rBmal1* expression pattern did not alter in LPS+PDTC and PDTC groups, suggests that LPS cannot act on this gene and NF- κ B is not required for the basal expression. Altered phases of all other clock genes in LPS+PDTC treatment suggest that LPS can act as NF- κ B dependent and independent manner. However, the altered phases of *rPer1*, *rCry1* and *rRora* in PDTC group suggest that NF- κ B is essential for their basal expression pattern (Fig. 65). The decreased expression levels of *rRev-erba* in LPS+PDTC group suggest that LPS can act as NF- κ B independent manner (Fig. 66).

In kidney, *rBmal1* did not alter its phase in LPS+PDTC and PDTC groups suggesting that LPS cannot alter its phase and NF- κ B is not essential for basal expression pattern. Altered phase of *rPer2* and *rCry2* in LPS+PDTC group suggest that LPS can act as NF- κ B independent manner. Altered phases of *rCry1* and *rRev-erba* in LPS+PDTC group suggest that LPS can act as NF- κ B dependent manner. Altered phase of *rPer1* in LPS+PDTC group suggest that LPS can as NF- κ B dependent and independent manner. Abolition of rhythmicity of *rRora* in LPS+PDTC and PDTC groups suggest that LPS can as NF- κ B dependent and independent manner and NF- κ B is essential for its basal expression pattern (Fig. 70). Decreased levels of *rPer1*, *rPer2*, and *rCry2* suggest that LPS can act as NF- κ B independent manner (Fig. 71).

In spleen, *rBmal1* did not alter its phase in LPS+PDTC and PDTC groups suggesting that LPS cannot alter its phase and NF- κ B is not essential for basal expression pattern. Altered phases of

rPer1, *rCry2* and *rRev-erba* in LPS+PDTC group suggest that LPS can act as NF- κ B dependent manner. Altered phases of *rPer2* and *rCry1* in LPS+PDTC suggest that LPS can act as NF- κ B independent manner. Abolition of rhythmicity of *rRora* in LPS+PDTC and altered phase in PDTC group suggest that LPS can act as NF- κ B dependent and independent manner and NF- κ B is essential for its basal expression pattern (Fig. 75). Unaltered levels of *rCry2* and *rRora* in LPS+PDTC group suggest that LPS can act as NF- κ B dependent manner (Fig. 76).

In microglia, liver, kidney, and spleen the altered phases of all immune genes in LPS+PDTC and PDTC group suggest that NF- κ B is essential for the basal expression pattern of immune genes (Fig. 60, 65, 70, 75). Further, the reduced levels of immune genes with PDTC treatment shows that NF- κ B activity is essential for the immune response caused by LPS administration in all the tissues studied (Fig. 61, 66, 71, 76). Correlation analysis and gene to gene network analysis had shown that NF- κ B has tissue specific role in regulating the clock and immunity (Fig. 63, 68, 73, 78).

Summary and Conclusions

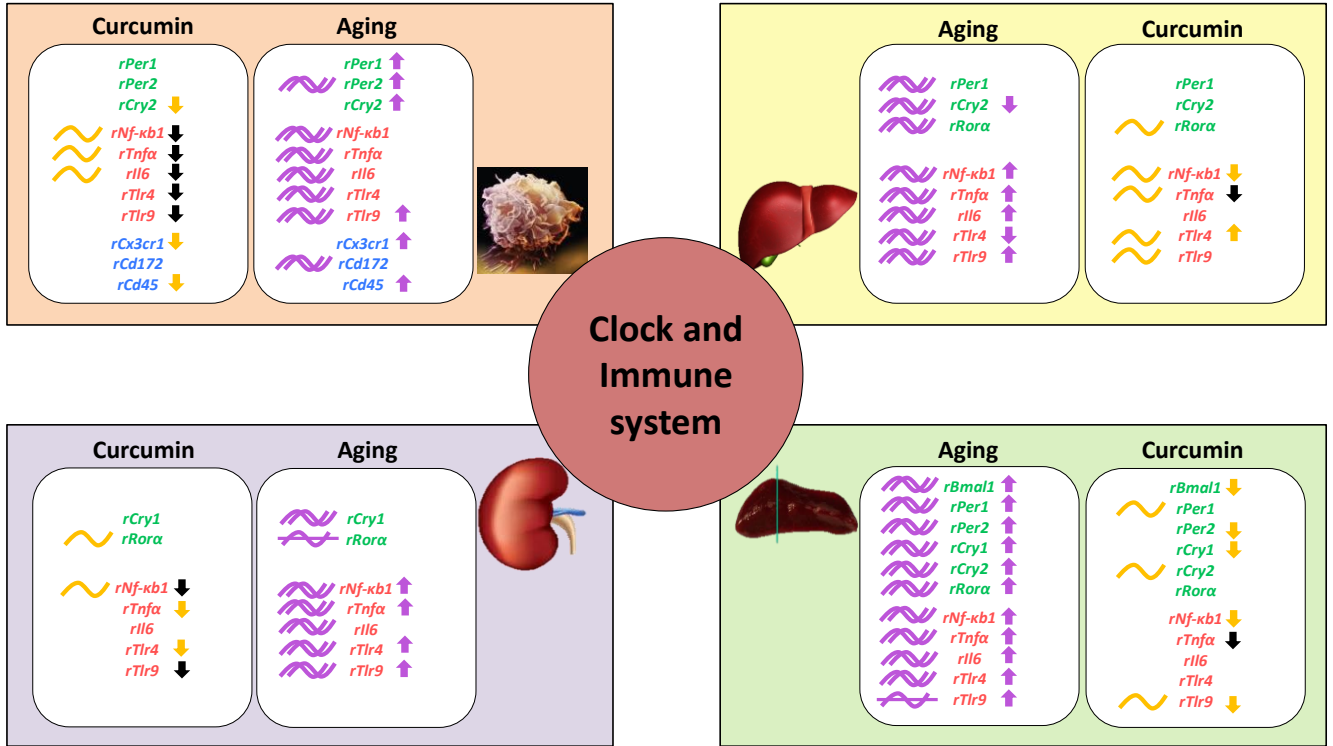
Summary and conclusions

Our studies demonstrated that clock and immune genes show tissue specific temporal expression pattern in microglia, liver, kidney, and spleen in young age. Microglia resting genes showed significant daily rhythms in microglia. Clock and inflammatory genes showed tissue specific correlations in young age. 5-HT also showed tissue specific daily rhythms in liver, kidney and spleen. With aging, *rPer2* in microglia; *rPer1*, *rCry2* and *rRora* in liver; *rCry1* and *rRora* in kidney; and all clock genes in spleen showed differential alterations in expression pattern. All the immune genes showed altered expression patterns in all the tissues studied. In microglia, *rCd172* showed altered expression pattern with aging. In microglia, correlations within clock genes and within inflammatory genes were significantly altered with aging. In liver and spleen correlations within clock genes and within inflammatory genes were significantly altered. The correlations between clock and immune genes were significantly altered with aging in all the tissues studied. 5-HT showed altered daily rhythms and mean levels in liver, kidney and spleen with aging. Curcumin administration showed restoration of daily rhythms of *rNf- κ b1*, *rTnfa* and *rIl6* in microglia; *rRora*, *rNf- κ b1*, *rTnfa*, *rTlr4* and *rTlr9* in liver; *rRora* and *rNf- κ b1* in kidney; *rPer1*, *rCry2* and *rTlr9* in spleen. Curcumin administration also restored the altered mean levels of *rCry2*, *rCx3cr1* and *rCd45* in microglia; *rNf- κ b1* and *rTlr4* in liver; *rTnfa* and *rTlr4* in kidney; *rBmall1*, *rPer2*, *rCry1*, *rNf- κ b1* and *rTlr9* in spleen. Curcumin differentially restored the correlations within and between clock and immune genes in all the tissues studied. Curcumin administration restored 5-HT daily rhythm in 24 h spleen. Our results demonstrated the chronobiotic role of curcumin in peripheral clocks.

Further, it was found that clock genes show tissue specific responses to the immunogen LPS. NF- κ B showed differential role in LPS induced alterations of clock genes expression in various tissues. LPS showed NF- κ B dependent activity on *rPer1* in all the tissues studied.

Overall, this study helps towards the development of new therapeutic strategies using the pleiotropic molecule curcumin to address several age related chrono-immune attritions. In addition, our study gave an insight into the cross-talk between clock and immune systems to underpin the molecular mechanisms involved in chrono-immunological pathologies.

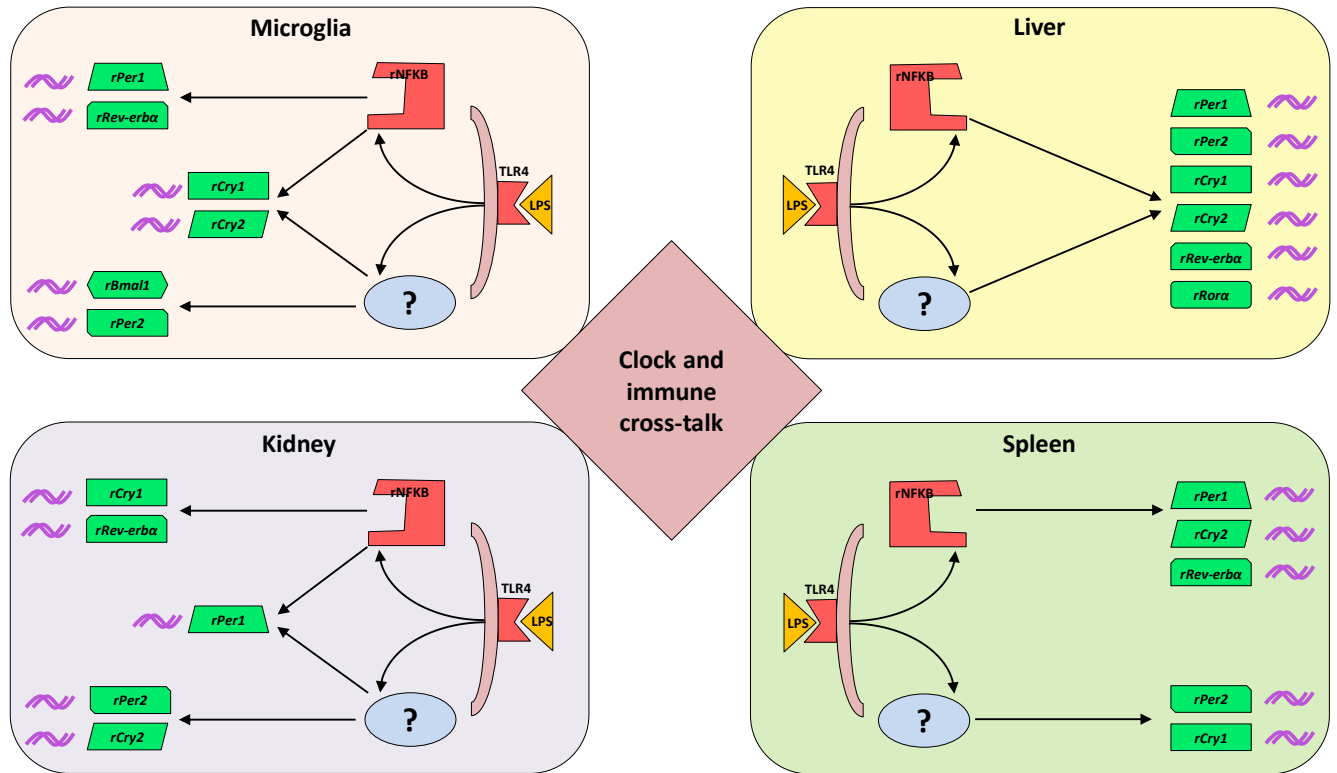
Fig. 80: Graphical representation of the summary from objective I and II



Schematic representation of effect of aging on various genes expression in various peripheral clocks and the chronobiotic role of curcumin on restoring the age induced alterations of various genes expression.

-  rhythmic expression (phase restoration)
-  altered rhythm
-  abolished rhythm
-  increased expression
-  decreased expression
-  decreased expression (restoration)

Fig. 81: Graphical representation of the summary from objective III



Schematic representation of LPS induced alterations of various clock genes in different peripheral clocks. The role of NF-κB on the LPS induced alterations of clock genes expression.

 altered expression

References

References

- Albers HE, Walton JC, Gamble KL, McNeill JK, Hummer DL (2017). The dynamics of GABA signaling: Revelations from the circadian pacemaker in the suprachiasmatic nucleus. *Front Neuroendocrinol* 44:35-82.
- Anand P, Kunnumakkara AB, Newman RA, Aggarwal BB (2007). Bioavailability of curcumin: problems and promises. *Mol Pharm* 4:807-818.
- Aravinthan AD, Alexander GJM (2016). Senescence in chronic liver disease: Is the future in aging? *J Hepatol* 65:825-834.
- Arjona A, Sarkar DK (2005). Circadian oscillations of clock genes, cytolytic factors, and cytokines in rat NK cells. *J Immunol* 174:7618-7624.
- Astafev AA, Patel SA, Kondratov RV (2017). Calorie restriction effects on circadian rhythms in gene expression are sex dependent. *Sci Rep* 7:9716.
- Aw D, Hilliard L, Nishikawa Y, Cadman ET, Lawrence RA, Palmer DB (2016). Disorganization of the splenic microanatomy in ageing mice. *Immunology* 148:92-101.
- Bachstetter AD, Morganti JM, Jernberg J, Schlunk A, Mitchell SH, Brewster KW, Hudson CE, Cole MJ, Harrison JK, Bickford PC, Gemma C (2011). Fractalkine and CX3CR1 regulate hippocampal neurogenesis in adult and aged rats. *Neurobiol Aging* 32:2030-2044.
- Balsalobre A (2002). Clock genes in mammalian peripheral tissues. *Cell Tissue Res* 309:193-199.
- Balsalobre A, Damiola F, Schibler U (1998). A serum shock induces circadian gene expression in mammalian tissue culture cells. *Cell* 93:929-937.
- Barichello T, Generoso JS, Simões LR, Goularte JA, Petronilho F, Saigal P, Badawy M, Quevedo J (2016). Role of Microglial Activation in the Pathophysiology of Bacterial Meningitis. *Mol Neurobiol* 53:1770-1781.
- Barish GD, Downes M, Alaynick WA, Yu RT, Ocampo CB, Bookout AL, Mangelsdorf DJ, Evans RM. A nuclear receptor atlas: macrophage activation. *Mol Endocrinol* 19:2466-2477.
- Becker D, Zahn N, Deller T, Vlachos A (2013). Tumor necrosis factor alpha maintains denervation-induced homeostatic synaptic plasticity of mouse dentate granule cells. *Front Cell Neurosci* 7:257.
- Benarroch EE (2008). Suprachiasmatic nucleus and melatonin: reciprocal interactions and clinical correlations. *Neurology* 71:594-598.
- Benarroch EE (2008). Suprachiasmatic nucleus and melatonin: reciprocal interactions and clinical correlations. *Neurology* 71:594-598.
- Birjandi SZ, Ippolito JA, Ramadorai AK, Witte PL (2011). Alterations in marginal zone macrophages and marginal zone B cells in old mice. *J Immunol* 186:3441-3451.
- Bolignano D, Mattace-Raso F, Sijbrands EJ, Zoccali C (2014). The aging kidney revisited: a systematic review. *Ageing Res Rev* 14:65-80.
- Bollinger T, Leutz A, Leliavski A, Skrum L, Kovac J, Bonacina L, Benedict C, Lange T, Westermann J, Oster H, Solbach W (2011). Circadian clocks in mouse and human CD4+ T cells. *PloS one* 6:e29801.
- Braun F, Rinschen MM, Bartels V, Frommolt P, Habermann B, Hoeijmakers JH, Schumacher B, Dolle ME, Müller RU, Benzing T, Schermer B (2016). Altered lipid metabolism in the aging kidney identified by three layered omic analysis. *Aging (Albany NY)* 8:441-457.

- Buhr ED, Takahashi JS (2013). Molecular components of the Mammalian circadian clock. *Handb Exp Pharmacol* 217:3-27.
- Buhr ED, Takahashi JS (2013). Molecular components of the Mammalian circadian clock. *Handb Exp Pharmacol* 217:3-27.
- Caldeira C, Oliveira AF, Cunha C, Vaz AR, Falcão AS, Fernandes A, Brites D (2014). Microglia change from a reactive to an age-like phenotype with the time in culture. *Front Cell Neurosci* 8:152.
- Campanelli CM (2012). American Geriatrics Society updated beers criteria for potentially inappropriate medication use in older adults: the American Geriatrics Society 2012 Beers Criteria Update Expert Panel. *J Am Geriatr Soc* 60:616.
- Canaple L, Rambaud J, Dkhissi-Benyahya O, Rayet B, Tan NS, Michalik L, Delaunay F, Wahli W, Laudet V (2006). Reciprocal regulation of brain and muscle Arnt-like protein 1 and peroxisome proliferator-activated receptor alpha defines a novel positive feedback loop in the rodent liver circadian clock. *Mol Endocrinol* 20:1715-1717.
- Cardona AE, Huang D, Sasse ME, Ransohoff RM (2006). Isolation of murine microglial cells for RNA analysis or flow cytometry. *Nat Protoc* 1:1947.
- Carniglia L, Ramírez D, Durand D, Saba J, Turati J, Caruso C, Scimonelli TN, Lasaga M (2017). *Mediators Inflamm* 5048616.
- Carniglia L, Ramírez D, Durand D, Saba J, Turati J, Caruso C, Scimonelli TN, Lasaga M (2017). Neuropeptides and microglial activation in inflammation, pain, and neurodegenerative diseases. *Mediators Inflamm* 2017:5048616.
- Castelo-Szekely V, Arpat AB, Janich P, Gatfield D (2017). Translational contributions to tissue specificity in rhythmic and constitutive gene expression *Genome Biol* 18:116.
- Cesta MF (2006). Normal structure, function, and histology of mucosa-associated lymphoid tissue. *Toxicol Pathol* 34:599-608.
- Chaves I, van der Horst GT, Schellevis R, Nijman RM, Koerkamp MG, Holstege FC, Smidt MP, Hoekman MF (2014). Insulin-FOXO3 signaling modulates circadian rhythms via regulation of clock transcription. *Curr Biol* 24:1248-1255.
- Chen J, Kieswich JE, Chiazza F, Moyes AJ, Gobbetti T, Purvis GS, Salvatori DC, Patel NS, Perretti M, Hobbs AJ, Collino M. IκB kinase inhibitor attenuates sepsis-induced cardiac dysfunction in CKD. *J Am Soc Nephrol* 28:94-105.
- Chi-Castañeda D, Ortega A (2018). Glial Cells in the Genesis and Regulation of Circadian Rhythms. *Front Physiol* 9:88.
- Cho H, Zhao X, Hatori M, Yu RT, Barish GD, Lam MT, Chong LW, DiTacchio L, Atkins AR, Glass CK, Liddle C, Auwerx J, Downes M, Panda S, Evans RM (2012). Regulation of Circadian Behavior and Metabolism by Rev-erba and Rev-erbβ. *Nature* 485:123-127.
- Cho JW, Lee KS, Kim CW (2007). Curcumin attenuates the expression of IL-1beta, IL-6, and TNF-alpha as well as cyclin E in TNF-alpha-treated HaCaT cells; NF-kappaB and MAPKs as potential upstream targets. *Int J Mol Med* 19:469-474.
- Christiansen SL, Bouzinova EV, Fahrenkrug J, Wiborg O (2016). Altered expression pattern of clock genes in a rat model of depression. *Int J Neuropsychopharmacol* 19(11).
- Christine M. Campanelli (2012). American Geriatrics Society Updated Beers Criteria for Potentially Inappropriate Medication Use in Older Adults. *J Am Geriatr Soc* 60:616-631.

- Curtis AM, Bellet MM, Sassone-Corsi P, O'Neill LA (2014). Circadian clock proteins and immunity. *Immunity* 40:178-86.
- Davalos D, Grutzendler J, Yang G, Kim JV, Zuo Y, Jung S, Littman DR, Dustin ML, Gan WB (2005). ATP mediates rapid microglial response to local brain injury in vivo. *Nat Neurosci* 8:752.
- de Goede P, Sen S, Su Y, Foppen E, Poirel VJ, Challet E, Kalsbeek A (2018). An Ultradian Feeding Schedule in Rats Affects Metabolic Gene Expression in Liver, Brown Adipose Tissue and Skeletal Muscle with Only Mild Effects on Circadian Clocks. *Int J Mol Sci* 19 pii: E3171.
- Delerive P, Monté D, Dubois G, Trottein F, Fruchart-Najib J, Mariani J, Fruchart JC, Staels B (2001). The orphan nuclear receptor ROR α is a negative regulator of the inflammatory response. *EMBO reports* 2:42-48.
- Denic A, Glasscock RJ, Rule AD (2016). Structural and functional changes with the aging kidney. *Adv Chronic Kidney Dis* 23:19-28.
- Deurveilher S, Semba K (2008) Reciprocal connections between the Suprachiasmatic nucleus and the midbrain raphe nuclei: A putative role in the circadian control of behavioral states. In: Monti JM, Pandi-Perumal SR, Jacobs BL, Nutt DJ (eds). *Serotonin and sleep: molecular, functional and clinical aspects*. Springer Science & Business Media. pp 103-129.
- Dibner C, Schibler U, Albrecht U (2010). The mammalian circadian timing system: organization and coordination of central and peripheral clocks. *Annu Rev Physiol* 72:517-549.
- Dickson DW, Crystal HA, Mattiace LA, Masur DM, Blau AD, Davies P, Yen SH, Aronson MK (1992). Identification of normal and pathological aging in prospectively studied nondemented elderly humans. *Neurobiol Aging* 13:179-189.
- Doi M, Takahashi Y, Komatsu R, Yamazaki F, Yamada H, Haraguchi S, Emoto N, Okuno Y, Tsujimoto G, Kanematsu A, Ogawa O (2010). Salt-sensitive hypertension in circadian clock-deficient Cry-null mice involves dysregulated adrenal Hsd3b6. *Nat Med* 16:67.
- Douma LG, Cheng KY, Lynch IJ, Holzworth M, Masten S, Barral D, Miller A, Esser KA, Wingo CS, Gumz ML (2018). Kidney-Specific KO of the Circadian Clock Protein BMAL1 Lowers Blood Pressure in Male C57BL/6J Mice. *The FASEB Jour* 32:905-906.
- Druzd D, Matveeva O, Ince L, Harrison U, He W, Schmal C, Herzel H, Tsang AH, Kawakami N, Leliavski A, Uhl O (2017). Lymphocyte circadian clocks control lymph node trafficking and adaptive immune responses. *Immunity* 46:120-32.
- Duguay D, Cermakian N (2009). The crosstalk between physiology and circadian clock proteins. *Chronobiol Int* 26:1479-513.
- Dürk T, Panther E, Müller T, Sorichter S, Ferrari D, Pizzirani C, Di Virgilio F, Myrtek D, Norgauer J, Idzko M (2005). 5-Hydroxytryptamine modulates cytokine and chemokine production in LPS-primed human monocytes via stimulation of different 5-HTR subtypes. *Int Immunol* 17:599-606.
- Dutta G, Zhang P, Liu B (2008). The lipopolysaccharide Parkinson's disease animal model: mechanistic studies and drug discovery. *Fundam Clin Pharmacol* 22:453-464.
- Edgar RS, Green EW, Zhao Y, van Ooijen G, Olmedo M, Qin X, Xu Y, Pan M, Valekunja UK, Feeney KA, Maywood ES, Hastings MH, Baliga NS, Meroow M, Millar AJ, Johnson CH, Kyriacou CP, O'Neill JS, Reddy AB (2012). Peroxiredoxins are conserved markers of circadian rhythms. *Nature* 485:459-464.
- Eglitis MA, Mezey É (1997). Hematopoietic cells differentiate into both microglia and macroglia in the brains of adult mice. *Proc Natl Acad Sci U S A* 94:4080-4085.

- Esquifino AI, Cano P, Jiménez-Ortega V, Fernández-Mateos P, Cardinali DP. Neuroendocrine-immune correlates of circadian physiology: studies in experimental models of arthritis, ethanol feeding, aging, social isolation, and calorie restriction. *Endocr* 32:1-9.
- Esquifino AI, Selgas L, Arce A, Della Maggiore V, Cardinali DP (1996). Twenty-four-hour rhythms in immune responses in rat submaxillary lymph nodes and spleen: effect of cyclosporine. *Brain Behav Immun* 10:92-102.
- Evans JA, Suen TC, Callif BL, Mitchell AS, Castanon-Cervantes O, Baker KM, Kloehn I, Baba K, Teubner BJ, Ehlen JC, Paul KN, Bartness TJ, Tosini G, Leise T, Davidson AJ (2015). *BMC Biol* 13:43.
- Farajnia S, Michel S, Deboer T, Tjebbe vanderLeest H, Houben T, Rohling JH, Ramkisoensing A, Yasenkov R, Meijer JH (2012). Evidence for neuronal desynchrony in the aged suprachiasmatic nucleus clock. *J Neurosci* 32:5891-5899.
- Ferrell JM, Chiang JY (2015). Circadian rhythms in liver metabolism and disease. *Acta Pharm Sin B* 5:113-122.
- Firsov D, Bonny O (2018). Circadian rhythms and the kidney. *Nat Rev Nephrol* 14:626-635.
- Flanary B (2005). The role of microglial cellular senescence in the aging and Alzheimer diseased brain. *Rejuvenation Res* 8:82-85.
- Fonken LK, Frank MG, Kitt MM, Barrientos RM, Watkins LR, Maier SF (2015). Microglia inflammatory responses are controlled by an intrinsic circadian clock. *Brain Behav Immun* 45:171-9.
- Fonken LK, Kitt MM, Gaudet AD, Barrientos RM, Watkins LR, Maier SF (2016). Diminished circadian rhythms in hippocampal microglia may contribute to age-related neuroinflammatory sensitization. *Neurobiol Aging* 47:102-12.
- Fontaine C, Rigamonti E, Pourcet B, Duez H, Duhem C, Fruchart JC, Chinetti-Gbaguidi G, Staels B (2008). The nuclear receptor Rev-erb α is a liver X receptor (LXR) target gene driving a negative feedback loop on select LXR-induced pathways in human macrophages. *Mol Endocrinol* 22:1797-1811.
- Fortier EE, Rooney J, Dardente H, Hardy MP, Labrecque N, Cermakian N (2011). Circadian variation of the response of T cells to antigen. *J Immunol* 187:6291-6300.
- Gallego M, Virshup DM (2007). Post-translational modifications regulate the ticking of the circadian clock. *Nat Rev Mol Cell Biol* 8:139-148.
- Gibbs JE, Blaikley J, Beesley S, Matthews L, Simpson KD, Boyce SH, Farrow SN, Else KJ, Singh D, Ray DW, Loudon AS (2012). The nuclear receptor REV-ERB α mediates circadian regulation of innate immunity through selective regulation of inflammatory cytokines. *Proc Natl Acad Sci U S A* 109:582-587.
- Godbout JP, Johnson RW (2006). Age and neuroinflammation: a lifetime of psychoneuroimmune consequences. *Neurol Clin* 24:521-538.
- Golombek DA, Rosenstein RE (2010). Physiology of Circadian Entrainment. *Physiol Rev* 90:1063-102.
- Gomez-Nicola D, Perry VH (2005). Microglial dynamics and role in the healthy and diseased brain: a paradigm of functional plasticity. *Neuroscientist* 21:169-84.
- Gumz ML, Stow LR, Lynch IJ, Greenlee MM, Rudin A, Cain BD, Weaver DR, Wingo CS (2009). The circadian clock protein Period 1 regulates expression of the renal epithelial sodium channel in mice. *J Clin Invest*. 119:2423-2434.

- Guo H, Brewer JM, Lehman MN, Bittman EL (2006). Suprachiasmatic regulation of circadian rhythms of gene expression in hamster peripheral organs: effects of transplanting the pacemaker. *J Neurosci* 26:6406-6412.
- Haloui M, Tremblay J, Seda O, Koltsova SV, Maksimov GV, Orlov SN, Hamet P (2013). Increased renal epithelial Na channel expression and activity correlate with elevation of blood pressure in spontaneously hypertensive rats. *Hypertension* 62:731-737.
- Hamesch K, Borkham-Kamphorst E, Strnad P, Weiskirchen R (2015). Lipopolysaccharide-induced inflammatory liver injury in mice. *Lab Anim* 49:37-46.
- Hanna L, Walmsley L, Pienaar A, Howarth M, Brown TM (2017). Geniculohypothalamic GABAergic projections gate suprachiasmatic nucleus responses to retinal input. *J Physiol* 595:3621-3649.
- Hara M, Minami Y, Ohashi M, Tsuchiya Y, Kusaba T, Tamagaki K, Koike N, Umemura Y, Inokawa H, Yagita K (2017). Robust circadian clock oscillation and osmotic rhythms in inner medulla reflecting cortico-medullary osmotic gradient rhythm in rodent kidney. *Scientific Repo* 7:7306.
- Hart EC, Charkoudian N (2014). Sympathetic neural regulation of blood pressure: influences of sex and aging. *Physiology (Bethesda)* 29:8-15.
- Hashiramoto A, Yamane T, Tsumiyama K, Yoshida K, Komai K, Yamada H, Yamazaki F, Doi M, Okamura H, Shiozawa S. Mammalian clock gene Cryptochrome regulates arthritis via proinflammatory cytokine TNF- α . *J Immunol* 184:1560-1565.
- Hastings MH, Maywood ES, Brancaccio M (2018). Generation of circadian rhythms in the suprachiasmatic nucleus. *Nat Rev Neurosci* 19:453-469.
- Hatori M, Gronfier C, Van Gelder RN, Bernstein PS, Carreras J, Panda S, Marks F, Sliney D, Hunt CE, Hirota T, Furukawa T (2017). Global rise of potential health hazards caused by blue light-induced circadian disruption in modern aging societies. *NPJ Aging Mech Dis* 3:9.
- Hayashi Y, Koyanagi S, Kusunose N, Okada R, Wu Z, Tozaki-Saitoh H, Ukai K, Kohsaka S, Inoue K, Ohdo S, Nakanishi H (2013). The intrinsic microglial molecular clock controls synaptic strength via the circadian expression of cathepsin S. *Sci Rep.* 3:2744.
- Hayashi Y, Koyanagi S, Kusunose N, Takayama F, Okada R, Wu Z, Ohdo S, Nakanishi H (2013). Diurnal spatial rearrangement of microglial processes through the rhythmic expression of P2Y12 receptors. *Jour of Neurolo Disord*.
- Herr N, Bode C, Duerschmied D (2017). The effects of serotonin in immune cells. *Front Cardiovasc Med* 4:48.
- Hewlings S, Kalman D (2017). Curcumin: a review of its' effects on human health. *Foods* 6:92.
- Hirsch EC, Hunot S (2009). Neuroinflammation in Parkinson's disease: a target for neuroprotection? *Lancet Neurol* 8:382-397.
- Hoeffel G, Squarzoni P, Garel S, Ginhoux F (2014). Microglial ontogeny and functions in shaping brain circuits. In *Macrophages: Biology and Role in the Pathology of Diseases* Springer, New York, NY 183-215.
- Hoesel B, Schmid JA (2013). The complexity of NF- κ B signaling in inflammation and cancer. *Mol Cancer* 12:86.
- Hong S, Dissing-Olesen L, Stevens B (2016). New insights on the role of microglia in synaptic pruning in health and disease. *Curr Opin Neurobiol* 36:128-34.

- Hood S, Amir S (2017). The aging clock: circadian rhythms and later life. *J Clin Invest* 127:437-446.
- Huang N, Chelliah Y, Shan Y, Taylor CA, Yoo SH, Partch C, Green CB, Zhang H, Takahashi JS (2012). Crystal structure of the heterodimeric CLOCK:BMAL1 transcriptional activator complex. *Science* 337:189-194.
- Ikegaya Y, Delcroix I, Iwakura Y, Matsuki N, Nishiyama N (2013). Interleukin-1 β abrogates long-term depression of hippocampal CA1 synaptic transmission. *Synapse* 47:54-7.
- Jagannath A, Butler R, Godinho SIH, Couch Y, Brown LA, Vasudevan SR, Flanagan KC, Anthony D, Churchill GC, Wood MJA, Steiner G, Ebeling M, Hossbach M, Wettstein JG, Duffield GE, Gatti S, Hankins MW, Foster RG, Peirson SN (2013). The CRTCL1-SIK1 pathway regulates entrainment of the circadian clock. *Cell* 154:1100-1111.
- Jagota A (2005). Aging and sleep disorders. *Indian J gerontol* 19:415-424.
- Jagota A (2012). Age-Induced Alterations in Biological Clock: Therapeutic Effects of Melatonin. In *Brain Aging and Therapeutic Interventions*, Springer 111-129.
- Jagota A, Kalyani D (2010). Effect of melatonin on age induced changes in daily serotonin rhythms in suprachiasmatic nucleus of male Wistar rat. *Biogerontology* 11:299-308.
- Jagota A, Mattam U (2017). Daily chronomics of proteomic profile in aging and rotenone-induced Parkinson's disease model in male Wistar rat and its modulation by melatonin. *Biogerontology* 18:615-630.
- Jagota A, Reddy MY (2007) The effect of curcumin on ethanol induced changes in suprachiasmatic nucleus (SCN) and pineal. *Cell Mol Neurobiol.* 27:997-1006
- Jones CR, Huang AL, Ptáček LJ, Fu YH (2013). Genetic Basis of Human Circadian Rhythm Disorders. *Exp Neurol* 243:28-33.
- Jones JR, Simon T, Lones L, Herzog ED (2018). SCN VIP Neurons Are Essential for Normal Light-Mediated Resetting of the Circadian System. *J Neurosci* 38:7986-7995.
- Journiac N, Jolly S, Jarvis C, Gautheron V, Rogard M, Trembleau A, Blondeau JP, Mariani J, Vernet-der Garabedian B. The nuclear receptor ROR α exerts a bi-directional regulation of IL-6 in resting and reactive astrocytes. *Proc Natl Acad Sci U S A* 106:21365-21370.
- Kaltschmidt B, Kaltschmidt C (2015). NF-KappaB in long-term memory and structural plasticity in the adult mammalian brain. *Front Mol Neurosci* 8:69.
- Keller M, Mazuch J, Abraham U, Eom GD, Herzog ED, Volk HD, Kramer A, Maier B (2009). A circadian clock in macrophages controls inflammatory immune responses. *Proc Natl Acad Sci U S A* 106:21407-21412.
- Kettenmann H, Hanisch UK, Noda M, Verkhratsky A (2011). Physiology of microglia. *Physiological reviews* 91:461-553.
- Kim P, Oster H, Lehnert H, Schmid SM, Salamat N, Barclay JL, Maronde E, Inder W, Rawashdeh O (2019). Coupling the Circadian Clock to Homeostasis: The Role of Period in Timing Physiology. *Endocr Rev* 40:66-95.
- Kramer A, Yang FC, Snodgrass P, Li X, Scammell TE, Davis FC, Weitz CJ (2001). Regulation of daily locomotor activity and sleep by hypothalamic EGF receptor signaling. *Science* 294:2511-2515.

- Kubera M, Maes M, Kenis G, Kim YK, Lasoń W (2005). Effects of serotonin and serotonergic agonists and antagonists on the production of tumor necrosis factor α and interleukin-6. *Psychiatry Res.* 134:251-258.
- Kukkemane K, Jagota A (2019). Therapeutic effects of curcumin on age-induced alterations in daily rhythms of clock genes and Sirt1 expression in the SCN of male Wistar rats. *Biogerontology* 20:405-419.
- Kwon Huh1, Hee-Kyung Hong3, Izabela Kornblum2, Vivek Kumar1,2, Nobuya Koike1, Ming
- Kwon I, Lee J, Chang SH, Jung NC, Lee BJ, Son GH, Kim K, Lee KH (2006). BMAL1 shuttling controls transactivation and degradation of the CLOCK/BMAL1 heterodimer. *Mol Cell Biol* 26:7318-7330.
- Ledford H, Callaway E (2017). Circadian clocks scoop Nobel Prize. *Nature* 550:18-18.
- Lee CC (2005). The circadian clock and tumor suppression by mammalian period genes. *Methods Enzymol* 393:852-861.
- Lee Y, Lee J, Kwon I, Nakajima Y, Ohmiya Y, Son GH, Lee KH, Kim K (2010). Coactivation of the CLOCK-BMAL1 complex by CBP mediates resetting of the circadian clock. *J Cell Sci* 123:3547-3557.
- Li H, Satinoff E (1998). Fetal tissue containing the suprachiasmatic nucleus restores multiple circadian rhythms in old rats. *Am J Physiol* 275:1735-1744.
- Li JD, Burton KJ, Zhang C, Hu SB, Zhou QY (2009). Vasopressin receptor V1a regulates circadian rhythms of locomotor activity and expression of clock-controlled genes in the suprachiasmatic nuclei. *Am J Physiol Regul Integr Comp Physiol* 296:824-830.
- Li S, Lin JD (2015). Transcriptional control of circadian metabolic rhythms in the liver. *Diabetes Obes Metab* 1:33-38.
- Liu Y, Chen Y, Zhang J, Liu Y, Zhang Y, Su Z. Retinoic acid receptor-related orphan receptor α stimulates adipose tissue inflammation by modulating endoplasmic reticulum stress. *J Biol Chem* 292:13959-13969.
- Liu Z, Patil IY, Jiang T, Sancheti H, Walsh JP, Stiles BL, Yin F, Cadenas E (2015). High-fat diet induces hepatic insulin resistance and impairment of synaptic plasticity. *PloS one* 10:e0128274.
- Logan RW, Wynne O, Levitt D, Price D, Sarkar DK (2013). Altered Circadian Expression of Cytokines and Cytolytic Factors in Splenic Natural Killer Cells of Per1^{-/-} Mutant Mice. *J Interferon Cytokine Res* 33:108-114.
- López-Otín C, Blasco MA, Partridge L, Serrano M, Kroemer G (2013). The hallmarks of aging. *Cell* 153:1194-217.
- Luo XG, Ding JQ, Chen SD (2010). Microglia in the aging brain: relevance to neurodegeneration. *Mol Neurodegener* 5:12.
- Maeso-Díaz R, Ortega-Ribera M, Fernández-Iglesias A, Hide D, Muñoz L, Hessheimer AJ, Vila S, Francés R, Fondevila C, Albillos A, Peralta C (2018). Effects of aging on liver microcirculatory function and sinusoidal phenotype. *Aging cell* 17:e12829.
- Manikonda PK, Jagota A (2012). Melatonin administration differentially affects age-induced alterations in daily rhythms of lipid peroxidation and antioxidant enzymes in male rat liver. *Biogerontology* 13:511-524.
- Martin F, Kearney JF (2002). Marginal-zone B cells. *Nat Rev Immunol.* 2:323-335.

- Mattam U, Jagota A (2014). Differential role of melatonin in restoration of age-induced alterations in daily rhythms of expression of various clock genes in suprachiasmatic nucleus of male Wistar rats. *Biogerontology* 15:257-268.
- Mattam U, Jagota A (2014). Differential role of melatonin in restoration of age-induced alterations in daily rhythms of expression of various clock genes in suprachiasmatic nucleus of male Wistar rats. *Biogerontology* 15:257-268.
- McLean AJ, Cogger VC, Chong GC, Warren A, Markus AM, Dahlstrom JE, Le Couteur DG (2003). Age-related pseudocapillarization of the human liver. *The Journal of Pathology: J Pathol* 200:112-117.
- Mebius RE, Kraal G (2005). Structure and function of the spleen. *Nat Rev Immunol* 5:606-16.
- Mieda M, Ono D, Hasegawa E, Okamoto H, Honma K, Honma S, Sakurai T (2015). Cellular clocks in AVP neurons of the SCN are critical for interneuronal coupling regulating circadian behavior rhythm. *Neuron* 85:1103-1016.
- Mohawk JA, Takahashi JS (2011). Cell autonomy and synchrony of suprachiasmatic nucleus circadian oscillators *Trends Neurosci* 34:349-358.
- Moravcová S, Pačesová D, Melkes B, Kyclerová H, Spišská V, Novotný J, Bendová Z (2018). The day/night difference in the circadian clock's response to acute lipopolysaccharide and the rhythmic Stat3 expression in the rat suprachiasmatic nucleus. *PLoS one* 13:e0199405.
- Morin LP (2007). SCN Organization Reconsidered. *J Biol Rhythms* 22:3-13.
- Nakagawa Y, Chiba K (2014). Role of microglial m1/m2 polarization in relapse and remission of psychiatric disorders and diseases. *Pharmaceuticals (Basel)* 7:1028-1048.
- Nakamura TJ, Nakamura W, Yamazaki S, Kudo T, Cutler T, Colwell CS, Block GD (2011). Age-related decline in circadian output. *J Neurosci* 31:10201-10205.
- Nakao A, Nakamura Y, Shibata S (2015). The circadian clock functions as a potent regulator of allergic reaction. *Allergy* 70:467-473.
- Nakazato R, Hotta S, Yamada D, Kou M, Nakamura S, Takahata Y, Tei H, Numano R, Hida A, Shimba S, Mieda M (2017). The intrinsic microglial clock system regulates interleukin-6 expression. *Glia* 65:198-208.
- Nakazato R, Takarada T, Yamamoto T, Hotta S, Hinoi E, Yoneda Y (2011). Selective upregulation of Per1 mRNA expression by ATP through activation of P2X7 purinergic receptors expressed in microglial cells. *J Pharmacol Sci* 2011:1107080583.
- Narasimamurthy R, Hatori M, Nayak SK, Liu F, Panda S, Verma IM (2012). Circadian clock protein cryptochrome regulates the expression of proinflammatory cytokines. *Proc Natl Acad Sci U S A* 109:12662-12667.
- Narasimamurthy R, Hatori M, Nayak SK, Liu F, Panda S, Verma IM (2012). Circadian clock protein cryptochrome regulates the expression of proinflammatory cytokines. *Proc Natl Acad Sci U S A* 109:12662-12667.
- Nimmerjahn A, Kirchhoff F, Helmchen F (2005). Resting microglial cells are highly dynamic surveillants of brain parenchyma in vivo. *Science* 308:1314-1318.
- Nobis CC, Labrecque N, Cermakian N (2016). Circadian control of antigen-specific T cell responses. *Chrono Physiol Ther* 6:65-74.

- Noguchi T, Leise TL, Kingsbury NJ, Diemer T, Wang LL, Henson MA, Welsh DK (2017). Calcium Circadian Rhythmicity in the Suprachiasmatic Nucleus: Cell Autonomy and Network Modulation. *eNeuro* 18;4. pii: ENEURO.0160-17.2017.
- Norden DM, Godbout JP (2013). Microglia of the aged brain: primed to be activated and resistant to regulation. *NeuroPathol Appl Neurobiol* 39:19-34.
- Nozaki Y, Hino S, Ri J, Sakai K, Nagare Y, Kawanishi M, Niki K, Funauchi M, Matsumura I (2017). Lipopolysaccharide-Induced Acute Kidney Injury Is Dependent on an IL-18 Receptor Signaling Pathway. *Int J Mol Sci* 18:2777.
- Oishi Y, Hayashi S, Isagawa T, Oshima M, Iwama A, Shimba S, Okamura H, Manabe I. Bmal1 regulates inflammatory responses in macrophages by modulating enhancer RNA transcription. *Sci Rep* 7:7086.
- Okada K, Yano M, Doki Y, Azama T, Iwanaga H, Miki H, Nakayama M, Miyata H, Takiguchi S, Fujiwara Y, Yasuda T (2008). Injection of LPS causes transient suppression of biological clock genes in rats. *J Surg Res* 145:5-12.
- Paolicelli RC, Bolasco G, Pagani F, Maggi L, Scianni M, Panzanelli P, Giustetto M, Ferreira TA, Guiducci E, Dumas L, Ragozzino D (2011). Synaptic pruning by microglia is necessary for normal brain development. *Science* 333:1456-1458.
- Park J, Miyakawa T, Shiokawa A, Nakajima-Adachi H, Tanokura M, Hachimura S (2014). Splenic stromal cells from aged mice produce higher levels of IL-6 compared to young mice. *Mediators Inflamm* 2014:826987.
- Parkhurst CN, Yang G, Ninan I, Savas JN, Yates III JR, Lafaille JJ, Hempstead BL, Littman DR, Gan WB (2013). Microglia promote learning-dependent synapse formation through brain-derived neurotrophic factor. *Cell* 155:1596-1609.
- Partch CL, Green CB, Takahashi JS (2014). Molecular architecture of the mammalian circadian clock. *Trends Cell Biol* 24:90-99.
- Pelegrí C, Vilaplana J, Castellote C, Rabanal M, Franch À, Castell M (2003). Circadian rhythms in surface molecules of rat blood lymphocytes. *Am J Physiol Cell Physiol* 284:67-76.
- Pizarro A, Hayer K, Lahens NF, Hogenesch JB (2013). CircaDB: a database of mammalian circadian gene expression profiles. *Nucleic Acids Res* 41:1009-1013.
- Poulose N, Raju R (2014). Aging and injury: alterations in cellular energetics and organ. *Aging Dis* 5:101-108.
- Prendergast BJ, Cable EJ, Patel PN, Pyter LM, Onishi KG, Stevenson TJ, Ruby NF, Bradley SP (2013). Impaired leukocyte trafficking and skin inflammatory responses in hamsters lacking a functional circadian system. *Brain Behav Immun* 32:94-104.
- Prendergast BJ, Cable EJ, Patel PN, Pyter LM, Onishi KG, Stevenson TJ, Ruby NF, Bradley SP (2013). Impaired leukocyte trafficking and skin inflammatory responses in hamsters lacking a functional circadian system. *Brain Behav Immun* 32:94-104.
- Priller J, Flügel A, Wehner T, Boentert M, Haas CA, Prinz M, Fernández-Klett F, Prass K, Bechmann I, de Boer BA, Frotscher M (2001). Targeting gene-modified hematopoietic cells to the central nervous system: use of green fluorescent protein uncovers microglial engraftment. *Nat med* 7:1356.
- Raghuram S, Stayrook KR, Huang P, Rogers PM, Nosie AK, McClure DB, Burris LL, Khorasanizadeh S, Burris TP, Rastinejad F (2007). Identification of heme as the ligand for the orphan nuclear receptors REV-ERB α and REV-ERB β . *Nat Struct Mol Biol* 14:1207-1213.

- Ransohoff RM, Cardona AE (2010). The myeloid cells of the central nervous system parenchyma. *Nature* 468:253.
- Reddy AB, Maywood ES (2007). Circadian Rhythms: Perturbations in the Liver Clock. *Curr Biol* 17:292-294.
- Reddy MY, Jagota A (2015). Melatonin has differential effects on age-induced stoichiometric changes in daily chronomics of serotonin metabolism in SCN of male Wistar rats. *Biogerontology* 16:285-302.
- Reghunandan, V, Reghunandan, R (2006). Neurotransmitters of the suprachiasmatic nuclei. *J Circadian Rhythm* 4:2.
- Reinke H, Asher G (2016). Circadian Clock Control of Liver Metabolic Functions. *Gastroenterology* 150:574-80.
- Ribas-Latre A, Baselga-Escudero L, Casanova E, Arola-Arnal A, Salvadó MJ, Bladé C, Arola L (2015). Dietary proanthocyanidins modulate BMAL1 acetylation, Npm1 expression and NAD levels in rat liver. *Sci Rep* 5:10954.
- Rohman MS, Emoto N, Nonaka H, Okura R, Nishimura M, Yagita K, Van Der Horst GT, Matsuo M, Okamura H, Yokoyama M (2005). Circadian clock genes directly regulate expression of the Na⁺/H⁺ exchanger NHE3 in the kidney. *Kidney Int* 67:1410-1419.
- Rosadini CV, Kagan JC (2017). Early innate immune responses to bacterial LPS. *Curr Opin Immunol* 44:14-19.
- Saderi N, Cazarez-Márquez F, Buijs FN, Salgado-Delgado RC, Guzman-Ruiz MA, del Carmen Basualdo M, Escobar C, Buijs RM (2013). The NPY intergeniculate leaflet projections to the suprachiasmatic nucleus transmit metabolic conditions. *Neuroscience* 246:291-300.
- Saijo K, Glass CK (2011). Microglial cell origin and phenotypes in health and disease. *Nat Rev Immunol* 11:775.
- Sakai T, Tamura T, Kitamoto T, Kidokoro Y (2004). A clock gene, period, plays a key role in long-term memory formation in *Drosophila*. *Proc Natl Acad Sci U S A* 101:16058-63.
- Sato S, Sakurai T, Ogasawara J, Takahashi M, Izawa T, Imaizumi K, Taniguchi N, Ohno H, Kizaki T (2014). A circadian clock gene, *Rev-erba*, modulates the inflammatory function of macrophages through the negative regulation of *Ccl2* expression. *The Jour of Immuno* 192:407-417.
- Satoh A, Shimosegawa T, Fujita M, Kimura K, Masamune A, Koizumi M, Toyota T (1999). Inhibition of nuclear factor- κ B activation improves the survival of rats with taurocholate pancreatitis. *Gut* 44:253-258.
- Sawada H, Hishida R, Hirata Y, Ono K, Suzuki H, Muramatsu SI, Nakano I, Nagatsu T, Sawada M (2007). Activated microglia affect the nigro-striatal dopamine neurons differently in neonatal and aged mice treated with 1-methyl-4-phenyl-1, 2, 3, 6-tetrahydropyridine. *J Neurosci Res* 85:1752-1761.
- Schafer DP, Lehrman EK, Kautzman AG, Koyama R, Mardinly AR, Yamasaki R, Ransohoff RM, Greenberg ME, Barres BA, Stevens B (2012). Microglia sculpt postnatal neural circuits in an activity and complement-dependent manner. *Neuron* 74:691-705.
- Scheiermann C, Gibbs J, Ince L, Loudon A (2018). Clocking in to immunity. *Nat Rev Immunol* 18:423.
- Scheiermann C, Kunisaki Y, Frenette PS (2013). Circadian control of the immune system. *Nature Reviews Immunology* 13:190.
- Scheiermann C, Kunisaki Y, Lucas D, Chow A, Jang JE, Zhang D, Hashimoto D, Merad M, Frenette PS (2012). Adrenergic nerves govern circadian leukocyte recruitment to tissues. *Immunity* 37:290-301.

- Schibler U, Gotic I, Saini C, Gos P, Curie T, Emmenegger Y, Sinturel F, Gosselin P, Gerber A, Fleury-Olela F, Rando G (2015). Clock-talk: interactions between central and peripheral circadian oscillators in mammals. *Cold Spring Harb Symp Quant Biol* 80:223-232.
- Schwartz M, Shechter R (2010). Systemic inflammatory cells fight off neurodegenerative disease. *Nat Rev Neurol* 6:405.
- Seung-Hee Yoo, Jennifer A. Mohawk^{1,2,7}, Sandra M. Siepka^{3,7}, Yongli Shan¹, Seong
- Sharaf A, Krieglstein K, Spittau B (2013). Distribution of microglia in the postnatal murine nigrostriatal system. *Cell Tissue Res* 351:373-382.
- Sharma VK (2003). Adaptive significance of circadian clocks. *Chronobiol Int* 20:901-919.
- Shimizu T, Watanabe K, Anayama N, Miyazaki K (2017). Effect of lipopolysaccharide on circadian clock genes *Per2* and *Bmal1* in mouse ovary. *J Physiol Sci* 67:623-628.
- Sierra A, Gottfried-Blackmore AC, McEwen BS, Bulloch K (2007). Microglia derived from aging mice exhibit an altered inflammatory profile. *Glia* 55:412-24.
- Silver AC, Arjona A, Walker WE, Fikrig E (2012). The circadian clock controls toll-like receptor 9-mediated innate and adaptive immunity. *Immunity* 36:251-261.
- Singh R, Sharma S, Singh RK, Cornelissen G (2016). Circadian time structure of circulating plasma lipid components in healthy Indians of different age groups. *Indian J Clin Biochem* 31:215-223.
- Sládek M, Rybová M, Jindráková Z, Zemanová Z, Polidarová L, Mrnka L, O'Neill J, Pácha J, Sumová A (2007). Insight into the circadian clock within rat colonic epithelial cells. *Gastroenterology* 133:1240-1249.
- Solt LA, Kojetin DJ, Burris TP (2011). The REV-ERBs and RORs: molecular links between circadian rhythms and lipid homeostasis. *Future Med Chem* 3:623-38.
- Solt LA, Wang Y, Banerjee S, Hughes T, Kojetin DJ, Lundasen T, Shin Y, Liu J, Cameron MD, Noel R, Yoo SH (2012). Regulation of circadian behaviour and metabolism by synthetic REV-ERB agonists. *Nature* 485:62.
- Squarzoni P, Oller G, Hoeffel G, Pont-Lezica L, Rostaing P, Low D, Bessis A, Ginhoux F, Garel S (2014). Microglia modulate wiring of the embryonic forebrain. *Cell Rep* 8:1271-1279.
- Stahl EC, Haschak MJ, Popovich B, Brown BN (2018). Macrophages in the Aging Liver and Age-Related Liver Disease. *Front Immunol* 9:2795.
- Stapleton CM, Jaradat M, Dixon D, Kang HS, Kim SC, Liao G, Carey MA, Cristiano J, Moorman MP, Jetten AM (2005). Enhanced susceptibility of staggerer (*ROR α sg/sg*) mice to lipopolysaccharide-induced lung inflammation. *Am J Physiol Lung Cell Mol Physiol* 289:144-152.
- Stojiljkovic MR, Ain Q, Bondeva T, Heller R, Schmeer C, Witte OW (2019). Phenotypic and functional differences between senescent and aged murine microglia. *Neurobiol Aging* 74:56-69.
- Stow LR, Gumz ML (2011). The circadian clock in the kidney. *J Am Soc Nephrol* 22:598-604.
- Sun Y, Yang Z, Niu Z, Peng J, Li Q, Xiong W, Langnas AN, Ma MY, Zhao Y (2006). MOP3, a component of the molecular clock, regulates the development of B cells. *Immunology* 119:451-60.
- Swirski FK, Nahrendorf M, Etzrodt M, Wildgruber M, Cortez-Retamozo V, Panizzi P, Figueiredo JL, Kohler RH, Chudnovskiy A, Waterman P, Aikawa E (2009). Identification of splenic reservoir monocytes and their deployment to inflammatory sites. *Science* 325:612-616.

- Takahashi JS (2017). Transcriptional architecture of the mammalian circadian clock. *Nat Rev Genet* 18:164-179.
- Takeda Y, Jothi R, Birault V, Jetten AM (2012). ROR γ directly regulates the circadian expression of clock genes and downstream targets in vivo. *Nucleic Acids Res* 40:8519-35.
- Taraborrelli C, Palchykova S, Tobler I, Gast H, Birchler T, Fontana A (2011). TNFR1 is essential for CD40, but not for lipopolysaccharide-induced sickness behavior and clock gene dysregulation. *Brain Behav Immun* 25:434-442.
- Tietz NW, Shuey DF, Wekstein DR (1992). Laboratory values in fit aging individuals--sexagenarians through centenarians. *Clin Chem* 38:1167-1185.
- Toh KL, Jones CR, He Y, Eide EJ, Hinz WA, Virshup DM, Ptáček LJ, Fu YH (2001). An hPer2 phosphorylation site mutation in familial advanced sleep phase syndrome. *Science* 291:1040-1043.
- Tremblay MÈ, Lowery RL, Majewska AK (2010). Microglial interactions with synapses are modulated by visual experience. *PLoS Biol* 8:e1000527.
- Tsukahara S, Tanaka S, Ishida K, Hoshi N, Kitagawa H (2005). Age-related change and its sex differences in histoarchitecture of the hypothalamic suprachiasmatic nucleus of F344/N rats. *Exp Gerontol* 40:147-55.
- Turek FW, Joshu C, Kohsaka A, Lin E, Ivanova G, McDearmon E, Laposky A, Losee-Olson S, Easton A, Jensen DR, Eckel RH (2005). Obesity and metabolic syndrome in circadian Clock mutant mice. *Science* 308:1043-1045.
- Turner VM, Mabbott NA (2017). Ageing adversely affects the migration and function of marginal zone B cells. *Immunology* 151:349-362.
- Turner VM, Mabbott NA (2017b). Influence of ageing on the microarchitecture of the spleen and lymph nodes. *Biogerontology* 18:723-738.
- Ueda HR, Hayashi S, Chen W, Sano M, Machida M, Shigeyoshi Y, Iino M, Hashimoto S (2005). System-level identification of transcriptional circuits underlying mammalian circadian clocks. *Nat Genet* 37:187-92.
- Van Cauter E, Leproult R, Kupfer DJ (1996). Effects of gender and age on the levels and circadian rhythmicity of plasma cortisol. *J Clin Endocrinol Metab* 81:2468-2473.
- VanGuilder HD, Bixler GV, Brucklacher RM, Farley JA, Yan H, Warrington JP, Sonntag WE, Freeman WM (2011). Concurrent hippocampal induction of MHC II pathway components and glial activation with advanced aging is not correlated with cognitive impairment. *J Neuroinflammation* 8:138.
- Vinod C, Jagota A (2016). Daily NO rhythms in peripheral clocks in aging male Wistar rats: Protective effects of exogenous melatonin. *Biogerontology* 17:859-71.
- Vinod C, Jagota A (2017). Daily Socs1 rhythms alter with aging differentially in peripheral clocks in male Wistar rats: therapeutic effects of melatonin. *Biogerontology* 18:333-45.
- von Bernhardi R (2007). Glial cell dysregulation: a new perspective on Alzheimer disease. *Neurotox Res* 12215-12232.
- Wagner S, Sagiv N, Yarom Y (2001). GABA-induced current and circadian regulation of chloride in neurones of the rat suprachiasmatic nucleus. *J Physiol* 537:853-869.

- Wakabayashi H, Nishiyama Y, Ushiyama T, Maeba T, Maeta H (2002). Evaluation of the effect of age on functioning hepatocyte mass and liver blood flow using liver scintigraphy in preoperative estimations for surgical patients: comparison with CT volumetry. *J Surg Res* 106:246-253.
- Wang GL, Salisbury E, Shi X, Timchenko L, Medrano EE, Timchenko NA (2008). HDAC1 cooperates with C/EBP α in the inhibition of liver proliferation in old mice. *J Biol Chem* 283:26169-26178.
- Wang T, Wang Z, Yang P, Xia L, Zhou M, Wang S, Du J, Zhang J (2016). PER1 prevents excessive innate immune response during endotoxin-induced liver injury through regulation of macrophage recruitment in mice. *Cell Death Dis* 7:e2176.
- Wang Y, Chen F, Rudic D, Fulton D. LPS induced circadian phase shift in macrophages. *J Immunol* 185:5796-5805.
- Wardyn JD, Ponsford AH, Sanderson CM (2015). Dissecting molecular cross-talk between Nrf2 and NF- κ B response pathways. *Biochem Soc Trans* 43:621-626.
- Wątroba M, Szukiewicz D (2016). The role of sirtuins in aging and age-related diseases. *Adv Med Sci* 61:52-62
- Webb IC, Coolen LM, Lehman MN (2013). NMDA and PACAP receptor signaling interact to mediate retinal-induced scn cellular rhythmicity in the absence of light. *PLoS One* 8:e76365.
- Wijisman CA, Van Heemst D, Hoogeveen ES, Slagboom PE, Maier AB, De Craen AJ, Van Der Ouderaa F, Pijl H, Westendorp RG, Mooijaart SP (2013). Ambulant 24-h glucose rhythms mark calendar and biological age in apparently healthy individuals. *Aging Cell* 12:207-213.
- Wu YH, Zhou JN, Van Heerikhuizen J, Jockers R, Swaab DF (2007). Decreased MT1 melatonin receptor expression in the suprachiasmatic nucleus in aging and Alzheimer's disease. *Neurobiol Aging* 28:1239-1247.
- Xi Y, Shao F, Bai XY, Cai G, Lv Y, Chen X (2014). Changes in the expression of the Toll-like receptor system in the aging rat kidneys. *PLoS One* 9:e96351.
- Xu XY, Meng X, Li S, Gan RY, Li Y, Li HB (2018). Bioactivity, health benefits, and related molecular mechanisms of curcumin: Current progress, challenges, and perspectives. *Nutrients* 10:1553.
- Yamazaki S, Straume M, Tei H, Sakaki Y, Menaker M, Block GD (2002). Effects of aging on central and peripheral mammalian clocks. *Proc Natl Acad Sci U S A* 99:10801-10806.
- Yang G, Chen L, Grant GR, Paschos G, Song WL, Musiek ES, Lee V, McLoughlin SC, Grosser T, Cotsarelis G, FitzGerald GA (2016). Timing of expression of the core clock gene Bmal1 influences its effects on aging and survival. *Sci Transl Med* 8:324ra16.
- Yang L, Chu Y, Wang LA, Wang Y, Zhao X, He W, Zhang P, Yang X, Liu X, Tian L, Li B (2015). Overexpression of CRY1 protects against the development of atherosclerosis via the TLR/NF- κ B pathway. *Int Immunopharmacol* 28:525-530.
- Yang L, Chu Y, Wang LA, Wang Y, Zhao X, He W, Zhang P, Yang X, Liu X, Tian L, Li B (2015). Overexpression of CRY1 protects against the development of atherosclerosis via the TLR/NF- κ B pathway. *Int Immunopharmacol* 28:525-530.
- Yang N, Williams J, Pekovic-Vaughan V, Wang P, Olabi S, McConnell J, Gossan N, Hughes A, Cheung J, Streuli CH, Meng QJ (2017). Cellular mechano-environment regulates the mammary circadian clock. *Nat Commun* 8:14287.
- Ye SM, Johnson RW (1999). Increased interleukin-6 expression by microglia from brain of aged mice. *J Neuroimmunol* 93:139-148.

- Yin L, Wu N, Curtin JC, Qatanani M, Szewergold NR, Reid RA, Waitt GM, Parks DJ, Pearce KH, Wisely GB, Lazar MA (2007). Rev-erb α , a heme sensor that coordinates metabolic and circadian pathways. *Science* 318:1786-1789.
- Yoo S, Mohawk JA, Slepka SM, Shan Y, Huh SK, Hong H, Kornblum I, Kumar V, Koike N, Xu M, Nussbaum J, Liu X, Chen Z, Chen ZJ, Green CB, Takahashi JS (2013). Competing E3 Ubiquitin Ligases Determine Circadian Period by Regulated Degradation of CRY in Nucleus and Cytoplasm. *Cell* 152: 1091–1105.
- Yoo SH, Yamazaki S, Lowrey PL, Shimomura K, Ko CH, Buhr ED, Slepka SM, Hong HK, Oh WJ, Yoo OJ, Menaker M (2004). PERIOD2:: LUCIFERASE real-time reporting of circadian dynamics reveals persistent circadian oscillations in mouse peripheral tissues. *Proc Natl Acad Sci U S A* 101:5339-5346.
- Zeeh J, Platt D. The aging liver: structural and functional changes and their consequences for drug treatment in old age. *Gerontology* 48:121-127.
- Zhang R, Lahens NF, Ballance HI, Hughes ME, Hogenesch JB (2014). A circadian gene expression atlas in mammals: implications for biology and medicine. *Proc Natl Acad Sci U S A* 111:16219-16224.
- Zhong X, Yu J, Frazier K, Weng X, Li Y, Cham CM, Dolan K, Zhu X, Hubert N, Tao Y, Lin F (2018). Circadian Clock Regulation of Hepatic Lipid Metabolism by Modulation of m6A mRNA Methylation. *Cell Rep* 25:1816-1828.
- Zhou H, S Beevers C, Huang S (2011). The targets of curcumin. *Curr Drug Target* 12:332-347.
- Zuber AM, Centeno G, Pradervand S, Nikolaeva S, Maquelin L, Cardinaux L, Bonny O, Firsov D (2009). Molecular clock is involved in predictive circadian adjustment of renal function. *Proc Natl Acad Sci U S A* 106:16523-16528.

Appendices

List of Figures

Figure no.	Page no.
Fig. 2: Figure depicting the circadian patterns	2
Fig. 2: Phase response curves of circadian rhythms	3
Fig. 3: Suprachiasmatic nucleus location and compartmentalization	5
Fig. 4: Afferent pathways of the SCN	6
Fig. 5: Efferent pathways of the SCN	7
Fig. 6: Melatonin synthesis pathway	8
Fig. 7: Molecular circadian gene network in mammals	10
Fig. 8: Light induced Per1 expression	12
Fig. 9: Peripheral clocks	13
Fig. 10: Integrative role of circadian clock	14
Fig. 11: Clock regulating the immune system	16
Fig. 12: Hallmarks of aging	17
Fig. 13: Schematic diagram showing various sleep disorders with aging	18
Fig. 14: Receptors regulating resting microglia	20
Fig. 15: Homeostatic functions of microglia	21
Fig. 16: Activation and polarization of microglia	22
Fig. 17: Resolution of microglia activation	23
Fig. 18: Microglial priming in the aged brain	25
Fig. 19: Age-primed microglia hypothesis of Parkinson's disease	26
Fig. 20: Circadian regulation of liver physiology	27
Fig. 21: Circadian disruption in liver and metabolic disorders	28
Fig. 22: Aging and liver disease	29

Fig. 23: Intrinsic circadian clocks in the kidneys	30
Fig. 24: Macroscopic and microscopic changes in the aging kidney and risk factors	31
Fig. 25: Temporal interactions between neuroendocrine and immune system	32
Fig. 26: NF- κ B target genes involved in inflammation development and progression	34
Fig. 27: Overview of the function of platelets and serotonin in inflammation and immunity	35
Fig. 28: Curcumin chemical structure	36
Fig. 29: A summary of the bioactivity and health benefits of curcumin	36
Fig. 30: Dissociation curves for clock, immune and microglia resting genes showing single peak	47
Fig. 31: Chromatograph showing the retention time for 5-HT	48
Fig. 32: Flowcytometry quadrant showing the microglial population	51
Fig. 33: Effect of curcumin administration on daily rhythms of various clock genes mRNA expression in microglia	57
Fig. 34: Effect of curcumin administration on daily rhythms of various immune genes mRNA expression in microglia	58
Fig. 35: Effect of curcumin administration on daily rhythms of microglia resting genes mRNA expression in microglia	59
Fig. 36: Effect of curcumin administration on mean 24 h levels of clock, immune and microglia resting genes in microglia	60
Fig. 37: Effect of curcumin administration on daily pulse of clock, immune, microglia resting genes in microglia	61
Fig. 38: Effect of curcumin administration on Pair wise correlations among clock, immune and microglia resting genes in microglia	63
Fig. 39: WGCNA analysis between clock, immune and microglia gene clusters in microglia	64
Fig. 40: Effect of curcumin administration on daily rhythms of clock genes in liver	82
Fig. 41: Effect of curcumin administration on daily rhythms of immune genes in liver	83
Fig. 42: Effect of curcumin administration on mean 24 h levels of clock and immune genes in liver	84
Fig. 43: Effect of curcumin administration on daily pulse of clock and immune genes in liver	85
Fig. 44: Effect of curcumin administration on Pair wise correlations between clock and immune genes in liver	86
Fig. 45: WGCNA analysis between clock and immune gene clusters in liver	88
Fig. 46: Effect of curcumin administration on daily rhythms of clock genes in kidney	93

Fig. 47: Effect of curcumin administration on daily rhythms of immune genes in kidney	94
Fig. 48: Effect of curcumin administration on mean 24 h levels of clock and immune genes in kidney	95
Fig. 49: Effect of curcumin administration on daily pulse of clock and immune genes in kidney	96
Fig. 50: Effect of curcumin administration on Pair wise correlations between clock and immune genes in kidney	98
Fig. 51: WGCNA analysis between clock and immune gene clusters in kidney	100
Fig. 52: Effect of curcumin administration on daily rhythms of clock genes in spleen	106
Fig. 53: Effect of curcumin administration on daily rhythms of immune genes in spleen	107
Fig. 54: Effect of curcumin administration on mean 24 h levels of clock and immune genes in spleen	108
Fig. 55: Effect of curcumin administration on Daily pulse of clock and immune genes in spleen	109
Fig. 56: Effect of curcumin administration on Pair wise correlations between clock and immune genes in spleen	111
Fig. 57: WGCNA analysis between clock and immune gene clusters in spleen	112
Fig. 58: Effect of curcumin administration on daily rhythms of 5-HT in liver, kidney and spleen	115
Fig. 59: Effect of curcumin administration on (a) Mean 24 hour (h) levels and (b) Daily pulse of 5-HT in liver, kidney and spleen	116
Fig. 60: Effect of PDTC on LPS induced alterations of daily rhythms of clock, immune and microglia resting genes in microglia	127
Fig. 61: Effect of PDTC on LPS induced alterations of Mean 24 h levels of clock, immune and microglia resting genes in microglia	128
Fig. 62: Effect of PDTC on LPS induced alterations of Daily pulse of clock, immune and microglia resting genes in microglia	129
Fig. 63: Effect of PDTC on LPS induced alterations of Pair wise correlations among clock, immune and microglia resting genes in microglia	130
Fig. 64 WGCNA analysis among clock, immune and microglia resting genes in microglia	131
Fig. 65: Effect of PDTC on LPS induced alterations of daily rhythms of clock and immune genes in liver	135
Fig. 66: Effect of PDTC on LPS induced alterations of Mean 24 h levels of clock and immune genes in liver	136
Fig. 67: Effect of PDTC on LPS induced alterations of Daily pulse of clock and immune genes in liver	137
Fig. 68: Effect of PDTC on LPS induced alterations of Pair wise correlations between clock and immune genes in liver	138
Fig. 69: WGCNA analysis between clock and immune genes clusters in liver	139
Fig. 70: Effect of PDTC on LPS induced alterations of daily rhythms of clock and immune genes in kidney	141

Fig. 71: Effect of PDTC on LPS induced alterations of Mean 24 h levels of clock and immune genes in kidney	142
Fig. 72: Effect of PDTC on LPS induced alterations of Daily pulse of clock and immune genes in kidney	143
Fig. 73: Effect of PDTC on LPS induced alterations of Pair wise correlations between clock and immune genes in kidney	144
Fig. 74: WGCNA analysis between clock and immune genes clusters in kidney	145
Fig. 75: Effect of PDTC on LPS induced alterations of daily rhythms of clock and immune genes in spleen	147
Fig. 76: Effect of PDTC on LPS induced alterations of mean 24 h levels of clock and immune genes in spleen	148
Fig. 77: Effect of PDTC on LPS induced alterations of Daily pulse of clock and immune genes in spleen	149
Fig. 78: Effect of PDTC on LPS induced alterations of Pair wise correlations between clock and immune genes in spleen	150
Fig. 79: WGCNA analysis between clock and immune genes clusters in spleen	151
Fig. 80: Graphical representation of the summary from objective I and II	171
Fig. 81: Graphical representation of the summary from objective III	172

List of Tables

S. no.	Page no.
Table 1: Components used for the cDNA synthesis.	45
Table 2: Reaction set up for cDNA synthesis	45
Table 3: components for qRT-PCR	45
Table 4: Reaction set up for qRT-PCR	45
Table 5: Primers list	46
Table 6: Effect of curcumin on age induced alterations of clock genes expression in microglia	65
Table 7: Effect of curcumin on age induced alterations of immune and microglia resting genes	66
Table 8: Effect of curcumin on age induced alterations of clock genes expression in liver	90
Table 9: Effect of curcumin on age induced alterations of immune genes expression in liver	91
Table 10: Effect of curcumin on age induced alterations of clock genes expression in kidney	102
Table 11: Effect of curcumin on age induced alterations of immune genes expression in kidney	103
Table 12: Effect of curcumin on age induced alterations of immune genes expression in spleen	110
Table 13: Effect of curcumin on age induced alterations of immune genes expression in spleen	114
Table 14: Effect of curcumin on age induced alterations of 5-HT levels	117
Table 15: Effect of NF- κ B inhibitor on LPS induced alterations of clock genes expression in microglia	132
Table 16: Effect of NF- κ B inhibitor on LPS induced alterations of immune and microglia resting genes expression in microglia	133
Table 17: Effect of NF- κ B inhibitor on LPS induced alterations of clock and immune genes in liver	140
Table 18: Effect of NF- κ B inhibitor on LPS induced alterations of clock and immune genes in kidney	146
Table 19: Effect of NF- κ B inhibitor on LPS induced alterations of clock and immune genes in spleen	152

Abbreviations

°C	:	degree centigrade/ degree Celsius
5-HIAA	:	5-Hydroxy indole acetic acid
5-HT	:	5-Hydroxytryptamine
5-HTOH	:	5-Hydroxy tryptophol
5-MIAA	:	5-Methoxy indole acetic acid
5-MTOH	:	5-Methoxy indole acetic acid
AANAT	:	Arylalkylamine N-acetyl transferase
AC	:	Adenylyl cyclase
AFMK	:	N-acetyl- N-formyl-5-methoxy kynuramine
AMK	:	N-acetyl-5-methoxy kynuramine
ANOVA	:	Analysis of Variance
ARNT	:	Arylhydrocarbon receptor nuclear translocator
Arntl	:	Arylhydrocarbon receptor nuclear translocator like
ASPS	:	Advanced Sleep Phase Syndrome
ATP	:	Adenosine triphosphate
AVP	:	Arginine vasopressin
bHLH	:	basic helix-loop-helix
Bmal1	:	Brain and muscle Arnt-like protein 1
BSA	:	Bovine serum albumin
CaM	:	Calmodulin
CAMK	:	Ca ²⁺ /calmodulin-dependent protein kinase
cAMP	:	Cyclic Adenosine Mono Phosphate
CAT	:	Catalase
CCGs	:	Clock controlled genes
CD	:	Cluster of differentiation
cDNA	:	Complementary DNA

CK	:	Casein kinase
CL	:	Cardiolipin
Clock	:	Circadian locomotor output cycles kaput
CRE	:	cAMP response element
CREB	:	cAMP response element binding protein
Cry	:	Cryptochrome
CSF	:	Cerebrospinal fluid
Ct	:	Cycle threshold
CTS	:	Circadian timekeeping system
DBP	:	D-box binding protein
DBPE	:	DBP-binding element
DD	:	constant dark
DNA	:	deoxy-ribo nucleic acid
DP	:	Dark phase
DSPS	:	Delayed Sleep Phase Syndrome
ECD	:	Electrochemical detection
EDTA	:	Ethylene di-amine tetra acetic acid
GABA	:	Gamma amino butyric acid
GHT	:	Geniculo-hypothalamic tract
Gi	:	G Inhibitory
GPCRs	:	G protein-coupled receptors
GRd	:	Glutathione reductase
GRP	:	Gastrin-releasing peptide
Gs	:	G stimulatory
GSH	:	Reduced glutathione
GSSG	:	Oxidized glutathione
h	:	Hour

HIOMT	:	Hydroxy indole -O-methyl transferase
H3	:	Histone 3
HAT	:	Histone Acetyl Transferase
HDAC	:	Histone Deacetylase
HSC	:	Hematopoietic stem cells
IGL	:	Inter-geniculate leaflet
IL	:	Interleukin
LD	:	Light Dark cycle
LGICs	:	Ligand-gated ion channels
LP	:	Light Phase
LPS	:	Lipopolysaccharide
MAO	:	Monoamine oxidase
MAPK	:	Mitogen activated protein kinase
MEK	:	Map ERK kinase
MEL	:	Melatonin
Max	:	Maximum
Min	:	Minimum
min	:	Minute
mg	:	milligram
mL	:	milliliter
mM	:	milli molar
MnSOD	:	Magnesium superoxide dismutase
mRNA	:	messenger RNA
miRNA	:	micro RNA
MT1	:	Melatonin receptor subtype1
MT2	:	Melatonin receptor subtype2
NAD ⁺	:	Nicotinamide adenine dinucleotide

NAMPT	:	Nicotinamide phosphoribosyl transferase
NAS	:	N-acetyl serotonin
NAT	:	N- Acetyl tryptamine
NE	:	Norepinephrine
NF- κ B	:	nuclear factor kappa-light-chain-enhancer of activated B cells
NO	:	Nitric Oxide
NOS	:	Nitric oxide synthase
Npas2	:	Neuronal PAS Domain Protein 2
NPY	:	Neuropeptide Y
O ₂ -	:	Superoxide anion radical
PACAP	:	Pituitary adenylyl cyclase activating peptide
PAS	:	Period-Arnt- Sim
PCD	:	Programmed cell death
PCR	:	Polymerase Chain Reaction
PD	:	Parkinson's disease
PDTC	:	Pyrrolidine dithiocarbamate
Per	:	Period
PHI	:	peptide histidine-isoleucin
PI3K	:	Phospho inositol -3 kinase
PK2	:	Prokineticin 2
PKA	:	Protein kinase A
PKC	:	Protein kinase C
PLC	:	Phospholipase C
PLMS	:	periodic leg movements in sleep
pM	:	Pico mole
qRT-PCR	:	Quantitative real time polymerase chain reaction
Rev-Erb α, β	:	Reverse-Erythroblastosis α, β

RHT	:	Retino-hypothalamic tract
RIPD	:	Rotenone induced Parkinson disease
RNA	:	Ribonucleic acid
ROR	:	Retinoic-acid related orphan nuclear receptors
RRE	:	ROR response elements
ROS	:	Reactive oxygen species
RP-HPLC	:	Reverse phase high pressure liquid chromatography
RRP	:	Retino-raphe pathway
RT	:	Room temperature
SCG	:	Superior cervical ganglion
SCN	:	Suprachiasmatic nucleus
SDB	:	Sleep disorder breathing
SDS	:	Sodium Dodecyl Sulfate
SIRT1	:	silent mating type information regulation 2 homolog 1
SIM	:	single minded protein
SN	:	Substantia nigra
SP	:	Substance P
Tlr	:	Toll like receptor
TPH	:	Tryptophan hydroxylase
TRP	:	Tryptophan
TTFL	:	Transcriptional Translational Feed back
UPS	:	Ubiquitin proteasome system
VIP	:	Vasoactive intestinal peptide
ZT	:	Zeitgeber time
µg	:	microgram
µL	:	microliter
µM	:	micro molar

Publications



Aging renders desynchronization between clock and immune genes in male Wistar rat kidney: chronobiotic role of curcumin

Neelesh Babu Thummadi · Anita Jagota

Received: 8 March 2019 / Accepted: 26 April 2019 / Published online: 16 May 2019
© Springer Nature B.V. 2019

Abstract Suprachiasmatic nucleus (SCN) contains the central clock that orchestrate circadian rhythms in physiology and behavior in mammals. Tightly interlocked transcriptional and translational feedback loops (TTFLs) comprising of various clock genes such as *Clock*, *Bmal1*, *Periods*, *Cryptochromes* etc. in the SCN, send the timing signals to peripheral clocks that governs local metabolism with similar TTFLs. Peripheral clocks in kidney regulates several circadian rhythms like blood pressure, immunity etc. However, aging leads to circadian and inflammatory disorders in kidney. Though there are increasing evidences on age associated perturbations, studies elucidating the rhythmic expression of clock and immune genes across aging in kidney are obscure. We therefore studied changes in daily rhythms of clock and immune genes in kidney. In this study we measured mRNA expression of clock genes *rBmal1*, *rPer1*, *rPer2*, *rCry1*, *rCry2*, *rRev-erb α* , *rRor α* , and inflammatory genes *rNf κ b1*, *rTnf α* , *rIl6*, *rTlr4* and *rTlr9* in 3, 12 and

24 months male Wistar rat kidney using qRT-PCR. From our study, we did not observe significant changes in clock genes expression except *rRor α* , but immune genes showed significant phase alterations as well as increase in mean 24 h levels. Pearson correlation analysis of data showed desynchronization between immune and clock genes expression. We further studied the effect of administration of curcumin which has anti-aging, anti-inflammatory, anti-oxidant etc. properties, and evaluated its chronobiotic properties. We here report differential effects of curcumin administration on daily rhythms of clock and immune genes expression.

Keywords Curcumin · Kidney · Clock genes · Immune genes · Aging · Peripheral clock

Introduction

In mammals, Suprachiasmatic nucleus (SCN) contains the central clock that synchronizes physiology, behavior and metabolism to the external environmental cues (*Zeitgebers*) (Jagota 2012; Roenneberg and Merrow 2016). SCN regulates circadian rhythms by core clock genes viz. *Clock*, *Bmal1*, *Periods*, *Cryptochromes*, *Rev-erb α* , *Ror α* etc. whose expression is orchestrated at transcriptional and translational levels to establish compact feedback loops that eventually result in ~ 24 h periodicity (Jagota 2012; Takahashi 2017).

Electronic supplementary material The online version of this article (<https://doi.org/10.1007/s10522-019-09813-6>) contains supplementary material, which is available to authorized users.

N. B. Thummadi · A. Jagota (✉)
Neurobiology and Molecular Chronobiology Laboratory,
Department of Animal Biology, School of Life Sciences,
University of Hyderabad, Hyderabad 500046, India
e-mail: ajsl@uohyd.ernet.in;
anitajagota01@gmail.com

AGE-INDUCED
DESYNCHRONIZATION
BETWEEN CLOCK AND
IMMUNE GENES EXPRESSION
IN MICROGLIA AND OTHER
PERIPHERAL CLOCKS IN
MALE WISTAR RATS:
CHRONOBIOTIC ROLE OF

Submission date: 22-Jul-2019 04:53PM (UTC+0530)

Submission ID: 1154021138

File name: (1.18M)

Word count: 40033

Character count: 201622

CURCUMIN

by Neelesh Babu Thummadi

AGE-INDUCED DESYNCHRONIZATION BETWEEN CLOCK AND IMMUNE GENES EXPRESSION IN MICROGLIA AND OTHER PERIPHERAL CLOCKS IN MALE WISTAR RATS: CHRONOBIOTIC ROLE OF CURCUMIN

ORIGINALITY REPORT

39%

SIMILARITY INDEX

5%

INTERNET SOURCES

37%

PUBLICATIONS

21%

STUDENT PAPERS

PRIMARY SOURCES

1

Neelesh Babu Thummadi, Anita Jagota. "Aging renders desynchronization between clock and immune genes in male Wistar rat kidney: chronobiotic role of curcumin", Biogerontology, 2019

Publication

26%

2

Submitted to University of Hyderabad, Hyderabad

Student Paper

4%

3

Kowshik Kukkemane, Anita Jagota. "Therapeutic effects of curcumin on age-induced alterations in daily rhythms of clock genes and Sirt1 expression in the SCN of male Wistar rats", Biogerontology, 2019

Publication

3%

4

Ushodaya Mattam, Anita Jagota. "Differential role of melatonin in restoration of age-induced alterations in daily rhythms of expression of

1%